Forecasting and decision-making in electricity markets with focus on wind energy

Jónsson, Tryggvi

Publication date:
2012

Document Version
Publisher's PDF, also known as Version of record

Forecasting and decision-making in electricity markets with focus on wind energy

Tryggvi Jónsson

Kongens Lyngby 2012
IMM-PHD-2012-269

Technical University of Denmark
Informatics and Mathematical Modelling
Building 321, DK-2800 Kongens Lyngby, Denmark
Phone +45 45253351, Fax +45 45882673
reception@imm.dtu.dk
www.imm.dtu.dk

IMM-PHD: ISSN 0909-3192

Preface

This thesis was prepared at the department of Informatics and Mathematical Modelling (Informatics), the Technical University of Denmark (DTU) in partial fulfilment of the requirements for acquiring the PhD degree in engineering. The project was funded jointly by ENFOR A/S and the Danish Agency for Science, Technology and Innovation through the Industrial Ph.D. initiative.

The thesis deals with analysis, forecasting and decision making in liberalised electricity markets with special focus on wind power. The impact of its presence on the market is analysed, models utilising this impact for prediction derived and tools facilitating better operation are presented.

The thesis consists of a summary report and eight research papers, written during the period November 2008 - February 2012. Five are either submitted to or published in international peer reviewed scientific journals, one is published as a research report at DTU Informatics and two either have or are to appear in conference proceedings.

Copenhagen, February 2012

Tryggvi Jónsson

Acknowledgements

First and foremost I would like to thank my supervisors in this project, Assoc. Prof. Pierre Pinson and Assoc. Prof. Niels Kjølstad Poulsen at DTU Informatics and Dr. Henrik Aa. Nielsen and Dr. Torben Skov Nielsen at ENFOR A/S for the excellent guidance, support and motivation. Same goes for my long time mentor and collaborator at DTU Informatics, Prof. Henrik Madsen.

Also I would like to thank Prof. Sarah M. Ryan at Iowa State University for her hospitality and collaboration during my stay with her department. Thanks are also extended to Prof. Leigh Tesfatsion and the others in the E3 group at Iowa State University for allowing me to participate in their meetings.

I would also like to thank my colleagues at DTU Informatics and ENFOR A/S for contributing to a inspiring working environment and their willingness assist when needed. In particular I want to thank my fellow Ph.D. student and collaborator Marco Zugno for joint work and the countless discussions about the issues of the energy sector and their solution. Fannar Örn Thordarson is also thanked for proofreading parts of the thesis. Thanks are also owed to the EU FP6 project Anemos.plus, and in particular DONG Energy for stimulating interactions.

Finally I would like thank my family, my wife Thorhildur and my daughters Brynhildur Freyja and Elinborg Dora for their patience, love and support.

Summary

This thesis deals with analysis, forecasting and decision making in liberalised electricity markets. Particular focus is on wind power, its interaction with the market and the daily decision making of wind power generators. Among recently emerged renewable energy generation technologies, wind power has become the global leader in terms of installed capacity and advancement. This makes wind power an ideal candidate to analyse the impact of growing renewable energy generation capacity on the electricity markets. Furthermore, its present status of a significant supplier of electricity makes derivation of practically applicable tools for decision making highly relevant.

The main characteristics of wind power differ fundamentally from those of conventional thermal power. Its effective generation capacity varies over time and is directly dependent on the weather. This dependency makes future production uncertain and difficult to contract even on a day-to-day basis. Consequently decisions about market bids for next-day delivery are based on production forecasts which are bound to come with some uncertainty. Naturally markets that experience large scale integration of wind power are affected by these different characteristics. The thesis presents analyses of how this impact is realised in markets significantly penetrated by wind power. Due to its representation by forecasts in the supply curve, such predictions are used to describe their non-linear influence on the market prices.

Methods adequately accounting for this effect in models for day-ahead forecasting of the prices are also presented in the thesis. Prompted by the volatile behaviour of electricity markets, considerable focus has been on time-varying and robust parameter estimates. The models derived are all based on well know methods from the statistical literature.

The stochastic production of wind turbines prompts the need for alternative methods for optimally bidding wind power to day-ahead markets. Such bidding strategies are formulated in this thesis, which utilise the information provided by the market models. Bids that maximise expected revenues are found and the possibility of risk averse behaviour is discussed.

Resumé
(summary in Danish)

Denne afhandling beskæftiger sig med analyse, prognoser og beslutningstagning i el markeder. Særlig fokus er sæt på vindkraft, dens samspil med markedet og vindkraftproducentens daglige beslutningstagning. Ud af de nyere kilder for vedvarende energi, vindkraft har påtaget sig en førerrolle som den mest avancerede og udbredte teknologi. Dette gør vindkraft til en ideal kandidat til at analysere hvilken effekt voksende el generation med vedvarende kilder har på el markeder. Endvidere, vindkraftens nuværende status som en betydningsfuld leverandør af elektricitet gør udviklingen af værktøjer til den daglige beslutningstagning meget relevant.

Vindkraftens karaktertræk adskiller sig fundamentalt fra disse for termiske kraftværker. Dens effektive generationskapacitet varierer over tid og afhænger af vejret direkte. Dette gør fremtidig produktion forbundet med usikkerhed og besværliggør handel selv på næste-dags basis. Som følge heraf må beslutninger vedrørende indmelding på marked for levering næste dag tages på grund af prognoser som i sagens natur er usikre. Markeder som i høj grad er penetreret af vindkraft bliver naturligvis påvirket af dette. Afhandlingen præsenterer analyser af hvordan denne effekt bliver realiseret i markeder med stor andel vindstrøm in dens produktionsportefølje. Grundet dens repræsentation i udbudskurven af prognoser, bliver sådanne forudsigelser brugt for at beskrive deres ikke-lineære påvirkning på markedspriserne.

Metoder for at tage højde for denne effekt på tilstrækkelig vis i modeller for forudsigelse af næste dags priser er også præsenteret i afhandlingen. Markedets varierende opførsel har gjort at adaptiv og robust parameter estimering har fået stor fokus. Modellerne er alle baseret på velkendte metoder fra den statistiske litteratur.

Vindmøllernes stokastiske produktionsevne skaber behøv for alternative metoder til at byde strøm ind på markedet optimalt. Sådanne indmeldingsstrategier er formuleret i denne afhandling, som gør nytte af den information prognosemodellerne leverer. Bud der maksimerer den forventede indtjening bliver fundet samt at muligheden for risikoavers adfærd bliver drøftet.

List of publications

Papers included in the thesis

A Tryggvi Jónsson, Pierre Pinson & Henrik Madsen (2010). On the market impact of wind energy forecasts. *Energy Economics* 32(2), pp. 313-320.

B Tryggvi Jónsson, Marco Zugno, Pierre Pinson & Henrik Madsen (2010). On the market impact of wind power (forecasts) - An overview of the effects of large-scale integration of wind power on the electricity market. In proceedings: *IAEE's 33rd International Conference.*

C Pierre Pinson, Tryggvi Jónsson, Marco Zugno, Juan-Miguel Morales & Henrik Madsen (2011). Statistical analysis of the impact of wind power on market quantities and power flows. Invited paper for: *IEEE Power and Energy Society General Meeting 2012.*

D Marco Zugno, Tryggvi Jónsson & Pierre Pinson (2012). Trading wind energy based on probabilistic forecasts of both wind generation and market quantities. Accepted for publication in: *Wind Energy (2011).*

E Tryggvi Jónsson, Sarah M. Ryan, Marco Zugno & Pierre Pinson (2012). Risk averse bidding of wind fower: formulation and properties. *IMM Technical Report 2012-03.*

F Tryggvi Jónsson, Pierre Pinson, Henrik Aa. Nielsen, Henrik Madsen & Torben Skov Nielsen (2012). Forecasting electricity spot prices accounting for wind power predictions. Accepted for publication in: *IEEE Transactions on Sustainable Energy*.

G Tryggvi Jónsson, Pierre Pinson, Henrik Aa. Nielsen & Henrik Madsen (2012). Predictive densities for day-ahead electricity prices using time-adaptive quantile regression. Submitted to *European Journal of Operational Research*.

H Tryggvi Jónsson, Pierre Pinson, Henrik Aa. Nielsen & Henrik Madsen (2012). Exponential smoothing approaches for prediction in real-time electricity markets. Submitted to *Energy Economics*.

Other Publications

In addition to the papers listed before, the following conference contributions were also prepared during the project period. Their content is however covered by the other paper and therefore they are not included in the thesis.

- Tryggvi Jónsson, Pierre Pinson, Henrik Madsen, Henrik Aa. Nielsen. Forecasting day-ahead electricity prices and regulation costs in markets with significant wind power penetration. EWEC'09, European Wind Energy Conference, Marseille, France. (oral presentation)
- Tryggvi Jónsson, Pierre Pinson, Henrik Madsen. The impact of wind power forecasts on electricity price behaviour in Denmark. EWEC'09, European Wind Energy Conference, Marseille, France. (poster)
- Tryggvi Jónsson, Pierre Pinson, Henrik Madsen. Point-and probabilistic forecasting of electricity spot prices International Symposium on Forecasting, Hong Kong, China, 2009. (oral presentation)
- Marco Zugno, Tryggvi Jónsson, Pierre Pinson. Trading wind energy in a liberalised electricity market: a real-world test case in Eastern Denmark. EWEC'10, European Wind Energy Conference, Warsaw, Poland, 2010. (poster)
- Marco Zugno, Tryggvi Jónsson, Pierre Pinson. Decision making strategies for trading wind power in deregulated energy markets. IAEE's 33rd International Conference, Rio de Janeiro, Brazil, 2010. (oral presentation)

Contents

Part I

Summary Report

CHAPTER 1

Introduction

For decades, electricity has been one of the most important building blocks of our society. Not only is it likely maintain this status but has an outlook to become even more important in the near and distant future. The globally increasing focus on curbing carbon emissions has fuelled large investments in research aimed at replacing all kinds of devices burning fossil fuel with similar ones relying on electricity. In parallel, electricity generation plants relying on renewable fuel sources have received increased attention. In particular, the wind power industry has bloomed and taken a leading role among the recently emerged renewable energy sources. Other plant types such as solar, geothermal and tidal power are evolving fast though.

Almost simultaneously, the electricity industry has been revolutionised and the deregulated electricity market has emerged as the future platform for the trade of this commodity. Despite being a relatively recent invention, these markets are typically designed for conventional power generators in full control of their production. This naturally poses problems for generation plants relying on recently emerged technology which fundamentally differs from those previously existing.

1.1 Thesis Objective

The main differences between the renewable energy sources like those previously mentioned and conventional power plants are owed to the characteristics of the fuel. Directly relying on nature for fuel supply causes the effective generation capacity of these plants to vary over time in a manner best characterised as stochastic. Thus contracting exact amount for future delivery can be problematic. With the fuel available however, these plants can generate electricity at virtually no cost and are not subject to the same constraints as the conventional ones.

These differences naturally call for different approaches to various aspects of their operation in general. Among those things is their participation in the market which is what eventually ensures the investor's payback. This thesis addresses some aspect of the interaction between wind power and electricity markets. The effect of its presence on the market is analysed and tools for assisting its participation in the market are presented. The latter involves analysis and development of tools for optimally bidding wind power to the market and also derivation of models that can provide the forecasts to be used in the decision making. More precisely the objectives of the thesis are as follows:

- To analyse and improve understanding of how electricity prices are influenced by large scale wind power integration.
- To analyse proposed bidding strategies for wind power producers, develop them further and understand which forecasts are required for adopting such strategies in practise.
- To utilise the interaction between wind power production and the market along with other known impact factors to construct models that are capable of issuing accurate forecasts of the day-ahead and real-time market prices.

The focus is thus on challenges that directly relate to the daily operation of a wind power producer. No attention is however paid to the long-term management challenges such producers face, e.g. pricing of financially settled contracts for risk management and pricing of long-term delivery contracts.

Due to the stochastic generation of wind turbines, their operators must rely on forecasts for trading on a day-ahead basis. The production forecasts therefore represent the wind power in the supply curve and not the actual production. This motivated that, in contrast to previous analysis of the relationship between wind power production and day-ahead prices (Morthorst, 2003, Moesgaard and Morthorst, 2008), the one presented in this thesis considers pro-

duction forecasts instead of actual production. In addition, by accounting the non-linear aspects of the analysed relationship through non-parametric models, the impact of wind power on the prices is shown to be more substantial than previously demonstrated.

These effects become an additional source of variation for the prices which already are known to exhibit features such as non-stationarity, multiple seasonal cycles, mean-reverting spikes, positive skewness and high kurtosis (Conejo et al., 2005, Panagiotelis and Smith, 2008, Kosater and Mosler, 2006). A common methodology for modelling the expected prices has therefore been the well known ARIMA model, fitted in terms of the logarithmically transformed prices (Conejo et al., 2005, Nogales et al., 2002, Weron, 2006). More in line with Karakatsani and Bunn (2008), the model presented in this thesis is estimated on the original scale of the prices. Correspondingly, forecasts are issued on the same scale. Recursive and robust parameter estimation are instead used to accommodate the varying dynamics of the prices. Similar transformations and parametric assumptions are also the literature's prevailing approach to density models for the prices (Panagiotelis and Smith, 2008, Higgs, 2009). Conversely, a semi-parametric density forecast method is presented in this thesis which also deals with untransformed data.

Alternatives to contracting the expected wind power production in the day-ahead market have received increased intention in the literature in recent years. The bidding strategy presented here builds on the work of Bremnes (2004), Pinson et al. (2007) and aims at maximising expected hourly revenues. Modifications are made to account for practical constraints and on the contrary to many previous studies, (e.g. Pinson et al., 2007, Matevosyan and Söder, 2006, who base their results on constant expectations for the market), trading is simulated based on actual forecasts for the cost of imbalances. The derivation of the model used to generate these forecasts is presented in the thesis as well. Similar to Olsson and Söder (2008), efforts are made to accommodate the regime switching behaviour of the imbalance costs in the modelling process.

The models presented are all developed with practical applicability in mind. Results are therefore in all cases derived by mimicking the real-life circumstances. The models used for analysis and forecasting are all statistical ones, built on established and well known models from the statistical literature. The characteristics of the subject has prompted focus on adaptive and robust parameter estimation along with other models that are able to capture varying dynamics. Most of the work presented in this thesis is done using data from the Western Danish grid area which comprises Jutland, Funen and the islands west of Størebælt. Papers B, C and D contain results for other areas though, in part or exclusively.

1.2 Thesis Outline

The thesis is divided into two parts. The first part contains a summary report which is meant to give a fairly non-technical overview of the main results of the thesis and provide background information on the problems dealt with and their empirical context. The second part comprises 8 research papers prepared during the project period. The contents of each paper is summarised briefly in the following:

Paper A was published in Energy Economics in 2010. The paper presents an analysis of the impact of wind power production forecasts on the day-ahead market prices in Western Denmark.

Paper B was published in the proceeding of the 33rd IAEE Conference in 2010. In this paper the analysis from Paper A is extended to the Eastern Danish grid area and variations in the relationship throughout the year are examined.

Paper C is an invited paper submitted to IEEE Power and Energy Society's General Meeting 2012. This paper presents an analysis similar to the one of Papers A and B using data from Western Denmark and Germany. Also the impact of German wind power production on domestic and cross-border power flows in Austria is analysed.

Paper D is a paper submitted to Wind Energy which presents a bidding strategy for a wind power producer based on production forecasts and predictions for the market outcome. The paper describes a 10 month long case study where participation in the market is simulated.

Paper E is a technical report published at DTU Informatics. In this report a general risk averse bidding strategy for wind power producers is presented. In addition, formulations suited for practical use are given along with a small case study used to exemplify the resulting bidding behaviour.

Paper F is a paper submitted to IEEE transactions on Sustainable Energy. It describes a model for the expected day-ahead electricity price which accounts for the impact of wind power predictions. The model is intended for forecasting of next day's prices and corresponding results are presented.

Paper G has been submitted to European Journal of Operational Research. The paper describes a model for predictive densities for the day-ahead electricity prices in Western Denmark. The model is built as an extension to the model from Paper F and is also intended for day-ahead forecasting.

Paper H is an article submitted to Energy Economics. It presents models for day-ahead prediction in the Danish real-time electricity market using theory from the exponential smoothing literature.

The remainder of the summary report is constructed as follows: Chapter 2 outlines the functions of liberalised electricity markets in general and the Nordic context of this thesis in particular. An introduction to the data set used for most model derivations is also presented in this chapter. Chapter 3 addresses the interaction between wind power and the market, both in terms of impact on prices and the bidding decision. The models for prediction are presented in Chapter 4 and finally concluding remarks and future perspectives are listed in Chapter 5.

CHAPTER 2

Electricity Markets

The electricity industry has undergone drastic reforms during the past two decades. The model of vertically integrated utilities has been abandoned and the potentially competitive functions of generation and retail separated from the natural monopolies of transmission and distribution.

The Chilean Chicago boys of the Pinochet cabinet are commonly credited for being the first to introduce the concepts of privatisation and deregulation to the electricity market in the early 1980's. In Europe, the transition towards deregulated electricity markets was initiated by the Thatcher government in the United Kingdom in 1990. The Nordic power exchange, Nord Pool, was opened in Norway in 1992 and gradually expanded its operations to the other Scandinavian countries throughout the decade. Following UK's example a number of other Commonwealth countries began deregulation of the electricity sector, most notably Australia in 1994 and New Zealand in 1998. Deregulation of markets in USA started in the northeastern states and in the state of California during the late 1990's followed by restructuring of markets in other parts of the union. Since then, market deregulation policies have been adopted in numerous countries. Today, a deregulated electricity markets have been established in most European countries and in many places in the Americas and Asia.

This worldwide unbundling of the electricity sector's vertical monopoly structure is generally praised as a successful one. The main benefits of this new

structure are commonly claimed to be increased transparency, lower prices and increased efficiency. None of these benefits are undisputed though. Despite that in principle an open auction should increase the transparency of any market, the complex pricing models and bid structure work towards the opposite. Indeed declining net prices (i.e. excluding taxes) were observed during the years around the millennium and it seems natural to accredit the deregulation process as the single most comprehensive change in the system for this reversed trend. However, these reductions were however neither felt by domestic consumers nor small and medium sized industrial ones due to increased taxation (Euorostat, 2007, Weron, 2006, Bunn, 2004). As of 2004 electricity prices have shown an increasing trend, including or excluding taxes (Euorostat, 2007, Eurostat, 2012). Whether this is a result of the market reform is unclear though given the development in the global economy in this period.

Critics on the other hand argue that incentives for new investment in generation and transmission capacity have been severely reduced. Among other examples, the massive blackout of 2003 in the north-eastern USA is used to support this claim. Furthermore, the California energy crisis of 2000-2001 is often used to exemplify the flaws of the deregulated markets.

During this period of market transition, most market operators have made numerous changes of the market framework intended to strengthen competition and ensuring an efficient market. Today the model of a liberalised electricity market seems to have converged to a design capable of serving its purpose. This chapter describes the general structure of modern electricity market and some of the major design variations. After a general introduction, a more detailed description of the Nordic Power Market is given as it serves as the context of all the empirical work done in this thesis.

2.1 Market Structure

Although the particularities of market design and institution roles vary between individual markets, the general framework remains similar among those who have adopted this new policy. In the following, the aim is to give an overview of the main existing structural variations of deregulated electricity markets.

2.1.1 Organisation

The backbone of a deregulated electricity market is typically the spot market (referred to as the forward market in some regions[1]). On these markets, electricity is traded for delivery within near future periods of fixed length, usually an hour or half an hour. Gate-closure is sometime between noon on the day before delivery and few hours before realisation. The market is organised by an independent operator which is responsible for collecting bids, calculating market clearing prices and determining the corresponding production and consumption schedules.

The transmission systems are generally considered natural monopolies. Hence, they have been put in the hands of system operators (SOs), formed for the purpose of managing the grid as state owned enterprises or thoroughly regulated private organisations. The responsibilities of the SO varies between countries to some extent. The European Transmission System Operators (TSOs) focus on operation and maintenance of the grid within their countries and connections to their neighbours only. The American Regional Transmission Organisations (RTOs) and Independent System Operators (ISOs) on the other hand have the additional function of being a market operator.

The SOs are responsible for maintaining constant balance between supply and demand, which is crucial for the operation of the system. For that purpose a real-time market is often organised by the SO even though other markets are operated by another organiser. The purpose of the real-time market is to settle deviations from previously entered contracts. Trading on these markets is often discouraged by a market structure unfavourable for speculation or gaming and other regulatory interventions. Many US market operators allocate capacity for the real-time market together with the clearing of the spot market by co-optimisation (Conejo et al., 2010). Just as for the spot market, the real-time market is referred to in different ways. Imbalance market and regulation market are two common ones and for those who favour the term forward market for the spot market think of the real-time market as the spot market.

In some areas an intermediate market is operated, allowing for adjustment of the contracts entered into on the spot market after its gate-closure. Finally, so-called over-the-counter (OTC) contracts are common. OTC contracts are agreements of electricity purchase and sale with delivery periods ranging from days or weeks up to years and settled according to a predetermined price or a pricing formula. Settlement of these contracts is done through a clearinghouse instead of on the market.

[1] Many, especially economists, argue that since the contracts traded on the markets here termed spot markets are for future delivery, they are indeed forward contracts as defined in the financial terminology.

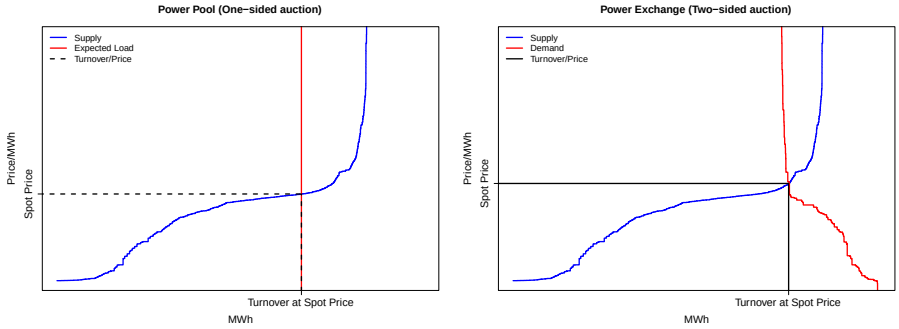

Figure 2.1: Price determination in a power pool (left) and in a power exchange (right). The plots are reconstructed version of similar plots in Weron (2006).

2.1.2 A Pool or an Exchange?

Electricity markets can be divided in two categories: power pools and power exchanges (Weron, 2006). The main differences between the two lies in i) the participation obligations of the generators and ii) the handling of the consumption.

A power pool is only meant to facilitate competition among generators. They submit their bids to the market as the price they request for their production and the corresponding volume. These bids are then cleared against the expected demand, i.e. the supply curve is vertical. Generators are obliged to participate in the pool so no transactions can be made outside the pool.

In contrast, participation in a power exchange is voluntary. The exchange auction is two-sided so bids are submitted by both generators and consumers. The role of the power exchange is to match the resulting supply and demand curves and announce the market clearing price along with the corresponding schedules for production and consumption.

The difference between the two price determination procedures is illustrated in Figure 2.1. Whereas expected load appears as a vertical demand curve for the one-sided auction, an actual demand curve is used in the two-sided auction. Hence, the market clearing price and the turnover volume are interdependent.

2.1.3 Price determination and Settlement

The most commonly applied model for price determination on the spot market is a bid-based security-constrained economic dispatch with either zonal or nodal prices. In other words, the price for a given delivery period is set as the intersection between the aggregated supply and demand curves while ensuring that transmission- and operation security constraints are respected.

The zonal or nodal prices are the result of finite transmission capacity. Although the principle behind the two is essentially the same when it comes to the price determination procedure, the finer spatial resolution of the nodal prices ensures that the physical constraints of the system are respected. On the other hand, the more coarse resolution of the zonal pricing scheme allows for the separation of the SO and the market operator as is commonly done in Europe. Since transmission capacity between zones and between nodes is limited, situations can occur where merit order dispatch prompts this capacity to be exceeded. This is handled by defining separate prices on either side of the congested line. In a nodal pricing system, also known as locational marginal pricing (LMP), each node can have a unique price. In a zonal pricing system however, prices can only differ at the zone level. Consequently, congested nodes are subsidised by uncongested ones in some situations.

Prices are generally determined as the highest accepted bid within the delivery period. In some markets though, e.g. the APX exchange in the UK and the Elbas market at Nord Pool, discriminatory or pay-as-bid settlement has been adopted.

Because bids on the regulation markets are activated in real-time, prices on these markets are determined ex post. Although some market operators (e.g. PJM (Ott, 2003)) calculate and broadcast an indicatory ex ante price during operation. Price- and settlement resolution can vary from being equal to that of the previously settled markets (e.g. APX UK) to having resolution of 5 minutes in both prices and settlement. Moreover, some market operators (e.g. Energinet.dk in Denmark) operate a real-time market with a price resolution equal to that of the spot market while imbalances are settled with higher resolution.

The single most notable difference among the pricing mechanism on the real-time markets is whether a single-price system is adopted or a two-price one. In a single price system, the same price is valid for all imbalances regardless of whether they are surpluses or deficits. So producers that produce more than their contracted volume sell their extra generation to those short of their contracts at a price directly resulting from the net imbalance of the system. In a two-price system, production deficits and surpluses are priced separately. In

other words, those overproducing sell their extra production to the market operator at one price and those who are not able to produce their full contracted volume buy their shortfall at another price.

2.2 The Nordic Power Market

Since the context of the entire empirical work done for the thesis is the two Danish price areas of the Nord Pool power exchange, the specific market design of Nord Pool is listed in the following.

Despite the name, Nord Pool is a power exchange and is the first of its kind to facilitate power trading across national borders. Following a new energy legislation in 1991 the Norwegian TSO, Statnett SF, began operating a domestic day-head spot market in the same year. Two years later the market operating activities were demerged into a subsidiary, Statnett Marked A/S, fully owned by Statnett SF. Cross-border trading began in 1996 following Svenska Kraftnät's acquisition of 50% of the shares in Statnett Marked A/S. Simultaneously, Statnett Marked A/S became Nord Pool ASA. The joint operation of a power exchange allowed both countries to continue their efforts towards a deregulated electricity sector. Since the opening of the market, Statnett's market had been plagued by price volatility, arising from it relying fully on hydroelectric power. Meanwhile, the oligopolistic structure of the Swedish power sector had prevented liberalisation (Carlsson, 1999). Nord Pool's day-ahead market, Elspot, then gradually expanded to encompass Finland in 1998, Western Denmark in 1999, Eastern Denmark in 2000 and Estonia in 2010. In addition, the German transmission grid area operated by Vattenfall was also a part of Nord Pool's markets during the years 2005-2009.

Besides operating Elspot, Nord Pool engaged in various other activities. In 1997 trading of financial forward contracts was launched along with a clearing service for these contracts. Other financial derivatives such as futures, options and Contracts for Difference (CfD) were later introduced in this market. A bilateral market for intra-day trading of power, Elbas, was opened in Sweden and Finland in 1999. Later it opened for trading in Eastern Denmark in 2004, followed by an opening in Western Denmark in 2007 and in Norway in 2009. Finally, Nord Pool ASA was involved in numerous consulting assignments.

Following the licensing of Nord Pool ASA as a regulated exchange and clearinghouse in 2002, all activities except the financial market were demerged into subsidiaries. The clearinghouse and the consulting business remained fully owned by Nord Pool ASA through Nord Pool Clearing ASA and Nord Pool Consulting ASA respectively. Physical exchange activities were established

under the name Nord Pool Spot ASA, which ownership was equally divided amongst Nord Pool ASA and the four Nordic TSOs.

Today Nord Pool ASA and its two fully owned subsidiaries have been acquired by NASDAQ OMX while Nord Pool's share in Nord Pool Spot ASA have been acquired by Statnett SF and Svenska Kraftnät - with equal shares. Currently, Nord Pool Spot ASA is therefore jointly owned by Statnett SF and Svenska Kraftnät with 30% each, and Energinet.dk and Fingrid Oy with 20% each (the Danish and the Finnish TSOs respectively). Nord Pool's market share is one of the highest in the world and has been increasing over the last three years despite fluctuating demand. With a 70% market share in 2008 it rose to 72%, 74% and 75% in 2009, 2010 and 2011 respectively (Nord Pool Spot AS, 2010, 2011, 2012).

2.2.1 Elspot

Elspot is a day-ahead market with gate-closure at noon on the day before delivery. Prices are determined by a bid-based security-constrained economic dispatch with zonal prices and a resolution of one hour. A map of the current zonal structure is shown in Figure 2.2. The market region comprises 13 price areas; 5 in Norway, 4 in Sweden, 2 in Denmark and 1 in Finland and Estonia. The price areas are bordered by bottlenecks in the transmission grid and, in the context of price determination, with internal transmission capacity practically infinite.

The Elspot system price is determined as the intersection between the aggregated supply and demand curves for the entire region in the same manner as illustrated in the right plot of Figure 2.1. This price is the one at which physical exchange is settled during hours where transmission across the grid bottlenecks does not reach their capacity. In addition, the system price serves as a reference price for almost all financial derivatives linked to Nord Pool. Only the CfDs have a partial reference in other prices. Two or more area prices are defined when the unconstrained merit order dispatch prompts scheduled transmission across price area borders to reach its capacity. The determination of an area price is illustrated in Figure 2.3. The procedure is essentially the same as for the system price but only based on the bids from the particular area while the full utilisation of the connections to the surrounding areas is regarded as price independent bids. Hence the parallel shift in the supply and demand curves in Figure 2.3.

Bids at Elspot can be placed as hourly ones or as block bids comprising multiple consecutive hours. Both bid types state a price and volume which can be defined in multiple intervals. The difference between the two is that whereas

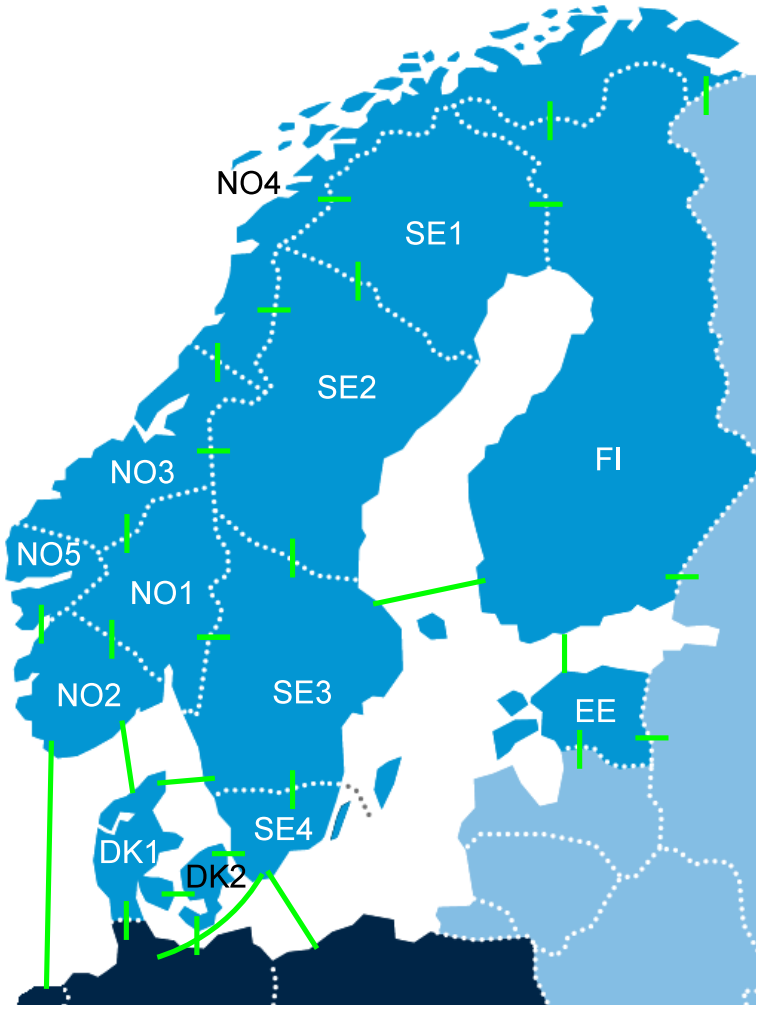

Figure 2.2: A map of Scandinavia sketching the price zone borders of Nord Pool. Source: www.nordpoolspot.com

the hourly bid is accepted if the specified price is lower than or equal to that of the marginal producer, the block bid is only accepted if the resulting average clearing price for the hours that constitute the block is higher than the bid price. The block bids are primarily used by producers that need to account for start-up and shut-down costs or physical constraints such as minimum running time in their bidding.

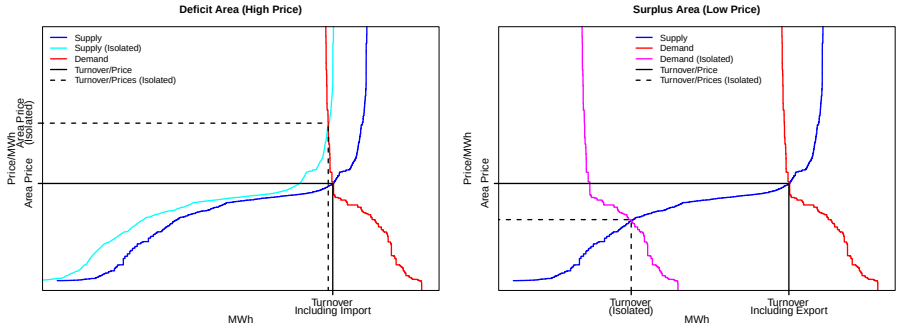

Figure 2.3: Determination of area prices at Nord Pool. The plots are a reconstruction of similar plots presented at .

2.2.2 Elbas

Elbas is opened for trading once the Elspot prices have been published and has gate-closure 1 hour prior to delivery. Elbas is a bid-ask market where bids for either purchase or sale of electricity are placed. The bids are prioritised according to price and submission time and are settled at the bid price. The acceptance of a bid across price areas is subject to capacity availability which is published along with the spot prices.

Compared to Elspot the traded volumes at Elbas are quite low or less than 1% of the total volume exchanged annually on Nord Pool's markets (Nord Pool Spot AS, 2010, 2011, 2012). For this reason Elbas is not considered as a potential forum for power exchange in the bidding strategy later described. Thus, no discussion about it is included in the remainder of this thesis although research on optimal participation in such markets exists (see, e.g., Conejo et al., 2010).

2.2.3 The Real-Time Market

In order to maintain grid stability, the Nordic TSOs each manage a real-time market in their countries. The three general imbalance scenarios that can occur are illustrated in Figure 2.4. The terms that have been adopted for these scenarios are based on the necessary counteraction for a generator. Thus a down-regulation hour is an hour of positive system imbalance or production surplus forcing producers to reduce their production. Contrarily, an up-regulation hour is an hour of production deficit requiring increased generation in the system. In principle, imbalances could be negated by the opposite actions of the consumers, but to date demand regulation on a notable scale has yet to leave

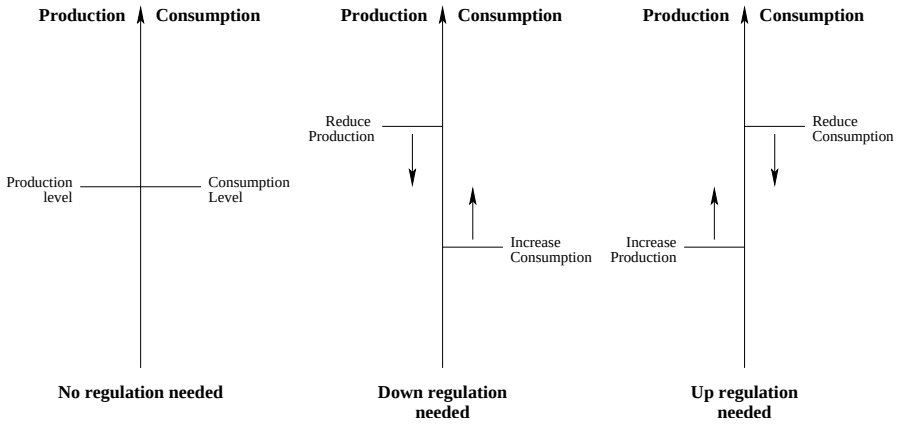

Figure 2.4: Possible scenarios of physical regulation need.

the drawing board.

Unless transmission lines across price zones are congested, it is the overall imbalance of the Nordic power system as a whole that determines whether an hour is defined as an up- or down-regulation hour. Accordingly, bids for regulation are accepted across area borders if possible. Should transmission capacity across area borders be exceeded, area specific regulation prices become effective. In these cases, it is the area's net imbalance that constitutes the definition of the regulation scenario.

Bids for regulating power are accepted until 45 minutes before the hour. The bids should state a price and a volume between 10 MW and 50 MW, to be available within 15 minutes from acceptance.

The pricing procedure for regulating power was harmonised for the whole Nordic region in 2009. Since then, generator imbalances and consumer imbalances are prices with different schemes. For the retailers a single price is defined at which all imbalances are settled. In contrast, two prices are defined on the suppliers' market. The producers short of their contracts buy their deficits at the up-regulation price while those overproducing sell their surplus at the down-regulation price. The hourly prices are determined as the most expensive regulation bid accepted within that hour for regulation in the active direction. Note that in this context the most expensive down regulation bid is the one with the lowest price.

For the producers, the regulation prices are bounded by the Elspot prices such that the up-regulation price can never deceed it and the down-regulation price can never exceed it. Furthermore, imbalances that negate the total system im-

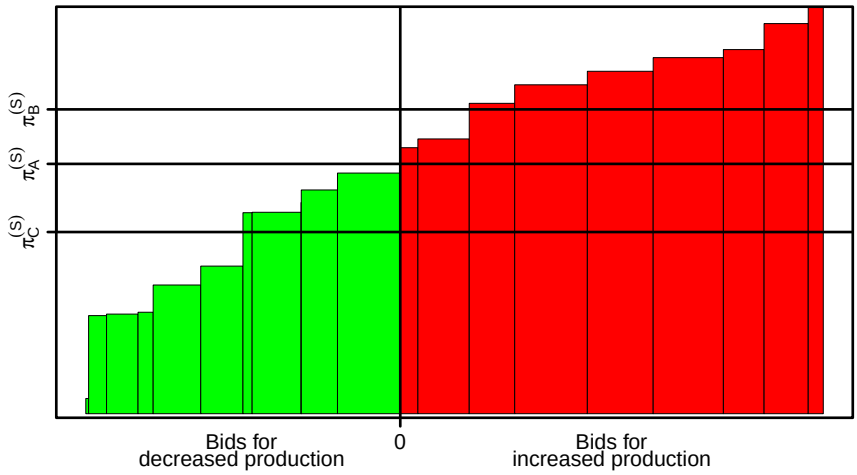

Figure 2.5: An example of a regulation supply curve.

balance are not penalised. This implies that at any given time, either the up-regulation or the down-regulation price is equal to the spot price.

An illustrative example of a supply curve for regulating power is shown in Figure 2.5. Bids for up-regulation (red) are accepted in ascending order from 0 and are simply bids for production. The down-regulation bids (green) on the other hand are accepted in descending order from 0 and can be viewed as bids for purchase of energy from generators that are scheduled for production. If a bid is accepted, the producer fulfils its contract by outsourcing the production to another producer instead of generating the power itself.

In order to further exemplify the pricing of regulating power, let the three horizontal lines in Figure 2.5 represent spot prices of hours for which the supply curve is valid. During the hour where $\pi_A^{(S)}$ is effective, both the up-and the down-regulation prices become that of the accepted bid furthest away from 0 if the system imbalance takes the corresponding sign. If however the spot price is $\pi_B^{(S)}$, the up-regulation price remains equal to the spot price if only the first two bids are activated. Only with the activation of the third bid the up-regulation price takes a different value than the spot price. Similarly, if the spot price is $\pi_C^{(S)}$, the down-regulation price remains equal to the spot price until the 5th bid for decreased production is accepted.

2.3 Empirical Data & Context

We round off the discussion on electricity markets by putting the market design into mathematical context and summarise the rationale behind the modelling choices made. The variable definitions presented in this section will be used in the analysis and the model derivations presented in the chapters that follow. A more detailed discussion of the various aspects of the information contained in this section is given in the papers devoted to the corresponding topic.

2.3.1 Definition of Market Variables

First let $\pi_t^{(S)}$, $\pi_t^{(\uparrow)}$ and $\pi_t^{(\downarrow)}$ denote the spot-, the up- and the down-regulation prices, respectively. Furthermore, define the up- and down-regulation penalties ($\psi^{(\uparrow/\downarrow)}$) as

$$\begin{aligned} \psi_t^{(\uparrow)} &= \pi_t^{(\uparrow)} - \pi_t^{(S)} \\ \psi_t^{(\downarrow)} &= \pi_t^{(S)} - \pi_t^{(\downarrow)}. \end{aligned} \tag{2.1}$$

The market design in the Nordic region implies that the following conditions are fulfilled at all times:

$$\pi_t^{(\uparrow)} \geq \pi_t^{(S)} \Rightarrow \psi_t^{(\uparrow)} \geq 0 \quad \forall t \tag{2.2}$$

$$\pi_t^{(\downarrow)} \leq \pi_t^{(S)} \Rightarrow \psi_t^{(\downarrow)} \geq 0 \quad \forall t \tag{2.3}$$

$$\pi_t^{(\uparrow)} = \pi_t^{(S)} \Rightarrow \psi_t^{(\uparrow)} = 0 \quad \text{if } \pi_t^{(\downarrow)} < \pi_t^{(S)} \quad \forall t \tag{2.4}$$

$$\pi_t^{(\downarrow)} = \pi_t^{(S)} \Rightarrow \psi_t^{(\downarrow)} = 0 \quad \text{if } \pi_t^{(\uparrow)} > \pi_t^{(S)} \quad \forall t. \tag{2.5}$$

From this it can be seen that any electricity generator not capable of providing regulating power maximises its earnings by selling all its production at the spot price. In other words, such a producer's involvement in the real-time market can only reduce revenues thus justifying the penalty naming.

Conditions (2.2) & (2.3) are the result of the real-time prices being bounded by the spot price. The latter two conditions, (2.4) & (2.5), are however due to that only producers that contribute to the overall imbalance are penalised. This pricing scheme introduces regime switching behaviour in the regulation prices, controlled by the net imbalance of the system and the available regulation power. More precisely, $\pi_t^{(\uparrow)}$ shares dynamics with the spot price during hours of production surplus and during deficit hours when the naturally determined up-regulation price does not exceed $\pi_t^{(S)}$. Likewise the dynamics of

$\pi_t^{(\downarrow)}$ are only unique during hours of net production surplus and a naturally determined down-regulation price lower than the spot price. For the penalties, $\psi_t^{(\uparrow/\downarrow)}$, these regimes are also present as the prices switch between being a constant zero and having dynamics on their own.

By definition, the regulation prices in each direction have two dynamical regimes. Taking into account the interdependence between how realisations from each regime can occur, the real-time prices can be thought of as a two-dimensional variable with dynamics switching between three regimes. A variable $I_t^{(\psi)}$, hereafter termed the imbalance sign, distinguishing between these regimes is defined as

$$\begin{aligned} I_t^{(\psi)} &= \operatorname{sgn}\{(\pi_t^{(\uparrow)} - \pi_t^{(S)}) + (\pi_t^{(\downarrow)} - \pi_t^{(S)})\} = \operatorname{sgn}\{\psi_t^{(\uparrow)} - \psi_t^{(\downarrow)}\} \\ &= \begin{cases} 1 & \text{during up-regulation hours} \\ 0 & \text{during hours of no regulation penalty} \\ -1 & \text{during down-regulation hours.} \end{cases} \end{aligned} \tag{2.6}$$

The imbalance sign describes which supply function defines the price or the penalty.

From a modelling perspective, the appeal of having the three regimes is that it allows models to be derived conditional to which supply the corresponding prices stem from. This is done by deriving models for expectations or densities which are conditional to $I_t^{(\psi)}$. Such models are more focused on capturing the dynamics of each regime. Afterwards, the forecasts for each regime can be mixed through modelling of the imbalance sign in order to obtain unconditional forecasts for the real-time market.

I should be noted that for the system operator, the states of the real-time market are not necessarily the same as for the producer. The TSO operates in higher temporal resolution with the actual physical balance of the system, which can change signs within an hour and is seldom precisely zero.

2.3.2 The Data

All empirical results presented in the thesis are derived using data from the two Danish price areas of Elspot. The areas are separated by the Størebælt channel and until recently there was no physical connection between the areas. In November 2010 however a 500 MW HVDC link connected the two areas. Apart from this connection the Western area (DK-1) is connected to Germany, Norway and Sweden. The Eastern area (DK-2) is connected to Germany and Sweden.

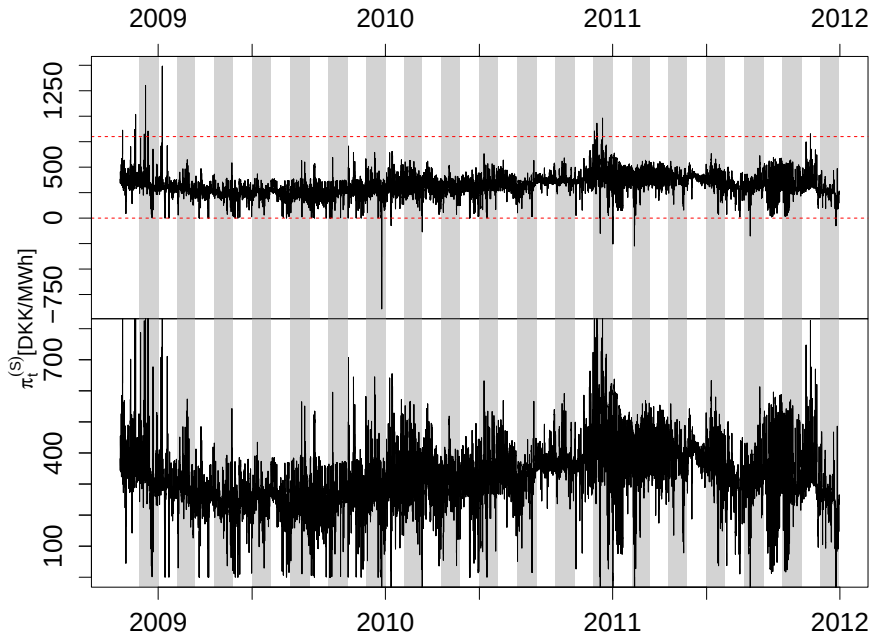

Figure 2.6: Time series plot of the spot prices in DK-1 from November 1st, 2008, until December 31st, 2011.

Model development is mainly done using data from DK-1 area and then extended to DK-2 when necessary. Thus, the data from DK-1 is used here to exemplify the main features of the prices. Observations similar to those listed here have been made for DK-2 though.

2.3.3 Spot Prices

Figure 2.6 presents time series plots of the spot prices in DK-1 for the period from November 1st, 2008, until December 31st, 2011. In order to better illustrate the average behaviour the prices are both plotted on a scale spanning their full range during the period and on a truncated scale.

Just like any other market in the world, the Elspot market was affected by the economic crisis in 2008. This resulted in a excessively volatile prices in the autumn of 2008. This period was followed by a one of relative tranquillity owing it, in part at least, to the decreasing fuel prices that fell dramatically on the world markets during this period. By the fall of 2009 the prices began to exhibit behaviour more similar to what was observed before the bank crisis in

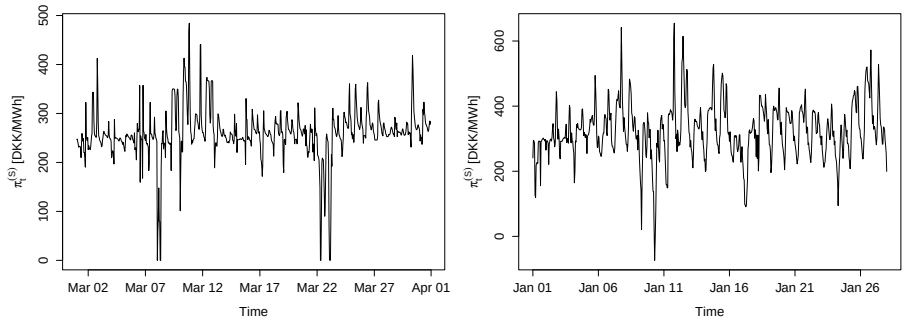

Figure 2.7: The spot prices in DK-1 during March 2009 (left) and January 2010 (right).

2008.

The prices seem to feature the characteristics commonly observed for such series like non-stationarity, heteroskedasticity and mean reverting spikes (Karakatsani and Bunn, 2008, Conejo et al., 2005, Panagiotelis and Smith, 2008, Kosater and Mosler, 2006). From Figure 2.7, which shows the time series for March 2009 and January 2010, daily and weekly seasonal patterns are also apparent. These seasonalities are mainly driven by the same feature of the load and how if affects the physical operation of the Nordic grid.

Whereas the intra-day and intra-week seasonal cycles of the prices are mainly explained by a single cause, variations in long-term behaviour are the accumulation of several things. For one, industrial demand for electricity goes hand in hand with the global and national economic development. Being a fair share in total demand, economic ups and downs will therefore impact the demand side of the electricity market substantially. On the other hand, operation costs for the various generation plants are highly dependent on fuel prices which are known to be quite volatile. In addition, the demand for electricity varies throughout the year, as well as the stock of hydro power. Thus, both the supply and demand have an annual seasonal cycle too. Being heavily weather dependent, this cycle intuitively seems less stable than the shorter ones. Determining that is however difficult due to the complexity of the long-term dynamics of electricity prices.

2.3.4 The Regulation Market

Table 2.1 lists the frequency of each imbalance sign during the period from November 1st, 2008, until December 31st, 2011. The regulation prices are quite

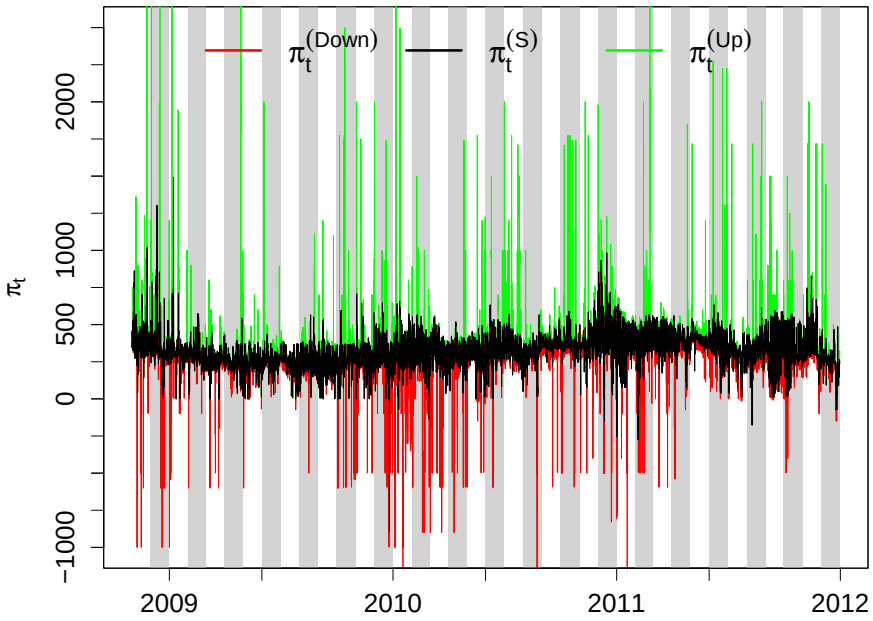

Figure 2.8: The spot-and regulation prices in DK-1 from November 1st, 2008, until December 31st, 2011.

often equal to the spot prices and, thus, share dynamics to considerable extent. During the hours where the prices differ however, the regulation prices have a more spikier behaviour. That is, excessive price spikes are both more frequent and more extensive than observed for the spot prices. This is shown in Figure 2.8 where the spot-and regulation prices are compared. Although the up-regulation prices up to 7447 DKK/MWh and down-regulation pries as low as -1700 DKK/MWh are observed during the period, the range of the y-axis is limited to -1000 and 2500 DKK/MWh in order to better illustrate the mean behaviour. This corresponds to that around 0.03% of each price series have a value beyond the scale of the plot.

These relatively frequent and excessive price spikes are mainly owed to the

Table 2.1: Frequency of imbalance signs from November 1st, 2008, until December 31st, 2011.

Direction:	$\downarrow$	$\sim$	$\uparrow$
Frequency [%]:	39.00	29.30	31.70

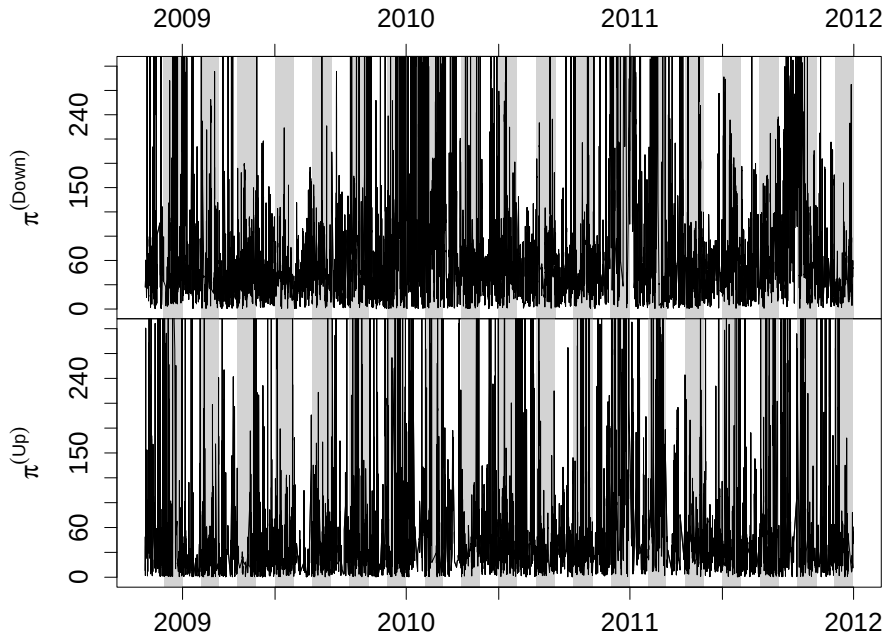

Figure 2.9: Time series plot of $\psi_t^{(\downarrow)}$ (top) and $\psi_t^{(\uparrow)}$ from November 1st 2008 until December 31st 2011. The plots y-axes are truncated at 300 DKK/MWh leaving 2% of the penalties outside the scale of the plot in each case.

limited supply of regulation services in both directions. During up-regulation hours, the supply is limited to the generation capacity that is not dispatched on the spot market and capable of delivering power within 15 minutes notice. For down-regulation, the supply curve comprises dispatched producers that are able to regulate their production within the same 15 minute notice. Compared to the supply function of Elspot, the short delivery notice and the physical limitations of the transmission grid yield a considerably steeper supply functions for regulating power. This high frequency of price spikes is naturally evident in the regulation penalties as well, which are plotted for the same period in Figure 2.9. Only penalties larger than 0 are plotted and the y-axes are truncated at 300 DKK/MWh in order to demonstrate the evolution of the average penalty during the period. The plots reveal that similar to the spot prices, the regulation penalties are non-stationary and heteroskedastic.

Due to its discrete definition, little information can be deducted from plotting the observations against time. However, there seems to be little reason to assume the probabilities of each imbalance sign to be stationary. Table 2.2 lists the

empirical frequencies of each imbalance scenario according to calendar years. Between the three full years of data, the frequency of both down-regulation hours and hours of no regulation penalties varies substantially. For these years, the share of up-regulation hours is more uniform. During the last two months of 2008 however, the frequency of up-regulation hours was much higher suggesting that the probabilities of up-regulation can vary within shorter periods.

In Paper H the varying probabilities of each state of $I_t^{(\psi)}$ are further demonstrated by using exponential smoothing. The exponentially smoothed averages of each state frequency are compared to identical tracking of a trinomial series, simulated using the period's empirical probabilities. For the sign probabilities being (close to) constant, their smoothed average should be similar to what is seen in the bottom panel of Figure 2.10. That is however far from being the reality as can be seen in the top panel of the same figure. The actual probabilities drift considerably more from their long-term averages.

Table 2.2: Frequency of imbalance signs by year.

	Sign Frequency [%]		
Period	$\downarrow$	$\sim$	$\uparrow$
2008	36.77	27.20	36.02
2009	42.00	26.97	31.03
2010	35.87	31.58	32.56
2011	39.49	29.71	30.80
2008-2011	39.00	29.30	31.70

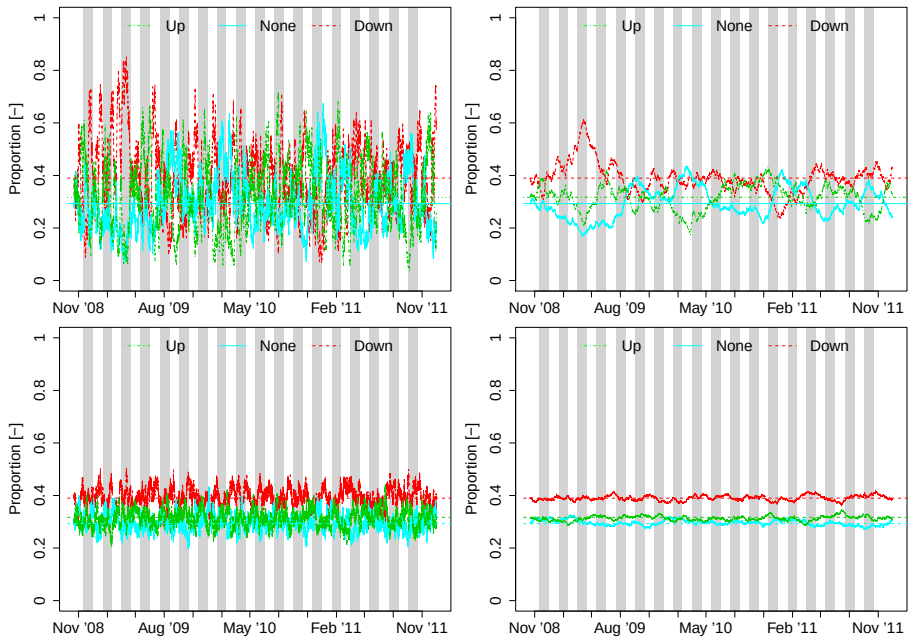

Figure 2.10: An exponential smoothed average of the observed $I_t^{(\psi)}$ sequence (top panel) and a simulated sequence (bottom panel) using $\lambda = 0.99$ (left panel) and $\lambda = 0.999$ (right panel).

CHAPTER 3

Wind Power and the Market

Another notable and recent development in the electricity sector is the rapid growth of generation by renewable sources. Fuelled by concerns for global warming and, to some degree, the desire to be less reliant on fuel imports from the Middle East, western countries have invested heavily in generation capacity of this sort. Among the recently emerged renewable sources for electricity generation, most of today's generation capacity is in wind turbines. Like other plants of its kind, generation capacity in the form of wind turbines is expensive per MW installed. Once installed however, they can produce energy at virtually no cost due to the absence of fuel expenses.

Both renewable energy generators in general and wind power producers in particular face the challenge of being non-dispatchable production. That is, since neither electricity nor the fuel for this type of generators is storable, the generation capacity varies constantly and is uncertain even for the very near future. Consequently, the power generated by these plants was in many cases managed centrally and outside the market through prioritisation schemes. With increasing share of renewables in the production portfolio however, producers are increasingly urged to sell their generation at the market.

By taking their production to the market, producers of wind energy become Balance Responsible Parties (BRPs). This entails that they have to settle deviations from their contracts on the real-time market and absorb the potentially associated cost. Being non-dispatchable the producers have to rely on

production forecasts for bidding on the market. Inevitably, such forecasts are not completely accurate, making it difficult to maintain balance between day-ahead contracts and realised production. This incites the wind power producer to seek other methods than precisely determining the volume for minimising imbalance costs.

In the general market perspective, the stochastic generation capacity of wind power turbines introduces new features to a supply curve that previously comprised conventional generators only. In addition, owing it to the non-existent marginal cost, the effect of these new features on the clearing price is quite strong.

In this chapter the interaction between the market and wind power producers is discussed from two perspectives. First the characteristics of a supply curve for a market penetrated by wind power are described along with the corresponding impact on the clearing prices. Further on, the bidding decision of a wind power producer in analysed.

3.1 Market Impact

An important first step in an analysis of the interaction between wind power production and any market is to determine how wind power should be represented. On the day-ahead market wind power is sold according to production forecasts, typically the expected production. Consequently, it is actually these forecasts that enter the supply curve and not the actual production. A collection of the production forecasts from individual producers are therefore the most appropriate form of wind power for inclusion in a day-ahead market analysis such as the one that follows. The wind power predictions used for the work of this thesis are an aggregation of 5 predictions each covering production in distinct parts of the DK-1 price area. These forecasts of course do not fully represent the expected production bid from all market participants in the area. Nonetheless, they share dependence on weather forecasts and thus provide a more accurate information on the amount of wind power that enters the supply curve than measurements.

The real-time prices are the result of, among other things, the difference between the bid wind power production and the realised one. Still assuming that the bids are well approximated by the forecast production, the expected value of this difference is 0 on a day-ahead basis. Then as time passes new information becomes available yielding a non-zero expected imbalance. Since the purpose of the real-time market analysis is solely to facilitate price forecasting on a day-ahead basis, it is limited to the information available at the forecasting

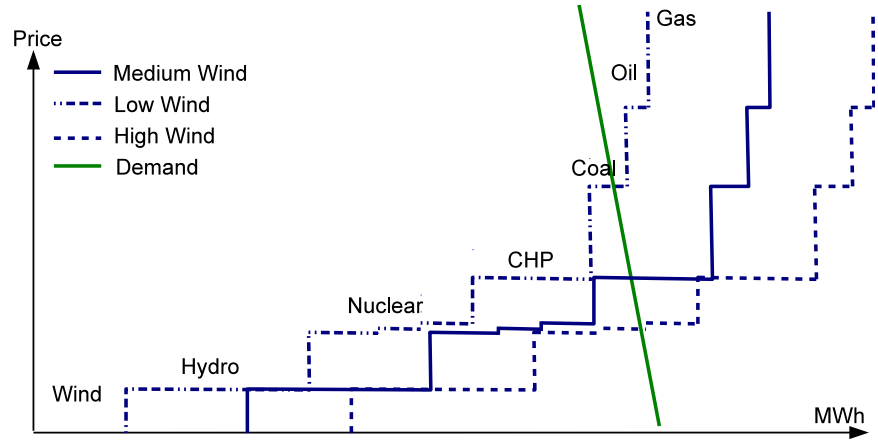

Figure 3.1: Electricity supply curve under different levels of expected wind power production.

time or the expected production.

3.1.1 Wind Power at the Spot Market

How the presence of wind power affects market clearing prices is the subject of Papers A & B. Its low marginal cost places wind power among the producers who receive the highest priority in the dispatching order. This, along with the stochastic availability, causes wind power to appear as a stochastic threshold in the supply function (Giabardo et al., 2010). This is illustrated in Figure 3.1 where a fictive example of a supply curve for the Nordic region is plotted under three different levels of expected (bid) wind production. The figure shows how wind power horizontally shifts the entire supply curve through its position on the very left of it.

How much the clearing prices are affected by this shift is determined by the shape of the remainder of the supply curve. Because of how steeply increasing the supply curve generally is at the high volume end and how inelastic the demand is, small shifts in the supply can cause huge differences in price. This results in a stronger relationship between wind power and prices during high consumption hours. This also means that two power systems similarly penetrated by wind power do not necessarily have to experience the impact on the prices to be equally extensive since it also depends on the steepness of the rest of the supply curve.

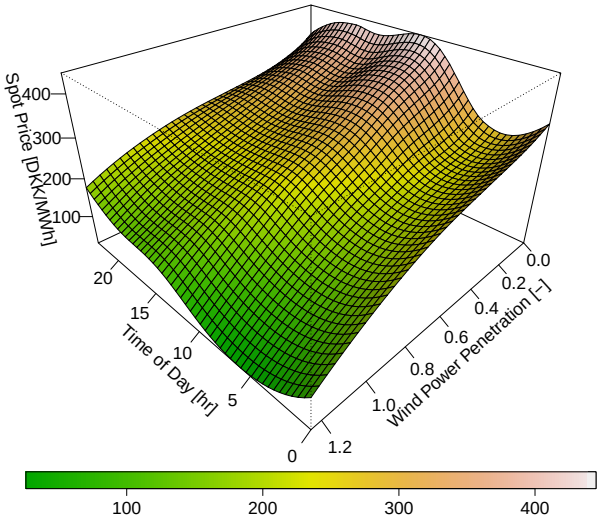

Figure 3.2: Average area spot price in DK-1 as a function of forecast wind power penetration and time of day.

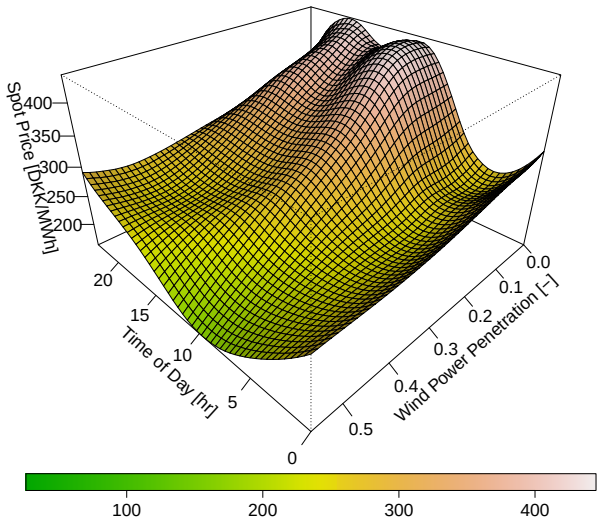

Figure 3.3: Average area spot price in DK-2 as a function of forecast wind power penetration and time of day.

This can be seen by comparing Figures 3.2 & 3.3 where the average spot price is plotted against the forecast hourly wind power penetration and the hour of the day for the two Danish price areas. These plots are presented in Paper B and are based on data for the period November 1st, 2008, until January 31st, 2010. In DK-1 around 25% of the annual consumption is generated by wind turbines. In the DK-2 on the other hand, wind power's share in the yearly demand is roughly half of that. So certainly DK-1 experiences higher wind power penetration and thus lower prices. For the range of wind power penetration shared by the two plots however, the impact is stronger in DK-2. That is, although the same type of impact is detected for both areas the prices in DK-2 are more affected by the same penetration level. This feature is illustrated further in Figure 3.4. The figure shows the average spot prices in the two areas as a function of the hourly forecast wind power penetration during the daytime hours (07:00 - 19:00) and the evening and night hours (19:00 - 07:00) separately. From there it is clear that the prices in DK-2 decline faster with increased wind power penetration than they do in DK-1 during the daytime hours. A potential explanation for this effect is the more direct access to inexpensive hydro power DK-1 has through its interconnection with Norway which yields a less steep supply curve.

Although it might be trivial to some readers, it is important to realise that it is the installed wind power capacity that determines its potential to impact the supply and thereby the prices. Meanwhile, it is the actual available capacity at each time that determines how much of this potential is realised. This is important because the annual generation of a wind turbine is only a fraction of its nominal capacity. Its ability to affect the prices is therefore much greater than that of a dispatchable generator with the same marginal costs and the same annual generation. More precisely, increasing the share of wind power in the annual generation by a single percent yields an elevated potential shift of the supply curve by one over the capacity factor of the newly installed turbines. Then, when capacity is dispersed over a relatively small area (e.g. Denmark), temporal correlation in production will cause this potential to be realised. Without harmonised growth in export potentials and wind power capacity, prices will increasingly exhibit regime switching and weather dependent behaviour as argued by Meibom (2007).

3.1.2 The Real-Time Market

The interaction between the regulation prices and wind power is more complex than for the spot prices since it affects both the supply and the demand side of the market. The regulation prices are the result of deviations from production and consumption schedules and how they are counterbalanced. Since

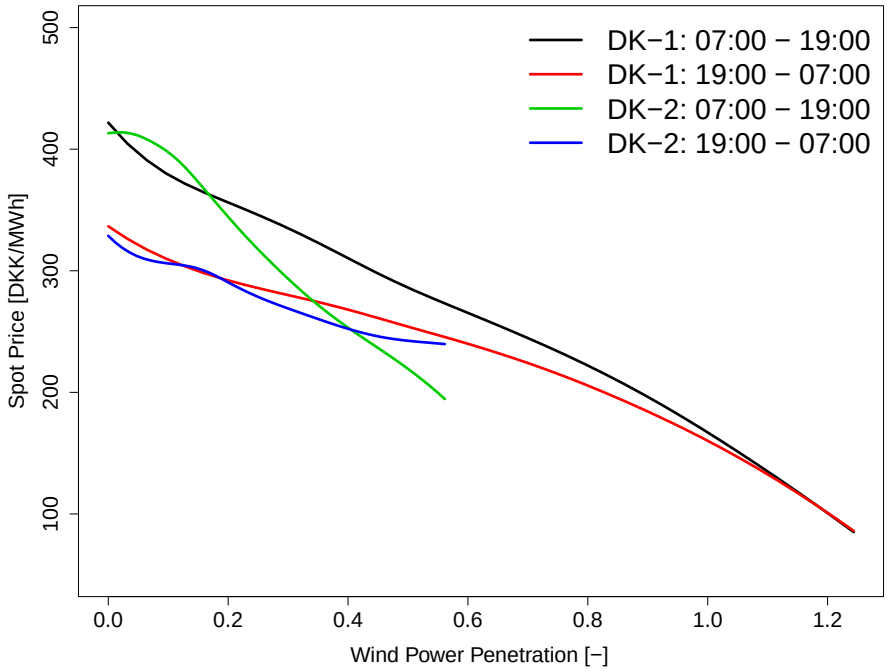

Figure 3.4: Electricity supply curve under different levels of expected wind power production.

the wind power production is subject to considerable uncertainty at the time of market clearing, deviations from the schedule are inevitable. These deviations then become demand for regulating power. Assuming all producers to bid their expected production, found by a well tuned model independent of other producer's model, these deviations should negate each other to a large extent with a sufficient number of producers. Given the limited number of weather forecast suppliers (which provide an essential input for the production forecasts) however, assuming the deviations to completely negate each other is in all likelihood unrealistic. Thus, one would expect the presence of wind power to impact the demand for regulating power. Other factors, also supporting this hypothesis are the limited number of producers and forecast service providers and that wind power forecasts are generally known to have a mean-dependent and asymmetric distribution (Lange, 2005). On the contrary, the shift in the supply curve and the inelastic load prompt many producers not to be scheduled for production during hours of high wind power production. Some of these producers have highly flexible generation plants which then are able to provide regulating services at a lower price than would be possible if they were dispatched on the spot market. In summary; both sides of the real-time auction

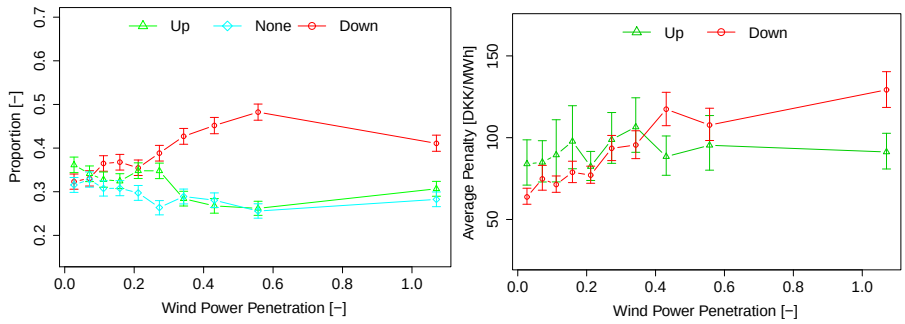

Figure 3.5: Average frequency of each imbalance sign (left) and average imbalance penalty (right) plotted against forecast wind power penetration.

are affected by the presence of wind power in the system.

As discussed in more detail in Papers B & H, a time-invariant analysis indicates a significant relation between the forecast hourly wind power penetration and some real-time market variables. More precisely, wind power penetration seems to affect both $I_t^{(\psi)}$ and $\psi_t^{(\downarrow)}$ while the impact on $\psi_t^{(\uparrow)}$ seem insignificant. This is illustrated in Figure 3.5 where, to the left, the average frequency of each imbalance sign is plotted against the forecast wind power penetration in the left plot. To the right the average regulation penalties are plotted against the same penetration forecasts. In both cases the plots are constructed by segmenting the data into 10 equally populated bins according to the penetration level and calculating the corresponding average.

Despite that the left plot in Figure 3.5 indicates a significant impact of the forecast wind power penetration on $I_t^{(\psi)}$, its inclusion in a model for the imbalance sign yields no improvement in forecasting skill. The effect observed in the plot is therefore most likely a result of coinciding seasonal pattern(s) and long-term variation in dynamics.

3.2 Market Participation

Just like any other commodity producer, a wind power producer's main interest is to maximise the financial yield of his investment. In general, profit measures for companies and investments have a time-resolution varying from several months to years. These measures are the milestones towards the ultimate goal of earning back the initial investment plus an acceptable profit mar-

gin. In the meantime, the investor manages the risk he is exposed to by entering into financial contracts which reduce both his potential earnings and losses and thereby stabilise the cash flow within the contract period. How much stabilising effect is obtained depends on the ratio between actual production and the hedged volume.

The pricing of these contracts is usually done based on long-term average of the prices and is not addressed in this thesis. In light of the results presented in the previous section, generator companies mostly or solely relying on wind power should take caution when entering such contracts. Since there is a negative dependency between the prices and the wind power production, a fixed volume contract will not cover the full production during hours when the contract generates positive cash flow. On the other hand, the same contract is likely to encompass more than the generated volume when the contract generates negative cash flow for the producer.

Even though stability has been ensured to a certain degree with financial derivatives, the revenues from the production are still paramount to most if not all generator companies. As earlier said, it is the quarterly and annual revenues that are of interest for the company's stakeholders. Hence, the ones responsible for the operation aim to maximise these revenues. On a non-leap year, the operator's objective is therefore to maximise the sum of 8760 hourly revenues in 365 decisions. At each decision time, limited information is available for the future which is all in the form of forecasts. A generator with dispatchable production unit is able to utilise these forecasts to arbitrage in time through minimisation of opportunity costs for different hours. For these producers, the long-term revenue optimisation is a matter of a sequence of interdependent decisions.

Since neither the fuel nor the final product can be stored, inter-hour opportunity cost optimisation for wind power producers is trivially solved. With no possibility for arbitrage, optimising long-term revenues directly corresponds to optimising the individual hourly revenues separately.

For a mathematical formalisation, let $\boldsymbol{R}$ denote the yearly revenue of a power producer during a year starting at time $t = 1$, generating electricity by wind turbines only. Furthermore let $\widetilde{W}_t$ be the amount of wind power bid/sold on the spot market in hour t and let $\rho_t(\widetilde{W}_t)$ be the corresponding hourly revenue so that

$$\boldsymbol{R} = \sum_{t=1}^{8760} \rho_t(\widetilde{W}_t). \tag{3.1}$$

Then the absence of arbitrage possibilities entails that at any decision time s, $s \in \{-12, 12, \ldots, 8724\}$ the bid $\widetilde{W}_t$ for hour t, occurring on the upcoming day, that

optimises the expected annual revenue is the one that maximises the expected revenue of hour t:

$$\widetilde{W}_t^* = \arg\max_{\widetilde{W}_t} \mathbb{E}[\boldsymbol{R}|\chi_s] = \arg\max_{\widetilde{W}_t} \mathbb{E}[\rho_t(\widetilde{W}_t)|\chi_s] \tag{3.2}$$

where χ_s is the information available at time s.

3.2.1 Expected Revenue Maximisation

Assuming that a wind power producer is not active in the Elbas market, its hourly revenue can be written as

$$\rho_t(\widetilde{W}_t) = \pi_t^{(S)} \widetilde{W}_t + C_t^{(\uparrow/\downarrow)} \tag{3.3}$$

where

$$C_t^{(\uparrow/\downarrow)} = \psi_t^{(\downarrow)} \max\{W_t - \widetilde{W}_t, 0\} + \psi_t^{(\uparrow)} \min\{W_t - \widetilde{W}_t, 0\} \tag{3.4}$$

is the hourly cost of imbalances or the cost of settling the difference between the submitted bid and the actual production, W_t.

In Paper D, Nord Pool's market design is shown to prompt that for a producer of wind power, who is a price taker, assuming the producer to maximising expected hourly revenues equivalent to minimising the expected hourly cost of imbalances. This yields the optimal bid to be found as

$$\widetilde{W}_t^* = F_{W_t}^{-1}\left(\frac{\mathbb{E}[\psi_t^{(\downarrow)}|\chi_s]}{\mathbb{E}[\psi_t^{(\downarrow)}|\chi_s] + \mathbb{E}[\psi_t^{(\uparrow)}|\chi_s]}\right) \tag{3.5}$$

where $F_{W_t}(\cdot)$ is the cumulative density function (CDF) of the wind power production during hour t.

Being an expectation optimisation, the bid found by Eq. (3.5) is completely risk neutral. This yields an optimal bid that is either close to 0 or nominal capacity when $\mathbb{E}[\psi_t^{(\uparrow)}|\chi_s] >> \mathbb{E}[\psi_t^{(\downarrow)}|\chi_s]$ or vice versa. In practise however, such bidding behaviour is frowned upon by the TSO which requires bids that reflect the expected production for their scheduling. This issue is addressed in paper D by constraining the bid such that it does not deviate more than a certain percentage from the expected production. A side effect of this constraining is reduced revenue risk through the smaller probability of large differences between bid and actual production.

The assumption of the producer being a price taker is necessary for the bid in Eq. (3.5) to be optimal. Being a price taker entails that the producer does not

affect the clearing price with its actions - neither the spot price nor the regulation prices. Although this might at first sight seem contradicting to the results presented in the previous section, it is not necessarily the case. The impact of wind power forecasts on the market demonstrated previously is the result of considering all wind power producers in the system collectively. Thus, the wind power production considered there comprises that of multiple individual generators of different capacity. Should the majority of the wind power producers maintain the policy of bidding their expected production to the market, a relatively small producer could deviate from that bid without affecting the price. If however the majority of producers were to adopt this strategy the price taker assumption might become problematic. Similarly if a single large producer was to do the same this assumption is presumably unrealistic. What the effect on the prices would be is hard to anticipate and impossible to analyse. Given the relatively small deviation band around the expected production that is likely to be accepted by the TSO, this impact might not be severe.

The risk, in terms of revenue, is not addressed explicitly in paper D though. The potential of a large loss during an hour of relatively small deviation from contracted volume, which is penalised extraordinary hard, remains unaccounted for. Even though such events did not occur in the 10 month long case study presented in the paper, the fact that the regulation prices are capped at 37500 DKK / MWh ($\approx$ 5000€ / MWh) (Energinet.dk, 2008) and suggest that such considerations might be relevant.

3.2.2 Risk Averse Bidding

In paper E a formulation of the optimal bidding problem with risk aversion is derived and discussed. Similar to Morales et al. (2010), risk is measured as Conditional Value-at-Risk (CVaR) (Rockafellar and Uryasev, 2000, 2002, Schultz and Tiedemann, 2006) and thus the objective function becomes

$$\widetilde{W}_t^* = \arg\max_{\widetilde{W}_t} \mathbb{E}[X_t] + \lambda \mathrm{CVaR}_\alpha[X_t] \tag{3.6}$$

where X_t can either be the hourly revenue ρ_t or the hourly (non-positive) imbalance costs $C_t^{(\uparrow/\downarrow)}$. Attitude towards risk is parameterised by λ, $0 \leq \lambda \leq 1$ and increases with higher risk-aversion. The CVaR at the α level is found as

$$\mathrm{CVaR}_\alpha(X) = \eta_\alpha - \frac{1}{\alpha}\mathbb{E}[\max\{(\eta_\alpha - X), 0\}] \tag{3.7}$$

where $\eta_\alpha = F_X^{-1}(\alpha)$ or the α-Value-at-Risk (VaR_α).

The inclusion of the CVaR-term prompts that optimisation in terms of $C_t^{(\uparrow/\downarrow)}$ and ρ_t no longer yields the same bid. This is because up- and down-regulation costs are generally more likely to be equally represented in the $(\alpha \cdot 100)\%$ least favorable imbalance costs than in the worst case revenues for a given hour. In context of the hourly revenue, being subject to up-regulation always reduces ρ_t (since involves purchase of energy). Being subject to down-regulation on the other hand increases the revenue as long as the down regulation price remains positive. Therefore, production surpluses will be increasingly favoured with higher λ and with ρ_t as an objective value. Alternatively with $C_t^{(\uparrow/\downarrow)}$ as an objective variable, deviations of equal magnitude and penalty have the same effect regardless of direction. Thus an increased weight on $\mathrm{CVaR}\left[C_t^{(\uparrow/\downarrow)}\right]$ will cause the bid to approach the expected production for the hour. The asymmetric imbalance cost expectation and the existing probability of negative down-regulation prices will prevent the bids from being exactly 0 or the expected production though, even if only the CVaR-term would be optimised. Consequently, λ can be chosen such that the imbalance cost optimisation trivially fulfils the TSO's requirement of bids reflecting expected production.

The choice between the two objective variables of the mean-CVaR strategy is in the end a matter of preference. Optimisation in terms of ρ_t can be regarded as the more conservative approach of the two since its CVaR term aims at minimising the probability of negative revenue at all times. With $C_t^{(\uparrow/\downarrow)}$ as an objective variable on the other hand the goal is only to minimise the deviation from the highest possible income. Therefore, if the producer has already entered financial contracts to stabilise his long-term risk, $C_t^{(\uparrow/\downarrow)}$ is a more appropriate choice. With no involvement in the financial market and with a generation portfolio solely consisting of wind turbines, choosing ρ_t as an objective might become an attractive choice. Although one has to bear in mind that the sub-additive property of CVaR prevents any goals for long-term revenue / risk from being set through the adaptation of this strategy. That is since the properties of the CVaR imply that

$$\mathrm{CVaR}\left[\sum_{i=1}^{N} X_i\right] \leq \sum_{i=1}^{N} \mathrm{CVaR}\left[X_i\right] \tag{3.8}$$

then

$$\mathrm{CVaR}[\boldsymbol{R}] \leq \sum_{t=1}^{8760} \mathrm{CVaR}\left[\rho_t(\widetilde{W}_t)\right]. \tag{3.9}$$

Thus there is not a direct linkage between hourly risk attitude and the actual long-term revenue risk.

3.2.3 Bidding of a Price Maker

In paper E it is suggested that for a single large producer the price taker assumption could be abandoned by discretising the decision space and subsequently solve a maxmax problem using decision dependent scenarios or scenario probabilities. The maxmax problem can be written as

$$\begin{aligned} \widetilde{W}_t^* &= \arg\max_{w \in \mathcal{W}} C^w(w;\alpha,\lambda) \\ C^w(w;\alpha,\lambda) &= \max \mathbb{E}\left[X_t|\mathcal{S}^w\right] + \lambda \mathrm{CVaR}_\alpha\left[X_t|\mathcal{S}^w\right] \end{aligned} \tag{3.10}$$

where $\mathcal{S}^w$ is a set of wind production-market scenarios that are valid for a certain range of $\widetilde{W}_t$.

Solving the problem given by Eq. 3.10 requires quite elaborate scenario generation framework which has to account for the interdependence between the producer's bidding and the market outcome and eventually the cleared load as well. In addition solving the problem is quite expensive computationally but is possible to parallelise. Although no empirical work was done on this problem, some thoughts on the scenario generation framework are presented in paper E.

CHAPTER 4

Market Forecasts

If the bidding strategies discussed in the previous chapter are to be adopted in practise, forecasts for wind power production and the market prices are required. Predictive densities for wind power production are necessary for all strategies along with expected values for constraining. The optimal quantile strategy also calls for expected imbalance penalties while adding the CVaR term calls for probabilistic price forecasts as well for scenario generation. In that context, optimisation in terms of the imbalance costs requires density forecasts of the regulation penalty. Choosing the revenue as an objective value requires probabilistic forecasts of the spot price as well.

Here the focus is on the price forecasts only. Wind power production forecast stemming from WPPT[1] have been made available for the case studies of the bidding strategies. A description of the ideas behind the models for the point forecasts and the probabilistic ones can be found in Nielsen et al. (2002) and Møller et al. (2008), respectively.

Given the intended application, the forecasts from the market models developed need to be available before gate-closure of the spot market. Thus, all search for explanatory variables is limited to information available before noon on the day before delivery. Correspondingly, all the forecasts analysed are based on information that is available at 11:00 am on the day prior to realisation. The forecasts are issued for all hours of the upcoming day and then

[1] The Wind Power Prediction Tool, see www.enfor.dk for further information

no predictions are made until 11:00 am the following day when the forecasting procedure is repeated. This implies that forecasts for each hour of the day have a distinct lead-time while it is identical for the same period of different days. That is, forecasts for the first hour of the day always have a lead-time of 13 hours while it is 14 hours at all times for the second hour of the day and so forth. For the spot market future information about the prices is available though and used. This prediction scheme is referred to as day-ahead forecasts in the remainder of this chapter and in the papers that address the forecasts.

A detailed description of the models developed is given in Papers F - H. In the following a brief summary and discussion of these models and the data used for their development is given.

4.1 Forecasts of the Spot Price

For the spot prices a model that describes their average behaviour was constructed as well as a one for their density. In addition to be required for some of the bidding strategies, the spot price forecasts provide important input to models for subsequent markets. On a more general note, accurate spot price forecasts are vital for many of the decisions many electricity producers and system operators have to be make.

4.1.1 Point Forecasts

Paper F describes a two-step model for the expected spot price on a day-ahead basis. In the first step, the spot price for hour t, $\pi_t^{(S)}$, is estimated as a function of the forecast load ($\widehat{L}_t$) and wind power production ($\widehat{W}_t$) for the same hour or

$$\pi_t^{(S)} = f(\widehat{L}_t, \widehat{W}_t) + \varepsilon_t \tag{4.1}$$

where $f(\cdot)$ is approximated by second order polynomials estimated at 24^2 distinct predetermined fitting points and ε_t is an error term with finite variance. Estimation of the polynomials' parameters is done by locally weighted regression (Cleveland and Devlin, 1988) where weights are assigned by a tri-cube kernel. Moreover, the parameters estimation is done recursively with an exponential forgetting factor, as shown in Nielsen et al. (2000), and robustified by applying the Huber influence function (Huber, 1981). Once the estimation is completed each day an intermediate forecast for next day's spot prices, $\widetilde{\pi}_t^{(S)}$, is found by bi-linear interpolation between the fitting points surrounding the actual values of $\widehat{L}_t$ and $\widehat{W}_t$.

The prediction error arising from $\widetilde{\pi}_t^{(S)}$:

$$\varepsilon_t = \pi_t^{(S)} - \widetilde{\pi}_t^{(S)}. \tag{4.2}$$

remains auto-correlated. Also some seasonal patterns persist despite the main source of seasonalities, the load, has been accounted for. The source of these features are multiple. Besides the obvious reason of the model being a statistical one, they are partly caused by the difference between the forecasts for the area's total load and wind power production and the actual bid. Also other factors such as pricing of hydro power, heating demand and interconnection capacity play an important role.

The second step is meant to account for the dynamics of ε_t. For this purpose, models from two different model classes were tried out which yielded two close to equally performing models. One is a double seasonal AR model of order with daily and weekly seasonal cycles. The regression parameters are estimated recursively with exponential forgetting (see e.g. Madsen, 2008, Ch. 11) and under a robust criteria (Huber, 1981). Furthermore, separate regression parameters are found for each lead-time, k. The model can be written as

$$\varepsilon_{t+k} = \boldsymbol{z}_t^T(k)\boldsymbol{\beta}_t(k) + \nu_{t+k} \tag{4.3}$$

where ν_t is a new noise term, centred and with finite variance and

$$\boldsymbol{z}_t(k) = [\ 1,\ \varepsilon_{t-1},\ \varepsilon_{t-2},\ \varepsilon_{t+k-24},\ \varepsilon_{t+k-48},\ \varepsilon_{t+k-168}]^T \tag{4.4}$$

$$\boldsymbol{\beta}_t(k) = [\ \beta_{0,t,k},\ \beta_{1,t,k},\ \ldots,\ \beta_{6,t,k}]^T. \tag{4.5}$$

The second model for ε_t is an additive seasonal Holt-Winters model (Winters, 1960, Taylor, 2003, Hyndman et al., 2008). Unlike the AR model, this one only includes a daily seasonal term. Similar to the AR model however, updating is done under a robust criteria following Gelper et al. (2010):

$$\widehat{\varepsilon}_{t+k|t} = \mu_t + D_{t+k-24} \tag{4.6}$$

where

$$\mu_t = \mu_{t-1} + \alpha_\mu g(\nu_t, \tau) \tag{4.7}$$

$$D_t = D_{t-24} + \alpha_D g(\nu_t, \tau). \tag{4.8}$$

The function $g(\cdot,\cdot)$ is the Huber influence function (Huber, 1981) and τ is its cutoff value.

Whereas the AR model performs marginally better than the Holt-Winters model, the latter has the appeal that it is less affected by missing data since only the

model update prevented and not the prediction as in the AR model's case. This makes the choice between them for practical implementation mostly a matter of preference.

After updating of and forecasting by the two models, the expected spot price is found as

$$\widehat{\pi}_t^{(S)} = \widetilde{\pi}_t^{(S)} + \widehat{\varepsilon}_t \tag{4.9}$$

4.1.2 Density Forecasts

A model that generates predictive densities for the spot prices is presented in paper G. The model depicts the density of v_t as defined by Eq. 4.3 in the previous section with the expected spot price and the forecast load as explanatory variables. Between the 5% and the 95% quantiles, the density is described by a series of Quantile Regression (QR) models (Koenker and Basset, 1978, Koenker, 2005) using the time-adaptive QR framework presented by Møller et al. (2008). This model is subsequently combined with a model for the distribution tails where they are assumed to be exponentially distributed. The rate parameter of each exponential distribution is updated every time a new observation becomes available without discounting of older observations.

The QR model has the same form for all quantiles τ:

$$Q_{v_t,t}(\tau) = F^{-1}_{v_t,t}(\tau) = \sum_{i=1}^{K} b_i(\widehat{\pi}_t^{(S)})\beta_{i,t}(\tau) + \widehat{L}_t\gamma_t(\tau) + e_t. \tag{4.10}$$

where $F^{-1}_{v_t,t}(\cdot)$ is the inverse CDF of v_t and b_i are natural cubic B-spline basis functions with no interception term. Furthermore, K is the number of knots used for the spline fitting, $\beta_{i,t}(\tau)$ and $\gamma_t(\tau)$ are regression parameters specific to each τ and e_t is an error term, centred and with finite variance.

Two new variables, one for each tail, are defined for modelling the tail:

$$\begin{aligned} z_t^{(l)} &= \max\{\widehat{Q}_{v_t,t}(0.05) - v_t, 0\} \\ z_t^{(u)} &= \max\{v_t - \widehat{Q}_{v_t,t}(0.95), 0\}. \end{aligned} \tag{4.11}$$

Both variable are assumed to be exponentially distributed,

$$\begin{aligned} z_t^{(l)} &\sim Exp(\lambda_t^{(l)}) \\ z_t^{(u)} &\sim Exp(\lambda_t^{(u)}) \end{aligned} \tag{4.12}$$

with rate parameters $\lambda_t^{(l)}$ and $\lambda_t^{(u)}$ for which a maximum likelihood estimate is obtained based on all previous observations of $z_t^{(l)}$ and $z_t^{(u)}$.

4.2 Prediction in the Regulation Market

Prompted by the derivation of the bidding strategy in Paper D, a description of the regulation market in terms of the imbalance penalties is sought. Two models that combined describe the expected imbalance penalty are derived. Although some steps towards a probabilistic description of the penalties were taken in Paper E, a thoroughly tested model was not derived. Paper H describes the models used for estimating the expected imbalance penalties which are used for providing inputs to the bidding strategy presented in Paper D.

Using the variable definitions from Section 2.3 and by applying the law of total expectation, the expected imbalance penalties can be written as

$$\mathbb{E}\left[\psi_t^{(\uparrow)}|\chi_s\right] = \mathbb{P}\left[I_t^{(\psi)} = 1|\chi_s\right] \cdot \mathbb{E}\left[\psi_t^{(\uparrow)}|\psi_t^{(\uparrow)} > 0, \chi_s\right] \tag{4.13}$$

$$\mathbb{E}\left[\psi_t^{(\downarrow)}|\chi_s\right] = \mathbb{P}\left[I_t^{(\psi)} = -1|\chi_s\right] \cdot \mathbb{E}\left[\psi_t^{(\downarrow)}|\psi_t^{(\downarrow)} > 0, \chi_s\right] \tag{4.14}$$

This allows for the problem to be partitioned into estimation of the probabilities of regulation in each direction, hereafter termed the imbalance sign, and forecasting of the penalties conditioned on they being different from zero.

The aim of dividing the problem up like this is to accommodate the regime switching behaviour of the regulation penalties. This can be especially useful when the use of external explanatory variables is considered since certain circumstances could for instance otherwise result in either a zero penalty or extremely high penalty and, thus, mitigating the observed effect of that variable. For applications where only the expected penalty is required on the other hand, estimating a model on the full series (including the zeros) could perform similarly if no helpful explanatory variables are found.

4.2.1 The Imbalance Sign

The pricing scheme of the regulation market makes deliberate imbalances irrational. Thus it is fair to assume that demand for regulative power mainly arises from unforeseen events (e.g. plant or grid malfunctions) and the forecasting error for load and wind power production. The latter stems from models which are commonly tuned to have to have prediction errors symmetric and centred at zero. Models of processes with constantly varying dynamics are however bound to forecasts that in the short term are biased. In some ways the model for the imbalance sign tracks theses biases, along with other short-term inconsistencies in planning, and translates them into probabilities for regulation in each direction.

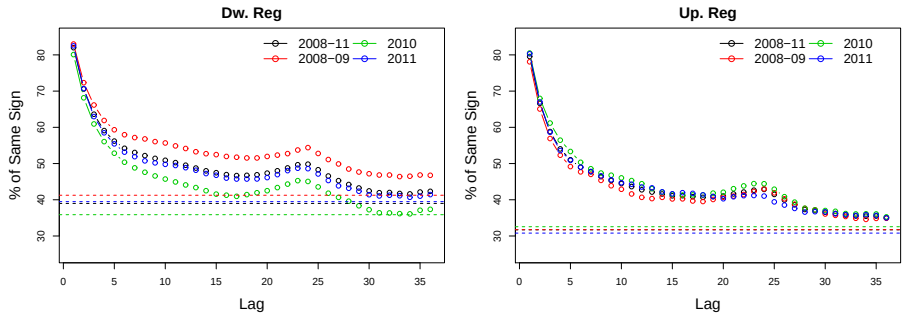

Figure 4.1: The proportion of lagged hours sharing imbalance sign with the current one is plotted for down- and up-regulation (left and right respectively)

What mainly impacts the imbalance sign is thus events taking place after the spot market is cleared. This prompts that variables with significant explanatory power are not available and correlation between day-ahead lags is small. The latter is demonstrated in Figure 4.1, where the proportion of lagged hours sharing imbalance sign with the current one is plotted for up- and down-regulation. Put mathematically the figure shows

$$\frac{1}{N}\sum_{t=1}^{N}\mathbf{1}(I_t^{(\psi)} = I_{t-k}^{(\psi)}), \quad k = 1,\ldots,37. \tag{4.15}$$

Results are shown for each year of the data period individually and combined for the whole period. Whereas the persistence between adjacent hours is quite high, the proportions decline rather quickly and become close to the overall probabilities on the day-ahead lags.

A Holt-Winters model with a daily seasonal cycle is used to estimate the probabilities of each state of $I_t^{(\psi)}$. By defining

$$\begin{aligned} \boldsymbol{I}_t^{(\uparrow/\downarrow)} &= \left[\; I_{t,1}^{(\uparrow/\downarrow)}, \quad I_{t,2}^{(\uparrow/\downarrow)}, \quad I_{t,3}^{(\uparrow/\downarrow)} \;\right] \\ &= \left[\; \mathbf{1}\{\pi_t^{(\downarrow)} < \pi_t^{(S)}\}, \quad \mathbf{1}\{\pi_t^{(S)} = \pi_t^{(\downarrow)} = \pi_t^{(\uparrow)}\} \quad \mathbf{1}\{\pi_t^{(\uparrow)} > \pi_t^{(S)}\} \;\right] \end{aligned} \tag{4.16}$$

for which it holds that

$$\sum_{i=1}^{3} I_{i,t}^{(\uparrow/\downarrow)} = 1,$$

the model's prediction equation is defined as

$$\widehat{\boldsymbol{I}}_{t+k|t}^{(\uparrow/\downarrow)} = \mu_t + D_{t+k-24} \tag{4.17}$$

where

$$\mu_t = \mu_{t-1} + \alpha_\mu e_t \tag{4.18}$$
$$D_t = D_{t-24} + \alpha_D e_t \tag{4.19}$$
$$\tag{4.20}$$

where in turn

$$e_t = \boldsymbol{I}_t^{(\uparrow/\downarrow)} - \boldsymbol{I}_{t|t-1}^{(\uparrow/\downarrow)}. \tag{4.21}$$

The smoothing parameters are estimated by maximum likelihood estimation and proper state probabilities are obtained by the inverse logit transformation or

$$\begin{aligned}
\widehat{\mathbb{P}}_{t+k|t}\left(I_{t+k}^{(\psi)} = -1\right) &= \widehat{\mathbb{P}}_{t+k|t}\left(I_{t+k,1}^{(\uparrow/\downarrow)} = 1\right) = \frac{\exp\left(\widehat{I}_{t+k|t,1}^{(\uparrow/\downarrow)}\right)}{1+\exp\left(\sum_{i\in\{1,3\}}\widehat{I}_{t+k|t,i}^{(\uparrow/\downarrow)}\right)} \\
\widehat{\mathbb{P}}_{t+k|t}\left(I_{t+k}^{(\psi)} = 1\right) &= \widehat{\mathbb{P}}_{t+k|t}\left(I_{t+k,3}^{(\uparrow/\downarrow)} = 1\right) = \frac{\exp\left(\widehat{I}_{t+k|t,3}^{(\uparrow/\downarrow)}\right)}{1+\exp\left(\sum_{i\in\{1,3\}}\widehat{I}_{t+k|t,i}^{(\uparrow/\downarrow)}\right)} \\
\widehat{\mathbb{P}}_{t+k|t}\left(I_{t+k}^{(\psi)} = 0\right) &= \widehat{\mathbb{P}}_{t+k|t}\left(I_{t+k,2}^{(\uparrow/\downarrow)} = 1\right) = \frac{1}{1+\exp\left(\sum_{i\in\{1,3\}}\widehat{I}_{t,i}^{(\psi)}\right)} \\
&= 1 - \left(\widehat{\mathbb{P}}\left(I_{t+k}^{(\psi)} = -1\right) + \widehat{\mathbb{P}}\left(I_{t+k}^{(\psi)} = 1\right)\right).
\end{aligned} \tag{4.22}$$

A more detailed description of the estimation process is given in Paper H.

4.2.2 The Imbalance Penalty

The models for the penalties are focused exclusively on observations when the penalties are actually realised. The models are therefore conditioned on the penalties being different from zero. Thus let

$$\begin{aligned}
\widehat{\psi}_{t|>0}^{(\downarrow)} &= \mathbb{E}\left[\psi_t^{(\downarrow)} | \psi_t^{(\downarrow)} > 0, \chi_s\right] \\
\widehat{\psi}_{t|>0}^{(\uparrow)} &= \mathbb{E}\left[\psi_t^{(\uparrow)} | \psi_t^{(\uparrow)} > 0, \chi_s\right]
\end{aligned} \tag{4.23}$$

and let $\psi_{t|>0}^{(\downarrow)}$ and $\psi_{t|>0}^{(\uparrow)}$ be the corresponding observations, defined as

$$\begin{aligned}
\psi_{t|>0}^{(\downarrow)} &= \begin{cases} \psi_t^{(\downarrow)} & \text{if } I_t^{(\psi)} = -1 \\ \text{Undefined} & \text{Otherwise} \end{cases} \\
\psi_{t|>0}^{(\uparrow)} &= \begin{cases} \psi_t^{(\uparrow)} & \text{if } I_t^{(\psi)} = 1 \\ \text{Undefined} & \text{Otherwise} \end{cases}
\end{aligned} \tag{4.24}$$

In paper H, the regulation penalty series are shown to have a diurnal seasonal cycle and also to include frequent spikes, some of the quite extreme. The severity of some of these spikes makes that estimation on the whole data set would yield parameters that solely focus on the residuals from these observations. Removing some of them is therefore necessary to obtain a description of the expected penalty. On the other hand, these spikes are a reality of the market and thus it is desirable to have them represented in the estimation set to some extent. Therefore in an effort to systematise the discarding of observations, the following procedure for removal of observations was adopted:

- Fit a robust RLS models on the form

$$\begin{aligned}\widehat{\psi}^{(\uparrow/\downarrow)}_{t+k|t} =& \phi_{0,t} + \phi_{1,t}\frac{\widehat{W}_{t+k|t}}{\widehat{L}_{t+k|t}} + \phi_{2,t}\widehat{\pi}^{(S)}_{t+k|t} \\ &+ \sum_{i\in Shr} \alpha_{i,t}\sin\left(\frac{2\pi i \cdot hr(t+k)}{24}\right) \\ &+ \sum_{i\in Chr} \beta_{i,t}\cos\left(\frac{2\pi i \cdot hr(t+k)}{24}\right) \\ &+ \sum_{i\in Swd} \gamma_{i,t}\sin\left(\frac{2\pi i \cdot wd(t+k)}{7}\right) \\ &+ \sum_{i\in Cwd} \delta_{i,t}\cos\left(\frac{2\pi i \cdot wd(t+k)}{7}\right)\end{aligned} \tag{4.25}$$

  for the penalties in each direction where $\widehat{W}_{t+k|t}$, $\widehat{L}_{t+k|t}$ and $\widehat{\pi}^{(S)}_{t+k|t}$ are the forecast wind power production, load and spot price as before. Moreover, $hr(t)$ and $wd(t)$ are integers taking their values according to the hour of the day and day of the week. The model is estimated using the full data set for various pairs of forgetting factor and cut-off value.

- Calculate the contribution of each individual observation to the RMSE
- Exclude the observations that contribute more than 0.5% to the total RMSE.

The model in Eq. (4.25) was chosen as one that could easily include double seasonality, multiple external variables and yet involved a limited number of parameters to vary. The elements of *Shr*, *Chr*, *Swd* and *Cwd* were found as the ones optimising the AIC criteria of the time-invariant version of Eq. (4.25) which yielded:

	Shr	*Chr*	*Swd*	*Cwd*
Down	{1}	{2}	∼	{2,3}
Up	{2,3}	{1}	{1,2}	{2}

The choice of the 0.5% limit is somewhat arbitrary but one important feature of having this limit is that it is the lowest one that discarded observations are not parameter specific. The resulting number of discarded observations is 85 for the up-regulation penalties and 29 for $\psi^{(\downarrow)}_{t|>0}$.

The models proposed for the penalties are Holt-Winters models both conditional to the forecast spot price. In addition, the model for the up-regulation penalty is also conditioned upon the forecast load and the model for the down-regulation penalties on the forecast wind power penetration. The models can be seen as a series of Holt-Winters models like the one in Eqs. (4.7) and (4.8), describing the average penalty around fitting points in $[\widehat{\pi}^{(S)}_t, \widehat{L}]$ or $[\widehat{\pi}^{(S)}_t, \widehat{W}/\widehat{L}]$. Like for the sign model, estimation procedure and performance is listed in Paper H along with relevant conclusions and comments.

CHAPTER 5

Conclusions and Further Perspectives

In order to understand the potential consequences of continuing growth in electricity generation by wind turbines, it is important to fully understand how current installations affect the system. The objective of this thesis has partly been to provide analysis that can improve this understanding. Through this analysis, it has been shown that the intuitively expected impact of wind power production on the prices does indeed exist. The hourly resolution of the analysis permits to conclude on the future market environment on numerous aspects. Given the geographical coverage of Denmark, spatial correlation in wind power generation will remain high. Hours of intermediate penetration levels will therefore become less frequent with increasing generation capacity. Instead there will be a tendency towards two different and weather dependent regimes in the hourly production mix. When the wind is blowing, wind turbines will be able to generate enough power to supply all demand and even much more. In still air on the other hand, production will be almost entirely thermal based. These weather depended regimes will then be transferred directly to the prices (Meibom, 2007).

An obvious effect of these prices regimes with current market structure is that earnings from the wind power producers will be severely reduced. This will in turn call for increased expenditures on subsidies and other support for the industry should the current production targets be met. The weather dependent

price regimes created by the increased wind power capacity will also incite those investing in other forms of generation capacity to emphasise flexibility rather than efficiency (Meibom, 2007). It is even plausible that either markets or ways of directly compensating flexibility and flexible capacity will emerge. One can even go so far to say that the establishment of such mechanism is paramount should the current market design of day-ahead settlement be retained during the foreseeable expansion of wind power capacity.

Great expansion of wind power generation capacity will also prompt an increasing number of hours of surplus energy in the system. This extra energy will then have to be either consumed, exported or shed. The two last options however do not contribute towards reaching the goal of having 50% of the consumption supplied for by wind energy by 2025 (Ea Energy Analyses, 2007). The most appealing option is therefore to consume this extra energy domestically. This calls for a tremendous flexibility on the consumption side however. Considerable efforts are currently being made for developing solution able to provide this flexibility and it is likely that such efforts will receive increased attention in coming years.

Increased flexibility on both sides of the supply and demand equation are therefore essential to accomplish, should the current production targets remain within reach. Because given the political effort required for obtaining the alternative solution of vastly expanded market area, and the corresponding investment in transmission capacity, it has to be seen as quite probable that much of the varying production has to be met by increased flexibility within current physical framework.

Regardless of what the future will entail for electricity markets, operational tools for a more efficient management of wind turbines will continue to develop. This thesis explores and provides a range of such tools that can contribute to better decision making of wind power producers.

The papers that address forecasting in the electricity market provide an appealing alternative to models working with logarithmically transformed data (e.g. Conejo et al., 2005, Panagiotelis and Smith, 2008, Higgs, 2009). This way inverse transformations are avoided along with the commonly associated loss of forecast quality. The result in paper F are a testimony of that price forecasts can be improved considerably by accounting for the non-linear effect of wind power on the prices where present. In paper G, the merits of the flexibility provided by the non-parametric approach to density modelling transpires through reliable predictions. There an appealing alternative to the conventional parametric models (Panagiotelis and Smith, 2008, Higgs, 2009) is given.

All together, the models presented seem to serve their purpose well in terms of practical applicability and quality. Like in any research however the results

obtained have prompted several new questions and ideas that would be interesting to pursuit.

In the present market environment, properly exploring the relevance of conventional risk management in the short-term is an interesting topic. An analysis of how such efforts relate to the long-term risk would be interesting to conduct, e.g. by studying the effect of the chosen VaR-quantile α and risk attitude parameter λ on the long-term revenues. This applies for both the hour-by-hour formulation presented in this thesis as well as approach of considering the daily risk as suggested by Morales et al. (2010). These analyses could potentially be accompanied by a derivation of a strategy that considers risk on different time scales simultaneously. Alternatives to the CVaR, focused on avoiding the utmost extreme losses would also be interesting to explore.

For any type of risk management in the day-ahead trading, models capturing the high penalty hours are important to obtain. Such models could come as density models, as spike forecasting models or a mixture of the two. Obtaining such models is however a challenging task since information on influential factors is unavailable at the prediction time. An interesting possibility would be to construct a model for joint predictive densities for the penalties and e.g. the demand and wind power imbalances. Such densities could subsequently serve as a basis for scenario generation.

The oligopolistic structure of electricity markets in general and the foreseeable development in the generation mix make the concept of market power an interesting research topic. How markets will be affected by strategic bidding behaviour of large producers will be interesting to follow. Both in terms of the effectiveness of the strategies adopted and also in context of market development.

Bibliography

John B. Bremnes. Probabilistic wind power forecasts using local quantile regression. *Wind Energy*, 7(1):47–54, 2004.

Derek W. Bunn. *Modelling prices in competitive electricty markets*, chapter 1 - Structural and Behavioural Foundations of Competitive Electricity Prices, pages 1–17. John Wiley & Sons, 2004.

Lennart Carlsson. International power trade - the nordic power pool. *Public Policy for the Private Sector*, Note no. 171, January 1999.

William S. Cleveland and Susan J. Devlin. Locally weighted regression: An approach to regression analysis by local fitting. *Journal of the American Statistical Association*, 83(403):596–610, 1988.

Antonio J. Conejo, Javier Contreras, Rosa Espínola, and Miguel A. Plazas. Forecasting electricity prices for a day-ahead pool-based electric energy market. *International Journal of Forecasting*, 21(3):435–462, 2005.

Antonio J. Conejo, Miguel Carrión, and Juan M. Morales. *Decision Making Under Uncertainty in Electricity Markets*. Springer, 2010.

Ea Energy Analyses. 50% wind power in denmark in 2025 - english summary. *Available at: http://www.talentfactory.dk/media(2513,1033)/081029_50pct._wind_power_in_dk_in_2025.pdf*, 2007.

Energinet.dk. *Regulation C2: The balancing market and balance settlement*, December 2008. URL http://www.energinet.dk. Doc. No. 251673-06 Rev. 2.

Euorostat. Gas and electricity market statistics. Technical report, Eurostat, 2007. URL www.eurostat.eu. Collection: Statistical books.

Eurostat, 2012. URL http://www.eurostat.eu.

Sarah Gelper, Roland Fried, and Cristophe Croux. Robust forecasting with exponential and Holt-Winters smoothing. *Journal of Forecasting*, 29(3):285–300, 2010.

Paolo Giabardo, Marco Zugno, Pierre Pinson, and Henrik Madsen. Feedback, competition and stochasticity in a day ahead electricity market. *Energy Economics*, 32(2):292–301, 2010.

Helen Higgs. Modelling price and volatility inter-relationships in the Australian wholesale spot electricity markets. *Energy Economics*, 31(5):748–756, 2009.

Peter J. Huber. *Robust Statistics*. John Wiley & Sons, Inc., Hoboken, NJ, USA, 1981.

Rob J. Hyndman, Anne B. Koehler, J. Keith Ord, and Ralph D. Snyder. *Forecasting with Exponential Smoothing - The State Space Approach*. Springer, New York, USA, 2008.

Nektaria V. Karakatsani and Derek W. Bunn. Forecasting electricity prices: The impact of fundamentals and time-varying coefficients. *International Journal of Forecasting*, 24(4):764–785, 2008.

Roger Koenker. *Quantile Regression*. Cambridge University Press, New York, NY, USA, 2005.

Roger Koenker and Gilbert Basset. Regression quantiles. *Econometrica*, 46(1): 33–50, 1978.

Peter Kosater and Karl Mosler. Can Markov regime-switching models improve power-price forecasts? Evidence from German daily power prices. *Applied Energy*, 83(9):943–958, 2006.

Matthias Lange. On the uncertainty of wind power predictions - Analysis of the forecast accuracy and statistical distribution of errors. *Journal of Solar Energy Engineering - Transactions of the ASME*, 127(2):177–184, 2005.

Henrik Madsen. *Time Series Analysis*. Chapman & Hall / CRC, London, UK, 2008.

J. Matevosyan and L. Söder. Minimization of imbalance cost trading wind power on the short-term power market. *IEEE Transactions on Power Systems*, 21(3):1396–1404, 2006.

Peter Meibom. Market consequences [in my view]. *IEEE Power and Energy Magazine*, 5(6):120–118, 2007.

Rune Moesgaard and Poul Erik Morthorst. The impact of wind power on electricity prices in denmark. In *EWEC 2008, European Wind Energy Conference, Business and Policy Track*, Brussels, Belgium, April 2008.

Jan Kloppenborg Møller, Henrik Aalborg Nielsen, and Henrik Madsen. Time-adaptive quantile regression. *Computational Statistics and Data Analysis*, 52 (3):1292–1303, 2008.

Juan M. Morales, Antonio J. Conejo, and Juan Pérez-Ruiz. Short-term trading for a wind power producer. *IEEE Transactions on Power Systems*, 25(1):554–564, 2010.

Poul Erik Morthorst. Wind power and the conditions at a liberalized power market. *Wind Energy*, 6(3):297–308, 2003.

Henrik Aa. Nielsen, Torben S. Nielsen, Alfred K. Joensen, Henrik Madsen, and Jan Holst. Tracking time-varying coefficient functions. *International Journal of Adaptive Control and Signal Processing*, 14(8):813–828, 2000.

Torben Skov Nielsen, Henrik Aalborg Nielsen, and Henrik Madsen. Prediction of wind power using time-varying coefficient functions. In *15th IFAC World Congress*, Barcelona, Spain, 2002.

Francisco J. Nogales, Javier Contreras, Antonio J. Conejo, and Rosario Espínola. Forecasting next-day electricity prices by time series models. *IEEE Transactions on Power Systems*, 17(2):342–348, 2002.

Nord Pool Spot AS. Exchange Information - Highest market share ever for Nord Pool Spot, January 2010. URL http://www.nordpoolspot.com/Message-center-container/Exchange-list/Exchange-information/No-022010-NPS---Highest-market-share-ever-for-Nord-Pool-Spot-/?year=2010&month=1.

Nord Pool Spot AS. Exchange Information - Highest volume ever for Nord Pool Spot, January 2011. URL http://www.nordpoolspot.com/Message-center-container/Exchange-list/Exchange-information/No-052011--Highest-volume-ever-for-Nord-Pool-Spot/?year=2011&month=1.

Nord Pool Spot AS. Exchange Information - Figures show record volume for Nord Pool Spot, January 2012. URL http://nordpoolspot.com/Message-center-container/Exchange-list/2012/1/No-022012---Figures-show-record-volume-for-Nord-Pool-Spot/?year=2012&month=1.

Magnus Olsson and Lennart Söder. Modeling real-time balancing power market prices using combined SARIMA and Markov processes. *IEEE Transactions on Power Systems*, 23(2):443–450, 2008.

Andrew L. Ott. Experience with PJM market operation, system design and implementation. *IEEE Transactions on Power Systems*, 18(2):528–534, 2003.

Anastasios Panagiotelis and Michael Smith. Bayesian density forecasting of intraday electricity prices using multivariate skew-t distributions. *International Journal of Forecasting*, 24(4):710–727, 2008.

Pierre Pinson, Christophe Chevallier, and George N. Kariniotakis. Trading wind generation from short-term probabilistic forecasts of wind power. *IEEE Transactions on Power Systems*, 22(3):1148–1156, 2007.

R. Tyrrell Rockafellar and Stanislav Uryasev. Optimization of Conditional Value-at-Risk. *The Journal of Risk*, 2(3):21–41, 2000.

R. Tyrrell Rockafellar and Stanislav Uryasev. Conditional Value-at-Risk for General Loss Distributions. *Journal of Banking and Finance*, 26(7):1443–1471, 2002.

Rudiger Schultz and Stephan Tiedemann. Conditional Value-at-Risk in Stochastic Programs with Mixed-Integer Recourse. *Mathematical Programming Series B*, 105(2-3):365–386, 2006.

James W. Taylor. Short-term electricity demand forecasting using double seasonal exponential smoothing. *Journal of Operational Research Society*, 54(8): 799–805, 2003.

Rafal Weron. *Modeling and Forecasting electricity loads and prices – A statistical approach*. John Wiley & Sons Ltd, 2006.

Peter R. Winters. Forecasting sales by exponentially weighted moving averages. *Management Science*, 6(3):324–342, 1960.

Part II

Papers

PAPER A

On the Market Impact of Wind Energy Forecasts

Authors:
T. Jónsson, P. Pinson, H. Madsen

Published in:
Energy Economics 32(2), pp. 313-320 (2010)

On the Market Impact of Wind Energy Forecasts

Tryggvi Jónsson[1,2] Pierre Pinson[2] Henrik Madsen[2]

Abstract

This paper presents an analysis of how day-ahead electricity spot prices are affected by day-ahead wind power forecasts. Demonstration of this relationship is given as a test case for the Western Danish price area of the Nord Pool's Elspot market. Impact on the average price behaviour is investigated as well as that on the distributional properties of the price. By using a non-parametric regression model to assess the effects of wind power forecasts on the average behaviour, the non-linearities and time variations in the relationship are captured well and the effects are shown to be quite substantial. Furthermore, by evaluating the distributional properties of the spot prices under different scenarios, the impact of the wind power forecasts on the price distribution is proved to be considerable. The conditional price distribution is moreover shown to be non-Gaussian. This implies that forecasting models for electricity spot prices for which parameters are estimated by a least squares techniques will not have Gaussian residuals. Hence the widespread assumption of Gaussian residuals from electricity spot price models is shown to be inadequate for these model types. The revealed effects are likely to be observable and qualitatively similar in other day-ahead electricity markets significantly penetrated by wind power.

1 Introduction

Since the beginning of the nineties, electricity markets around the world have undergone drastic reforms, resulting in a more deregulated structure. The backbone of these changes has been the adoption of wholesale electricity markets, in which producers and distributors bid for purchase and sale of electricity. Commonly, these bids are placed through a central clearing mechanism which determines a spot price at which electricity is traded. However due to

[1]ENFOR A/S, Lyngsø Allé 3, DK-2970 Hørsholm, Denmark
[2]DTU Informatics, Technical University of Denmark, Richard Petersens Plads, building 321, DK-2800 Kgs. Lyngby, Denmark

the complex nature of the commodity in question, the dynamics of these spot prices are only partially understood, making them difficult to accurately forecast. Nevertheless, understanding of the price dynamics (and the resulting increased predictability) is paramount for all market participants and regulators, for the purpose of planning, trading, risk management or alternatively market design (see e.g. Daneshi and Daneshi, 2008).

The complex nature of spot prices arises from numerous causes. First of all, anti-gaming policies along with the instantaneous nature of electricity and restrictions on its transmission make arbitrage over time and space nearly impossible (Boogert and Dupont, 2005, Sewalt and de Jong, 2003). Secondly, demand for electricity, seen from a short-term perspective, is highly inelastic and has distinctive and complex characteristics in the first two moments, (see e.g. Taylor and McSharry, 2007 or Panagiotelis and Smith, 2008 and references therein). Thirdly, the electricity supply function is discontinuous, convex and steeply increasing at the high demand end (Nord Pool Spot AS, 2006a, Karakatsani and Bunn, 2008). In parallel, the presence of non-dispatchable renewable energy sources causes frequent variations in the shape of the supply function, due to their low marginal costs and potential prioritisation (Giabardo and Zugno, 2008). In addition, market design is generally complex and frequently changing support schemes for some plant technologies often lead to modifications of the market design as well. Finally, the oligopolistic structure in many markets has given rise to a debate about to what extent market power is exercised. Although controversial, evidence of market power being put to force has been documented on many major electricity markets (see e.g. Eggertsson, 2003, Schwarz et al., 2007, Christensen et al., 2007 and also Karakatsani and Bunn, 2008 for other sources). A main objective of the present paper is to demonstrate that wind power forecasts have an impact on the market, and to describe how they quantitatively affect prices on the electricity market.

The combination of all the factors listed above results in a price behaviour unlike what is observed for most other traded commodities as the price time-series often exhibits periodicity, inter- and intra-day correlations, trends, mean reverting spikes, positive skewness and heavy tails (see e.g. Conejo et al., 2005, Panagiotelis and Smith, 2008, Kosater and Mosler, 2006, for empirical evidence of this). Furthermore, the increased emphasis on renewable energy sources around the world has made the dynamics of spot prices even more complex. The price characteristics have become more extreme and made prices even harder to predict - partly due to the very volatile nature of many of these energy sources.

Several papers have been dedicated to describing the short-term dynamics of electricity spot prices, either by (i) relying solely on previous values, i.e. in a univariate time-series modelling framework (Huisman et al., 2006, Conejo

et al., 2005, Cuaresma et al., 2004), (ii) by accounting for the price's response to demand, fuel prices or weather conditions (Vehviläinen and Pyykkönen, 2005, Ruibal and Mazumdar, 2008, Mandal et al., 2006, Nogales and Conejo, 2006), or (iii) by using regime-switching approaches (Kosater and Mosler, 2006, González et al., 2005). However as correctly stated by Karakatsani and Bunn (2008), the models presented in those papers have a number of limitations. Firstly, fuel prices and weather conditions only affect the supply function indirectly and their influence on the elements of the supply function is highly non-linear. Therefore, those factors ought to be supplemented by, or transformed into, information that more directly affects the supply function and the behaviour of market participants in general, as suggested by Karakatsani and Bunn (2008) and Longstaff and Wang (2004). Secondly, most research works have been focused on daily averages or baseload / peakload averages which conceal to some or full extent the distinct intra-day variations of the prices. Recently, higher frequency analysis have appeared though (e.g. Huisman et al., 2006, Longstaff and Wang, 2004, Karakatsani and Bunn, 2008).

Operationally, energy produced by non-dispatchable energy sources is commonly bid into the markets using forecasts of the future production. In the case of wind power, production forecasting is a major and rapidly growing research field and has been the topic of countless papers (see e.g Giebel et al., 2003, Costa et al., 2008, for a state of the art review). Some efforts have been made to optimise the bidding of wind energy into deregulated electricity markets based on these forecasts, and in some cases on information about their situation-dependent uncertainty as well (Pinson et al., 2007, Matevosyan and Söder, 2006, Bathurst et al., 2002). These studies however have all regarded wind power as a price taker, and therefore not considered its potential effects on prices. Although this approach is suitable when concentrating on individual wind power generators, wind power as a whole is in fact a price maker as originally suggested by Skytte (1999) and Morthorst (2003), due to its extremely low marginal cost. In areas where wind power has a significant share in the generation portfolio, the most substantial short-term changes in the global supply function arise from variations in wind power generation. As shown by Giabardo et al. (2010), estimated future wind power generation[1] appears as a stochastic threshold in the supply function. The present paper presents an analysis of how electricity spot prices, for the case of the Western Danish price area (DK-1) of Nord Pool's Elspot market, are affected by wind power forecasts. The analysis puts emphasis on the effects of such forecasts on the mean behaviour of the prices, on the intra-day variations of these effects, as well as on the corresponding impact on the distributional characteristics of day-ahead electricity prices. Some studies have been presented on the effects of actual power generated by wind turbines on the spot prices in the area (Skytte, 1999, Morthorst,

[1] And thereby wind power capacity due to the low marginal costs and sometimes prioritisation of wind power

2003, Moesgaard and Morthorst, 2008, Enevoldson et al., 2006) and they have shown this effect to exist — as also expected by economical arguments. However, these studies have been bounded to linear effects on the mean behaviour and have therefore neither captured the full extent of this impact nor any of the distributional effects. Furthermore, as the analysis are carried out on the actual measured power output they only show the presence of a relation between wind power generation and spot prices, rather than proving wind power to be a price maker on the market. Consequently, the resulting models can not be used for forecasting.

Showing wind power as a price maker in a short-term perspective, implies raising the question: *"What will the electricity spot prices be, if it is believed that the wind will/will not blow?"* As an answer to this question, the relationship between wind power forecasts and spot prices is shown not only to exist, but also to be highly non-linear and time dependent. Furthermore, it is demonstrated that the correlation between demand and wind power forecasts should not be neglected since it is in fact the ratio between the forecasted wind power generation and the forecasted load that has the strongest association with the spot prices. In parallel, this proportional contribution of wind power to the supply is shown to have substantial influence on the distribution of the spot prices as well.

For the demonstration of these effects, a non-parametric regression model is employed. The relationship between forecasted wind power production and electricity spot prices is estimated for every hour of the day. This dependency is estimated by assuming that the relationship can be locally described with a second order polynomial. For estimation, a least squares criteria is employed allowing for the mean effect of forecasted wind power penetration on the prices to be extracted. Despite the facts listed about the (non-Gaussian) properties of the conditional spot price distribution, this approach serves well for estimating the mean behaviour of the spot prices, partially due to the non-linear properties of the model and the large amount of data used as input to analysis. Employing such a criteria for the non-parametric regression model prevents however from any inference on the effects of wind power forecasts on distributional properties of spot prices to be made. Therefore, the evaluation of these effects is performed by directly analysing the first four moments of the price distributions under different scenarios of the ratio between forecasted wind power and forecasted load. The wind power forecasts used are generated by WPPT[2] (see Nielsen et al., 2002), a wind power forecasting tool that has been successfully used in Denmark over the past years and was used for bidding aid by almost every wind turbine owner in DK-1 during the period in question.

The remainder of the paper is structured as follows: Section 2 describes the

[2]The Wind Power Prediction Tool

market structure at Elspot and the data set used as input to the analysis. Section 3 provides a brief introduction to the mathematical approach to the modelling. In Section 4, an analysis of how the mean behaviour of the spot prices is affected by wind power forecasts is given, while the impact of these forecasts on the price distribution is the topic of Section 5. Finally, concluding remarks are given in Section 6 along with some general discussion.

2 Nord Pool's Elspot

2.1 Market Setting

The analysis presented in this paper is done on data from the Western Danish price area (DK-1) of Nord Pool's Elspot market. Elspot is a day-ahead physical delivery market for electricity. It is currently operating in the entire Scandinavia (Denmark, Finland, Norway and Sweden) and in the so called Kontek area, located in Northeastern Germany.

At Elspot, spot prices are set by a market equilibrium model, where supply and demand curves of all market participants are matched on a day-ahead basis. Gate closure is at noon each day for the period midnight to midnight in the following day and prices are published later in the day with a resolution of one hour. The one hour prices are calculated by matching the collaborative supply and demand curves, calculated from the bids and ask prices placed by the market participants (see Nord Pool Spot AS, 2006a,b, for details). This price, found from bids from all market participants, defines the system price from which the area prices are defined.

Due to transmission constraints, the region covered by Elspot is divided into several price areas. Physical constraints on transmission define the outer bounds of each price area, implying that transmission capacity within an area can be regarded as unlimited. The area spot prices are calculated in the same manner as the system price, but only considering the bids within the area along with possible utilisation of the transmission lines to surrounding areas (see Nord Pool Spot AS, 2006b, for details). The area prices, which determine at what price physical trading is done within an area, can therefore differ quite considerably between areas. If none of the interconnections between areas are fully utilised, the system price is valid in the whole region. However, this is seldom the case and therefore is modelling of the area spot prices appropriate when short term dynamics and forecasting are considered.

The DK-1 price area consists of Jutland, Funen and the islands west of the Great Belt. The area is an interesting context for investigation of electricity spot prices

as it can be said to represent the future of liberalised electricity markets. This is because it has relatively large connections to its surrounding areas, and is heavily penetrated by an inexpensive, non-dispatchable energy source, i.e. wind power. In fact, DK-1 is currently the grid area in the world that has the largest share of wind power in its generation portfolio, with more than 20% of its annual consumption generated by wind turbines.

2.2 The Data

The data, which the analysis here presented is carried out on, covers the period from January 4th 2006 to October 31st 2007. It consists of hourly area spot prices along with hourly consumption measurements for the area[3] and wind power forecasts (in MW) with a temporal resolution of 15 minutes, made at 07:00 on the day before delivery for lead times up to 48 hours. The forecasts are made using WPPT (see Nielsen et al., 2002).

If the analysis is to be true to the criteria of analysing future electricity prices, both measures entering the wind power-load ratio have to be forecasts instead of actual measurements. When load forecasts are made using state of the art load forecasting models (e.g. Taylor and McSharry, 2007), the relationship between the actual load and the predicted load can be described as

$$L_t = \widehat{L}_t + \varepsilon_t \quad \text{where} \quad \varepsilon_t \sim N(0, \sigma^2) \tag{1}$$

where L_t is the actual load, $\widehat{L}_t$ is the predicted load and σ^2 is the finite variance of the residuals, ε_t. Hence, by adding a Gaussian noise with the appropriate variance to the load measurements, a time series that has the characteristics of an actual load forecast series is obtained. The standard deviation of the noise is chosen as 2% of the average load for the period, since it reflects the performance of state of the art load forecasting models (see e.g. Taylor and McSharry, 2007). The use of simulated load forecasts gives rise to some deviations from the real-life situation though. First of all, the residuals of actual load forecasts are bound to have some autocorrelation in the lags up to the prediction horizon. This is not reflected in the simulated residuals. However, for forecasts of such a degree of accuracy as load forecasts are in general, the small prediction error is reflected by a small residual autocorrelation as well. The influence of the missing autocorrelation structure is therefore only marginal. Secondly, since both load forecasts and wind power predictions are typically based on weather forecasts, some correlation between the errors of the two might be observed in practise. This is however not the case when simulated forecasts are used since the computer generated noise, added to the load forecasts, is

[3] Available at http://www.energinet.dk/en/menu/Market/Market.htm and at http://www.nordpoolspot.com

not correlated to the real error of the wind power predictions. The error of the wind-load forecasting ratio will therefore have characteristics that differ slightly from what would be observed if both were actual forecasts. Nevertheless, the mean of the errors will still be zero in both cases and other effects are minor. These potential dissimilarities from the practical situation are ignored in the analysis to follow due to their small impact on the results.

Hourly wind energy forecasts in MWh also have to be derived. This is done by linearly interpolating between each two adjacent forecasts in every hour and taking the result as the production in MWh for that 15 minute period. These interpolations are then summed up for each hour. So in mathematical terms, an hourly forecast is obtained by

$$\widehat{V}_t^{(h)} = \sum_{i=2}^{5} 0.25 \cdot \left(\frac{\widehat{V}_{t,q(i-1)}^{(q)} + \widehat{V}_{t,q(i)}^{(q)}}{2} \right) \tag{2}$$

where $\widehat{V}_t^{(h)}$ (hereafter noted as $\widehat{V}_t$) is the hourly wind energy forecast for hour t, and $\widehat{V}_{t,q(i)}^{(q)}$ is the 15 minute wind power forecast for quarter i within hour t.

In order to account for the correlation between demand and wind power forecasts, the wind power penetration level, $\widehat{V}_t^{(p)}$, is defined as

$$\widehat{V}_t^{(p)} = \frac{\widehat{V}_t}{\widehat{L}_t}, \tag{3}$$

Finally, it should be emphasised that no extreme events are excluded from the data set.

3 Non-parametric regression modelling of day-ahead electricity prices

The relationship between, area spot price and wind power generation is far from being linear. It is therefore essential for obtaining a proper estimate of the effects of wind power forecasts on the area spot price to account for these non-linearities. The problem of estimating a complex non-linear relationship between variables is however not a trivial one. But by assuming that the relationship is locally linear or locally describable by a low order polynomial the problem is much more convenient to deal with. One could locally solve a weighted least squares problem as described in detail for the general case in (Cleveland and Devlin, 1988, Nielsen et al., 2000, Madsen and Holst, 2000).

Let a model for the spot prices at time t, P_t, be defined as

$$P_t = \boldsymbol{\theta}(\boldsymbol{x}_t) + \varepsilon_t, \tag{4}$$

where $\boldsymbol{\theta}(\cdot)$ is a vector of coefficient functions and ε_t is a noise term. Furthermore, $\boldsymbol{x}_t$ is a vector of explanatory variables. In this case those variables are some direct or derived form of a wind power forecast, $\widehat{V}_t$, and an hour of the day indicator, k_t.

The functions $\boldsymbol{\theta}(\cdot)$ are estimated at a number of distinct points by approximating the functions using polynomials and fitting the resulting linear model locally to each of these fitting points. More specifically, let $\boldsymbol{U} = \begin{bmatrix} \widehat{V}_U & k_U \end{bmatrix}^T$ denote a particular fitting point, chosen from a set of m total fitting points, and let $\boldsymbol{p}_2(\boldsymbol{U})$ be a column vector of terms in the corresponding 2*nd*-order polynomial, i.e.

$$\boldsymbol{p}_2(\boldsymbol{U}) = \begin{bmatrix} 1 & \widehat{V}_U & k_U & \widehat{V}_U^2 & \widehat{V}_U k_U & k_U^2 \end{bmatrix}^T. \tag{5}$$

Furthermore, let $\boldsymbol{\phi}_U = \begin{bmatrix} \phi_{U,1} & \cdots & \phi_{U,7} \end{bmatrix}^T$ denote the coefficient vector at $\boldsymbol{U}$. Now the linear model

$$P_U = \boldsymbol{p}_2(\boldsymbol{U})^T \boldsymbol{\phi}_U + \varepsilon_U \tag{6}$$

can be used to describe the spot price in the close vicinity of $\boldsymbol{U}$ and can be fitted locally using weighted least squares (WLS), i.e.

$$\widehat{\boldsymbol{\phi}}(\boldsymbol{U}) = \underset{\boldsymbol{\phi}_U}{\arg\min} \sum_{i=1}^{N} w_U(\boldsymbol{x}_i) \left(P_i - x_i^T \boldsymbol{\phi}_U \right)^2 \tag{7}$$

where $\boldsymbol{x}_i = \boldsymbol{p}_2(\boldsymbol{U}_i)$ and for which a unique closed-form solution exists provided that the matrix with rows $\boldsymbol{x}_i$ corresponding to non-zero weights has a full rank. The weights are assigned as

$$w_U(\boldsymbol{x}_i) = W\left(\frac{||\boldsymbol{x}_i - \boldsymbol{x}||_2}{h(\boldsymbol{x})} \right) \tag{8}$$

where $W(\cdot)$ is a decreasing weight function taking non-negative arguments. Furthermore, $h(\boldsymbol{x})$ is the bandwidth used for the particular fitting point, i.e. the maximum euclidean distance between a fitting point and an observation resulting in a non-zero weight being assigned in Eq. (7). This implies that a small bandwidth will result in a very flexible model with low bias and high variance while applying a large bandwidth yields a more rigid model having higher bias but lower variance. For readers familiar to exponential smoothing, applying a small bandwidth corresponds to having a low level of smoothing in the model. The bandwidth can therefore be said to be a scalar controlling

the rate at which the weight of an observation, in the estimation, decreases with distance from the fitting point. From this it follows that the argument which $W(\cdot)$ takes is the relative distance between the fitting point and the other point falling within the bandwidth. Following Cleveland and Devlin (1988) and Nielsen et al. (2000), a tri-cube kernel is chosen as a weight function so

$$W(u) = \begin{cases} (1-u^3)^3 & u \in [0,1) \\ 0 & u \in [1,\infty) \end{cases}. \tag{9}$$

Turning back to the global view on the model, it can be seen that for an arbitrary chosen $\boldsymbol{U}$, out of a set of m fitting points, there can be found a parameter vector ϕ_U. From these, the elements of $\boldsymbol{\theta}(\boldsymbol{x}_t)$ are estimated as

$$\widehat{\boldsymbol{\theta}}(\boldsymbol{x}_t) = \widehat{\boldsymbol{\theta}}(\boldsymbol{p}_2(\boldsymbol{U} = \boldsymbol{x}_t)) = \boldsymbol{p}_2^T(\boldsymbol{U})\widehat{\phi}(\boldsymbol{U}) \tag{10}$$

where $\widehat{\phi}(\boldsymbol{U})$ is the WLS estimate of $\phi_{\boldsymbol{U}}$.

The bandwidth, $h(\boldsymbol{x})$ is chosen so that at any given time 30% of all observations fulfil $||\boldsymbol{x}_i - \boldsymbol{x}||_2 \leq h(\boldsymbol{x})$. In other words, the bandwidth is varied according to the local density of the data by letting $h(\boldsymbol{x})$ be equal to the distance of the qth-nearest $\boldsymbol{x}_i$ to $\boldsymbol{x}$, where q is 30% of the total number of observations (see e.g. Cleveland and Devlin, 1988, for details). The choice of the criteria that 30% of the observations should fall within the bandwidth is made since it was desired to obtain as local estimates as possible and 30% was the smallest bandwidth that resulted in a full rank design matrix at all times. This criteria is applied for estimation in all $m = 24^2$ fitting points.

Despite what has been stated previously in this paper regarding the conditional distribution of the spot prices, using this sort of least squares technique is deemed suitable for this analysis. This is because the model is only used for assessing the average dependency between the variables and for such estimates, Gaussian estimators are generally known to be the best ones for most types of data. Furthermore, the non-Gaussianity of the residuals is reduced by the model's non-linearity. This aside, as will be demonstrated later on in the paper (Figure 5), despite the prices not being normally distributed, their distribution has a bell shaped form, making the Gaussian assumption not completely inappropriate. In addition, the analysis is carried out on a very extensive data set containing hourly observations for 22 consecutive months. Therefore, will the impact of each individual extreme only be minimal. Hence, the use of robust least squares or similar techniques is not necessary.

How the method is applied in the analysis to follow can be summarised as follows. First the data is scaled so all variables are between $[-1,1]$. Then a grid of $m = 24 \times 24$ equidistant fitting points is defined. For each of these fitting points, $\boldsymbol{U}_{m_i}$, the following steps are taken:

1. Calculate the euclidean distances between every observation and the fitting point of interest. Applying the bandwidth principle previously described, these distances are normalised by that corresponding to the qth-nearest neighbour, where q is set to 30%, and thereby form the input to Eq. (9).

2. Compute the estimate $\hat{\Phi}(\boldsymbol{U}_{m_i})$ of the local polynomial coefficients at the fitting point $\boldsymbol{U}_{m_i}$ by solving Eq. (7).

3. Obtain the local estimate of the spot price at $\boldsymbol{U}_{m_i}$ from Eq. (10) with $p_2(\boldsymbol{U}_{m_i})$ as the polynomial for the particular fitting point as described by Eq. (5).

The mean spot price for any point $\boldsymbol{U}$ can be obtained by bilinear interpolation from the local estimates calculated at each fitting point. This finally yields a smooth trend surface like those shown and commented on in the following.

4 General trend: the effect of forecasts on the mean price

On a day-ahead basis, the area spot price is subject to a considerable uncertainty. It can therefore rightfully be stated that the future spot price has some unknown distribution and the model presented in the previous section can be used, if applied correctly, to provide information about the mean in this distribution.

In Figure 1 the average spot price in DK-1 is estimated as a function of both the time of the day and the forecasted wind energy production measured in MWh per hour. From the figure, it is quite obvious that forecasts of large wind power production in a given hour will, on average, result in a lower spot price in that hour, since when going along the wind power-axis, in the increasing direction, the mean price decreases. During the night, the average price varies from around $30€/MWh$ for a forecasted low wind power production down to around $18€/MWh$ for the hours with forecasted large wind power production. During the day, this difference between the two extremes in forecasted quantities of wind power produced is somewhat larger as the prices go from around $50-55€/MWh$ down to around $30€/MWh$. Due to the infrequent occurrence of the installed wind power capacity being fully utilised, the wind power-axis only reaches 1500 MWh which is somewhat lower than the full utilisation[4]. Observations above the 1500 MWh limit are nevertheless used for

[4]Installed wind generation capacity in DK-1 was around 2400 MW during the considered period.

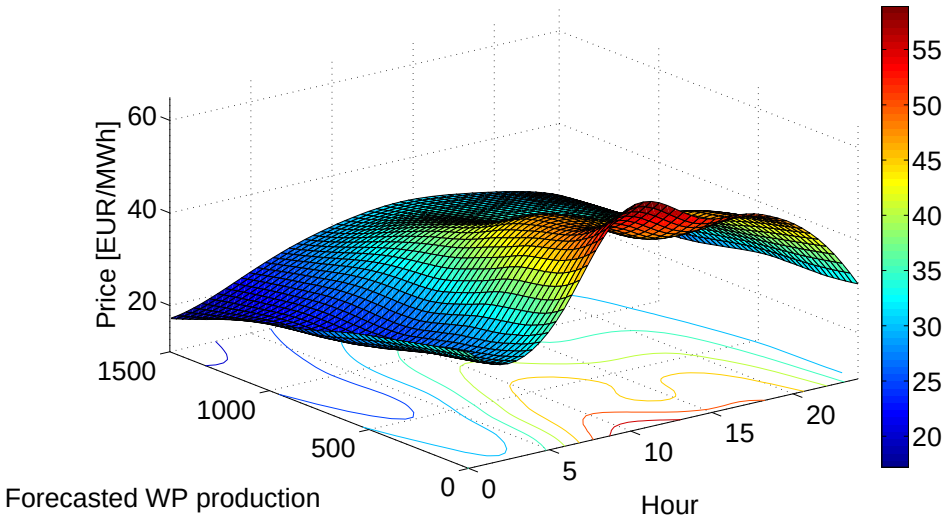

Figure 1: The dependence of the spot prices on forecasted wind power production and its variation throughout the day

estimation when it is relevant.

What is also very interesting is that the daily price raise, during the hours of the day where consumption reaches its daily peak, evens out as wind power production in the system increases. The reason for this is that the virtually nil marginal cost of the wind turbines shifts the supply curve to the right when more wind power is produced and therefore it takes more consumption to reach the steep end of it. In other words, the increased production of the turbines means that less cost efficient plants otherwise covering the base load, will be covering the peaks only. This in turn prevents the even less cost efficient generators from being utilised during the hours when demand peaks.

As stated earlier, the demand for electricity varies severely throughout the day and the week. The same quantity of wind power, measured in MWh, can therefore have quite different effects on the price depending on the time of the day and the week. More specifically, electricity demand is generally lower during the evening and the night and therefore will a large volume of wind power produced in these hours make up for a larger share of the total demand than the same quantity would do during the day. This in turn will cause the equilibrium point of the supply and demand curves to be placed lower during the evening and the night than it would during the day. In order to eliminate these effects, to some extent at least, the wind power forecasts can be included as

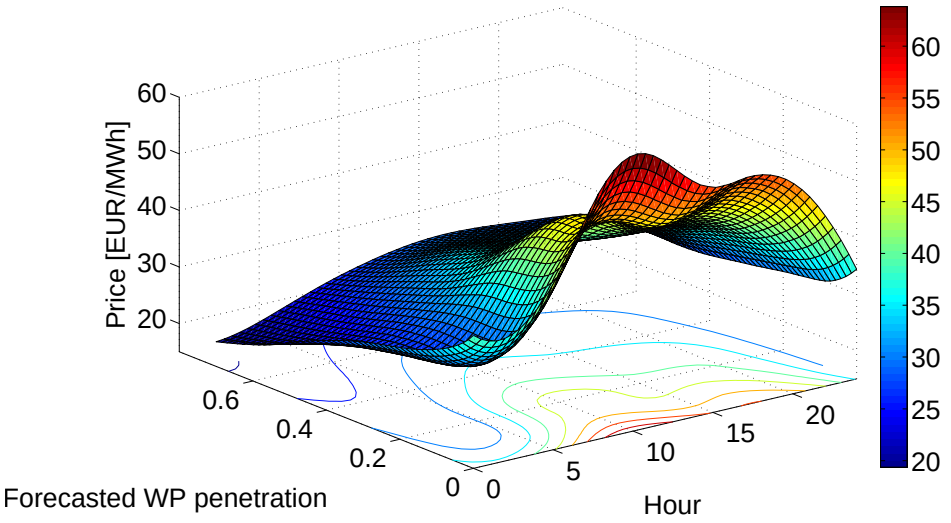

Figure 2: The dependence of the spot prices on forecasted wind power penetration and its variation throughout the day

the proportional contribution to the total supply instead of its absolute contribution. In other words, by substituting the forecasted wind power production, $\widehat{V}_t$, with the forecasted wind power penetration defined in Eq. (3), $\widehat{V}_t^{(p)}$, a better prediction of the price equilibrium is gained from the wind power forecasts.

There are certainly other ways of deriving a number representing the interaction between wind power predictions and load forecasts. For instance, the difference between the forecasts could be considered instead of the ratio between the two. Although the relationship will then appear differently, simulations indicate that the extent of the impact will be approximately the same. It is also intuitively appealing to work with values that are between 0 and 1. Therefore, further analysis is only presented on $\widehat{V}_t^{(p)}$ as it is defined in Eq. (3).

In Figure 2 a smooth estimate of the spot price, as a function of the time of the day and forecasted wind power penetration, is given. The figure shows the same type of effects as described before. However, the effects are more dramatic than seen in Figure 1 since the same actual production now has different effects depending on what time of the day and the week[5] the production occurs. The average spot price is again considerably lower at times where wind power production has been predicted to be large. The difference between the

[5] Due to the weekly variation in the load

two extremes in forecasted production is roughly the same during night hours, while the difference has increased during the day. During the day, the average spot price is around $55 - 60€/MWh$ when nothing of the demand is supplied by wind power. The average prices then rapidly diminishes with a small increase in wind power penetration, and after a short stand still as the penetration approaches 20%, the sharp decline continues up to around 40% predicted penetration, for which the average spot price is around $35€/MWh$. When the forecasted wind penetration has reached 40%, a decrease in average price per penetration percent becomes more subtle and as the forecasted wind power penetration reaches 80%, the average spot price has declined to around $22 - 25€/MWh$.

Some general information about the characteristics of the supply function can also be deduced from the figure. The rather sharp gradient changes in the average price in the lower penetration end of the plot are a clear indication of the discontinuity of the supply function. Wind power quickly pushes the steepest end of the supply curve to the right side of the equilibrium point, and thereby out of the generation portfolio for that hour, explaining the sharp decline in the average price. After stabilising itself, the average price decreases rapidly again when another threshold is pushed out of the equilibrium. The final subtle decline, and the night time behaviour can also be explained by considering the shape of the underlying supply function, since the equilibrium point has then reached the flatter part of the supply function where cheaper energy sources such as Norwegian hydro power and wind power are placed.

Even though it is clear from Figure 2 that forecasted wind power does in fact influence the spot prices, it is hard to point out how big the actual effects are. In Figures 3 and 4 the extent of the effects are better illustrated. In Figure 3 the average spot price is shown for predicted wind power penetration on certain intervals in the period which the data set spans. It shows how the average spot price generally decreases as the share of wind power in the system increases.

In Figure 4, the impact of forecasted wind power penetration is formulated in terms of reduction in price compared to no wind being present in the system. For doing this, the assumption is made that wind power penetration under 4%, corresponding to a production of approximately 80 MWh per hour, has very little or no effects on the spot prices. Observations falling on this interval are taken as a reference point and represents the situation when no wind power is predicted to enter the system. Comparing the average spot price for the reference group, which is €44.43, to that of the remaining observations, where the average is €36.68, shows that the spot prices drop on average by 17.5% when the forecasted wind power penetration exceeds 4%. In Figure 4, the penetration levels above 4% have been divided into intervals of 6-10% and the bars represent how much lower on average, the price is during periods of the given

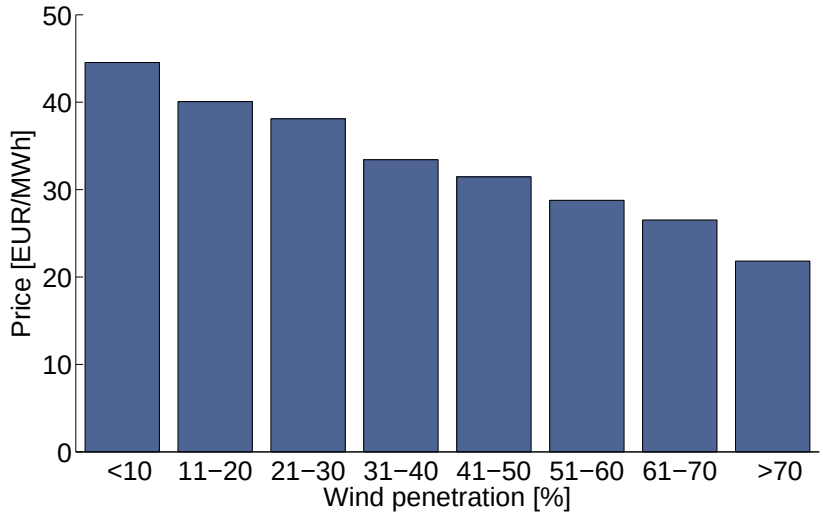

Figure 3: Average spot price, categorised by intervals of forecasted wind power penetration, in DK-1 in the period January 4th 2006 - October 31st 2007

penetration interval, compared to the reference "no wind" situation. The plot clearly illustrates that the spot prices tend to decrease as the forecasted wind power penetration increases.

The extent and the characteristics of the effects that have been shown to exist here indicate that properly accounting for them will be of serious help when electricity spot prices are to be forecasted in an area penetrated by wind power to some or large extent. These effects are consistent with what intuitively would be expected and would provide a forecasting model with vital information about the current shape of the supply function and thereby a good indication about the equilibrium point. However although the existence of these effects is undisputed, it can be debated whether they are for the good or worse, now when the share of wind power stands to be increased all over the world. Less expensive electricity might sound appealing for many at first, especially put in context with marginal bidding. On the other hand, this results in less contribution to the enormous initial investments of power plants of any kind. This will in turn reduce investors' interest in investing in new plants. Furthermore, lower electricity prices pose a threat to the existence of flexible power plants that produce electricity at high marginal costs. These plants however contribute heavily to a much needed stability in the energy supply.

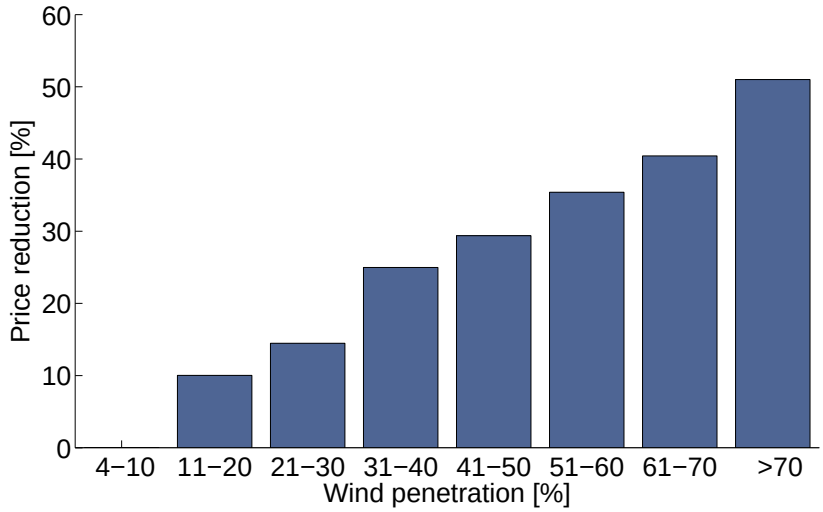

Figure 4: Reduction in average spot price, compared to the "no wind" situation, for different levels of forecasted wind power penetration in DK-1 in the period January 4th 2006 - October 31st 2007

5 Effects of wind power forecasts on price distributional properties

Having established that forecasted wind power penetration certainly affects the mean spot price in DK-1, the question remains whether it affects the distribution of the prices as well. Equipped with more comprehensive knowledge about the relationship between price volatility and one or more of its fundamental causes (in this case wind power forecasts), one may better explain and hereby estimate future volatility levels while conditioning it upon these causes, e.g. in a non-parametric fashion. For carrying out the distribution analysis, the data set is divided into bins, according to forecasted wind power penetration, so that approximately 2500-3000 observations belong to each segment. Then the properties of the price distribution are estimated within each bin.

In Figure 5, histograms of the electricity prices are shown for different levels of forecasted wind power penetration. The figure illustrates, what already has been established, that the mean price shifts towards zero as forecasted wind power penetration increases. Furthermore, the positive skewness of the price distribution is quite evident from the figure as well as the fact that the heavy tail diminishes with increased forecasted wind power penetration. This translates

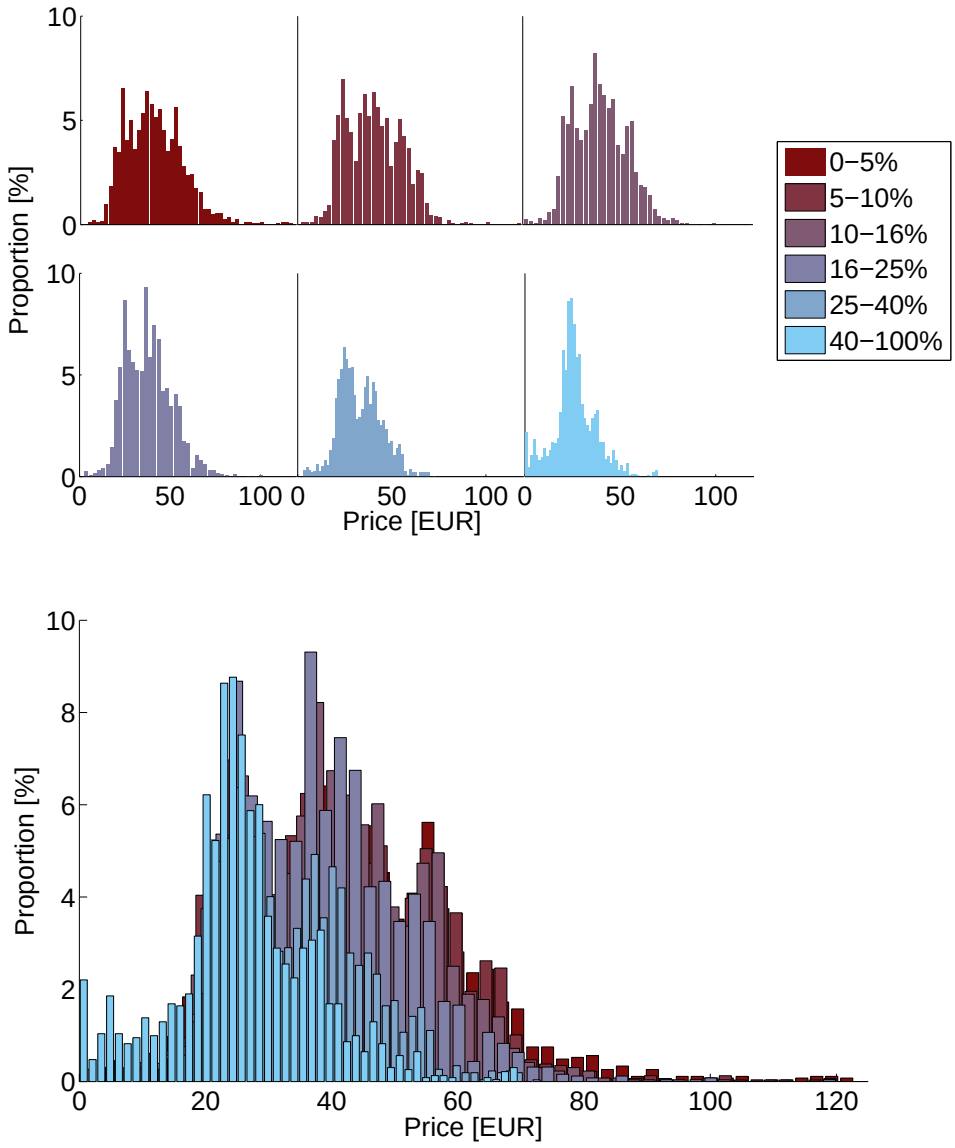

Figure 5: Distribution of prices for different intervals of forecasted wind power penetration

to the statement that the probability of extremely high prices is much lower when the wind power penetration is predicted to be high.

The difference in distribution properties is summarised in Table 1. The first two lines in the table show the shift of mean, already discussed, and reduction in standard deviation, indicating less volatility of the prices. Lines 3 and 4 show how the skewness and kurtosis of the distributions change for the different levels of penetration. Despite the fact that no obvious pattern is detectable in lines 3 and 4, they represent quite dissimilar distributions. Taking the penetration intervals from left to right in the table, the first distribution is rather skewed and with high kurtosis, due to the heavy tail seen in Figure 5. Then as the wind power penetration increases in the 2nd and 3rd intervals, the tail becomes not as heavy, while the mean does not shift all that much, explaining the decrease in both skewness and kurtosis. When the penetration reaches the level of the 4th interval, the mean has shifted more while the rather high prices still occur. Hence, the increase in skewness and kurtosis. For predicted wind power penetration between 25-40% these extreme price situations no longer occur, reflected in a decrease both in skewness and kurtosis. This threshold effect is yet another non-linear effect introduced in the market by wind power or wind power forecasts. Finally, for the highest forecasted penetration interval, the frequency of very low prices increases substantially, explaining the reduction of skewness and increase in kurtosis. So to summarise, going from a low wind power penetration to high, generally leads to a lower skewness due to the diminishing frequency of very high prices along with the increased probability of very low prices.

Another thing that catches the eye in Figure 5 is the relatively high proportion of prices equal to zero in the histogram representing the highest penetration interval. Over 2% of the times when wind penetration is above 40%, electricity spot prices are $0 €/MWh$. Although ill-detectable from the figure, this situation rarely occurs for the 25 - 40% penetration interval, while it does not occur for the lower levels of penetration. For the four lower ones, the minimum price does however approach zero as the forecasted penetration increases. The oc-

Table 1: Properties of the spot price distribution for different scenarios of forecasted wind power penetration

	0-5%	5-10%	10-16%	16-25%	25-40%	40-100%
Mean	42.98	41.13	40.26	38.10	33.24	26.02
Std. Dev.	16.95	15.32	14.18	13.08	11.35	11.23
Skewness	0.82	0.48	0.39	0.63	0.32	0.29
Kurtosis	4.41	3.39	3.40	4.05	3.04	4.09

currence of the spot price being $0€/MWh$ will result in a negative cash flow for producers subject to imbalance costs in that hour. In other words, it will pay off, even for producers with no marginal production costs, not to produce electricity. This further supports what was stated at the end of previous section about the down side of increased wind power penetration under current market conditions.

From a modelling perspective, the dissimilarity of the spot price distribution between different levels of forecasted wind power penetration strongly indicates that estimating prediction intervals conditioned on the wind power predictions is worth the effort. It is quite obvious that the spot prices are not Gaussian distributed and therefore it must be deemed highly unlikely that models constructed with least squares techniques will have Gaussian residuals. Prediction intervals for such models should therefore be estimated using other techniques. In fact the distributions are so far from parameterised distributions that it seems reasonable to conclude that non-parametric approaches, like for instance quantile regression (Møller et al., 2008), will return the most reliable prediction intervals.

6 Conclusions and Discussion

The analysis presented in this paper demonstrates the dramatic impact of predicted wind power penetration in the system on not only the level of the spot prices but also their distributional characteristics. The spot price is, on average, shown to decrease with increased predicted wind power penetration, while intra-day price variations diminish to some extent. As all this happens in a non-linear manner, the use of the non-parametric regression model for the analysis proves to be very beneficial. Furthermore, wind power forecasts are shown to cause threshold effect in the price behaviour, with e.g. the appearance of zero prices, or the removal of extreme prices. They could therefore contribute to an understanding of some of the non-linearities and regime-switching behaviour in the prices. The results of this paper therefore support some of the conclusions of Karakatsani and Bunn (2008) such that aspects of plant dynamics should be considered when models of the short-term dynamics of electricity spot prices are to be derived. It would therefore be interesting to derive a forecasting model for these prices that accounts for the impact of forecasted wind-to-load ratio (see e.g. Jónsson, 2008). When developing such an approach, accounting for the uncovered non-linearities in the relationship between forecasted wind power penetration and day-ahead electricity prices will be essential.

The findings of this paper confirm what previous studies of the impact of

wind power on electricity spot prices have shown, that wind power has a non-negligible impact on day-ahead electricity prices. Here however, based on the claim that it is instead the predicted wind power penetration that should be seen as an explanatory variable, the impact is shown to be more substantial than previously recorded (Enevoldson et al., 2006, Moesgaard and Morthorst, 2008). The corresponding relationship moreover turns out to be highly non-linear, and the distributional characteristics of prices are also affected. The results also show that a simple assumption like Gaussianity commonly made for the estimation of prediction intervals of electricity prices (e.g. Nogales and Conejo, 2006) does not hold. The fact that the spot prices themselves are so far from being Normally distributed will certainly be reflected in the residual distribution of a forecasting model, which parameters are estimated with a least squares criteria. Furthermore, as the price distribution has also been shown to be dependent on an external signal, prediction intervals should be generated accounting for this relation, thus yielding conditional prediction intervals. The analysis therefore indicates that estimating the uncertainty conditioned on an explanatory variable, e.g. wind power forecasts, in a non-parametric fashion could increase the resolution of probabilistic forecasts of electricity spot prices.

In this paper, the scope has been the Western Danish price area (DK-1) at Nord Pool. This price area may be seen as representative of the future deregulated electricity with significant penetration of renewable energy generation. Although the share of wind power in DK-1 is larger than anywhere else in the world, it is very plausible that the effects, revealed here, can also be detected in other market areas as well, penetrated by wind power to some extent — for instance in Spain or Germany. Similar causes would have similar effects, the principal ones being varying availability of the fuel and extremely low marginal costs.

The severe impact of wind power forecasts on all behaviour of the electricity prices is also interesting to consider in the context of market design and with the long-term development of the production portfolio in Denmark in mind — where the intention is to increase the share of wind power generation up to 50% of the electricity consumption by 2025 (Ea Energy Analyses, 2007). With the current market structure of marginal bidding, the frequency of hours where the spot price is zero is bound to increase along with growing wind power penetration in the system in a similar manner as has been demonstrated here. This will further enhance the stochastic threshold effect demonstrated here, and thereby increase price volatility and cause it to have alternating weather dependent patterns (Meibom, 2007). This aside, higher risk premium will be required on investments in all sorts of new energy generation capacity and investment in conventional power generation capacity will be more focused on flexibility than efficiency since those plants will have to rely more on the increased demand on the balance markets as a source of in-

come (Meibom, 2007). The impact of wind power on the price making at the electricity markets should therefore be given careful thought when the possibility of increasing the share of wind power, and non-dispatchable energy sources in general, in the generation portfolio is discussed. Especially, the fact that wind power penetration has some non-linear effects on the prices should be taken into consideration, as it implies that current market situation can not be scaled directly for analysing the future circumstances. In the context of market design, it will also be interesting to monitor the market's response to other renewable sources reaching the status of making up for a significant share of the energy supply. Those sources in all likelihood being solar or wave energy in the medium term. Whether this will level out the effect of increased wind power or magnify them will play an important role in future development of the market structure.

7 Acknowledgements

The authors would like to thank Energinet.dk, the danish Transmission system operator, and Nord Pool ASA for providing data for the analysis, publicly available at http://www.energinet.dk/en/menu/Market/Market.htm and at http://www.nordpoolspot.com. Authors are also grateful to Henrik Aa. Nielsen at ENFOR A/S for fruitful discussions and useful comments and Torben Skov Nielsen at ENFOR A/S for providing wind power predictions.

References

Graeme N. Bathurst, Jennie Weatherill, and Goran Strabac. Trading wind generation in short term energy markets. *IEEE Transactions on Power Systems*, 17 (3):782–89, 2002.

Alexander Boogert and Dominique Dupont. On the effectiveness of the anti-gaming policy between the day-ahead and real-time electricity markets in the Netherlands. *Energy Economics*, 27(5):752–770, 2005.

Bent Jesper Christensen, Thomas Elgaard Jensen, and Rune Mølgaard. Market power in power markets: Evidence from forward prices of electricity. *CREATES Research Paper No. 2007-30. Available at http://ssrn.com/abstract=1150145*, 2007.

William S. Cleveland and Susan J. Devlin. Locally weighted regression: An approach to regression analysis by local fitting. *Journal of the American Statistical Association*, 83(403):596–610, 1988.

Antonio J. Conejo, Javier Contreras, Rosa Espínola, and Miguel A. Plazas. Forecasting electricity prices for a day-ahead pool-based electric energy market. *International Journal of Forecasting*, 21(3):435–462, 2005.

Alexandre Costa, Antonio Crespo, Jorge Navarro, Gil Lizcano, Henrik Madsen, and Everaldo Feitona. A review on the young history of wind power short-term prediction. *Renewable & Sustainable Energy Reviews*, 12(6):1725–1744, 2008.

Jesús Crespo Cuaresma, Jaroslava Hlouskova, Stephan Kossmeier, and Michael Obersteiner. Forecasting electricity spot-prices using linear univariate time-series models. *Applied Energy*, 77(1):87–106, 2004.

Hossein Daneshi and A Daneshi. Price forecasting in deregulated electricity markets - a bibliographical survey. In *The 3rd IEEE International Conference on Electric Utility Deregulation, Restructuring, and Power Technology (DRPT2008)*, Nanjing, China, April 2008.

Ea Energy Analyses. 50% wind power in denmark in 2025 - english summary. *Available at: http://www.talentfactory.dk/media(2513,1033)/081029_50pct._wind_power_in_dk_in_2025.pdf*, 2007.

Haukur Eggertsson. The scandinavian elecricity power market and market power. Master's thesis, Technical University of Denmark, DTU, Kgs. Lyngby, Denmark, 2003. Available at http://www2.imm.dtu.dk/pubdb/views/publication_details.php?id=2533.

Svend W. Enevoldson, Poul Alberg Østergaard, Poul Erik Morthorst, and Rune Moesgaard. Vindkraftens betydning for elprisen i danmark. Technical report, IBT-Wind, 2006. In Danish.

Paolo Giabardo and Marco Zugno. Competitive bidding and stability analysis in electricity markets using control theory. Master's thesis, Informatics and Mathematical Modeling, Technical University of Denmark, DTU, Kgs. Lyngby, Denmark, 2008. Available at www2.imm.dtu.dk/~pp/thesis.htm.

Paolo Giabardo, Marco Zugno, Pierre Pinson, and Henrik Madsen. Feedback, competition and stochasticity in a day ahead electricity market. *Energy Economics*, 32(2):292–301, 2010.

Gregor Giebel, George Kariniotakis, and Richard Brownsword. The state-of-the-art in short-term prediction of wind power - a literature overview. *EU project Anemos, Deliverable Report D1.1, Available at http://anemos.cma.fr/download/ANEMOS_D1.1_StateOfTheArt_v1.1.pdf*, 2003.

Alicia Mateo González, Antonio Muñoz San Roque, and Javier García-González. Modeling and forecasting electricity prices with input/output

hidden markov models. *IEEE Transactions on Power Systems*, 20(1):13–24, 2005.

Ronald Huisman, Christian Huurman, and Ronald Mahieu. Hourly electricity prices in day-ahead markets. *Energy Economics*, 29(2):240–248, 2006.

Tryggvi Jónsson. Forecasting of electricity prices accounting for wind power predictions. Master's thesis, Informatics and Mathematical Modeling, Technical University of Denmark, DTU, Kgs. Lyngby, Denmark, 2008.

Nektaria V. Karakatsani and Derek W. Bunn. Forecasting electricity prices: The impact of fundamentals and time-varying coefficients. *International Journal of Forecasting*, 24(4):764–785, 2008.

Peter Kosater and Karl Mosler. Can Markov regime-switching models improve power-price forecasts? Evidence from German daily power prices. *Applied Energy*, 83(9):943–958, 2006.

Francis A. Longstaff and Ashley W. Wang. Electricity forward prices: A high-frequency empirical analysis. *The Journal of Finance*, 59(4):1877–1900, 2004.

Henrik Madsen and Jan Holst. *Modelling Non-Linear and Non-Stationary Time Series (Lecture Notes)*. IMM, DTU, Kgs. Lyngby, Denmark, 2000.

Paras Mandal, Tomonobu Senjyu, and Toshihisa Funabashi. Neural networks approach to forecast several hour ahead electricity prices and loads in deregulated markets. *Energy Conversion & Management*, 47(15-16):2128–2142, 2006.

Julija Matevosyan and Lennart Söder. Minimization of imbalance cost trading wind power on the short-term power market. *IEEE Transactions on Power Systems*, 21(3):1396–1404, 2006.

Peter Meibom. Market consequences [in my view]. *IEEE Power and Energy Magazine*, 5(6):120–118, 2007.

Rune Moesgaard and Poul Erik Morthorst. The impact of wind power on electricity prices in denmark. In *EWEC 2008, European Wind Energy Conference, Business and Policy Track*, Brussels, Belgium, April 2008.

Jan K. Møller, Henrik Aa. Nielsen, and Henrik Madsen. Time-adaptive quantile regression. *Computational Statistics and Data Analysis*, 52(3):1292–1303, 2008.

Poul Erik Morthorst. Wind power and the conditions at a liberalized power market. *Wind Energy*, 6(3):297–308, 2003.

Henrik Aa. Nielsen, Torben S. Nielsen, Alfred K. Joensen, Henrik Madsen, and Jan Holst. Tracking time-varying coefficient functions. *International Journal of Adaptive Control and Signal Processing*, 14(8):813–828, 2000.

Torben Skov Nielsen, Henrik Aalborg Nielsen, and Henrik Madsen. Prediction of wind power using time-varying coefficient functions. In *15th IFAC World Congress*, Barcelona, Spain, 2002.

F.J. Nogales and Antonio J. Conejo. Electricity price forecasting through transfer function models. *Journal of Operational Research Society*, 57(3):350–356, 2006.

Nord Pool Spot AS. *Bidding in Nord Pool Spot's Elspot Market*, 2006a. Available at www.nordpoolspot.com.

Nord Pool Spot AS. *Calculation of System- and Area prices*, 2006b. Available at www.nordpoolspot.com.

Anastasios Panagiotelis and Michael Smith. Bayesian density forecasting of intraday electricity prices using multivariate skew-t distributions. *International Journal of Forecasting*, 24(4):710–727, 2008.

Pierre Pinson, Christophe Chevallier, and George N. Kariniotakis. Trading wind generation from short-term probabilistic forecasts of wind power. *IEEE Transactions on Power Systems*, 22(3):1148–1156, 2007.

Claudio M. Ruibal and Mainak Mazumdar. Forecasting the mean and the variance of electricity prices in deregulated markets. *IEEE Transactions on Power Systems*, 23(1):25–32, 2008.

Hans-Gunter Schwarz, Christoph Lang, and Sonja Meier. Market power in the german wholesale electricity market: What are the political options? *Available at SSRN, http://ssrn.com/abstract=1028201*, 2007.

Michael Sewalt and Cyriel de Jong. Negative prices in electricity markets. *Commodities Now. Available at http://www.erasmusenergy.com/articles/91/1/Negative-prices-in-electricity-markets/Page1.html*, 2003.

Klaus Skytte. The regulating power market on the nordic power exchange nord pool: An econometric analysis. *Energy Economics*, 21(4):295–308, 1999.

James W. Taylor and Patrick E. McSharry. Short-term load forecasting methods: An evaluation based on european data. *IEEE Transactions on Power Systems*, 22(4):2213–2219, 2007.

Iivo Vehviläinen and Tuomas Pyykkönen. Stochastic factor model for electricity spot price - the case of the nordic market. *Energy Economics*, 27(2):351–367, 2005.

PAPER B

On the market impact of wind power (forecasts) - An overview of the effects of large-scale integration of wind power on the electricity market

---

Authors:
T. Jónsson, M. Zugno, P. Pinson, H. Madsen

In proceedings:
IAEE's 33rd International Conference

On the market impact of wind power (forecasts) - An overview of the effects of large-scale integration of wind power on the electricity market

Tryggvi Jónsson[1,2] Marco Zugno[2] Pierre Pinson[2] Henrik Madsen[2]

Abstract

Large-scale integration of wind power, and non-dispatchable renewable generation units in general, implies substantial changes in the dynamics of deregulated electricity markets. The varying production capacity of such plants along with their extremely low marginal costs introduces greater volatility of the prices and increases the demand for flexible generation units for regulation and frequency control. The paper illustrates the magnitude and the characteristics of the effects wind power has on the electricity spot prices and on the penalties associated with producers' imbalances when its share in the generation portfolio is substantial. Trough statistical analysis the relationship between prices and forecasted wind power production is shown to be highly non-linear and to exhibit strong seasonal behavior. Finally, the paper touches upon how the sign of the regulation need, i.e. whether production surpluses or deficits will be penalized, can be modeled accounting for the non-linearities imposed on the prices by large-scale integration of wind power in a power system.

Notation and Abbreviations

Although variables and abbreviations are introduced as the paper progresses, its notation is summarized here for the sake of clarity.

[1]ENFOR A/S, Lyngsø Allé 3, DK-2970 Hørsholm, Denmark
[2]DTU Informatics, Technical University of Denmark, Richard Petersens Plads, building 321, DK-2800 Kgs. Lyngby, Denmark

Symbol	Description	Unit
W	Wind Power Production	MWh
π	Price	DKK/MWh
ψ	Regulation Penalty	DKK/MWh
ρ	Revenue	DKK
G	Total production in the system(area)	MWh
L	Total consumption in the system(area)	MWh
χ	Available information	$-$
PTU	Programme time unit	h

Superscript	Description
$(\uparrow)/(\downarrow)$	Up / Down (regulation)
(S)	Spot (Price)

Subscript	Description
t	PTU t
k	Lead Time from t

Accent	Description
$\widehat{\ }$	Forecast
$\sim$	Bid

1 Introduction

The debate on global warming caused by emission of greenhouse gases has increased the focus on the utilization of renewable energy sources around the world. With a prominent share in the total emission of carbon dioxide world wide, electricity generation has been of great interest in that prospective, resulting in ambitious targets for reducing emissions in many countries. This paper discusses the impact of large-scale integration of one of these sources, wind power, on deregulated electricity markets. The impact is shown to be nonlinear, time-varying on different scales and of such extent that it should not be neglected when future plans for the integration of renewable energy are made. In addition, ways of utilizing these effects for more efficient trading of wind power through forecasting are discussed. The results presented here are obtained using data from the two Danish grid areas of the Nordic power exchange for a period of 25 consecutive months starting in January 2008. Despite being case specific, the results shown here are likely to hold for other power exchanges of similar structure.

The transition of electricity markets towards a more deregulated structure began in the early nineteen nineties for the purpose of increasing transparency and efficiency in the electricity sector and has been ongoing ever since. These

markets can provide an excellent platform for producers of renewable energy to sell their production as transactions are based on very short time periods. Even so, the fact that many of these markets were constituted before the emergence of renewable energy sources has lead to some aspects of these markets such as relatively long time between gate-closure and delivery, being unfavorable for producers of such energy. The reason lies in the fundamental difference between conventional power generation and power production by renewable energy sources that the former can be scheduled in advance while the latter depends entirely upon the forces of nature. This characteristic of renewable energy, the resulting low marginal costs and potential prioritization, causes frequent variations in the shape of the supply function (Giabardo et al., 2010). One of the aims of this paper is to map these variations by directly estimate prices as a function of forecasted wind power production.

The backbone of many of these markets are day-ahead spot markets with gate-closure around noon on the day before delivery. Selling energy on a day-ahead basis implies that wind energy producers have to rely on forecasts of their future production with the same lead time (see e.g. Giebel et al., 2003, Costa et al., 2008, for a state of the are review). Naturally, those forecasts are subject to errors which consequently become an integrated part of the supply curve. Hence, the analysis presented in this paper is done using forecasts of wind power production instead of actual measured production. Furthermore, following the suggestions of Jónsson et al. (2010), it is the proportion of the total demand supplied by wind power, termed wind power penetration, that is used for assessing this relation. By doing so, the impact of seasonal variation in the demand is excluded from the relationship. Subsequently, using conditional parametric methods, the relationship between day-ahead spot prices is shown to have the aforementioned characteristics.

In addition, the relationship between the forecasted wind power penetration and the active regulation direction on the real-time imbalance market in the two areas is investigated. As the discrete formulation of the problem prevents the same methods as for the spot price to be used, this relationship is estimated by segmenting the data by the wind power penetration and calculate the proportion of active regulation in each direction within each bin. Subsequently, hypothesis testing is used in order to confirm that the means are truly different from each other. Finally, thoughts on how the results of this paper can be utilized for improved trading of wind power are discussed and model formulations presented.

2 The Nordic Power Market

The Nordic power exchange, Nord Pool[1], operates markets for trading both physical as well as financial power contracts. The physical markets are organized by Nord Pool Spot ASA, a company jointly owned by the transmission system operators (TSOs) in Denmark, Finland, Norway, Sweden and the mother company Nord Pool ASA, each with a 20% share. Besides these countries, the markets operate in Northeastern Germany[2] and since recently, in Estonia as well.

The physical markets are two, Elspot and Elbas. Elspot is a day ahead spot market on which hourly contracts for next day delivery are traded with a gate closure at noon. After collecting bids for purchase and sale of energy, the system price is derived by matching the aggregated supply and demand curves for the whole region. The system price is calculated without regard to transmission limitations and is the reference for nearly all financial contracts. Furthermore, it is the price at which physical contracts are settled if transmission capacity is sufficient throughout the market region. However, due to limited transmission capacity across the nations' borders and within some member countries, the region is split up in several price areas. Each area price is found in the same manner as the system price merely considering bids from that area while viewing the production deficits or surpluses of the neighboring areas as price independent bids for purchase or sale. In the event of transmission capacity being fully utilized somewhere in the region, physical contracts are settled at the corresponding area prices.

Elbas is an intraday market where bilateral contracts are traded in real time up to one hour prior to delivery. Transactions between parties in different areas are subject to the availability of transmission capacity. Unfortunately, Elbas suffers from illiquidity as only 0.3% of the volume traded each year at Nord Pool is sold on Elbas.

The TSO in each country is responsible for frequency control in their area(s). For that purpose they operate a real-time balance market or regulation market at which producers and retailers have to settle deviations from their contracts. Here producers with flexible generation units state how much they are willing to increase or decrease their production in a given hour within 15 minutes notice and at what cost. The TSO then accepts bids in real time based on their monitoring of the system's frequency. The regulation price for a given hour is defined as the most expensive regulation power activated during that hour. Further functional details of these markets differ slightly between the countries

[1] www.nordpool.com, www.nordpoolspot.com

[2] The area is commonly referred to as KONTEK

and in order to stick with relevant matters, only the Danish market is outlined.

In Denmark, regulation prices are constrained by the spot price in such a manner that nothing can be gained by deliberately being out of balance. This implies that the price for up regulation is at lowest equal to the spot price whereas the down regulation price can never exceed the spot price. Furthermore, individual imbalances that counterbalance the system's net imbalance go unpenalized which entails that only one of the two regulation prices is different from the spot price at any given time.

Denmark comprises two price areas bordered by the Great Belt channel which separates the islands of Zealand and Funen. The area west of the channel is called DK-1 while the eastern part is referred to as DK-2. Denmark has been a leading nation in the integration of wind power and currently around 18 % of its annual electricity production is produced by wind turbines[3]. In DK-1 this share is much higher though as ca. 25% of the area's annual power consumption is supplied by wind power. On the contrary the same figure for DK-2 is 12%. Other energy sources with significant share in the generation mix are coal plants with around 50% share, natural gas with approximately 20% and waste-to-energy plants with 5% for both areas combined.

3 The Data

Since wind power is a non-dispatchable energy source, producers rely on forecasts of future production when trading on a day-ahead basis. Consequently, wind power enters the supply curve in the form of a forecast which naturally will deviate from the actual production. For this reason, impact of wind power on any market dynamics should be viewed upon in terms of the forecasts actually entering the supply curve instead of actual production measurements. It can be debated whether other market fundamentals, known at the time of price calculation, should enter such an analysis as forecast or as observations. However in order to allow for any inference on whether or not the inclusion of wind power in a forecasting model for the market is legitimate, only information available before gate-closure is used in the following. Hence, the results presented are solely based on forecasts available at the time of bidding unless otherwise specified.

The data used in the analysis consist of hourly observations of prices in the two Danish areas for the period from the beginning of 2008 and through January 2010. These observations have been made publicly available by Energinet.dk[4],

[3] Source: http://www.nordpoolspot.com/reports/Production_split/

[4] www.energinet.dk

the Danish TSO, through their website. Furthermore, publicly available load forecasts for the same period were obtained from Nord Pool Spot's website. Finally, predictions of wind power production are acquired from a commercial wind power forecasting model, WPPT[5] (Nielsen et al., 2002). Both forecasting series are for their totals within each area, with a temporal resolution of 1 hour and issued at 10 o'clock on the day before their realization.

4 Wind Power's Impact on the Market

Jónsson et al. (2010) suggests that the impact of wind power on the market should be analyzed with reference to the proportional contribution of wind power to the total consumption. By doing so, the correlation among prices and demand can be eliminated and thus will the analysis only reveal the direct impact of wind power on the market. We therefore define the (forecasted) wind power penetration at any given hour t as

$$\frac{\widehat{W}_{t|t-k}}{\widehat{L}_{t|t-k}}$$

where W_t is the wind power production during that hour, L_t is the consumption at during the same period and k is the time between gate-closure and actual delivery.

4.1 Impact on Day-Ahead Prices

As in Jónsson et al. (2010), the relationship between wind power penetration and spot prices are assessed with the aid of a conditional parametric model. The mathematical formulation of the model was originally introduced by Cleveland and Devlin (1988), but in order to make the paper self-contained a short formulation specifically for the problem at hand follows.

Let a model for the spot prices at time t, $\pi_t^{(S)}$, be defined as

$$\pi_t^{(S)} = \boldsymbol{\theta}(\boldsymbol{x}_t) + \varepsilon_t, \tag{1}$$

where $\boldsymbol{\theta}(\cdot)$ is a vector of coefficient functions and ε_t is a noise term. Furthermore, $\boldsymbol{x}_t$ is a vector of explanatory variables. In this case those variables are the forecasted wind power penetration, $\widehat{\zeta}_t$, and an hour of the day indicator, κ_t.

[5] www.enfor.dk

The functions $\boldsymbol{\theta}(\cdot)$ are estimated at a number of distinct points by approximating the functions using polynomials and fitting the resulting linear model locally to each of these fitting points. More specifically, let $\boldsymbol{U} = \begin{bmatrix} \widehat{\zeta}_U & \kappa_U \end{bmatrix}^T$ denote a particular fitting point, chosen from a set of m total fitting points, and let $\boldsymbol{p}_2(\boldsymbol{U})$ be a column vector of terms in the corresponding 2*nd*-order polynomial, i.e.

$$\boldsymbol{p}_2(\boldsymbol{U}) = \begin{bmatrix} 1 & \widehat{\zeta}_U & \kappa_U & \widehat{\zeta}_U^2 & \widehat{\zeta}_U\kappa_U & \kappa_U^2 \end{bmatrix}^T. \tag{2}$$

In addition, let $\boldsymbol{\phi}_U = \begin{bmatrix} \phi_{U,1} & \dots & \phi_{U,7} \end{bmatrix}^T$ denote the coefficient vector at $\boldsymbol{U}$. Now the linear model

$$\pi_U^{(S)} = \boldsymbol{p}_2(\boldsymbol{U})^T\boldsymbol{\phi}_U + \varepsilon_U \tag{3}$$

can be used to describe the spot price in the close vicinity of $\boldsymbol{U}$ and can be fitted locally using weighted least squares (WLS), i.e.

$$\widehat{\boldsymbol{\phi}}(\boldsymbol{U}) = \underset{\boldsymbol{\phi}_U}{\arg\min} \sum_{i=1}^{N} v_U(\boldsymbol{x}_i)\left(\pi_i^{(S)} - x_i^T\boldsymbol{\phi}_U\right)^2 \tag{4}$$

where $\boldsymbol{x}_i = \boldsymbol{p}_2(\boldsymbol{U}_i)$ and for which a unique closed-form solution exists provided that the matrix with rows $\boldsymbol{x}_i$ corresponding to non-zero weights has a full rank. The weights are assigned as

$$v_U(\boldsymbol{x}_i) = V\left(\frac{||\boldsymbol{x}_i - \boldsymbol{x}||_2}{h(\boldsymbol{x})}\right) \tag{5}$$

where $V(\cdot)$ is a decreasing weight function taking non-negative arguments. Furthermore, $h(\boldsymbol{x})$ is the bandwidth used for the particular fitting point, i.e. the maximum euclidean distance between a fitting point and an observation resulting in a non-zero weight being assigned in Eq. (4). This implies that a small bandwidth will result in a very flexible model with low bias and high variance while applying a large bandwidth yields a more rigid model with higher bias but lower variance. For readers familiar to exponential smoothing, applying a small bandwidth corresponds to having a low level of smoothing in the model. The bandwidth can therefore be said to be a scalar controlling the rate at which the weight of an observation in the estimation process, decreases with distance from the fitting point. This implies that the argument which $V(\cdot)$ takes is the relative distance between the fitting point and the other point falling within the bandwidth. Following Cleveland and Devlin (1988) and Nielsen et al. (2000), a tri-cube kernel is chosen as a weight function so

$$V(u) = \begin{cases} (1-u^3)^3 & u \in [0,1) \\ 0 & u \in [1,\infty) \end{cases}. \tag{6}$$

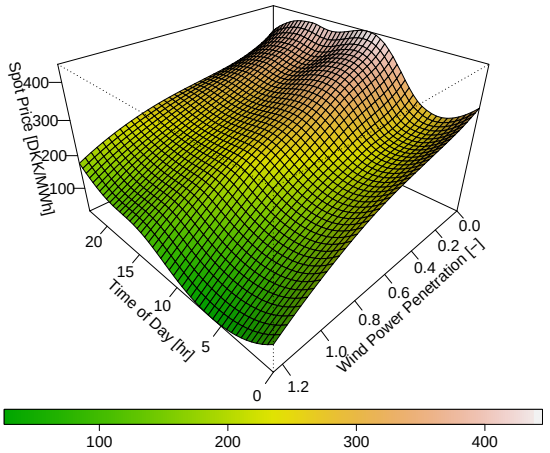

Figure 1: Surface plots of the average spot price in DK-1 as a function of wind power penetration and its variation throughout the day

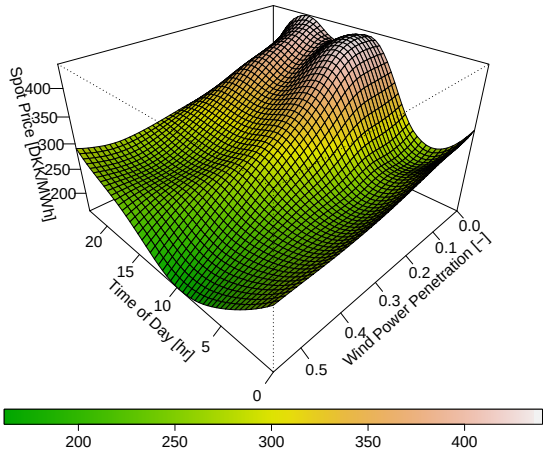

Figure 2: Surface plots of the average spot price in DK-2 as a function of wind power penetration and its variation throughout the day

Turning back to the global view on the model, it can be seen that for an arbitrary chosen $\boldsymbol{U}$, out of a set of m fitting points, there can be found a parameter vector ϕ_U. From these, the elements of $\boldsymbol{\theta}(\boldsymbol{x}_t)$ are estimated as

$$\widehat{\boldsymbol{\theta}}(\boldsymbol{x}_t) = \widehat{\boldsymbol{\theta}}(\boldsymbol{p}_2(\boldsymbol{U} = \boldsymbol{x}_t)) = \boldsymbol{p}_2^T(\boldsymbol{U})\widehat{\boldsymbol{\phi}}(\boldsymbol{U}) \tag{7}$$

where $\widehat{\boldsymbol{\phi}}(\boldsymbol{U})$ is the WLS estimate of $\boldsymbol{\phi_U}$.

The bandwidth, $h(\boldsymbol{x})$ is chosen so that at any given time 30% of all observations fulfil $||\boldsymbol{x}_i - \boldsymbol{x}||_2 \leq h(\boldsymbol{x})$. In other words, the bandwidth is varied according to the local density of the data by letting $h(\boldsymbol{x})$ be equal to the distance of the qth-nearest $\boldsymbol{x}_i$ to $\boldsymbol{x}$, where q is 30% of the total number of observations (see e.g. Cleveland and Devlin, 1988, for details). This criteria is applied for estimation in all $m = 24^2$ fitting points.

How the method is applied in the analysis to follow can be summarized as follows. First the data is scaled so all variables are between $[-1, 1]$. Then a grid of $m = 24 \times 24$ equidistant fitting points is defined. For each of these fitting points, $\boldsymbol{U}_{m_i}$, the following steps are taken:

1. Calculate the euclidean distances between every observation and the fitting point of interest. Applying the bandwidth principle previously described, these distances are normalized by that corresponding to the qth-nearest neighbor, where q is set to 30%, and thereby form the input to Eq. (6).

2. Compute the estimate $\hat{\Phi}(\boldsymbol{U}_{m_i})$ of the local polynomial coefficients at the fitting point $\boldsymbol{U}_{m_i}$ by solving Eq. (4).

3. Obtain the local estimate of the spot price at $\boldsymbol{U}_{m_i}$ from Eq. (7) with $p_2(\boldsymbol{U}_{m_i})$ as the polynomial for the particular fitting point as described by Eq. (2).

The mean spot price for any point $\boldsymbol{U}$ can be obtained by bilinear interpolation from the local estimates calculated at each fitting point. This finally yields a smooth trend surface like those shown and commented on in the following.

Figures 1 and 2 show a surface plot of the average behavior of the spot prices as a function of wind power penetration and time of the day in DK-1 and DK-2 respectively. The same is shown as contour plots in Figure 3. Although wind power's contribution to the supply seems the have a somewhat less effect during the night in DK-1, the impact of wind power is quite evident throughout the whole day. Conversely for DK-2, the impact of wind power seems to be primarily bounded to the day and the evening. The plots show how the increased wind power penetration gradually excludes the less cost-efficient energy sources. The varying gradient is a result of the discontinuity of the supply function and its steepness for high values. Moreover, the plots exhibit quite

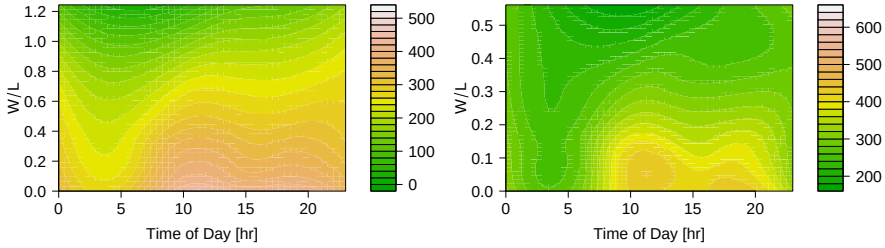

Figure 3: Contour plot of the average spot price in DK-1 (left) and DK-2 (right) as a function of wind power penetration and time of day

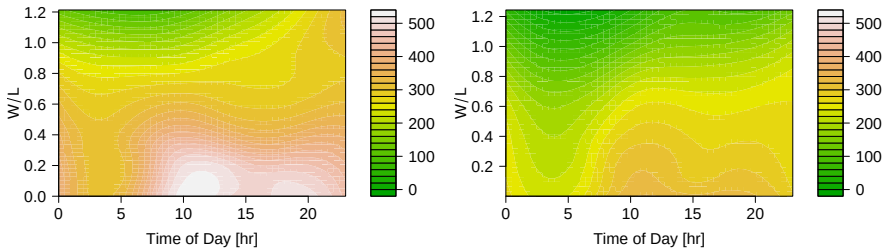

Figure 4: Contour plot of the average spot price in DK-1 in 2008 (left) and 2009 (right) as a function of wind power penetration and time of day

clearly the intra-day variation of the prices with two peaks in the morning and the early evening. However, it is interesting that for DK-1 this daily seasonality diminishes to some extend with increased penetration of wind power.

In Figures 4 and 5, the same relationship as before is plotted for 2008 and 2009 separately. Whereas the high fuel prices of 2008 are evident from the higher overall level of the left hand side figures, the behavioral pattern is otherwise quite consistent between the two years for both areas. Apart from the level shift, the high prices of 2008 also boosts the intra-day variation in the prices. This is a consequence of the large share of the load supplied by hydro- and wind power during night. Hence making the prices less dependent on the prices of fossil fuels during night than they are during the day where demand peaks.

The prices at Nord Pool are generally dominated by the water level in the hydro power reservoirs in North. This level has a strong yearly seasonal pattern which should be reflected in the impact of other sources as well. We therefore estimate the impact of wind power penetration for each quarter of the year separately, resulting in the plot displayed in Figures 6 and 7. In order to avoid

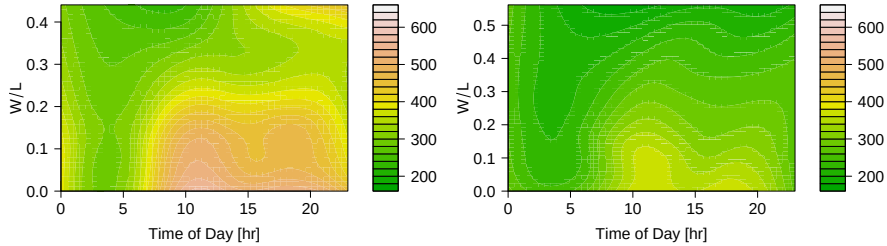

Figure 5: Contour plot of the average spot price in DK-2 in 2008 (left) and 2009 (right) as a function of wind power penetration and time of day

effects from the different price level between years, only data from 2009 are used for the construction of these plots. The general pattern in the relationship remains the same between the quarters although changes in the price level are evident. However, it seems as the impact of wind power is more substantial during periods where there water reserve is low (2nd quarter). The cause of this is most likely that the lowest end of the supply curve is almost entirely made up of wind power during those periods. Hence magnifying its impact.

To summarize, the stochastic threshold in the supply curve, resulting from the presence of wind power (Giabardo et al., 2010), is quite evident from the plots presented. Above all, it is shown that the relationship between share of wind power in the generation portfolio and the spot prices is both existent and highly nonlinear. An interesting feature of this relation is that the daily seasonality of the prices vanishes to a certain degree during hours of high wind power penetration. Furthermore, the long-term variation in the link between the two suggests that recursivity or seasonality with long cycles should be used if the results are to be used as a basis for forecasting models.

4.2 Impact on the Imbalance Sign

As explained in Zugno et al. (2010), knowledge about the real-time regulation market is extremely beneficial when placing a bid for wind power production. If it exists, information about the impact of wind power on any aspects of the regulation market could play an important role in obtaining such forecasts. This prompts us to investigate whether, and subsequently to what extent, the anything can be told about the regulation direction from forecasts of wind power penetration.

What formally determines whether a given PTU t is defined as an up regulation

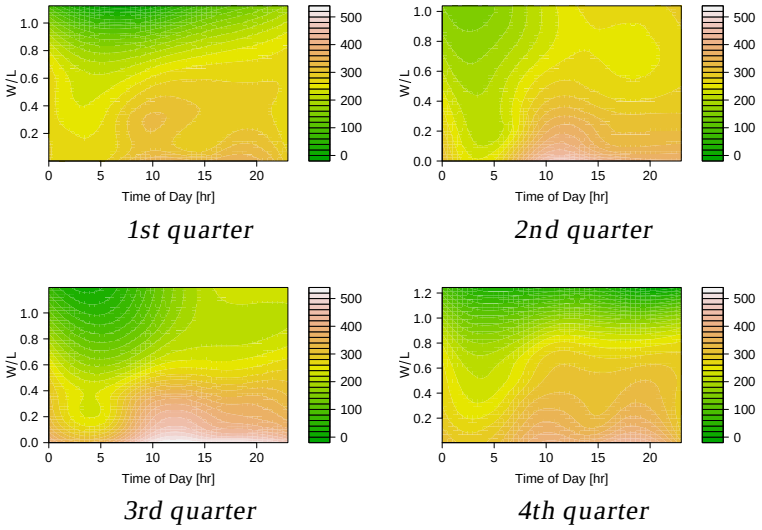

Figure 6: Contour plot of the average spot price in DK-1 as a function of wind power penetration and time of day, estimated for each quarter of the year

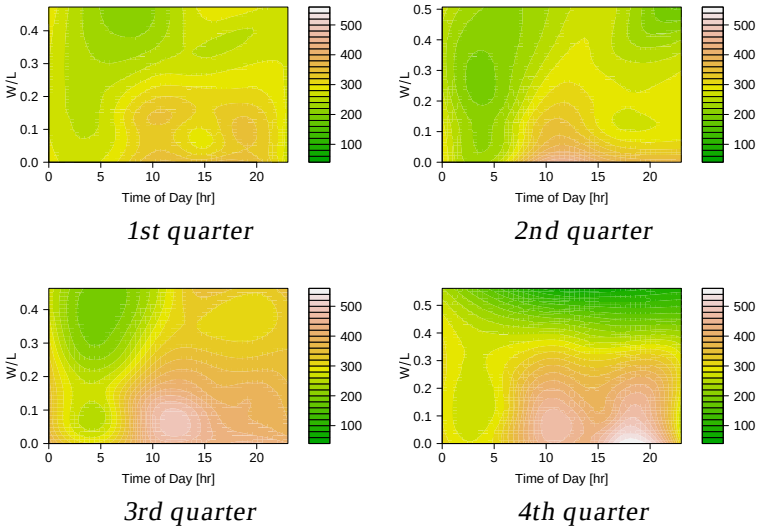

Figure 7: Contour plot of the average spot price in DK-2 as a function of wind power penetration and time of day, estimated for each quarter of the year

hour or a down regulation hour is

$$\text{sign}\left\{\left(\widetilde{G}_t - G_t\right) - \left(\widetilde{L}_t - L_t\right)\right\} \tag{8}$$

where G_t is the total volume produced in the area, L_t is the total demand and the accent $\widetilde{\cdot}$ signals the volume traded for the same quantities. Eq. (8) takes the value -1 during production surplus hours or down regulation hours, while it becomes 1 during hours of production deficit, that is during up regulation hours. The market's regulative framework implies that the maximum potential revenue for any given hour is received by either producing exactly the contracted quantity of electricity or by counterbalancing the system's imbalance with one's own. From a trading perspective we are therefore interested in placing our bids in such a manner that they fall on the "correct side" of the system imbalance and not necessarily precisely bidding the produced quantity. Hence a more relevant formulation of Eq. (8) for this purpose is to formulate it in terms of the regulation penalty, $\psi^{(\uparrow/\downarrow)}$, as

$$\text{sign}\left\{\left(\pi_t^{(\uparrow)} - \pi_t^{(S)}\right) + \left(\pi^{(\downarrow)} - \pi_t^{(S)}\right)\right\} = \text{sign}\left\{\psi_t^{(\uparrow)} + \psi^{(\downarrow)}\right\}. \tag{9}$$

where $\pi_t^{(S)}$ is the spot price at time t, $\pi_t^{(\uparrow)}$ is the up regulation price and $\pi_t^{(\downarrow)}$ is the down regulation price. Furthermore the regulation penalties are defined as

$$\psi_t^{(\downarrow)} = \pi_t^{(\downarrow)} - \pi_t^{(S)} \leq 0 \quad \text{and} \quad \psi_t^{(\uparrow)} = \pi_t^{(\uparrow)} - \pi_t^{(S)} \geq 0 \tag{10}$$

for which it should hold that only one is different from zero at any given time.

In harmony with Eq. (8), Eq. (9) should take the value -1 during down regulation hours and the value 1 during up regulation hours. What differs however between the two is that the latter only becomes different from zero during hours when imbalances can prompt a penalty or put differently reduced revenue.

We now define two indicator variables, one for each direction of regulation, as

$$I_t^{(\uparrow)} = \begin{cases} 1 & \text{if } \pi^{(\uparrow)} > \pi^{(S)} \\ 0 & \text{otherwise} \end{cases}, \quad I_t^{(\downarrow)} = \begin{cases} 1 & \text{if } \pi^{(\downarrow)} < \pi^{(S)} \\ 0 & \text{otherwise} \end{cases}. \tag{11}$$

Now the data is segmented into 20 equally sized bins according to the forecasted wind power penetration. That is the first bin will include observations from hours for which wind power penetration is below the 5% sample quantile, the second one will contain observations for which $\widehat{W}/\widehat{L}$ is between the 5% and 10% sample quantile, etc. In Figure 8, the averages of $I^{(\uparrow/\downarrow)}$ within each bin are plotted against the median penetration within the same bin for each area. The y-axis of the plots therefore translates to the proportion of hours within each

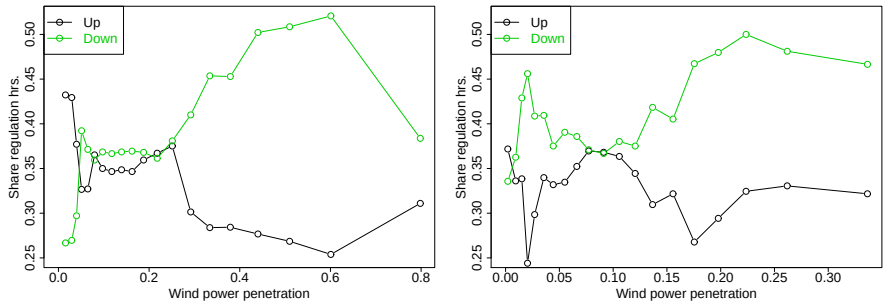

Figure 8: Proportion of regulation hours in each direction under different levels of wind power penetration for DK-1 (left) and DK-2 (right)

bin that have a particular imbalance sign. In order to verify that the bin means are truly different from each other, hypothesis testing is used. More specifically, the null hypothesis that the mean of a single bin is equal to that of any other bin is tested against the alternative hypothesis that the means are different. In this case testing of the means of two bernoulli variables is appropriate.

The plots reveal, what is also strongly supported by hypothesis testing, that there is a considerable difference between those proportions among the bins. The increased proportion of down regulation hours for hours with wind power penetration above the sample median is quite interesting. The production is obviously bounded by the installed capacity and thus the errors as well. The high share of down regulation can then be interpreted as the producers' reluctance to bid close to their nominal capacity out of fear of having close to one sided risk. Alternatively, this increase could be caused by the forecasting models' incapability to accurately forecast production close to full production. What contradicts the latter is though for how low production this increase becomes observable. Nevertheless, the explanation for this is most likely a mixture of both. For the same reasons, the higher share of up regulation hours for the absolutely lower penetration level in DK-1 is peculiar. The expectance of very low production should leave one the very little probability of under producing. Consequently proportions near the opposite is what intuitively would be expected. This aside, the lines' strong negative correlation is also of interest. It implies that the increase or decrease in the shares are mainly at the cost of the opposite regulation direction while the proportion of hours with no regulation penalty is less affected.

The values plotted are obtained by a static splitting of the data and therefore would any long-term time variation of the relation plotted not be revealed. As will be demonstrated later on in the paper, this variation is present in the imbalance sign. Its presence can however only act as a diminishing factor on the

relationship as it is an additional source of noise in the data set. Thus estimating the relation adaptively could only increase the difference between bins and never reduce it.

In order to assess the daily variation in the relationship between imbalance sign and wind power penetration the same procedure is repeated, now for each hour of the day separately. The result is shown in Figures 9 and 10 for DK-1 and DK-2 respectively. Doing so reveals that the relation is strongest during the daytime hours which coincides nicely with what was observed for the spot price. Apart from that, what has been said earlier generally holds for each hour. The difference between hours is so large though that the within-day seasonality of this effect should somehow be accounted for in a forecasting model.

5 Briefly on the Bidding Decision

One possible utilization of the effects demonstrated in the previous section is to use them for short-term forecasting of the market dynamics. These forecasts in turn can contribute to better decision making when wind power is sold on deregulated electricity markets with benefits for both the individual producer as well as the system as a whole. The details of how trading of wind power can be improved and the resulting benefits are described in (Zugno et al., 2010, Pinson et al., 2007, and references therein). Nevertheless, for the sake self-containment, the formulation of the decision making problem will be discussed briefly here.

Recall the definition of the regulation penalty from Eq. (10). One self's imbalance cost for a given PTU can then be found as

$$\rho_t^{(\uparrow/\downarrow)} = \begin{cases} \psi_t^{(\downarrow)} \left(W_t - \widetilde{W}_t \right) & \text{if } \left(W_t - \widetilde{W}_t \right) > 0 \\ \psi_t^{(\uparrow)} \left(W_t - \widetilde{W}_t \right) & \text{if } \left(W_t - \widetilde{W}_t \right) < 0 \end{cases} \tag{12}$$

When trading wind power the ultimate goal must always be to maximize revenue while paying some regard to the risk implied by the volume sold in the process. The revenue of one PTU t can be calculated in terms of $\psi_t^{(\uparrow/\downarrow)}$ and W_t assuming a wind power producer does not consider the Elbas market as a

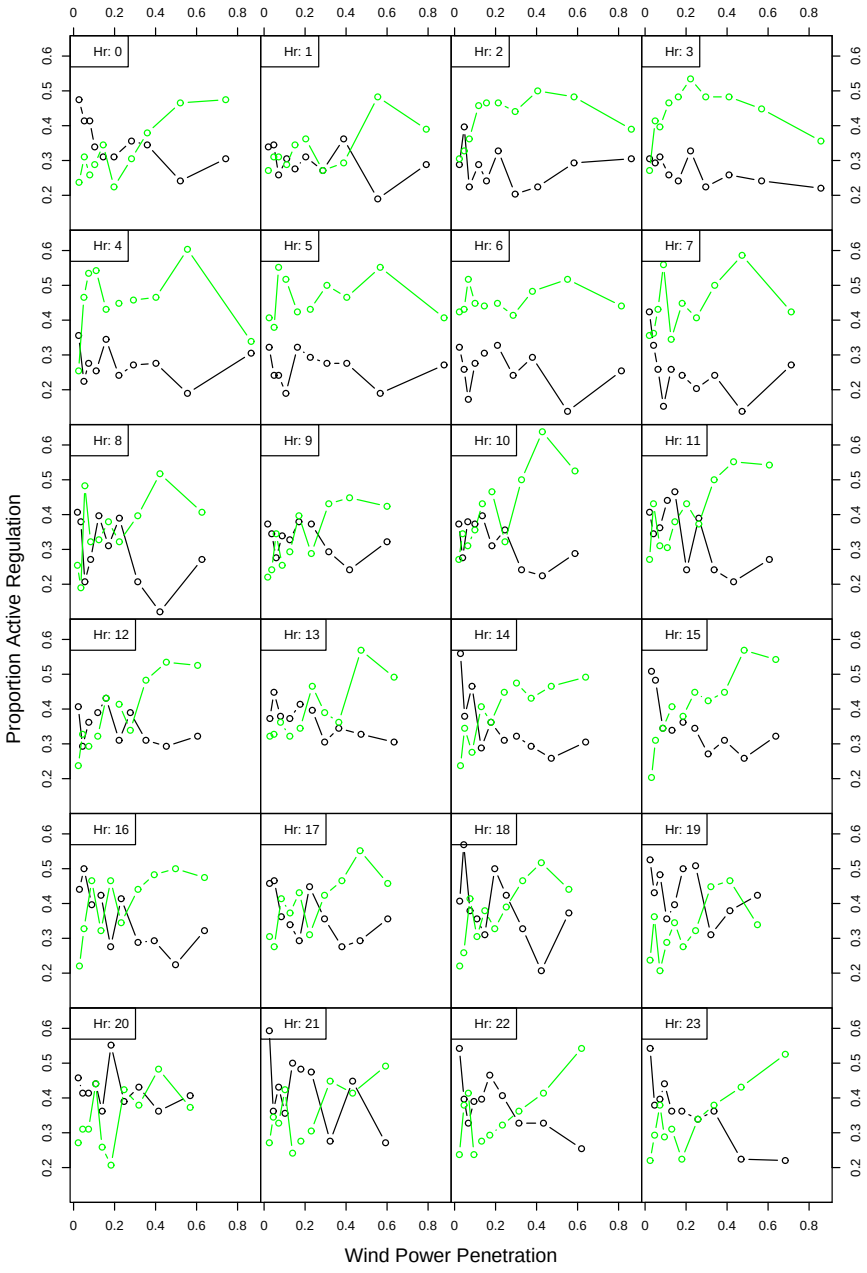

Figure 9: Proportion of regulation hours in each direction under different levels of wind power penetration in DK-1 estimated for each hour of the day separately. Following the convention from Figure 8, green is used for down regulation and black for up regulation.

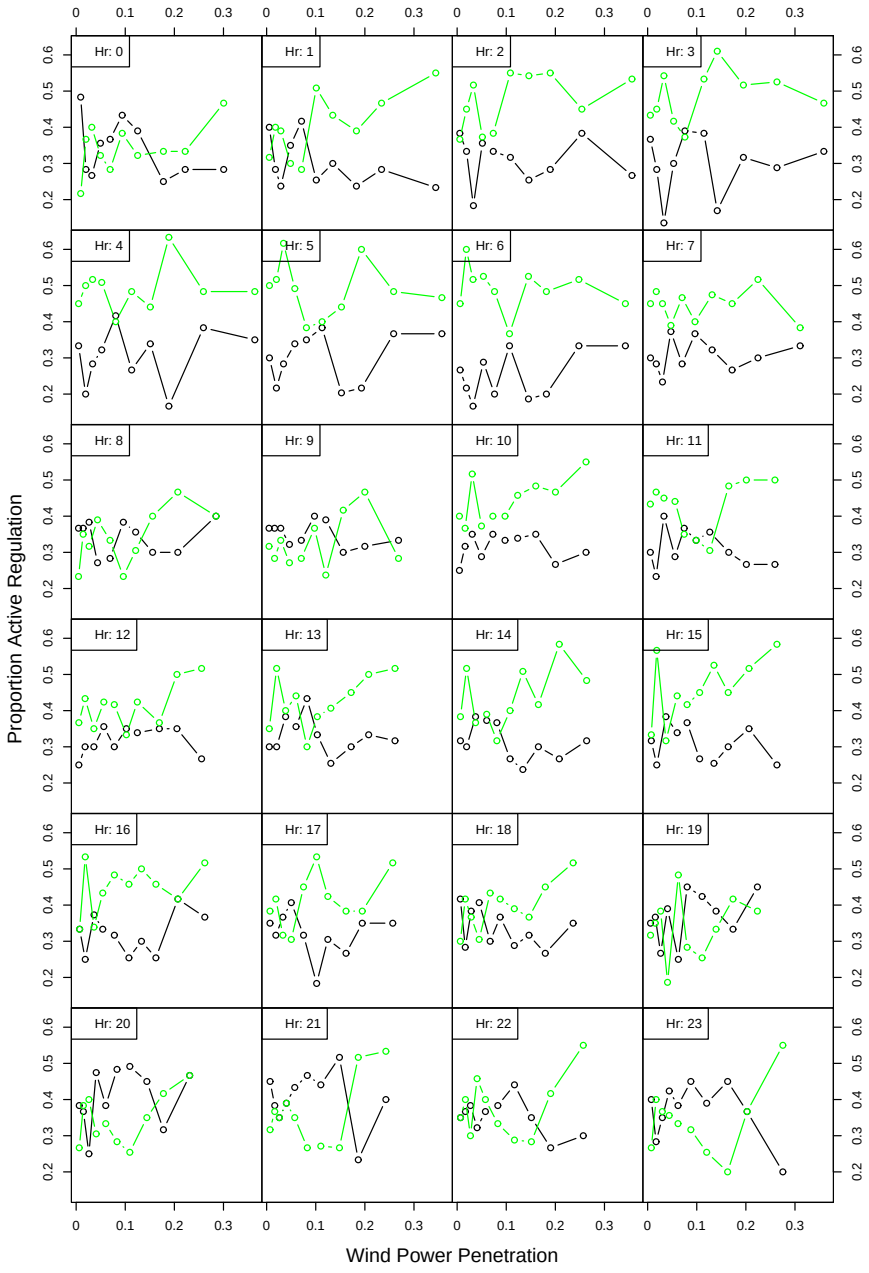

Figure 10: Proportion of regulation hours in each direction under different levels of wind power penetration in DK-2 estimated for each hour of the day separately. Following the convention from Figure 8, green is used for down regulation and black for up regulation.

realistic option for trading as

$$\begin{aligned}\rho_t = &\ \pi_t^{(S)} W_t + \psi_t^{(\downarrow)} \max\left\{W_t - \widetilde{W}_t, 0\right\} \\ &+ \psi_t^{(\uparrow)} \min\left\{W_t - \widetilde{W}_t, 0\right\} \\ = &\ \pi_t^{(S)} W_t + \psi_t^{(\downarrow)} \left(W_t - \widetilde{W}_t\right) I\left\{W_t > \widetilde{W}_t\right\} \\ &+ \psi_t^{(\uparrow)} \left(W_t - \widetilde{W}_t\right) I\left\{W_t < \widetilde{W}_t\right\}.\end{aligned} \tag{13}$$

When a bid is placed, none of the prices are known and at least in the case of wind power, neither are the produced volumes. These quantities therefore need to be regarded by the trader as stochastic variables and he must decide on the decision variable $\widetilde{W}$, by maximizing his expected revenue depending on the stochastic variables $\pi_t^{(S)}$, W_t ,$\pi_t^{(\uparrow/\downarrow)}$ / $\psi_t^{(\uparrow/\downarrow)}$ or the expectations for those, which in turn depend on the information available at the bidding time, χ_t. The expectation of Eq. (13) can be expressed as

$$\begin{aligned}\mathbb{E}\left[\rho_t|\chi_t\right] = &\ \mathbb{E}\left[\pi_t^{(S)}|\chi_t\right] \mathbb{E}\left[W_t\middle|\chi_t\right] \\ &+ \mathbb{P}\left[\pi_t^{(\downarrow)} < \pi_t^{(S)}\middle|\chi_t\right] \mathbb{E}\left[\psi_t^{(\downarrow)}\middle|\pi_t^{(\downarrow)} < \pi_t^{(S)}, \chi_t\right] \\ &\cdot \mathbb{E}\left[\left(W_t - \widetilde{W}_t\right) I\left\{W_t > \widetilde{W}_t\right\}\middle|\chi_t\right] \\ &+ \mathbb{P}\left[\pi_t^{(\uparrow)} > \pi_t^{(S)}\middle|\chi_t\right] \mathbb{E}\left[\psi_t^{(\uparrow)}\middle|\pi_t^{(\uparrow)} > \pi_t^{(S)}, \chi_t\right] \\ &\cdot \mathbb{E}\left[\left(W_t - \widetilde{W}_t\right) I\left\{W_t < \widetilde{W}_t\right\}\middle|\chi_t\right]\end{aligned} \tag{14}$$

assuming

$$\mathbb{E}\left[\pi_t^{(S)}\middle|\widetilde{W}\right] = \mathbb{E}\left[\pi_t^{(S)}\right] \text{ and } \mathbb{E}\left[\pi_t^{(\uparrow/\downarrow)}\middle|\widetilde{W}_t\right] = \mathbb{E}\left[\pi_t^{(\uparrow/\downarrow)}\right],$$

i.e. that the individual wind power producer neither influences the spot price nor the regulation price by his actions. It should be emphasized that there is a difference between the results of the previous chapter, where wind power in the system as a whole is considered, and the impact of the actions of a single producer.

At this point it is important to realize that the highest achievable revenue for a wind power producer is obtained by receiving the spot price for all produced power[6]. Hence maximizing the revenue is exactly the same as minimizing the

[6]Because wind turbines can not provide regulation power. For plants that have the possibility of selling regulating power this might not hold.

imbalance costs. The maximum revenue is thereby found by minimizing the contribution of the last two terms in Eq. (13).

Hence, the objective is to minimize the total imbalance costs, $\rho_t^{(\uparrow/\downarrow)}$, from Eq. (12). Now define

$$\widehat{\psi}_{k|t}^{(\downarrow)} = \mathbb{P}[\psi_{t+k}^{(\downarrow)} < 0|\chi_t]\mathbb{E}[\mathbb{E}[\psi_{t+k}^{(\downarrow)}|\psi_{t+k}^{(\downarrow)} < 0]|\chi_t]$$
$$\widehat{\psi}_{k|t}^{(\uparrow)} = \mathbb{P}[\psi_{t+k}^{(\uparrow)} > 0|\chi_T]\mathbb{E}[\mathbb{E}[\psi_{t+k}^{(\uparrow)}|\psi_{t+k}^{(\uparrow)} > 0]|\chi_t]$$

and assume that in addition to the forecasts defined above, probabilistic forecasts for the wind power generation are available. Making the price taker assumptions previously discussed, $\mathbb{E}[\rho_t^{(\uparrow/\downarrow)}|\chi_t]$ can be written as

$$\begin{aligned}
\mathbb{E}\left[\rho_k^{(\uparrow/\downarrow)}|\chi_t\right] &= \widehat{\psi}_{k|t}^{(\downarrow)}\mathbb{E}\left[\left(W_k - \widetilde{W}_k\right) I\left\{W_k - \widetilde{W}_k > 0\right\}\Big|\chi_t\right] \\
&\quad + \widehat{\psi}_k^{(\uparrow)}\mathbb{E}\left[\left(W_k - \widetilde{W}_k\right) I\left\{W_k - \widetilde{W}_k < 0\right\}\Big|\chi_t\right] \\
&= \widehat{\psi}_{k|t}^{(\downarrow)}\int_{-\infty}^{\infty}\left(y - \widetilde{W}_k\right) I\left\{W_k - \widetilde{W}_k > 0\right\} f_k(y)dy \\
&\quad + \widehat{\psi}_{k|t}^{(\uparrow)}\int_{-\infty}^{\infty}\left(y - \widetilde{W}_k\right) I\left\{W_k - \widetilde{W}_k < 0\right\} f_k(y)dy \\
&= \widehat{\psi}_{k|t}^{(\downarrow)}\int_{\widetilde{W}_k}^{W^{(max)}}\left(y - \widetilde{W}_k\right) f_k(y)dy + \widehat{\psi}_{k|t}^{(\uparrow)} \\
&\quad \cdot \int_0^{\widetilde{W}_k}\left(y - \widetilde{W}_k\right) f_k(y)dy
\end{aligned} \tag{15}$$

where $W^{(max)}$ is the wind power generation capacity. As each term in this equation is ≤ 0 the minimum expected imbalance costs can be found as the solution to

$$\begin{aligned}
\frac{\delta\mathbb{E}\left[\rho_k^{(\uparrow/\downarrow)}|\chi_t\right]}{\delta\widetilde{W}_k} &= -\widehat{\psi}_{k|t}^{(\uparrow)}\int_0^{\widetilde{W}_k} f_k(y)dy - \widehat{\psi}_{k|t}^{(\downarrow)}\int_{\widetilde{W}_k}^{W^{(max)}} f_k(y)dy \\
&= -\widehat{\psi}_{k|t}^{(\uparrow)}(F_k(\widetilde{W}_k) - \underbrace{F_k(0)}_{=0}) - \widehat{\psi}_{k|t}^{(\downarrow)}(\underbrace{F_k(W^{(max)})}_{=1} - F_k(\widetilde{W}_k)) \\
&= F_k(\widetilde{W}_k)(\widehat{\psi}_{k|t}^{(\downarrow)} - \widehat{\psi}_{k|t}^{(\uparrow)}) - \widehat{\psi}_{k|t}^{(\downarrow)}
\end{aligned} \tag{16}$$

where $F_k(\widetilde{W}_k)$ is the CDF of $W_k|\chi_t$. Solving Eq. (16) yields

$$F_k(\widetilde{W}_k) = \frac{|\widehat{\psi}_{k|t}^{(\downarrow)}|}{|\widehat{\psi}_{k|t}^{(\downarrow)}| + \widehat{\psi}_{k|t}^{(\uparrow)}} \tag{17}$$

and therefore the optimal bid is found as the $\frac{|\widehat{\psi}^{(\downarrow)}_{k|t}|}{|\widehat{\psi}^{(\downarrow)}_{k|t}|+\widehat{\psi}^{(\uparrow)}_{k|t}}$-quantile of $F_k(\widetilde{W}_k)$.

In conclusion, forecasts of the regulation market are of main interest, alongside wind power forecast, when optimizing the bid of wind power into a day-ahead market. This is of course given the regulative framework as it is on Nord Pool.

6 Other Aspects of Power Market Forecasting

There are several ways of formulating a forecasting model for $\psi^{(\uparrow/\downarrow)}$, required for solution of the trading decision problem. The market's structure implies that the regulation prices, $\pi^{(\uparrow/\downarrow)}$, essentially comprise two processes each. One set of dynamics are detected during hours of active regulation while the prices are identical to the spot prices at other times. For this reason, it is decided to first estimate the probabilities of regulation in each direction and subsequently forecast the penalty itself, conditioned upon active regulation in the corresponding direction. Forecasting the penalties themselves instead of the prices and subsequently subtract the spot price has the obvious advantage that the penalties are bounded by zero in one direction. In the following, some ideas about how to model the probabilities of active regulation in each direction are presented.

The imbalance sign, Eq. (9), exhibits like every other power market data series seasonal behavior and alternating drift patterns. This can be demonstrated by viewing the values in Table 1 together with the plots in Figure 11. The table states the proportions of each possible outcome of (9) during parts of and the whole data period. If the probabilities of each regulation scenario were static, an exponentially smoothed tracking of them would result in a figure like the one on the left in Figure 11. The figure illustrates tracking of a series simulated from the proportions of 2009. Reality however is that the imbalance sign is a non-stationary process and therefore does an exponentially smoothed tracking of the proportions for 2009 result in the plot on the right. The proportions, which can be interpreted as the unconditional probabilities of regulation in each direction, vary quite severely throughout the year making a static model inappropriate. Furthermore, by zooming in on the plot also reveals a seasonal pattern as is illustrated in Figure 12.

A pragmatic approach to modeling series with the characteristics described above is the Holt-Winters method (Winters, 1960). In its standard form, it is suitable for series with one seasonal pattern. However it is extended to account

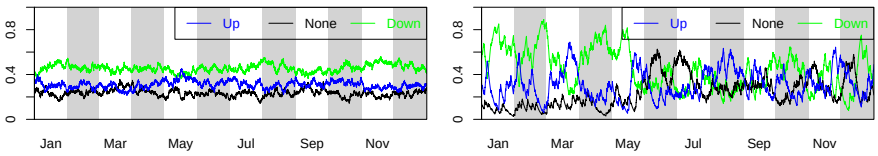

Figure 11: Simulated static imbalance sign probabilities (left) and actual tracked probabilities (right)

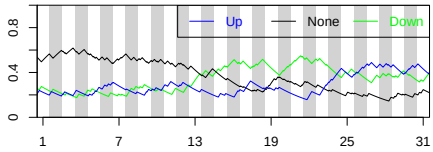

Figure 12: Exponentially smoothed tracking of the unconditional imbalance sign probabilities in July 2009

for double-seasonality in Taylor (2003). Now let us define

$$I_t^{(\psi)} = \left(\; I\{\psi^{(\downarrow)} < 0\}, \quad I\{\psi^{(\downarrow)} = \psi^{(\uparrow)} = 0\}, \quad I\{\psi^{(\uparrow)} > 0\} \; \right)$$

for which it holds that

$$\sum_{i=1}^{3} I_{i,t}^{(\psi)} = 1.$$

Then the probabilities of regulation in each direction occurring can be tracked by simple exponential smoothing, using forgetting factor λ ($0 < \lambda < 1$), by

$$\widehat{I}_t^{(\psi)} = (1-\lambda) I_t^{(\psi)} + \lambda \widehat{I}_t^{(\psi)}$$

from which the k-step ahead estimate for sign probabilities can be found as

$$\widehat{I}_{t+k|t}^{(\psi)} = \widehat{I}_t^{(\psi)}$$

Table 1: Proportion of regulation hours during 2008, 2009 and for the whole data period for both Danish price areas

	DK-1			DK-2		
Period	$\downarrow$	$\sim$	$\uparrow$	$\downarrow$	$\sim$	$\uparrow$
2008	35.00	30.48	34.50	44.66	24.08	31.25
2009	42.00	26.97	31.02	41.17	27.38	31.43
2008-10	38.66	29.19	32.13	43.36	25.37	31.26

and a response type prediction can subsequently be found as

$$\mathbb{E}[\text{sgn}\{\psi^{(\uparrow)} + \psi^{(\downarrow)}\}] = \max\{\widehat{I}_t^{(\psi)}\}.$$

Given the properties of λ it is automatically ensured that $I_t^{(\psi)}$ will sum to 1 at all times. Hence, the probabilities are obtained directly from the estimate.

The probabilities can be decomposed into a mean, trend and one or more seasonal components by writing the tracking of them as a Holt-Winters model. After trials of with the inclusion of different model components a Holt-Winters model including a mean term and two seasonal terms with daily and weekly seasonalities is derived. The additive form of Holt-Winters model is preferable due to the zeros in the observations and the resulting risk of some model components taking a value close to zero. The model can therefore be written as

$$\mu_t = \alpha_\mu(I_t^{(\psi)} - (d_{t-s_1} + w_{t-s_2})) + (1-\alpha_\mu)\mu_{t-1} \tag{18}$$

$$d_t = \alpha_D(I_t^{(\psi)} - (\mu_t + w_{t-s_2})) + (1-\alpha_D)d_{t-s_1} \tag{19}$$

$$w_t = \alpha_W(I_t^{(\psi)} - (\mu_t + d_{t-s_1})) + (1-\alpha_W)w_{t-s_2} \tag{20}$$

where μ_t is the mean term, d_t and w_t represent the within-day and within-week seasonalities while the αs are smoothing coefficients.

A forecast for lead time k can be found from the estimated components as

$$\widehat{I}_{t+k|t}^{(\psi)} = \mu_t + h_t^{(k)} + d_{t+k-s_1} + w_{t+k-s_2}. \tag{21}$$

Since the updating of the different components of the model is done with different frequencies, the output's property of its elements automatically sum to 1 is lost. Whereas the response forecast is still found as

$$\mathbb{E}[\text{sgn}\{\psi^{(\uparrow)} + \psi^{(\downarrow)}\}] = \max\{\widehat{I}_t^{(\psi)}\},$$

the sign probabilities are now found by applying the (inverse) multinomial logit transformation. Hence by choosing the "no regulation penalty" scenario

as a reference, the sign probabilities are found as:

$$\mathbb{P}\left(\text{sgn}\{\psi^{(\uparrow)}-\psi^{(\downarrow)}\}=-1\right)=\frac{\exp\left(\widehat{I}_{t,1}^{(\psi)}\right)}{1+\exp\left(\sum_{i\in\{1,3\}}\widehat{I}_{t,i}^{(\psi)}\right)}$$

$$\mathbb{P}\left(\text{sgn}\{\psi^{(\uparrow)}-\psi^{(\downarrow)}\}=1\right)=\frac{\exp\left(\widehat{I}_{t,3}^{(\psi)}\right)}{1+\exp\left(\sum_{i\in\{1,3\}}\widehat{I}_{t,i}^{(\psi)}\right)}$$

$$\begin{aligned}\mathbb{P}\left(\text{sgn}\{\psi^{(\uparrow)}-\psi^{(\downarrow)}\}=0\right)&=\frac{1}{1+\exp\left(\sum_{i\in\{1,3\}}\widehat{I}_{t,i}^{(\psi)}\right)}\\&=1-\left(\mathbb{P}\left(\text{sgn}\{\psi^{(\uparrow)}-\psi^{(\downarrow)}\}=-1\right)\right.\\&\quad\left.+\,\mathbb{P}\left(\text{sgn}\{\psi^{(\uparrow)}-\psi^{(\downarrow)}\}=1\right)\right).\end{aligned}$$

By writing Eq. (18)-(20) in their error-correction form

$$\mu_t=\mu_{t-1}+\alpha_\mu(I_t^{(\psi)}-d_{t-s_1}-w_{t-s_2}-\mu_{t-1})=\mu_{t-1}+\alpha_\mu\varepsilon_t \tag{22}$$

$$d_t=d_{t-s_1}+\alpha_D(I_t^{(\psi)}-\mu_t-w_{t-s_2}-d_{t-s_1})=d_{t-s_1}+\alpha_D\varepsilon_t \tag{23}$$

$$w_t=w_{t-s_2}+\alpha_W(I_t^{(\psi)}-\mu_t-d_{t-s_1}-w_{t-s_2})=w_{t-s_2}+\alpha_W\varepsilon_t \tag{24}$$

where ε_t is the prediction error for $k=1$.

Using the error-correction form allows for the Holt-Winters model to be written on the state space form as (Hyndman et al., 2002)

$$\boldsymbol{X}_t=\boldsymbol{A}\boldsymbol{X}_{t-1}+\boldsymbol{B}\varepsilon_t \tag{25}$$

$$\boldsymbol{Y}_t=\boldsymbol{C}_t\boldsymbol{X}_t+\boldsymbol{D}\varepsilon_t \tag{26}$$

where

$$\boldsymbol{X_t}=\begin{pmatrix}\mu_{1,t}&\mu_{1,t-1}&d_{1,t}&\dots&d_{1,t-s_1}&w_{1,t}&\dots&w_{1,t-s_2}\\\mu_{2,t}&\mu_{2,t-1}&d_{2,t}&\dots&d_{2,t-s_1}&w_{2,t}&\dots&w_{2,t-s_2}\\\mu_{3,t}&\mu_{3,t-1}&d_{3,t}&\dots&d_{3,t-s_1}&w_{3,t}&\dots&w_{3,t-s_2}\end{pmatrix}^T,$$

and $\boldsymbol{A},\boldsymbol{B},\boldsymbol{C}_t,\boldsymbol{D}$ are matrices of appropriate size containing the matrix formulation of Eq. (22) - (24).

On the state space formulation, the k-step ahead prediction is obtained by

$$\widehat{I}_{t+k|t}^{(\psi)}=\widehat{Y}_{t+k|t}=\boldsymbol{C}^{(k)}\boldsymbol{X}_t \tag{27}$$

where $\boldsymbol{C}^{(k)}$ is a slightly modified version of $\boldsymbol{C}$ for $k > 1$ while $\boldsymbol{C}^{(1)} = \boldsymbol{C}$. Once $\widehat{I}^{(\psi)}_{t+k|t}$ is obtained response and probability forecasts are found by the same convention as outlined above.

Writing the model on a state space form has the advantage that it can be extended to include features such as external variables and time-varying parameters. In that context, the sum of the Holt-Winters components would constitute a time-varying mean to which external variables would add extra information.

7 Conclusions and Discussion

The findings of this paper confirm the findings of previous studies of the impact of wind power on electricity spot prices (Moesgaard and Morthorst, 2008, Enevoldson et al., 2006, Jónsson et al., 2010), that wind power has a non-negligible impact on day-ahead electricity prices. Moreover, wind power is shown to influence the active regulation direction as well. All effects are shown to be both non-linear and time-varying. Thus should models aimed at capturing such influences be chosen accordingly. With the current market structure, knowledge about the impact of wind power on the market can be used to improve forecasts of the market dynamics and thereby contribute to better decision making for all market participants. Especially will better understanding of the market improve the competitiveness of emerging and established renewable energy sources since it allows them to be more strategic in their bidding, resulting in less imbalance costs for them and less stability issues for the grid operators (Zugno et al., 2010).

This paper's scope has been the two Danish price areas at Nord Pool. Despite that these areas have a relatively large share of wind power in their total installed capacity, the results presented here are likely to hold for other areas where wind power has the ability to shift the supply curve. The current structure of Nord Pool leaves producers only with one realistic option of settling their imbalances, namely the real-time market. This is most likely the cause for the substantial influence the forecasted wind power penetration has on the active regulation direction since producers do not have the possibility of correct their day-ahead contracts by other means. It would therefore be interesting to carry out similar study on a market with more a liquid intraday market and yet with wind power production on a similar scale. In addition, the impact of wind power on higher order moments of the market variable has been left untouched in this paper. Study of these aspect would nevertheless be interesting and relevant as it could help explain some of the volatility in the system.

The substantial impact of wind power forecasts on all behavior of the electricity

prices is also interesting to consider in the context of market design and with the long-term development of the production portfolio in Denmark in mind - where the intention is to increase the share of wind power generation up to 50% of the electricity consumption by 2025 (Ea Energy Analyses, 2007). With the current market structure of marginal bidding, the frequency of hours where the spot price is zero or negative is bound to increase along with growing wind power penetration in the system in a similar manner as has been demonstrated here. This will further enhance the stochastic threshold effect mentioned, resulting in increased price volatility and cause it to have alternating weather dependent patterns (Meibom, 2007). This aside, higher risk premium will be required on investments in all sorts of new energy generation capacity. Meanwhile investment in conventional power generation capacity will be more focused on flexibility rather than efficiency since those plants will have to rely more on the increased demand on the balance markets as a source of income (Meibom, 2007). The impact of wind power on the price making at the electricity markets should therefore be given careful thought when the possibility of increasing the share of wind power, and non-dispatchable energy sources in general, in the generation portfolio is discussed. Especially, the fact that wind power penetration has some non-linear effects on the prices should be taken into consideration, as it implies that current market situation can not be scaled directly for analyzing the future circumstances. In the context of market design, it will also be interesting to monitor the market's response to the emergence of other renewable sources. Whether this will level out the effect of increased wind power or magnify them will play an important role in future development of the market structure.

8 Acknowledgments

The work presented has been partly supported by the European Commission through the EU FP6 project Anemos.plus (contract N° 038692), which is hereby acknowledged. The authors would also like to thank Henrik Aa. Nielsen and Torben Skov Nielsen at ENFOR A/S for fruitful discussions and their inputs.

References

William S. Cleveland and Susan J. Devlin. Locally weighted regression: An approach to regression analysis by local fitting. *Journal of the American Statistical Association*, 83(403):596–610, 1988.

Alexandre Costa, Antonio Crespo, Jorge Navarro, Gil Lizcano, Henrik Madsen, and Everaldo Feitona. A review on the young history of wind power short-

term prediction. *Renewable & Sustainable Energy Reviews*, 12(6):1725–1744, 2008.

Ea Energy Analyses. 50% wind power in denmark in 2025 - english summary. *Available at: http://www.talentfactory.dk/media(2513,1033)/081029_50pct._wind_power_in_dk_in_2025.pdf*, 2007.

Svend W. Enevoldson, Poul Alberg Østergaard, Poul Erik Morthorst, and Rune Moesgaard. Vindkraftens betydning for elprisen i danmark. Technical report, IBT-Wind, 2006. In Danish.

Paolo Giabardo, Marco Zugno, Pierre Pinson, and Henrik Madsen. Feedback, competition and stochasticity in a day ahead electricity market. *Energy Economics*, 32(2):292–301, 2010.

Gregor Giebel, George Kariniotakis, and Richard Brownsword. The state-of-the-art in short-term prediction of wind power - a literature overview. *EU project Anemos, Deliverable Report D1.1, Available at http://anemos.cma.fr/download/ANEMOS_D1.1_StateOfTheArt_v1.1.pdf*, 2003.

Rob J. Hyndman, Anne B. Koehler, Ralph D. Snyder, and Simone Grose. A state space framework for automatic forecasting using exponential smoothing methods. *International Journal of Forecasting*, 18(3):439–454, 2002.

Tryggvi Jónsson, Pierre Pinson, and Henrik Madsen. On the market impact of wind energy forecasts. *Energy Economics*, 32(2):313–320, 2010.

Peter Meibom. Market consequences [in my view]. *IEEE Power and Energy Magazine*, 5(6):120–118, 2007.

Rune Moesgaard and Poul Erik Morthorst. The impact of wind power on electricity prices in denmark. In *EWEC 2008, European Wind Energy Conference, Business and Policy Track*, Brussels, Belgium, April 2008.

Henrik Aa. Nielsen, Torben S. Nielsen, Alfred K. Joensen, Henrik Madsen, and Jan Holst. Tracking time-varying coefficient functions. *International Journal of Adaptive Control and Signal Processing*, 14(8):813–828, 2000.

Torben Skov Nielsen, Henrik Aalborg Nielsen, and Henrik Madsen. Prediction of wind power using time-varying coefficient functions. In *15th IFAC World Congress*, Barcelona, Spain, 2002.

Pierre Pinson, Christophe Chevallier, and George N. Kariniotakis. Trading wind generation from short-term probabilistic forecasts of wind power. *IEEE Transactions on Power Systems*, 22(3):1148–1156, 2007.

James W. Taylor. Short-term electricity demand forecasting using double seasonal exponential smoothing. *Journal of Operational Research Society*, 54(8): 799–805, 2003.

Peter R. Winters. Forecasting sales by exponentially weighted moving averages. *Management Science*, 6(3):324–342, 1960.

Marco Zugno, Pierre Pinson, and Tryggvi Jónsson. Decision making strategies for trading wind power in deregulated energy markets. In *IAEE's 33rd International Conference*, Rio de Janeiro, Brazil, 2010.

PAPER C

Statistical Analysis of the Impact of Wind Power on Market Quantities and Power Flows

---

Authors:
P. Pinson, T. Jónsson, M. Zugno, J.M. Morales, H. Madsen

Appears in:
IEEE Power and Energy General Meeting 2010

Statistical Analysis of the Impact of Wind Power on Market Quantities and Power Flows

Pierre Pinson[2] Tryggvi Jónsson[1,2] Marco Zugno[2] Juan-Miguel Morales[2] Henrik Madsen[2]

Abstract

In view of the increasing penetration of wind power in a number of power systems and markets worldwide, we discuss some of the impacts that wind energy may have on market quantities and cross-border power flows. These impacts are uncovered through statistical analyses of actual market and flow data in Europe. Due to the dimensionality and nonlinearity of these effects, the necessary concepts of dimension reduction using Principal Component Analysis (PCA), as well as nonlinear regression are described. Example application results are given for European cross-border flows, as well as for the impact of load and wind power forecasts on Danish and German electricity markets.

1 Introduction

Wind power capacities are rapidly expanding in a number of countries, maybe most noticeably in Europe, the US and China. This is facilitated by direct and indirect incentives, for instance in the form of feed-in tariffs or of prioritization in electricity pools. Both variability and limited predictability of that renewable energy source will yield a radical shift in the paradigms of power systems management. The parallel development of other forms of renewable energy e.g. solar and wave, may contribute to dampen or inversely magnify the undesirable effects of wind power on the physical operation of power systems as well as market characteristics. A recent status of the deployment of renewable energy capacities worldwide is available in Renewable Energy Policy Network (2011).

Electricity network and markets were designed based on a long history of dealing with various forms of dispatchable generation, for which the concepts

[1]ENFOR A/S, Lyngsø Allé 3, DK-2970 Hørsholm, Denmark
[2]DTU Informatics, Technical University of Denmark, Richard Petersens Plads, building 321, DK-2800 Kgs. Lyngby, Denmark

of unit commitment, economic dispatch, contingency analysis made sense in view of the technical characteristics of the physical units. The increasing penetration of wind power challenges these practices, owing to its impact on market quantities and cross-border flows. As an illustrative example, the impact of wind power predictability is now regularly accounted for in network expansion and future offshore grid studies Trötscher and Korpås (2011), Tande el.al. (2008). It is of utmost importance to properly characterize and model the effects of wind on markets and power flows before we may be able to project ourselves in the future with scenarios of substantial renewable energy penetration. For the example of Denmark, the objective is to have 50% of the electricity consumption met by wind energy by 2025 Ea Energy Analyses (2007). This has triggered a number of technical and economical analyses focused on market value, investment and power flows, as in Lindbo (2007) for instance. Note that game-changers may also appear, most likely in the form of various forms of demand-side management Strbac (2008).

Both meteorological and economical effects are at the roots of this impact: *(i)* wind power generation over a region is directly influenced by the geographical coverage of weather systems, while *(ii)* wind energy has a direct consequence on market quantities due to the so-called merit-order effect which places wind at the very left of the market supply curves. Complex network effects then add on to yield the final power flows. In view of the complexity brought in by all these combined aspects, system studies of the effect of wind on market quantities and power flows may necessitate relying on crude simplifications and on simulations. Recent examples of these detailed system studies partly based on simulations include Gerber et al. (2012) for the case of the UK system in 2020 and Hagspiel (2012) concentrating on the Swiss power system at the horizon 2030. Toy model simulations can actually highlight some of the effects of wind on electricity markets, as in Giabardo et al. (2010). Simplified system and toy models may however mask some of the effects that are aimed at being uncovered. This is the reason why inversely, statistical *ex-post* analyses of some of the key variables can already give a fair picture, without looking at a complete modeling of all meteorological, market and network effects. Example statistical analyses of market quantities were for instance performed in Morthorst (2003), Jónsson et al. (2010) and Gelabert et al. (2011) for the case of the Danish and Spanish electricity markets, respectively.

In this paper, we review the methodological aspects necessary for the statistical analysis of the impact of wind power on market quantities and power flows (Section 2). Especially, we insist on the nonlinear nature of this impact, and on its potential nonstationarity. In parallel, owing to the potentially large dimensions of datasets to be analysed, we also discuss dimension reduction (based on Principal Component Analysis) that may prove necessary when looking at power flows over the whole electricity network of a region. Subsequently, an

example application to the case of the Nord Pool (Western Denmark control zone - DK1) and EEX (Germany) markets considered in Section 3. Similarly in Section 4, we look at the case of power flows related to the Austrian control block, and of cross-border power flows over the whole ENTSO-E (European Network of Transmission System Operators for Electricity) system. The paper finally ends in Section 5 with conclusions, implications of the findings, as well as perspectives for future work.

2 Methodological aspects

In this Section we review some statistical modeling concepts necessary for the various applications covered in the following, that is, the impact of wind on both market quantities and power flows. These concepts include nonlinear regression based on local polynomial models, as well as PCA for dimension reduction.

2.1 Nonlinear regression with local polynomial models

Whatever the variables of interest, the set of observations consists of time-series of measurements. We denote by $\{y_t\}$, $t = 1,\ldots,T$, the observed time-series for the response variable, and by $\mathbf{x}_t^\top = [x_t^1 \ldots x_t^i \ldots x_t^m]$ the vector of m explanatory variables at time t. In a practical setup, the response variable may be the day-ahead electricity price or the overall system balance of a TSO's network, and generated wind power the explanatory variable for instance.

The relationship between explanatory and response variables is written in the form of a general regression model,

$$y_t \;=\; \theta(\mathbf{x}_t) + \epsilon_t, \qquad t = 1,\ldots,T. \tag{1}$$

The noise term $\{\epsilon_t\}$, $i = 1,\ldots,T$, is a sequence of independent and identically distributed (i.i.d.) random variables with unknown distribution F. It is assumed that F has a zero mean and a finite variance σ_ϵ^2. In general, it is assumed that both $\mathbf{x}$- and y-values can be normalized. Therefore, they are all contained in the unit interval, while $\epsilon_t \in [-1,1]$, $\forall t$.

Based on the concept of local polynomial regression, it is assumed that θ may be locally approximated by k-order polynomials. Most common instances of local polynomial regression include kernel smoothing ($k = 0$) and local linear regression ($k = 1$). Note that in practice, the curse of dimensionality imposes

that the dimension of $\mathbf{x}$ has to be low, say less than 3 (for a discussion on that issue, see (Hastie and Tibshirani, 1990, pp. 83-84)).

θ is approximated at a number of fitting points, chosen based on a rule of thumb or after consideration of the data distribution. Let us focus on a single fitting point $\widetilde{\mathbf{x}} = [\widetilde{\mathbf{x}}^1, \ldots, \widetilde{\mathbf{x}}^m]$ only. The k-order local polynomial approximation $\mathbf{z}_t$ of the vector of explanatory variables $\mathbf{x}_t$ is given by:

$$\mathbf{z}_t^\top = \mathbf{p}_k^\top(\mathbf{x}_t). \tag{2}$$

For instance if $k = 1$, $\mathbf{p}_1(\mathbf{x}_t) = [1 \;\; \mathbf{x}_t]$.

In parallel, write $\underline{\boldsymbol{\theta}}$ the vector of local coefficients at $\widetilde{\mathbf{x}}$, so that locally at $\widetilde{\mathbf{x}}$ one obtains the following linear model

$$y_t = \mathbf{z}_t^\top \underline{\boldsymbol{\theta}}, \quad t = 1, \ldots, T, \tag{3}$$

which is then fitted by minimizing a weighted loss of the form

$$\hat{\underline{\boldsymbol{\theta}}} = \arg\min_{\underline{\boldsymbol{\theta}}} \sum_{t=1}^{T} w_t \rho(y_t - \mathbf{z}_t^\top \underline{\boldsymbol{\theta}}) \tag{4}$$

with the w_t weights assigned by a Kernel function, i.e.

$$w_t = K(\mathbf{x}_t, \widetilde{\mathbf{x}}) \;\; = \prod_i \omega\left(\frac{|x_t^i - \widetilde{x}^i|_i}{h^i}\right). \tag{5}$$

In the above, $|.|_i$ denotes a chosen distance on the i-th dimension of $\mathbf{x}$ (typically the Euclidean distance), and $\mathbf{h} = [h^1 \; \ldots \; h^m]$ is the bandwidth for that particular fitting point $\widetilde{\mathbf{x}}$. As an example, ω can be defined as a tricube function,

$$\omega(v) = \begin{cases} (1 - v^3)^3, & v \in [0,1] \\ 0 & , \; v > 1 \end{cases}, \tag{6}$$

as introduced and discussed in e.g. Cleveland and Devlin (1988). This type of estimation procedure may also be made adaptive in order to account for smooth temporal changes in the regression, if aiming at accounting for seasonal variations in the effects of interest for instance. The weights in Eq. (4) would then include a time decay, e.g. in the form of exponential forgetting, in order to gradually discount older observations.

For the fitting of these local linear models, the type of regression will decide upon the loss function to be minimized. In the case where the mean effect is to be modelled, they are to be fitted using weighted least-squares. ρ then takes the form of a quadratic loss function, such that

$$\rho(\epsilon) = \epsilon^2 / 2. \tag{7}$$

If aiming to perform quantile regression instead, for a given nominal proportion τ, $\tau \in [0,1]$, one chooses an asymmetric piecewise linear loss function ρ_τ as

$$\rho_\tau(\epsilon) = \begin{cases} (\tau-1)\epsilon, & \epsilon < 0 \\ \tau\epsilon, & \epsilon > 0 \end{cases} . \tag{8}$$

For an overview of the theory and application of quantile regression, we refer to Koenker (2005).

Finally when the local coefficients are calculated at all fitting points, the complete coefficient functions $\hat{\boldsymbol{\theta}}(\mathbf{x})$ can be obtained by linear or spline interpolation of the local coefficients. This will be illustrated in the example applications below.

2.2 Generalization to higher dimensions using Principal Component Analysis (PCA)

The case of a single response variable was considered so far only. This setup may be suitable if looking at the impact of one or more variables (say, wind and load) on day-ahead market prices. If concentrating however on the effect of wind power on a set of variables over a network e.g. power flows, the dimension n of the response variable will be greater than 1, and potentially very large. The model of Eq. (1) therefore needs to be generalized as

$$\mathbf{y}_t = \theta(\mathbf{x}_t) + \epsilon_t, \qquad t = 1,\ldots,T, \tag{9}$$

where $\mathbf{y}_t = [y_t^1 \ \ldots \ y_t^n]$ is now a multivariate response.

In order to ease the estimation of the coefficient functions θ, a first necessary step consists in reducing the dimension of the problem. This is done here in a PCA framework, by summarizing the information from the n-dimensional response in a q-dimensional basis of Principal Components (PCs), $q << n$. These PCs are chosen so that they maximize their ability to explain the variance of the original multivariate response. For an overview of PCA, of the properties of the PCs, and more generally of multivariate data analysis, we refer to Lattin et al. (2003). A more applied introduction focused on atmospheric sciences can be found in Wilks (2006). In the power systems literature, PCA for dimension reduction was for instance employed in Burke and O'Malley (2011) for studying spatially distributed wind power generation in Ireland.

Before to apply the PCA itself, the multivariate response is first centred and normalized. The benefits of such preprocessing are discussed in Wilks (2006).

Subsequently, finding the PCs for the multivariate response $\mathbf{y}$ is performed by diagonalizing the covariance matrix of the data,

$$\mathbf{R}_y = \frac{1}{T}\sum_{t=1}^{T}\mathbf{y}_t\mathbf{y}_t^\top. \tag{10}$$

After diagonalizing, the PCs are obtained as the eigenvectors of $\mathbf{R}_y$ with the largest corresponding eigenvalues. The number of PCs to be selected is decided upon through graphical and/or numerical methods Lattin et al. (2003). The ratio of the sum of the selected eigenvalues over that for all eigenvalues gives the share of the variance in the response data explained by these PCs. In the following we will use the average eigenvalue method for PC selection, as in Zugno et al. (2011). We denote by $\widetilde{\mathbf{y}}_j$, $j = 1,\ldots,q$ the obtained PCs ($q << n$). All observed values $\mathbf{y}_t$ for the response variables can consequently be written as a linear combination of the PCs,

$$\mathbf{y}_t = \sum_{j=1}^{q}\alpha_t^j\widetilde{\mathbf{y}}_j + \nu_t, \quad \forall t, \tag{11}$$

with an additional random noise ν_t originating from the unexplained variance in the data. A projection operator $\mathbf{P}$ can then be introduced, permitting to project the original response into the space spanned by the PCs,

$$\mathbf{P} = [\widetilde{\mathbf{y}}_1 \ \ldots \ \widetilde{\mathbf{y}}_q]. \tag{12}$$

$\mathbf{P}$ allows projecting standardized response values $\mathbf{y}_t$ in the basis defined by the principal components, since Eq. (11) can be rewritten as

$$\mathbf{y}_t = \mathbf{P}^\top\boldsymbol{\alpha}_t + \nu_t, \quad \forall t, \tag{13}$$

with $\boldsymbol{\alpha}_t = [\alpha_t^1 \ \ldots \ \alpha_t^q]$.

Finally by combining the models of Eqs. (9) and (11), one obtains

$$\mathbf{y}_t = \sum_{j=1}^{q}\theta(\mathbf{x}_t)\widetilde{\mathbf{y}}_j + \varepsilon_t, \qquad t = 1,\ldots,T, \tag{14}$$

where the noise ε_t combines the original noise from the regression model with the additional one coming from the PCA decomposition. In other words in the basis formed by the PCs, the coefficients $\boldsymbol{\alpha}_t$ are replaced by coefficient functions of the explanatory variables $\mathbf{x}$ similar to that of Eq. (1). These coefficient functions can be estimated in the same fashion as in Section 2.1.

3 Application to electricity market quantities

A first and highly relevant application to the methodology presented for uncovering the nonlinear effect of wind power on some response variable consists in looking at the effect of wind power on prices in electricity markets. This effect was first looked at in Morthorst (2003), which attempted to find a linear relationship between observed wind power generation and prices in the Nord Pool day-ahead market in Western Denmark. Since then, Jónsson et al. (2010) argued that *(i)* the relationship of interest is actually between day-ahead prices and the predicted values for load and wind power, while *(ii)* such a relationship is most surely nonlinear. These aspects are discussed below, after introducing the set of available data.

3.1 Available data

For this study of the impact of wind power on electricity market quantities, focus is given to two markets highly penetrated by wind energy, namely the Nord Pool and EEX ones. More precisely, the Western Denmark area of the Nord Pool (often referred to as DK1) is looked at since corresponding to the control zone with the highest wind power penetration (more than 20% of the energy consumption met by wind energy). Long records of market quantities (day-ahead and imbalance prices, imbalance sign, etc.) are available for those markets.

In parallel in both cases, relevant forecast and measured data are freely available at the websites of the corresponding network operators. Energinet.dk is the TSO in Denmark. In Germany, only the wind information at the control zones of RWE, Eon and Vattenfall is considered, since accounting for most of the wind capacities. Overall, the data include day-ahead wind power forecasts, as well as measured wind power generation and load. We simulate the availability of load forecasts by adding noise to the measurements, with a variance consistent to reported accuracy of load forecasts for a country today (between 2 and 4% Mean Average Percent Error - MAPE).

Overall, the data for the Danish test case cover a period from the 1st of January 2008 to the 13th February 2008, while those for Germany are for the two years of 2006-2007.

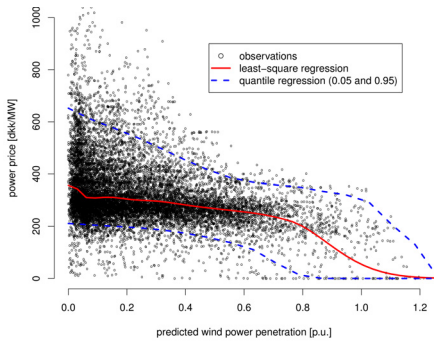

Nord Pool, Western Denmark area (DK1) - 1.1.2008 to 13.2.2010

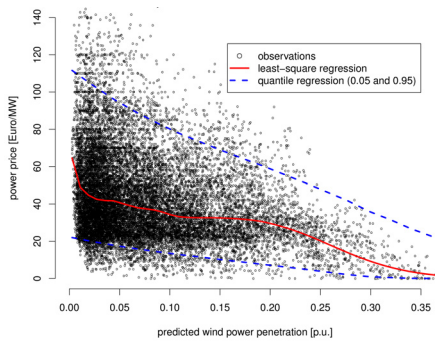

EEX - 1.1.2006 to 31.12.2007

Figure 1: The relationship between predicted wind power penetration and the day-ahead market prices in the Nord Pool and EEX day-ahead markets.

3.2 Sample results focused on day-ahead prices

We follow the argument of Jónsson et al. (2010) such that the predicted values for the load and the wind power generation are those that impact the day-ahead prices in these electricity markets. This argument is directly motivated by their clearing mechanism based on bids that are in turn based on predictions.

We first work with a single explanatory variable only, the predicted wind power penetration, defined as the ratio of wind power and load forecasts. It represents the foreseen share of wind in the day-ahead electricity mix at the time of market clearing and for each time unit over the following day. The response variable is the corresponding day-ahead price for every time unit. The scatter plots representing the empirical relationship between these explanatory and response variables in the Nord Pool and EEX markets are gathered in Fig. 1.

Local polynomial regression is employed for characterizing the evolution of day-ahead prices as a function of predicted wind power penetration. On the one hand, the least-square fitting gives the mean trend, while on the other hand quantile regression with nominal proportions $\tau = 0.05$ and $\tau = 0.95$ yields prediction intervals with a 90% nominal coverage rate. Note that for this response variable the data are log-transformed before fitting the regression models, even though the results are presented in the original space of the variable. We use 30 fitting points, with a nearest-neighbour bandwidths covering local neighbor-

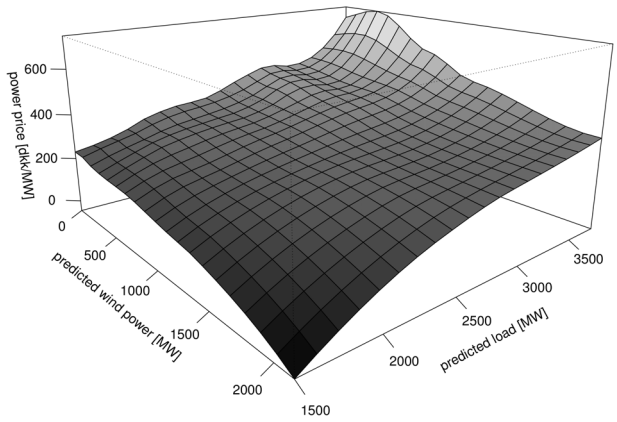

Figure 2: The relationship between predicted wind power generation, predicted load, and the day-ahead market prices in the Nord Pool day-ahead market, Western Denmark area (DK1), 1.1.2008 to 13.2.2010.

hoods corresponding to 10% of the data.

The mean trend is qualitatively similar for both markets, with day-ahead prices decreasing with increasing predicted wind power penetration, even though there may be some quantitative differences. Maybe the most important one is that the day-ahead price appears to tend more rapidly towards 0 in the EEX market, already at around 35% predicted wind power generation, while it is only the case in Denmark when this explanatory variable gets closer to 100% penetration. The bands given by quantile regression also illustrate how the price variability and convergence towards 0 differ for the two markets.

To further detail the dependence between day-ahead prices and predicted load and wind power generation, the local polynomial regression approach is upgraded so that both predicted variables are simultaneously seen as explanatory ones ($m = 2$). We use 20 fitting points for each variable (leading to a total of 400 fitting points), with a nearest-neighbour bandwidths covering local neighborhoods corresponding to 20% of the data. The resulting smooth surface is depicted in Fig. 2 for DK1 and for least-square regression only. It confirms the joint role of predicted load and wind power: the former induces an upward pressure on prices, while the latter pushes them back down, the impact of wind being greater at lower load values.

Similar analysis may be performed for other market quantities and other markets, with focus on the various moments of their distributions. The uncovered

dependencies may then be used as additional knowledge for the building of relevant forecast methodologies of market quantities. Example recent works in that direction include Jónsson et al. (2011) focusing on the prediction of day-ahead prices accounting for wind power predictions, and Jónsson et al. (2011) looking at the specific case of imbalance sign characterization and prediction.

4 Application to power flows

A second relevant application of the statistical approaches described in the present paper relates to the analysis of power flows within and over one or more control zones. The results we gather and discuss in the following are based on some of the data and work of Klöckl and Pinson (2009) for the analysis of power flows related to the Austrian control block, and of Zugno et al. (2011) for the analysis of cross-border power flows over the whole ENTSO-E system. For confidentiality reasons, some of the results may not be detailed.

4.1 Example focus on the Austrian control block

The underlying motivation of the work performed in Klöckl and Pinson (2009) was to perform an *ex-post* analysis of available power flow data within Austria, as well as of cross-border power flows, in relation with some of the publicly available data from EEX and the German TSOs. These data basically are the same than those considered in Section 3.2, i.e. wind power forecasts, wind power and load measurements, as well as all market quantities. They cover the period of 2006-2007. A basic question to be answered is how much the German wind power and market influence the power flows experienced by the Austrian TSO.

The Austrian control block is operated by the TSO APG (Austrian Power Grid), for an installed generation capacity of more than 19 GW (12 GW in hydro power units), while the maximum load is less than 10 GW. This control zone is physically linked to six different control blocks and a total of nine control zones. Two independent analyses were performed focused on *(i)* all the cross-border flows, and *(ii)* the power flows over 23 400kV-systems throughout Austria, in order to uncover the impact of German wind and market quantities on all these power flows. Dimension reduction was necessary in the latter case: most of the variance in the power flows of the 23 400kV-systems could be explained with 4 PCs only.

Let us give here a set of results focusing on the impact of predicted wind power penetration in Germany and of day-ahead prices in the EEX market on the

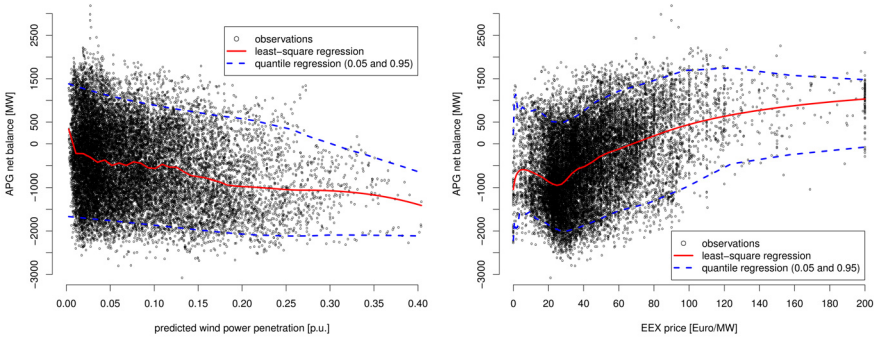

Predicted wind power penetration in Germany

EEX day-ahead prices

Figure 3: The impact of predicted wind power penetration in Germany and the EEX day-ahead prices on the APG net balance over 2006-2007.

APG net balance. This contrasts with the more detailed analysis of individual cross-border and 400kV-systems power flows which can be found in Klöckl and Pinson (2009). The APG net balance is calculated as the sum of all power export minus the sum of all import at a given time. It is expressed here in MW. Fig. 3 gathers the scatter plots for that analysis, while depicting the regression curves for the mean effect (least-square regression), as well as 90% prediction intervals defined by the quantile regression curves with nominal proportions of 0.05 and 0.95.

The plots in Fig. 3 reveals that the Austrian control block tends to export more as the EEX price gets higher, but also to import more as the predicted wind power penetration in Germany is greater. Actually the mean trend is that Austria only imports when there is almost no wind power penetration in Germany. One also observes that obviously these are trends only, with large intervals around this mean trend, showing that other effects are to be accounted for. For instance, it may be crucial to account for daily and seasonal variations in the power flow patterns. This is illustrated by Fig. 4 which depicts the mean impact of predicted wind power penetration in Germany on the total balance of the APG control block, also as a function of the time of the day. It shows how Austria has a typical cycle of importing at night and exporting during the day, when there is no or almost no wind power penetration in Germany. As this wind power penetration increases, even though there still are variations over the day, the Austrian control block tends be in an import situation at any hour of the day. In general, we have observed that it is highly beneficial to account for potential diurnal and seasonal variations in our analysis of power flows.

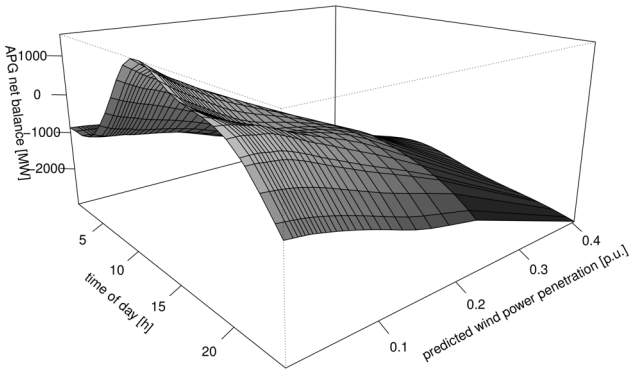

Figure 4: The impact of predicted wind power penetration in Germany on the APG net balance over 2006-2007, as function of the time of the day.

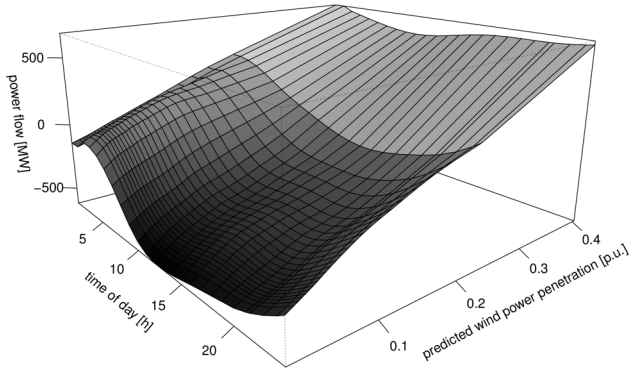

Figure 5: The impact of predicted wind power penetration in Germany on cross-border power flows between DK1 and Norway over 2006-2008.

4.2 General results related to ENTSO-E system

The type of study performed for the Austrian control block was generalized to the whole ENTSO-E system. The dataset there consists of hourly cross-border power flows between 34 European and bordering extra-European countries, over a 3 year period covering 2006 to 2008. After quality check, the study is

restricted to 68 cross-border interconnections. The overall question studied is similar to the above section, i.e. related to the impact of German wind and market quantities on the whole set of European cross-border flows. The analysis performed is fully covered by Zugno et al. (2011).

For this dataset, 8 PCs were deemed enough to represent the overall dynamics of the cross-border power flows over the ENTSO-E system, explaining 82% of the original variance in the data. Local polynomial models were then used on the PCs, conditioned by the predicted wind power penetration in Germany, EEX day-ahead prices, as well as the time of the day.

Out of the extensive analysis covered, let us show an illustrative example results in Fig. 5, which depicts the impact of predicted wind power penetration in Germany on cross-border power flows between DK1 and Norway over 2006-2008. As wind power penetration is predicted to be greater in Germany, the situation switches from DK1 importing power from Norway to exporting. Consistent behaviour was observed at the interconnection between DK1 and Germany. This is in line with intuitive economic reasoning, such that an hydro-dominated control zone like the Norwegian one tend to withhold production when energy prices are low due to significant wind power penetration, and inversely increase production when prices are high. This result is in fact similar to that of Fig. 4 for the case of Norway. A noticeable difference though is that Austria is directly interconnected to the German network, while it is not the case of Norway. Overall in view of the work of Zugno et al. (2011), the data available today permits to quantify how much German wind and market quantities impact cross-border flows over the whole ENTSO-E system. The identified PCs may be seen as modes of propagation of power flows, which are more of less stimulated depending on various explanatory variables. This analysis may be refined in the future by also accounting for wind and market-related variables in other countries as well.

5 Conclusions

The effect of wind power generation on electricity markets and power flows is recognized but not always understood and quantified. Owing to the potential complexity of modelling all meteorological, economical and network aspects involved, we suggest that an interesting alternative to full system studies consists in performing statistical *ex-post* analyses of the datasets available at market and network operators. When acknowledging the potentially nonlinear and nonstationary impact of wind power on these quantities, the regression techniques (and related estimation concepts) come fairly natural. Also the issue of the dimensionality of the dataset involved may be dealt with based on

statistical dimension reduction techniques e.g. the PCA approach employed here.

It is not possible to cover in a single paper all the analyses that could be performed based on the datasets available. We have therefore pointed at further reading for more extensive studies. Overall, it appears that load and wind power forecast have a significant impact on today's market quantities. This impact can be characterized as nonlinear and nonstationary, and quantified through appropriate statistical regression techniques. Similarly, these variables, or the market price used as a proxy, highly influence power flows within and between control zones. This effect was evidenced and modeled for the case of the APG control block, as well as for the all interconnectors of the ENTSO-E system. Note that the impact of forecast errors should also be thoroughly studied, as they are known to induce unscheduled power exchanges.

Here only the effect of some explanatory variables e.g. predicted wind power generation, on market quantities and power flows was considered. Interestingly, the time dimension could also be accounted for in a straightforward manner by generalizing the methodological concepts presented in a time-varying regression framework. This would then permit to *(i)* assess the way uncovered effects evolved over the past years, for instance as a function of installed wind capacities, and *(ii)* tentatively predict what the future effects of more substantial renewable energy penetration levels on electricity markets and power flows may be. Obviously, these predictions would be based on stationarity assumptions, which would be very weak in view of the non-negligible changes to be expected in market and power systems operations in the foreseeable future.

Such a statistical approach should be considered as part of, or jointly with, other system studies. They can provide valuable insight to TSOs and policy makers, while allowing market participants to refine their forecasting and participation strategies. Note that importantly, it is the spatio-temporal dynamics of all types of renewable energy sources that should be seen as explanatory variables in the future, in view of the future plans for deployment of renewable energy capacities.

Acknowledgment

This work was partly supported by the European Cost Action "WIRE: Weather Intelligence for Renewable Energies" (ES1002), and by the Austrian Power Grid through the project "Impact of Stochastic Generation on EU Cross-border Flows". The European Network of Transmission System Operators for Electricity (ENTSO-E), APG, Energinet.dk and Nord Pool A/S are also acknowledged

for their role in providing the dataset.

References

REN21, “Renewable 2011 - Global Status Report,” Tech. rep., Renewable Energy Policy Network for the 21st Century, 2011 [http://www.ren21.net].

T. Trötscher, M. Korpås, “A framework to determine optimal offshore grid structures for wind power integration and power exchange,” *Wind Energy*, vol. 14, pp. 977-992, 2011.

J.O. Tande, M. Korpås, L. Warland, K. Uhlen, and F. van Hulle, “Impact of a TradeWind offshore wind power capacity scenarios on power flows in the European HV network,” in *Proc. 7th Int. Wind Integration Workshop*, Madrid, Spain, may 2008.

Ea Energy Analyses,”50% wind power in Denmark by 2025 - English summary,” Tech. rep., Ea Energy Analyses, Copenhagen, Denmark, 2007 [http://www.ea-energianalyse.dk/reports].

H.H. Lindbo, “50% wind in Denmark 2025 - A technical economical analysis,” in *IEA workshop* (technical presentation), Paris, 2007 [http://www.iea.org/work/2007/grids/Linboe.pdf].

G. Strbac, “Demand side management: benefits and challenges,” *Energy Policy*, vol. 36, pp. 4419-4426, 2008.

A. Gerber, M. Qadrdan, M. Chaudry, J. Ekanayake, N. Jenkins, “A 2020 GB transmission network study using dispersed wind farm power output,” *Renewable Energy*, vol. 37, pp. 124-132, 2012

S. Hagspiel, A. Papaemannouil, M. Schmid, G. Andersson, “Copula-based modeling of stochastic wind power in Europe and implications for the Swiss power grid,”, *Applied Energy*, available online, 2012.

P. Giabardo, M. Zugno, P. Pinson, H. Madsen, “Feedback, competition and stochasticity in a day-ahead electricity market,” *Energy Economics*, vol. 32, pp. 292-301, 2010.

P. Morthorst, “Wind power and the conditions at a liberalized power market,” *Wind Energy*, vol. 6, pp. 297-308, 2003.

T. Jónsson, P. Pinson, H. Madsen, “On the market impact of wind energy forecasts,” *Energy Economics*, vol. 32, pp. 313-320, 2010

L. Gelabert, X. Labandeira, P. Linares, “An ex-post analysis of the effect of renewables and cogeneration on Spanish electricity prices,” *Energy Economics*, vol. 33, pp. 59-65, 2011.

T. Hastie, R. Tibshirani, *Generalized Additive Models*, Chapman & Hall, London, 1990.

W.S. Cleveland, S.J. Devlin, "Locally weighted regression: An approach to regression analysis by local fitting," *Journal of the American Statistical Association*, vol. 83, pp. 596-610, 1988.

R. Koenker, *Quantile Regression*, Cambridge University Press, 2005.

J. Lattin, J.D. Carroll, P.E. Green, *Analyzing Multivariate Data*, Duxbury Applied Series, 2003.

D.S. Wilks, *Statistical Methods in the Atmospheric Sciences*, 2nd Ed., Academic Press, International Geophysics Series, 2006.

D.J. Burke, M. O'Malley, "A study of principal component analysis applied to spatially distributed wind power," *IEEE Transactions on Power Systems*, vol. 26, pp. 2084-2092, 2011.

M. Zugno, P. Pinson, H. Madsen, B. Klöckl, "The impact of wind power on European cross-border power flows," *IEEE Transactions on Power Systems*, submitted, 2011.

T. Jónsson, P. Pinson, H.Aa. Nielsen, H. Madsen, T.S. Nielsen, "Forecasting day-ahead electricity prices accounting for the impact of wind power generation," *IEEE Transactions on Sustainable Energy*, In PRESS, 2011.

T. Jónsson, P. Pinson, H.Aa. Nielsen, H. Madsen, "Exponential Smoothing Approaches for Prediction in Electricity Regulation Markets,"*Energy Economics*, submitted, 2012.

B. Klöckl, P. Pinson, "Effects of increasing wind power penetration on the physical operation of large electricity market systems," in *IEEE-CIGRE Symposium*, Calgary, Canada, 2009.

PAPER D

Trading wind energy based on probabilistic forecasts of both wind generation and market quantities

---

Authors:
M. Zugno, T. Jónsson, P. Pinson

Accepted for publication in:
Wind Energy (2012)

Trading wind energy based on probabilistic forecasts both of wind generation and of market quantities

Marco Zugno[2] Tryggvi Jónssonl[1,2] Pierre Pinson[2]

Abstract

Wind power is not easily predictable and non-dispatchable. Nevertheless, wind power producers are increasingly urged to participate in electricity market auctions in the same manner as conventional power producers. The aim of this paper is to propose an operational strategy for trading wind energy in liberalised electricity markets and to assess its performance. At first the so-called optimal quantile strategy is revisited. It is proved that without market power, i.e. under the price-taker assumption, this strategy maximises expected market revenues. Forecasts of wind power production, of day-ahead and real-time market prices and of the system imbalance are inputs to this strategy. Subsequently, constraining of the bid that maximises the expected revenues is proposed as a way to overcome the strategy's disregard of practical limitations and, at the same time, of risk. Two constraining techniques are introduced: constraining in the decision space and in the probability space. Finally, the trade of a wind power producer is simulated in a test-case for the Eastern Danish (DK-2) price area of the Nordic Power Exchange (Nord Pool) during a 10 month period in 2008. The results of the test-case show the financial benefits of the aforementioned strategy as well as the consequent interaction with the electricity market. This study will support a demonstration in the framework of the EU project ANEMOS.plus.

[1]ENFOR A/S, Lyngsø Allé 3, DK-2970 Hørsholm, Denmark
[2]DTU Informatics, Technical University of Denmark, Richard Petersens Plads, building 321, DK-2800 Kgs. Lyngby, Denmark

Nomenclature

Main symbols:

ρ_k	Wind power producer revenues at trading period k
W_k	Wind power production at trading period k
π_k	Market price at trading period k
C_k	Negative wind power producer revenues due to imbalance at trading period k
ψ_k	Unit regulation costs for positive and negative imbalances at trading period k
$W^{(max)}$	Installed wind power capacity
r_k	Quantile of wind power distribution at trading period k
P_k	Probability of imbalance direction at trading period k
a_v	Parameter determining the width of the bound to the optimal bid in the decision space
a_p	Parameter determining the width of the bound to the optimal bid in the probability space

Superscripts:

$^{(S)}$	Referring to the day-ahead market
$^{(\uparrow/\downarrow)}$	Referring to the real-time market
$^{(\uparrow)}$	Referring to up-regulation in the real-time market
$^{(\downarrow)}$	Referring to down-regulation in the real-time market
*	Optimal
$\tilde{}$	Contracted at the day-ahead market
$\hat{}$	Forecast

1 Introduction

In liberalised electricity markets, competition stands as the fundamental mechanism ensuring the efficient operation of the system. Competition is implemented through the establishment of a market (or multiple markets operating under different rules and gate-closures) where energy is traded. Bids for sale and purchase are collected by the market operators, which are responsible for optimally scheduling the dispatch of energy and allocating sufficient power reserve. The backbone of most liberalised electricity markets are the day-ahead markets, often referred to as *spot* markets (in Europe) or *forward* markets (in the U.S.), on which most of the trading takes place. Typically these markets offer a platform for trading energy to be delivered / withdrawn within a certain period during the upcoming day. The minimum period length is referred to as *trading*

period in this paper; every contract covers one or more trading periods.

Although most renewables are not easily predictable and non-dispatchable, renewable power producers are increasingly urged to participate in electricity markets in the same manner as producers of conventional energy. Here we specifically concentrate on wind energy, which has been the most rapidly growing renewable energy source over the last decade. Our developments and conclusions could however be similarly applied for other types of non-dispatchable renewables e.g. solar energy.

Wind power generation is the typical example of a stochastic and non-dispatchable renewable energy source. Although the possibility of curtailing power exists, it is not economically sound as long as the electricity price (including potential subsidies) remains positive. As a result, trading wind energy in a day-ahead electricity market requires forecasts of wind power production, which can be performed only with limited accuracy, as discussed in Madsen et al. (2005). Reviews of the state of the art of wind power forecasting methods and operational tools can be found in Giebel et al. (2003), Costa et al. (2008), Monteiro et al. (2009), while Botterud et al. (2010) discusses their application in electricity markets.

Differences between contracted and actual energy production (e.g. due to forecasting errors) have to be settled on the intra-day and/or the real-time markets. Due to shorter lead-time from gate closure to delivery, these markets might reduce the revenues of producers that cause imbalance, as more flexible market players are called to equilibrate the system – generally at higher costs. Joint operation of wind and hydro power has recently emerged as a way to reduce imbalance costs among other benefits, see for instance Angarita et al. (2009) or Montero and Perez (2009). However, this solution is only conceivable for market participants having both energy sources in their portfolio. For other producers, the most practical option for imbalance settlement is to rely on the market. Although it is sometimes possible to adjust contracts through existing intra-day markets, the volumes exchanged there are generally low, as illustrated by Weber (2010) for the main European electricity markets. Producers are therefore most often forced to rely on the real-time market, where bids for regulation are activated by the TSO close to real-time, and producers are charged for their imbalances, which are determined post-delivery. Hence, the only way for them to reduce imbalance costs is to bid optimally into the day-ahead market, so that the risk of facing losses on the real-time market is minimised. This bid is optimised conditioned upon the information available at the time of contracting, both in terms of future wind power production and market prices.

The penalties faced by electricity producers in the real-time market are generally asymmetric, in some cases even single sided, i.e. they are only to be paid

by the producers that increase the overall imbalance with their own. This incites market participants whose portfolio includes a stochastic component to be more strategic in their approach to bidding, see Skytte (1999). Indeed it can be analytically shown that under these conditions the optimal day-ahead market bid for a wind energy producer is a certain quantile of the distribution of wind power generation, see for instance Bremnes (2004), Linnet (2005), Pinson et al. (2007). This optimal quantile is a dynamic function of the day-ahead and the imbalance prices, which are not known a priori. Market experience shows that such optimal bids might significantly differ from the point forecasts of wind power production (consisting of the conditional expectation for each lead time). In practice, however, point forecasts are still commonly used when contracting wind power in the day-ahead market. A more theoretical discussion about quantile forecasts being optimal bids in electricity markets can be found in Gneiting (2011).

The existing literature has already described and analysed a number of strategies for trading wind power in the day-ahead market, with different approaches with regards to the uncertainty in production and in market prices. As a basic approach, some authors consider that traditional point forecasts of wind power generation may be used for analysing the value of wind energy in electricity markets, e.g. Angarita-Márquez et al. (2007), Barthelmie et al. (2008), Chang et al. (2009). Furthermore, Bathurst et al. (2002) models wind generation uncertainty through Markov probability tables and chooses, in a discrete decision space, the bid that minimises the expected costs. Alternatively, Galloway et al. (2006) suggests the construction of a utility cost function to model the financial risk of wind power producers participating in the market, using persistence forecasting of wind power and average values as price forecasts. The stochastic optimisation algorithm described in Matevosyan and Söder (2006) uses scenarios of wind power production as input along with historical imbalance prices. Besides, Pinson et al. (2007) makes use of probabilistic forecasts of wind power and yearly or quarterly average values of imbalance prices in order to determine the optimal quantile bid, in a fashion resembling that of Bremnes (2004). The same strategy is implemented in Gibescu et al. (2008), using probabilistic forecasts and measured data for wind speed and yearly averages as estimates of the day-ahead and real-time prices. Finally, Morales et al. (2010) proposes a linear programming technique for optimising the trade of wind energy in day-ahead, intra-day and real-time markets. The uncertainty in both wind power production and market prices is modelled through simple ARIMA / ARMA models. All these works and strategies either only account for uncertainty in wind power generation but disregard uncertainty in the market quantities, or include both but make use of simple forecasting methods.

In this work, we revisit the quantile strategy described in Bremnes (2004) and Pinson et al. (2007) and generalise it by considering stochastic rather than de-

terministic market prices. State-of-the-art probabilistic forecasts both of wind power generation and of market quantities are considered as input. These market quantities include the regulation sign, which can be down-regulation, up-regulation or no regulation, as well as the unit regulation costs. This strategy is formulated in Section 2 as a stochastic optimisation problem, which aims at the maximisation of the expected revenues (or utility) of the market participant. This approach is hereafter referred to as Expected Utility Maximisation (EUM). Having the maximisation of the expected value of the revenues as the objective, such an approach directly relates to a long-term optimisation of the market performance of the wind power producer. It is also shown through an example that, due to the uncertainties involved and potentially large forecast errors, such a strategy may occasionally lead to severe losses from a single contract. For instance this might occur when the regulation sign forecast wrongly assigns a high probability to an imbalance direction that is not realised. It is proposed in Section 3 to constrain the EUM bid in terms of deviations from the point forecasts, either in the quantity space or in the probability space. The two constraining methods are proposed with two different ranges of the allowed interval in the decision space. The motivation for this constraining is twofold. From a practical perspective, constraining the bid is beneficial, because system operators are reluctant to allow large deviations from the point forecasts. This is because efficient system planning requires market bids to closely reflect the actual delivery of energy. Moreover, since point forecasts have been used as operational bids since wind energy started to be traded on electricity markets, such point forecasts act as anchors in the mind of the operators. From a different point of view, this work shows that by setting a constraint on the allowed deviation from the point forecast, the trader can reduce the impact of forecasting errors and increase its risk-aversion. Next, in Section 4, the participation of a wind power portfolio in the Nord Pool market (Eastern Denmark price area) over a period of 10 months in 2008 is considered in order to evaluate the actual performance of the aforementioned trading strategies. To our knowledge a test-case of such length, combining state-of-the-art forecasts of wind power production, day-ahead and imbalance prices, as well as observed wind production and market data, has never been performed. The results of the exercise show the possibility for wind power producers to significantly reduce their imbalance costs and control the risk of dramatic losses.

The contribution of this paper to the state-of-the-art on the subject is threefold. First of all, the derivation of the optimal quantile strategy is extended to the case where market prices are stochastic. Owing to this formulation, probabilistic forecasts both of wind power production and of market quantities are needed by the decision maker. Secondly, we introduce constraining of the bid as a way to account for issues related to the practical implementability of the strategy and, in parallel, risk-aversion. Finally, we present a realistic test-case simulating wind power trading, and we assess the market value of state-of-the

art probabilistic forecasts of wind power production and of market quantities.

The derivation of the optimal quantile strategy presented in this paper is valid under the price-taker assumption, i.e. the wind power producer cannot influence market prices with its bid. Therefore, the aim of this work is to propose operational strategies and to assess the market value of forecasts under this hypothesis. In future markets with increasing penetration of wind power this assumption might not hold, since wind power producers might impact the total system imbalance and therefore influence the price formation mechanisms with their trading strategy. By introducing the constraining of the bid, this issue is partly addressed, since constrained strategies result in lower imbalance and, therefore, limit the impact on prices. The derivations and the results presented in this paper thus constitute a valuable starting point and a reference for further research on the subject, where the dependence structure between wind power production and market prices is taken into account.

The work presented here will support and serve as the basis for a real-world demonstration of stochastic approaches to wind power participation in electricity markets in the framework of the EU project ANEMOS.plus.

2 The Expected Utility Maximisation (EUM) bidding strategy

This section is devoted to the introduction of the strategy maximising the expected utility of a wind power producer participating at both the day-ahead and the real-time energy markets. At first, the strategy is derived in Section 2.1. Then, the forecasts needed in order to decide on the optimal bid are described in Section 2.2. Finally, possible shortcomings of the strategy are discussed based on a test-case in Section 2.3.

2.1 Derivation of the EUM strategy

In electricity day-ahead markets, power producers have to indicate the amount of energy they are willing to deliver at any trading period through a bid submitted to the market operator. Bids are collected with a certain lead-time to the physical delivery of energy. For example, at the Nord Pool day-ahead market the deadline for submission is at noon on the day prior to delivery. Let $\widetilde{W}_k$ denote the amount of energy contracted in the day-ahead market and let W_k be the stochastic production of wind energy, both for the k-th trading period. The power producer will then have to correct the stochastic imbalance $W_k - \widetilde{W}_k$ on

the real-time market. This is because the possibility of trading on the intra-day market is disregarded, due to its general illiquidity. Hence, the total revenues of the generator, ρ_k, can be expressed as the sum of the revenues, $\rho_k^{(S)}$ and $\rho_k^{(\uparrow/\downarrow)}$, obtained at the day-ahead and the real-time market respectively

$$\rho_k = \rho_k^{(S)} + \rho_k^{(\uparrow/\downarrow)} \tag{1}$$

The revenues at the day-ahead market can be determined as the multiplication of the contracted energy $\widetilde{W}_k$ with the day-ahead market price $\pi_k^{(S)}$

$$\rho_k^{(S)} = \pi_k^{(S)} \widetilde{W}_k \tag{2}$$

The real-time market revenues are positive if $W_k > \widetilde{W}_k$ (energy surplus to be sold) and negative if $W_k < \widetilde{W}_k$ (energy deficit to be purchased)

$$\rho_k^{(\uparrow/\downarrow)} = \begin{cases} \pi_k^{(\downarrow)}(W_k - \widetilde{W}_k), & W_k \geq \widetilde{W}_k \\ \pi_k^{(\uparrow)}(W_k - \widetilde{W}_k), & W_k < \widetilde{W}_k \end{cases} \tag{3}$$

In this expression, $\pi_k^{(\downarrow)}(\pi_k^{(\uparrow)})$ represents the unit down(up)-regulation price which is paid to (by) an overproducing (underproducing) generator. At Nord Pool real-time prices are restricted such that

$$\begin{aligned} \pi_k^{(\downarrow)} &\leq \pi_k^{(S)} \\ \pi_k^{(\uparrow)} &\geq \pi_k^{(S)} \end{aligned} \tag{4}$$

at all times. Then depending on the total imbalance of the system, the inequality sign is substituted by an equality sign in at least one of the two inequalities in Equation (4). More specifically, let the net system imbalance be denoted as

$$(\widetilde{G}_k - G_k) - (\widetilde{L}_k - L_k) \tag{5}$$

where $\widetilde{G}_k$ and G_k denote the total (i.e. summed over all the producers dispatched at the day-ahead market) energy production, contracted and realised respectively, for the k-th trading period. Similarly, $\widetilde{L}_k$ and L_k represent the contracted and realised consumption, respectively, for the consumers and the retailers scheduled at the day-ahead market. Notice that when the quantity in Equation (5) is different from zero, real-time bids have to be activated in order to restore energy balance. During hours of power surplus, i.e. when the net system imbalance in Equation (5) is < 0, the following holds for the prices

$$\begin{aligned} \pi_k^{(\downarrow)} &\leq \pi_k^{(S)} \\ \pi_k^{(\uparrow)} &= \pi_k^{(S)} \end{aligned} \tag{6}$$

This situation is commonly referred to as down-regulation. Conversely during hours of power deficit (when the system net imbalance in Equation (5) is > 0), commonly termed up-regulation, it holds that

$$\begin{aligned} \pi_k^{(\downarrow)} &= \pi_k^{(S)} \\ \pi_k^{(\uparrow)} &\geq \pi_k^{(S)} \end{aligned} \tag{7}$$

Finally during hours of perfect balance between load and production then

$$\pi_k^{(S)} = \pi_k^{(\downarrow)} = \pi_k^{(\uparrow)} \tag{8}$$

In this way, only the producers contributing to the overall system imbalance risk being penalised, while the ones acting to reduce it receive the day-ahead price for their realised production, when transactions on both the day-ahead and the real-time markets are combined. The rationale behind this choice of market design is that producers should not be allowed to profit from their imbalances. However, it should be pointed out that there are exceptions to this. For instance, the Dutch APX electricity market is just one example of a market where energy imbalance can actually be rewarded.

Now Equation (1) can be reformulated as:

$$\rho_k = \pi_k^{(S)} W_k + C_k^{(\uparrow/\downarrow)}. \tag{9}$$

Assuming that the wind power producer is a price-taker individually, which is reasonable if it does not hold a significant share of the total production, the term $\pi_k^{(S)} W_k$ in Equation (9) is independent of its decision. That is, neither the day-ahead price $\pi_k^{(S)}$ nor the wind power production W_k are influenced by the bidding policy adopted in the day-ahead market. This implies that curtailment is not considered as an option, for the reasons discussed in Section 1. The term $\pi_k^{(S)} W_k$ represents the revenues that the producer could achieve if it had perfect information on its future wind power production (i.e. if contracted power and wind power production are equal: $\widetilde{W}_k = W_k$). The second term in Equation (9) can be made explicit as

$$C_k^{(\uparrow/\downarrow)} = \begin{cases} \psi_k^{(\downarrow)}(W_k - \widetilde{W}_k), & W_k \geq \widetilde{W}_k \\ \psi_k^{(\uparrow)}(W_k - \widetilde{W}_k), & W_k < \widetilde{W}_k \end{cases} \tag{10}$$

where the variables $\psi_k^{(\downarrow)}$ and $\psi_k^{(\uparrow)}$ represent the unit regulation costs for positive and negative imbalances at the real-time market, and are given by

$$\psi_k^{(\downarrow)} = \pi_k^{(\downarrow)} - \pi_k^{(S)} \tag{11}$$

$$\psi_k^{(\uparrow)} = \pi_k^{(\uparrow)} - \pi_k^{(S)} \tag{12}$$

The quantity in Equation (10) therefore accounts for negative revenues, which represent the losses for the producer contracting $\widetilde{W}_k$ at the day-ahead market in comparison to the case of perfect information. At Nord Pool it holds that $C_k^{(\uparrow/\downarrow)} \leq 0$ at all times. Elsewhere (e.g. APX in the Netherlands), $C_k^{(\uparrow/\downarrow)} > 0$ might occur. Regarding the latter case, economists argue that although situations where producers can gain from their imbalance are possible, this cannot be exploited in the sense of strategic bidding. The argument is that the expectation $\mathbb{E}\left\{C_k^{(\uparrow/\downarrow)}|\chi\right\}$ of the losses given the information available at the moment of bidding is negative. As a consequence, the producers are expected to suffer losses from their imbalance in the long run, although in some trading periods they might be able to gain from it. Interested readers are referred to Boogert and Dupont (2005) for a detailed discussion.

As one can see from Equations (4), (11) and (12), at Nord Pool $\psi_k^{(\downarrow)} \leq 0$ and $\psi_k^{(\uparrow)} \geq 0$, and they are equal to zero in the cases of up- and down-regulation respectively. It should also be noted that both the unit regulation costs in Equations (11) and (12) are stochastic variables as the day-ahead price and the imbalance prices are not known in advance by the power producer.

It is assumed from now on that the wind power producer is *rational* (see e.g. Binmore (2008) for a conceptual introduction) and that its objective is the maximisation of the expected value of its total revenues. The set of bids $\widetilde{\mathbf{W}}^*$ maximising the total revenues is

$$\widetilde{\mathbf{W}}^* = \arg\max_{\widetilde{\mathbf{W}}} \mathbb{E}\left\{\sum_{k=i_{TP}}^{f_{TP}} \rho_k\right\} \tag{13}$$

where i_{TP} and f_{TP} are the shortest and the longest lead-times considered in the optimisation, respectively. Here the commonly accepted assumption of independence of decisions for different trading periods is followed. However it may be argued that market dynamics should be accounted for, see for instance Alvarado (1999), Liu (2006), Giabardo et al. (2010). Under the assumption of time-independent decisions over time, the maximisation of the sum of the revenues over time is equal to the maximisation of the revenues obtained at each single k. The optimal bid at the day-ahead market is then

$$\widetilde{W}_k^* = \arg\max_{\widetilde{W}_k} \mathbb{E}\{\rho_k\} \tag{14}$$

Since the first term in Equation (9) is not dependent on the decision on the day-ahead market, the maximisation of the expected revenues in Equation (14) is equivalent to the maximisation of the expectation of the regulation costs, which

are non-positive

$$\widetilde{W}_k^* = \arg\max_{\widetilde{W}_k} \mathbb{E}\left\{C_k^{(\uparrow/\downarrow)}\right\} \tag{15}$$

The problem in Equation (15) is a variant of the well known linear terminal loss problem (also called the newsvendor problem), see for instance Raiffa and Schlaifer (1964), in which the imbalance costs to be borne by the decision maker are stochastic, asymmetric and piecewise linear. Under the assumption that the unit up- and down-regulation costs are independent of the power producer's imbalance, these stochastic costs can be replaced by *certainty equivalents* in the optimisation problem. Assuming that the considered wind power producer is relatively small, such a simplification seems quite reasonable as the producer is a price-taker. Nevertheless, it is clear that some variables could influence wind power production and real-time costs at the same time. This could be the case of e.g. weather related variables in a relatively small power system. This issue goes beyond the scope of this article, but it certainly calls for future research in modelling variables influencing both prices and wind power production.

According to the theory of certainty equivalents, see Raiffa and Schlaifer (1964), the rational decision maker can determine the optimal decision without taking into account the whole distribution function of the unit costs. Instead an equivalent problem is solved, in which the stochastic unit costs are substituted by certain deterministic functions of the unit costs themselves. It is proved below that maximising $C_k^{(\uparrow/\downarrow)}$ in Equation (10) is equivalent to maximising the expectation of the following function with deterministic unit costs

$$\overline{C}_k^{(\uparrow/\downarrow)} = \begin{cases} \widehat{\psi}_k^{(\downarrow)}(W_k - \widetilde{W}_k) & W_k \geq \widetilde{W}_k \\ \widehat{\psi}_k^{(\uparrow)}(W_k - \widetilde{W}_k) & W_k < \widetilde{W}_k \end{cases} \tag{16}$$

where $\widehat{\psi}_k^{(\downarrow)}$ and $\widehat{\psi}_k^{(\uparrow)}$ denote the expected values of the unit regulation costs $\psi_k^{(\downarrow)}$ and $\psi_k^{(\uparrow)}$. The expectation of the imbalance costs in Equation (10) can be expanded as

$$\begin{aligned} \mathbb{E}\left\{C_k^{(\downarrow/\uparrow)}\right\} = &\int_0^{+\infty}\int_0^{\widetilde{W}_k} \psi_k^{(\uparrow)}(W_k - \widetilde{W}_k) dP_{W_k} dP_{\psi_k^{(\uparrow)}} \\ &+ \int_{-\infty}^{0}\int_{\widetilde{W}_k}^{W^{(max)}} \psi_k^{(\downarrow)}(W_k - \widetilde{W}_k) dP_{W_k} dP_{\psi_k^{(\downarrow)}} \end{aligned} \tag{17}$$

where $W^{(max)}$ is the installed capacity of the wind power producer. Still assuming independence between the unit regulation costs and wind power pro-

duction the integrations can be separated so that one gets to

$$\begin{aligned}\mathbb{E}\left\{C_k^{(\downarrow/\uparrow)}\right\} = &\int_0^{+\infty} \psi_k^{(\uparrow)} dP_{\psi_k^{(\uparrow)}} \int_0^{\widetilde{W}_k} (W_k - \widetilde{W}_k) dP_{W_k} \\ &+ \int_{-\infty}^{0} \psi_k^{(\downarrow)} dP_{\psi_k^{(\downarrow)}} \int_{\widetilde{W}_k}^{W^{(max)}} (W_k - \widetilde{W}_k) dP_{W_k}\end{aligned} \tag{18}$$

This is by definition equal to

$$\begin{aligned}\mathbb{E}\left\{C_k^{(\downarrow/\uparrow)}\right\} = &\widehat{\psi}_k^{(\uparrow)} \int_0^{\widetilde{W}_k} (W_k - \widetilde{W}_k) dP_{W_k} \\ &+ \widehat{\psi}_k^{(\downarrow)} \int_{\widetilde{W}_k}^{W^{(max)}} (W_k - \widetilde{W}_k) dP_{W_k}\end{aligned} \tag{19}$$

which is equal to the expected value of the equivalent loss in Equation (16).

The problem of maximising the expectation of the utility in Equation (16) is a standard linear terminal loss problem, which can then be treated as the general case in Raiffa and Schlaifer (1964). The proof is omitted here and only the expression for the Expected Utility Maximisation (EUM) bid is given

$$\widetilde{W}_k^* = F_{W_k}^{-1}\left(\frac{\left|\widehat{\psi}_k^{(\downarrow)}\right|}{\widehat{\psi}_k^{(\uparrow)} + \left|\widehat{\psi}_k^{(\downarrow)}\right|}\right) \tag{20}$$

where F_{W_k} is the cumulative distribution function of the wind power production W_k. Therefore, the EUM bid $\widetilde{W}_k$ is a quantile of the distribution of the stochastic variable W_k corresponding to the probability given by the fraction

$$\widetilde{r}_k^* = \frac{\left|\widehat{\psi}_k^{(\downarrow)}\right|}{\widehat{\psi}_k^{(\uparrow)} + \left|\widehat{\psi}_k^{(\downarrow)}\right|} \tag{21}$$

2.2 Input forecasts to the EUM strategy

From the treatment in Section 2.1 it follows that the determination of the optimal bid requires forecasts of both wind power production and imbalance costs.

As far as wind power production is concerned, a probabilistic forecast is needed, as the distribution F_{W_k} of the generation W_k appears in Equation (20). Here the non-parametric probabilistic tool described in Pinson (2006) and Pinson and Kariniotakis (2010) is considered. This tool provides the user with a set of forecast quantiles of the wind power distribution for each trading period. Let us

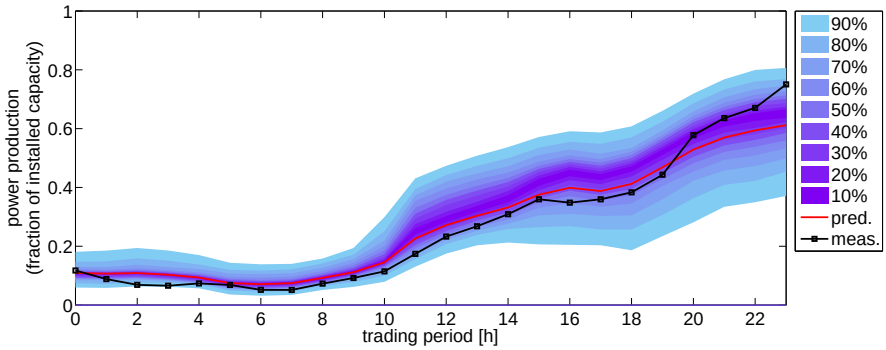

Figure 1: Example of probabilistic forecast of production for a wind power portfolio in Eastern Denmark. The forecast was issued on the previous day at 11am.

denote the α-quantile of wind power production at time k with $q_{W_k}(\alpha)$, such that

$$F_{W_k}\left(q_{W_k}(\alpha)\right) = \alpha \tag{22}$$

The provided forecasts are then

$$\widehat{q}_{W_k}(\alpha) = \mathbb{E}\left\{q_{W_k}(\alpha)\,|\,M,\boldsymbol{\theta},\chi_t\right\} \tag{23}$$

for different values $\alpha \in [0,1]$. The expectation on the right side of Equation (23) is conditioned on the choice of the model M, on its estimated parameters $\boldsymbol{\theta}$ and on the information χ_t available at the time t when the forecast is issued. It holds trivially that $t < k$. In the example of Nord Pool t might be 11am (one hour before the deadline for bidding), while k could be any of the hours in the following day. From now on the condition on the expectation is discarded in order to lighten the notation. However, the reader should keep this in mind whenever a forecast is defined. An example of quantile forecast can be seen in Figure 1. The complete forecast of the function F_{W_k} can then be obtained from the set of forecast quantiles $\widehat{q}_{W_k}(\alpha)$ by linear interpolation.

The expected values of the regulation costs $\widehat{\psi}_k^{(\downarrow)}$ and $\widehat{\psi}_k^{(\uparrow)}$ need to be forecast as well. Methods for forecasting the day-ahead market price $\pi_k^{(S)}$, as well as the unit imbalance costs $\psi_k^{(\downarrow)}$ and $\psi_k^{(\uparrow)}$, conditioned upon the regulation sign[1], are

[1] In Jónsson (2012) a given hour is defined as up-regulation hour if $\psi_k^{(\uparrow)} > 0$ and a down-regulation hour if $\psi_k^{(\downarrow)} < 0$.

described in Jónsson (2012). The following forecasts are therefore available

$$\widehat{\pi}_k^{(S)} = \mathbb{E}\left\{\pi_k^{(S)}\right\} \tag{24}$$

$$\widehat{\psi}^{(\downarrow)}_{k|\psi_k^{(\downarrow)}<0} = \mathbb{E}\left\{\psi_k^{(\downarrow)}|\psi_k^{(\downarrow)} < 0\right\} \tag{25}$$

$$\widehat{\psi}^{(\uparrow)}_{k|\psi_k^{(\uparrow)}>0} = \mathbb{E}\left\{\psi_k^{(\uparrow)}|\psi_k^{(\uparrow)} > 0\right\} \tag{26}$$

Jónsson (2012) also presents a method for estimating conditional posterior probabilities of imbalance in each direction being penalised at any given time k, defined as

$$P_k^{(\downarrow)} = P\left\{\psi_k^{(\downarrow)} < 0\right\} \tag{27}$$

$$P_k^{(\uparrow)} = P\left\{\psi_k^{(\uparrow)} > 0\right\} \tag{28}$$

From a pure trading perspective this is equivalent to predicting the sign of the actual imbalance as the trader is indifferent to imbalances he/she is not penalised for. The models for $\widehat{\psi}^{(\downarrow)}_{k|\psi_k^{(\downarrow)}<0}$, $\widehat{\psi}^{(\uparrow)}_{k|\psi_k^{(\uparrow)}>0}$ and $\widehat{P}_k^{(\uparrow/\downarrow)}$ are all conditional Holt-Winters models with a diurnal seasonality. For the penalty forecasts, the models are conditioned upon the forecast system load and the forecast spot price for the area, while the direction probability model is conditioned upon the forecast wind power penetration (i.e. the ratio between the forecast wind power production in the whole system and the forecast system load).

An example of forecasts of the regulation signs is shown in Figure 2. It should be noticed that the two probabilities in the figure do not sum to 1. Indeed, the probability of no regulation $P_k^{(0)}$ might also be positive, and at any time k it holds

$$P_k^{(\uparrow)} + P_k^{(\downarrow)} + P_k^{(0)} = 1 \tag{29}$$

The expected values $\widehat{\psi}_k^{(\downarrow)}$ and $\widehat{\psi}_k^{(\uparrow)}$ can then be determined according to the law of total expectation

$$\widehat{\psi}_k^{(\downarrow)} = \widehat{\psi}^{(\downarrow)}_{k|\psi_k^{(\downarrow)}<0}\widehat{P}_k^{(\downarrow)} + \widehat{\psi}^{(\downarrow)}_{k|\psi_k^{(\downarrow)}=0}(1-\widehat{P}_k^{(\downarrow)}) = \widehat{\psi}^{(\downarrow)}_{k|\psi_k^{(\downarrow)}<0}\widehat{P}_k^{(\downarrow)} \tag{30}$$

$$\widehat{\psi}_k^{(\uparrow)} = \widehat{\psi}^{(\uparrow)}_{k|\psi_k^{(\uparrow)}>0}\widehat{P}_k^{(\uparrow)} + \widehat{\psi}^{(\uparrow)}_{k|\psi_k^{(\uparrow)}=0}(1-\widehat{P}_k^{(\uparrow)}) = \widehat{\psi}^{(\downarrow)}_{k|\psi_k^{(\uparrow)}>0}\widehat{P}_k^{(\uparrow)} \tag{31}$$

In the cases when both $\widehat{\psi}_k^{(\downarrow)}$ and $\widehat{\psi}_k^{(\uparrow)}$ are zero the ratio in Equation (21) is not defined. In these cases the producer might bid the median, corresponding to the 0.5 quantile, which maximises the expected market revenues in the general case where the forecast penalties in the two regulation directions are equal.

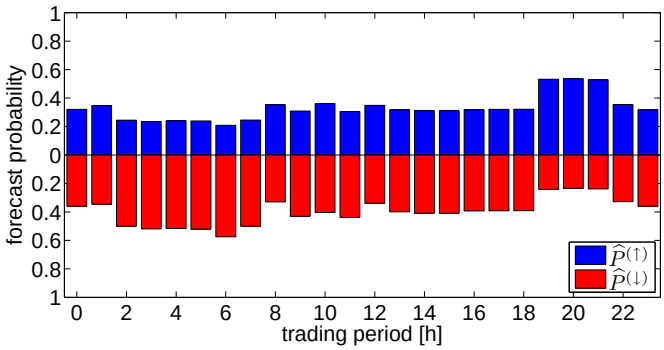

Figure 2: Example of forecast probabilities of up ($\widehat{P}^{(\uparrow)}$) and down ($\widehat{P}^{(\downarrow)}$) regulation in DK-2.

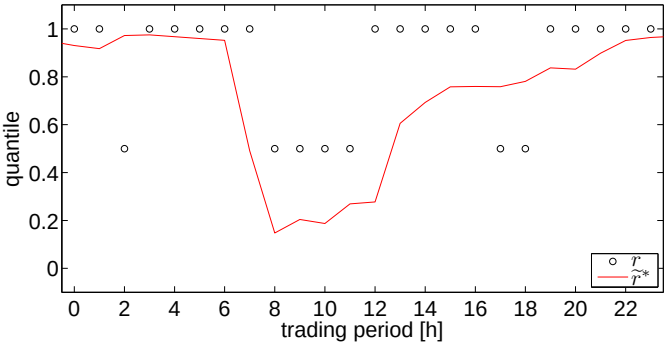

Figure 3: Optimal forecast ($\widetilde{r}^*$) and measured (r) ratios for a wind power portfolio in DK-2 on a selected day.

Figure 3 plots an example of forecast, $\widetilde{r}_k^*$, and measured, r_k, ratios in Equation (21) for a power producer in Eastern Denmark participating in Nord Pool. The resulting bid maximising the expected revenues is shown in Figure 4. As one can see from the scale employed on the y-axis of the figure, the bid is shown as a fraction of the total installed capacity. The point forecast, which is currently the reference for wind power producers participating in day-ahead markets, is also shown for comparison.

2.3 Testing the EUM bid

This section presents the setup and the results obtained in a test-case simulating energy trading in Nord Pool. Its aim is to assess the performance of the

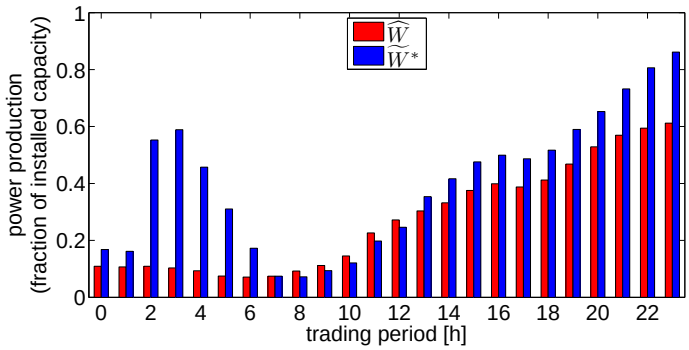

Figure 4: Example of point forecast ($\widehat{W}$) and EUM bid ($\widetilde{W}^*$) for a wind power portfolio in DK-2.

EUM bidding strategy compared to the traditional point forecast bidding. Afterwards, the main drawbacks of the EUM strategy are discussed, along with the reasons motivating the introduction of more risk-averse strategies, which are presented in Section 3.

In this test-case, the DK-2 (Denmark East) market area has been considered as the geographic location of the wind power plants of a virtual power producer. Data and forecast availability motivate the choice of a 10-month period of simulation, spanning from the 1st March 2008 to the 31st December 2008. The size of the producer is not defined, and all the results are scaled to its installed capacity. It is assumed, though, that the producer is a price-taker, i.e. that changes in its bidding policy do not influence the market. This implies that its size is small relatively to the total installed capacity in the region.

The data set used consists of measured wind power production, point and probabilistic forecasts of wind power production, observed regulation costs and the market forecasts previously described. All data refer to the DK-2 market area and have a temporal resolution of 1 hour. Based on point forecasts issued by WPPT, see Nielsen (2002), enf (2011), probabilistic wind power forecasts are obtained by the method described in Pinson and Kariniotakis (2010) and Pinson (2006) while market forecasts have been obtained as outlined in Jónsson (2012). All observations used are publicly available on www.energinet.dk.

For the sake of performing a realistic test-case, the forecasts of wind power production, of day-ahead and real-time market prices and of imbalance direction probabilities used in this study were issued before 11am of the previous day. Because the day-ahead gate closure at NordPool is noon, these forecasts are precisely the information available for producers bidding on the day-ahead

market.

Table 1 shows the economic results of the wind power producer in both the cases of point forecast bidding and of EUM bid. The third column represents the reduction in the imbalance costs in Equation (10) with respect to the case of point forecast bidding. Imbalance cost reduction is a relevant index for assessing the quality of a bidding strategy for wind power producers. Indeed, there is a "fatal" part, i.e. which could be achieved no matter how bad a bidding strategy is employed, that is implicitly included in the total producer profits. For example, a producer could at least earn its realised wind power production times the down-regulation price just by never participating at the day-ahead market. On the contrary, imbalance costs represent what the wind power producer can actually improve by employing a more advanced strategy. Furthermore, the imbalance cost reduction with respect to a reference bid, the point forecast in this example, provides with an upper bound for performance improvement, i.e. the 100% reduction that would be achieved by bidding with perfect information. The value of imbalance cost reduction in the first row is trivially 0, while one can notice that the improvement obtained with the EUM is 2.3%.

Figure 5 shows the subtraction of the cumulative revenues obtained with the EUM strategy and the cumulative revenues obtained with the point forecast bid for each trading period in the test-case. The difference in revenues is positive overall, meaning that the EUM bid is outperforming the point forecast bid in the long run. On the other hand, the performance of the EUM bid appears to be rather volatile and characterised by steep drops, for instance around the 1200th and the 4500th hours in the figure. This suggests that the producer adopting the EUM strategy is exposed to the risk of significant losses stemming from a single contract. It can be shown that the losses are due to inaccurate forecasts of the regulation costs or sign. What the EUM aims at is, essentially, to set the day-ahead market bid on the "safe" side of the decision space, i.e. on the imbalance direction that will not be penalised at the real-time market and paid at the day-ahead price $\pi_k^{(S)}$. As Figure 3 shows, by doing this the optimal ratio $\widetilde{r}_k^*$, and therefore the EUM strategy, results in being somewhat "extreme". In

Table 1: Economic results for the wind power producer in the test-case performed from the 1st March 2008 to the 31st December 2008 with real market data and forecasts issued for the DK-2 market area.

Strategy	Net revenue per installed MW (€/MW)	Imbalance cost per installed MW (€/MW)	Imbalance cost reduction (%)	Price per MWh (€/MWh)
Point forecast	94436.40	4076.51	0.00	54.48
EUM	94529.96	3982.95	2.30	54.54

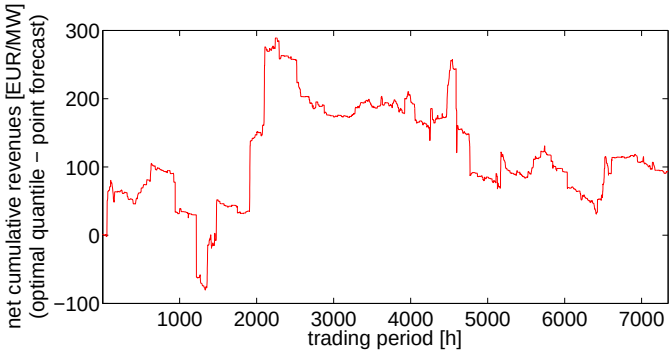

Figure 5: Subtraction of the cumulative revenues per installed MW using the EUM bid and the cumulative revenues using the point forecast. Its positive value signals an improvement in the performance.

fact, when the forecasts indicate that one regulation direction is far more likely than another, $\widetilde{r}_k^*$ tends to the extreme values 0 or 1, as shown in the early and late hours of the day in Figure 3. Figure 4 shows that this yields a bid that is significantly different from the point forecast during these hours. Generally situations where the EUM bid is close to the nominal capacity or zero are not rare. Hence the producer is in the situation of probably having a great imbalance in the forecast "safe" regulation direction. In the case that the forecasts leading to $\widetilde{r}_k^*$ are correct, the imbalance is paid at the day-ahead price $\pi_k^{(S)}$, with no loss for the producer. On the other hand, if the forecast turns out to be incorrect the producer will have to pay regulation costs for a high amount of energy, resulting in one of the significant losses shown in Figure 5. Furthermore, the wind power producer using the EUM strategy can be expected to incur large imbalances, which are unwanted by the TSO. This casts doubt on the possibility of using the EUM strategy in practice.

3 Constraining the EUM bid

As an extension to the EUM strategy, a parameter for constraining the bid is introduced in this section as a way to reduce the expected imbalance level. There are several motivations for doing this. As Section 2 discussed, the EUM bid is often quite far from the point forecast. On the other hand market authorities require that the energy bid be representative of the actual (or forecast) production of a generator. Hence an excessive deviation of the bid from the expected production could be seen as a way to take advantage of the market and thus it could be penalised. Secondly, a strategy causing high imbalance

levels might influence the price formation mechanism, especially with respect to the regulation prices. If this happens, the price-taker assumption is violated and, therefore, the model of the market becomes inconsistent.

As a matter of fact, the point forecast bid is a robust decision when the producer is seeking to minimise the impact on the system imbalance. Indeed, the point forecast commonly minimises the expectation of the squared deviation from the energy production W_k

$$\widehat{W}_k = \arg\min_x \mathbb{E}\left\{(x - W_k)^2\right\} \tag{32}$$

It should be pointed out, though, that different criteria could be employed Bessa et al. (2011). The most commonly used least-squares criterion only makes the point forecast optimal in the sense of minimising imbalance volumes (in squared values), with no economic considerations. Therefore, a compromise between the EUM bid and the point forecast could reconcile revenue maximisation with practical implementability of the strategy, with respect both to monitoring of the bid by the TSO and to potential violations of the price-taker assumption. Moreover, seeking a compromise between these two strategies is intuitively related to the reduction of risk. Indeed, as discussed above, the EUM strategy is exposed to the risk of large losses under price-forecasting errors. By trying to render the bid less extreme, i.e. closer to the point forecast, the producer would reduce the amount of regulating power, and therefore losses, in these cases. This will be illustrated in the test-case in Section 4. Finally, energy traders are somehow bound to the point forecast, which has traditionally been bid on the day-ahead market and has proved to be reliable over the years. For this reason it is desirable for an operational strategy not to deviate too much from it.

The main idea in this section is that the bid should somehow be bounded to some values around the point forecast. In this way extreme bid values - and hence extreme losses - are avoided. Constraints can be imposed in the decision space, so that the bid $\widetilde{W}_k^*$ is limited within a certain interval $\left[\underline{W}_k, \overline{W}_k\right]$. The mathematical formulation is described in Section 3.1. As an alternative, the limit can be imposed in the probability space so that the optimal ratio $\widetilde{r}_k^*$ is limited in a similar interval $[\underline{r}_k, \overline{r}_k]$. This is introduced in Section 3.2.

3.1 Constraints in the decision space

In this section we propose the determination of the allowed interval for the bid as a function of the expected value of wind power production $\widehat{W}_k$.

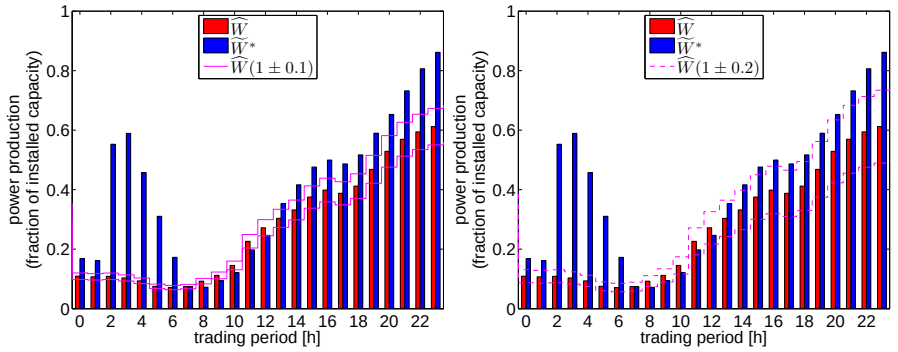

Constraints in value ($a_v = 0.1$)

Constraints in value ($a_v = 0.2$)

Figure 6: Point forecast ($\widehat{W}$), EUM bid ($\widetilde{W}^*$) and allowed interval with constraints on the decision space.

The allowed interval of the decision space is centred around the point forecast

$$\widehat{W}_k = \mathbb{E}\{W_k\} \tag{33}$$

and has radius equal to a certain percentage of this value itself. Two values for the radius are used in the application case-study, i.e. 10% and 20% of $\widehat{W}_k$. Naturally the larger the allowed interval the more risk-neutral the strategy. The suggested bid in this case can be determined as

$$\widetilde{W}_k^{v,a_v} = \min\left\{\max\left\{\widetilde{W}_k^*, \widehat{W}_k \cdot (1 - a_v)\right\}, \widehat{W}_k \cdot (1 + a_v)\right\} \tag{34}$$

where a_v is to be set to either 0.1 or 0.2. Figures 6a and 6b show the EUM bid and the point forecast $\widehat{W}_k$ along with the allowed intervals with $a_v = 0.1$ and $a_v = 0.2$.

3.2 Constraints in the probability space

In the second method proposed here, the ratio $\widetilde{r}_k^*$ in Equation (21) is allowed to span a certain interval in the probability space. This interval is centred around the value of the cumulative distribution at the point forecast $\widehat{W}_k$

$$\widehat{r}_k = F_{W_k}\left(\widehat{W}_k\right) \tag{35}$$

The radius of the interval is then to be set to a certain fraction of the probability space. In this work the radii 0.1 and 0.2 are used. The constrained bid can then

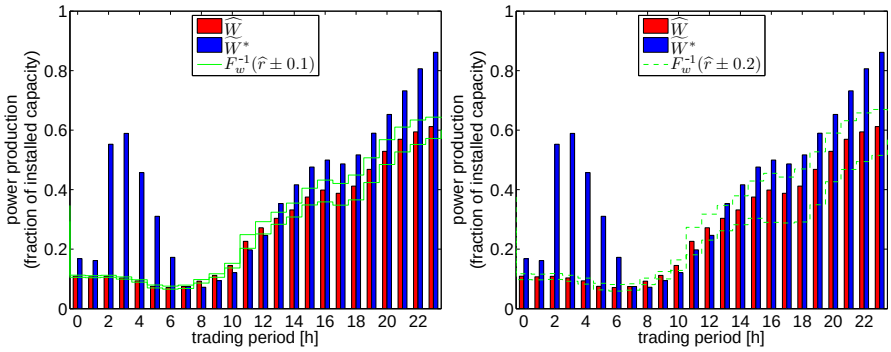

Constraints in probability ($a_p = 0.1$)

Constraints in probability ($a_p = 0.2$)

Figure 7: Point forecast ($\widehat{W}$), EUM bid ($\widetilde{W}^*$) and allowed interval with constraints on the probability space.

be determined as

$$\widetilde{W}_k^{p,a_p} = {F_{W_k}}^{-1}\left(\min\left\{\max\left\{\widetilde{r}_k^*, \widehat{r}_k - a_p\right\}, \widehat{r}_k + a_p\right\}\right) \tag{36}$$

where a_p is to be set to 0.1 or 0.2 according to the desired risk aversion of the bid. Figures 7a and 7b show the EUM bid and the point forecast $\widehat{W}_k$ along with the allowed intervals with $a_p = 0.1$ and $a_p = 0.2$.

4 Test case results

In this section we discuss the results of a test-case simulating the strategies presented above in a realistic market situation. The setup of the test-case is the same as described in Section 2.3. Section 4.1 discusses the performance of the bidding strategies from the point of view of the producer and its economic result, while Section 4.2 discusses the implications of the proposed strategies from a system point of view.

4.1 Economic advantage of the strategies

The main economic results for the power producer are shown in Table 2. This shows the total revenues of the producer and its imbalance losses per MW of installed capacity, the percentage reduction in imbalance losses obtained by the

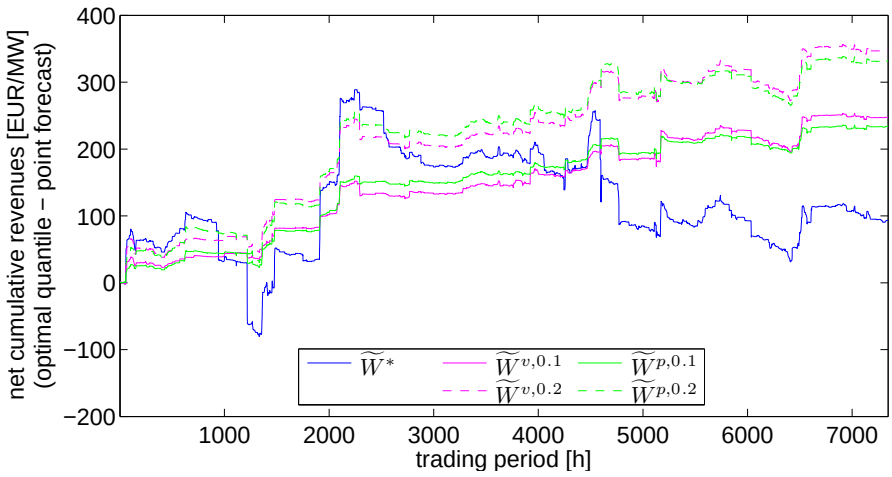

Figure 8: Improvement of the cumulative revenues for the strategies described in Sections 2 and 3 with respect to the point forecast bidding strategy.

strategy compared to the case of point forecast bidding and the average price per MWh paid to the producer.

As one can see, the constrained strategies introduced in the previous section produce better results than the plain EUM one. The reduction in imbalance costs amounts to around 6% when the constraint limit is set to 10% (both in value and in probability) and to around 8.5% when it is set to 20%. A slightly better performance is obtained by constraining in value than in probability. As far as the last column of Table 2 is concerned it should be mentioned that with perfect information on wind power production the energy would have been sold at an average price of €56.83 in the considered period.

The improved profits obtained with these strategies, compared to that of using the point forecast bidding, are illustrated in Figure 8. Indeed, this figure displays the difference between the cumulative revenues obtained by using the EUM strategy and its constrained versions and the revenues obtained by bidding the point forecast. All the cumulative revenues in this plot are expressed in € per MW of installed wind power capacity. It can be seen how the EUM bid ($\widetilde{W}$) is the least efficient strategy, apart from the point forecast bidding. The constrained strategies, besides performing better than the EUM, are also less exposed to significant isolated losses.

In view of the results above, there is clearly a relationship between range of the constraint and net revenues. Intuitively, there is also a relationship with risk,

since as pointed out in Section 3 an increase in the allowed bid range results in a higher risk of a large imbalance, and therefore a higher risk of large losses. In principle, the full joint probability distribution of wind power production and market prices should be employed in order to assess risk quantitatively. An *a posteriori* approach is followed here, in that risk is assessed by analysing the realised standard deviation of the hourly imbalance losses.

Figures 9a and 9b show the imbalance cost reduction obtained in the test-case as a function of the parameters a_v and a_p. The trend is increasing in both cases up to a certain value of the parameter (approximately 0.6 and 0.2 for a_v and a_p respectively). Increasing the constraining parameter further beyond these critical values results in less profits. This is because the distribution of the producer's hourly revenues is bounded on the upper side by $\pi_k^{(s)} W_k$. By allowing larger deviations from the point forecasts, this maximum value of the revenues is reached during more and more trading periods. In this way the rate of growth of the revenues slows down, as fewer trading periods offer possible improvements. Meanwhile, when forecasts are not perfect the risk of losses increases. When the critical level of the constraining parameter is reached, the increased losses exceed the revenue growth, resulting in the negative slopes on the right sides of Figures 9a and 9b. This decline is only stopped when the allowed bid interval is large enough to contain the optimal quantiles for all trading periods, as in the flat part of the curve on the right side of Figure 9b. At that point the constrained strategy is in practice equal to the original EUM strategy.

The empirical standard deviation of the hourly imbalance losses is plotted in Figure 9c and 9d. As one can see in Figure 9d, the EUM strategy (to which the constrained strategy converges when the constraining parameter a_p is just above 0.6) is the riskiest strategy, since it incurs the highest standard deviation of hourly losses. Strategies with lower values of the constraining parameters are subject to lower risk, but the trend is not monotonic all the way down to the point forecast (achieved with $a_v = a_p = 0$). The latter strategy would in fact be very risk-averse in case of equal penalties for up- and down-regulation. In a realistic case with different penalties, the most risk-averse constrained strategy is obtained for a value a_v slightly lower than the one delivering best revenues, while the value a_p that delivers the highest revenues is to a good approximation the one that is minimising the standard deviation of the losses.

Furthermore, Table 2 and Figures 9a and 9b indicate that the EUM strategy does not achieve the best performance among the considered strategies in the simulated market period. One would expect that a 10-month period is long enough for considering the incidence of isolated losses on the cumulative revenues negligible, so that the EUM strategy achieves the optimal performance. On the contrary, this study seems to suggest that the EUM strategy is not opti-

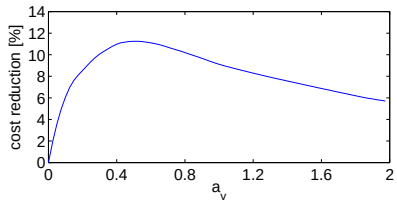

Imbalance loss reduction with constraints in value

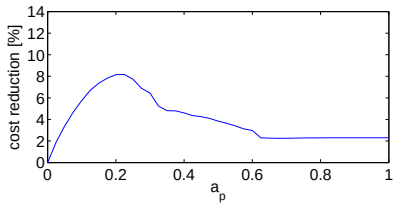

Imbalance loss reduction with constraints in probability

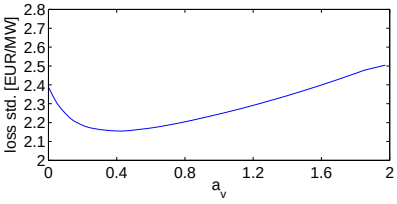

Imbalance loss standard deviation with constraints in value

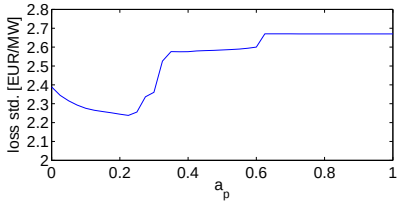

Imbalance loss standard deviation with constraints in probability

Figure 9: Producer's imbalance loss reduction and standard deviation in the test-case as a function of constraining parameter.

mal in practice. Indeed, even from a theoretical point of view the EUM bid is optimal only under the assumption that probabilistic forecasts of wind power production and of market prices are correct. In practice, errors in the probabilistic forecasts might cause the loss of optimality that is observable in this test-case. On the other hand the constrained strategies seem to limit the negative effects of forecast errors both by reducing the risk of losses stemming from single hourly-contracts and by achieving a better performance in the long run.

4.2 Interaction with the system

This section sheds some light on the effects of the strategies presented in Sections 2 and 3 in terms of energy imbalance introduced in the system.

Table 3 shows the simulation results in terms of imbalance direction. The first three columns show the energy imbalance brought to the system by the wind producer in the considered 10 months, in total and divided between positive, i.e. producer being long (second column), and negative imbalance, i.e. pro-

ducer being short (third column). All the values are expressed in hours of operation at nominal capacity, i.e. they are obtained by dividing the total energy imbalance (MWh) over the simulation by the installed capacity (MW). It can be seen that the more risk-neutral the strategy, the higher the overall energy imbalance. In this sense, the EUM strategy appears to have an extreme behaviour, pushing the total imbalance from less than 500 hours of operation, obtained with the point forecast bid, to over 700 hours. The four constrained strategies appear to have a limited effect on the overall imbalance. The strategies with tighter bounds ($\pm$ 10% in value and $\pm$ 0.1 in probability) cause only a negligible increase, while when the ones with the less restrictive bounds ($\pm$ 20 % in value and $\pm$ 0.2 in probability) are used the total imbalance rises by 35 hours at most.

Furthermore, an evaluation of the second and the third columns shows that generally more advanced strategies tend to bid above the actual production. This means that the producer is more often short rather than long. In fact, one can see that the difference between the values in the second and the third columns, which is almost zero with the point forecast bidding, tends to spread markedly when other strategies are used. This result might at a first sight look counterintuitive, since penalties are on average higher for up-regulation than for down-regulation. Nevertheless other factors, i.e. skewness of wind power production distribution, have an influence on this. According to expectations, the prevalence of up-regulation power is more evident when less risk-averse strategies are used.

The fourth and the fifth columns of Table 3 show the percentage of market hours during which the producer is long and short respectively. It can be seen that the variation in number of regulation hours, despite the significant variation in the imbalance volumes, is at most 1.5%. This indicates that the proposed strategies change the volumes of the energy imbalance but not the general trend in the number of up- or down-regulation periods. Finally, the last two columns show the maximum value of energy imbalance, again expressed in hours of operation at nominal capacity, during a single hour. Interestingly only the row corresponding to the EUM bid shows a considerable increase, which underlines the fact that constraining the EUM bid is an effective method to limit the maximum value of imbalance.

Table 4 looks at the producer's imbalance from a different perspective. This table separates the results for the imbalance into two components: the component opposite to the overall system imbalance, which is paid at the day-ahead market price and is shown in the second and the fourth columns, and the component in the same direction, which is paid at the day-ahead price minus the imbalance cost and is shown in the third and fifth columns. While in the case of the EUM bid the third column shows a significant increase, its val-

ues are roughly unchanged with the tighter constraints and slightly increased with the looser ones. In turn, the second column increases by a significant amount in most cases. These two facts indicate that the increase in energy imbalance caused by the use of more advanced strategies, which has been discussed above, actually involves only the direction in which the producer is not penalised, i.e. the one paid at the day-ahead price. There are two implications of this. On one hand, part of the energy imbalance is shifted to the opposite direction with respect to the system imbalance (second column in Table 4), thus contributing to restoring the overall balance – yet on a marginal level due to the price-taker assumption. In other words, the proposed constrained strategies are able to better "read" the feedback signal sent by the regulation prices and adapt to it, thus reducing the system imbalance. On the other hand, the variation in imbalance could become significant if the proposed strategies become common practice for producers. As a result, this could influence the formation of the regulation prices as well as possibly change the direction of the system imbalance. While it has been shown that the trading behaviour of wind power producers is capable of affecting day-ahead prices at NordPool even at the current level of market penetration, see Jónsson et al. (2010a,b), the relationship with the real-time market penalties, which are the quantities that ultimately determine the optimal bid in Equation (20), has not been investigated yet. In the event that the trading strategies presented above become common practice, they might influence the real-time penalties and no longer be optimal, and could possibly destabilise the system. Then, the market power of wind power producers should be accounted for if efficient bidding strategies are to be designed for producers with a large total capacity or for combined producers. This can be achieved by modelling energy markets as closed-loop systems, see for instance Liu (2006), Giabardo et al. (2010).

5 Conclusions

In this work, the optimal quantile strategy for trading wind power in liberalised energy market is revisited. It is shown that this strategy maximises the expected value of the market revenues (utility), under the assumption that the wind power producer is a price-taker, i.e. its market strategy is not capable of influencing price formation. The use of the Expected Utility Maximisation (EUM) strategy in practice requires probabilistic forecasts of wind power production, point forecasts of day-ahead and real-time market prices and of the imbalance sign probabilities. All these forecasts can be provided by state-of-the-art forecasting techniques.

An evaluation of the EUM strategy in a realistic test-case in Nord Pool highlights both its improved performance and its risk-neutral nature. The former

Table 2: Economic results for the wind power producer in the test-case.

Strategy	Net revenue per installed MW (€ / MW)	Imbalance cost per installed MW (€ / MW)	Imbalance cost reduction (%)	Price per MWh (€ / MWh)
Point forecast	94436.40	4076.51	0.00	54.48
EUM	94529.96	3982.95	2.30	54.54
Constrained (±10% value)	94684.18	3828.74	6.08	54.63
Constrained (±20% value)	94784.27	3728.64	8.53	54.68
Constrained (±10% probability)	94670.78	3842.13	5.75	54.62
Constrained (±20% probability)	94768.55	3744.37	8.15	54.67

Table 3: Energy imbalance of the wind power producer in the test-case.

Strategy	Energy imbalance (h)			Imbalance hours (%)		Max value (h / h)	
	Total	> 0	< 0	> 0	< 0	> 0	< 0
Point forecast	484.92	235.94	248.98	45.45	54.47	0.54	0.70
EUM	755.29	269.93	485.35	46.28	53.72	0.66	0.89
Constrained (±10% value)	495.91	236.48	259.43	44.26	55.73	0.56	0.68
Constrained (±20% value)	519.70	244.82	274.88	44.06	55.91	0.58	0.68
Constrained (±10% probability)	488.94	237.82	251.12	46.09	53.91	0.57	0.68
Constrained (±20% probability)	514.62	245.98	268.64	46.60	53.40	0.59	0.68

Table 4: Energy imbalance of the wind power producer in the test-case.

Strategy	Energy imbalance (h)			Imbalance hours (%)	
	Total	Day-Ahead price	Penalty	Day-Ahead price	Penalty
Point forecast	484.92	277.71	207.21	62.81	37.19
EUM	755.29	498.66	256.62	65.14	34.86
Constrained (±10% value)	495.91	286.72	209.19	63.16	36.84
Constrained (±20% value)	519.70	304.85	214.85	63.59	36.41
Constrained (±10% probability)	488.94	281.93	207.00	62.72	37.28
Constrained (±20% probability)	514.62	301.74	212.87	63.39	36.61

is underlined by a 2.3% reduction of the imbalance costs. As far as the latter is concerned, the test-case shows that this strategy is exposed to a number of significant losses that take place in short periods of time. These losses are caused by the use of inaccurate forecasts which cause the bid to differ significantly from the actual wind power production.

Constraining of the bid is then introduced in two different versions: with constraints in the decision space and in the probability space. The main idea is that bounding the bid to a certain interval around the point forecast can help reduce the distance of the bid from the actual wind power production. This heuristic can solve some issues, associated with the control of market authorities of the producer's bid as well as with its influence on the price formation mechanism. Indeed, constrained strategies generally reduce the imbalance introduced by the wind power producer in the system, thus lowering the potential impact on real-time prices and the sub-optimality of the strategy in a price-maker market environment. Moreover, the risk of incurring high regulation costs is also reduced by using constrained strategies.

Furthermore, the test-case is extended in order to assess the performance of the constrained strategies. The results of the simulation show that the constrained strategies outperform both the point forecast and the EUM strategies. The latter fact shows that constraining the EUM bid is also an effective way for reducing the impact of forecast errors on long-term revenues. At a second stage in the test-case, the interactions between a producer employing this strategy and the overall system are analysed. It is shown that only the EUM bid causes a significant increase in the total energy imbalance compared to the point forecast bid. The constrained strategies increase the amount of regulated energy at most by about 10% in the case of less restrictive bounds, while the increase is negligible when the strategies with tighter bounds are adopted. Moreover, it is pointed out that this increase in the regulated power involves only the component in the opposite direction compared to the overall system imbalance. As a result, the constrained strategies might be able to reduce the overall imbalance, thus marginally benefiting the system, at least as long as they do not become common practice.

We underline that the obtained results hold as long as the wind power producer does not own a significant share of the overall production capacity. When this hypothesis is not true, the power producer cannot be considered a price-taker. It is expected that in this case the performance of the proposed strategies decreases. In addition, the assertion that these strategies may be beneficial to the system by reducing the overall imbalance might prove incorrect. This is because such a large producer -or many smaller producers using the same bidding policy- might change the direction of the system imbalance, thus contributing positively to it rather than reducing it. For these reasons, an in-

teresting future development of this work could be to study the relationship between the bid of a large wind power producer and the formation of the regulation prices in the real-time market. This could then lead to the formulation of optimal bidding strategies of practical use for large wind power producers, as well as more stable from a system point of view.

Similarly, modelling explanatory variables influencing wind power production and energy market prices at the same time is of clear interest for future research. This would account for the situation where a high penetration of wind power in the system is able to influence the prices, although the considered wind power producer is too small to have any sort of market power on its own.

Besides, trading on the intra-day market could also be included in the problem under the assumption of sufficient liquidity of this market. As shown in Morales et al. (2010), this trading floor gives market participants further possibilities for reducing the risk of losses. Indeed, producers can employ forecasts with a shorter lead-time (typically one hour) with clear advantages in terms of accuracy. Therefore, an assessment of the advantages both for the producers and the system obtained by increasing the liquidity of balancing markets would be particularly interesting.

Finally, another direction for further research could be to account for the dynamic aspects of the market. In this way the assumption of independence of decisions in different trading periods would be overcome. The dynamic view of the market could include, for instance, modelling competition among producers as well as the market participation of mixed portfolios. In the latter case a typical situation could be the coupling of wind power with hydro power or energy storage, both of which allow for shifts in the trade of power between different trading periods. This research could lead to the determination of more advanced bidding strategies in competitive market environments, possibly for producers with a diversified portfolio of energy sources.

6 Acknowledgements

The work presented has been partly supported by the European Commission, which is hereby greatly acknowledged, under the Anemos.plus project (ENK6-CT2006-038692). The authors would also like to give credit to DONG Energy, ENFOR, Nord Pool and Energinet.dk for their role in providing the data used in this work. In particular, the authors would like to thank Torben S. Nielsen and Henrik Aa. Nielsen from ENFOR, as well as John Tøfting, Jes Smed and Lars Kruse from DONG Energy for the constructive discussions that enhanced

the level of this research. Finally, we express our gratitude to the Editor of this journal and to the three anonymous referees for providing insightful comments and suggestions for improving this manuscript.

References

ENFOR's website, June 2011. URL http://www.enfor.dk.

Fernando Alvarado. The stability of power system markets. *IEEE Transactions on Power Systems*, 14(2):505–511, 1999.

Jorge L. Angarita, Julio Usaola, and Jorge Martínez-Crespo. Combined hydro-wind generation bids in a pool-based electricity market. *Electric Power Systems Research*, 79(7):1038–1046, 2009.

Jorge L. Angarita-Márquez, Carlos A. Hernandez-Aramburo, and Julio Usaola-Garcia. Analysis of a wind farm's revenue in the British and Spanish markets. *Energy Policy*, 35(10):5051–5059, 2007.

R.J. Barthelmie, F. Murray, and S.C. Pryor. The economic benefit of short-term forecasting for wind energy in the UK electricity market. *Energy Policy*, 36 (5):1687–1696, 2008.

G.N. Bathurst, J. Weatherill, and G. Strbac. Trading wind generation in short-term energy markets. *IEEE Transactions on Power Systems*, 17(3):782–789, 2002.

R.J. Bessa, V. Miranda, A. Botterud, and J. Wang. 'Good' or 'bad' wind power forecasts: A relative concept. *Wind Energy*, 14(5):625–636, 2011.

K. Binmore. *Game theory: a very short introduction*. Oxford University Press, 2008.

Alexander Boogert and Dominique Dupont. On the effectiveness of the anti-gaming policy between the day-ahead and real-time electricity markets in the Netherlands. *Energy Economics*, 27(5):752–770, 2005.

Audun Botterud, Jianhui Wang, Vladimiro Miranda, and Ricardo J. Bessa. Wind power forecasting in U.S. electricity markets. *The Electricity Journal*, 23(3):71–82, 2010.

John B. Bremnes. Probabilistic wind power forecasts using local quantile regression. *Wind Energy*, 7(1):47–54, 2004.

Junying Chang, Bart C. Ummels, Wilfried G.J.H.M. van Sark, and Huub P.G.M. den Rooijen. Economic evaluation of offshore wind power in the liberalized Dutch power market. *Wind Energy*, 12(5):507–523, 2009.

A. Costa, A. Crespo, J. Navarro, G. Lizcano, H. Madsen, and E. Feitosa. A review on the young history of the wind power short-term prediction. *Renewable and Sustainable Energy Reviews*, 12(6):1725–1744, 2008.

S. Galloway, G. Bell, G. Burt, J. McDonald, and T. Siewerski. Managing the risk of trading wind energy in a competitive market. *Generation, Transmission and Distribution, IEE Proceedings*, 153(1):106–114, 2006.

P. Giabardo, M. Zugno, P. Pinson, and H. Madsen. Feedback, competition and stochasticity in a day ahead electricity market. *Energy Economics*, 32(2):292–301, 2010.

M. Gibescu, W. L. Kling, and E. W. Van Zwet. Bidding and regulating strategies in a dual imbalance pricing system: case study for a Dutch wind producer. *International Journal of Energy Technology and Policy*, 6(3):240–253, 2008.

G. Giebel, G. Kariniotakis, and R. Brownsword. The state of the art in short-term prediction of wind power – a literature overview. Technical report, EU project ANEMOS, Deliverable Report D-1.1, available online: http://www.anemos-project.eu, 2003.

Tilmann Gneiting. Quantiles as optimal point forecasts. *International Journal of Forecasting*, 27(2):197–207, 2011.

T. Jónsson. *Forecasting and decision-making in electricity markets with focus on wind energy*. PhD thesis, DTU Informatics, Technical University of Denmark, Kgs.Lyngby, Denmark, 2012.

T. Jónsson, P. Pinson, and H. Madsen. On the market impact of wind energy forecasts. *Energy Economics*, 32(2):313–320, 2010a.

T. Jónsson, M. Zugno, H. Madsen, and P. Pinson. On the market impact of wind power (forecasts) – An overview of the effects of large-scale integration of wind power on the electricity market. In *IAEE's 33rd International Conference*, Rio de Janeiro, Brazil, 2010b.

U. Linnet. Tools supporting wind energy trade in deregulated markets. Master's thesis, Technical University of Denmark, 2005.

Y. Liu. *Network and temporal effects on strategic bidding in electricity markets*. PhD thesis, University of Hong Kong, 2006.

Henrik Madsen, Pierre Pinson, George Kariniotakis, Henrik Aa. Nielsen, and Torben S. Nielsen. Standardizing the performance evaluation of short-term wind power prediction models. *Wind Engineering*, 29(6):475–489, 2005.

J. Matevosyan and L. Söder. Minimization of imbalance cost trading wind power on the short-term power market. *IEEE Transactions on Power Systems*, 21(3):1396–1404, 2006.

C. Monteiro, R. Bessa, V. Miranda, A. Botterud, J. Wang, and G. Conzelmann. Wind power forecasting: State-of-the-art 2009. Technical Report ANL/DIS-10-1, Argonne National Laboratory, 2009.

Fernando Peran Montero and Juan J. Perez. Pump up the volume: Using hydro storage to support wind integration. *Renewable Energy World*, 12(5):80–88, 2009.

Juan M. Morales, Antonio J. Conejo, and Juan Pérez-Ruiz. Short-term trading for a wind power producer. *IEEE Transactions on Power Systems*, 25(1):554–564, 2010.

Torben Skov Nielsen. *Online prediction and control in nonlinear stochastic systems*. PhD thesis, Technical University of Denmark, 2002.

P. Pinson. *Estimation of the uncertainty in wind power forecasting*. PhD thesis, Ecole des Mines de Paris, France, 2006.

P. Pinson and G. Kariniotakis. Conditional prediction intervals of wind power generation. *IEEE Transactions on Power Systems*, 25(4):1845–1856, 2010.

P. Pinson, C. Chevalier, and G.N. Kariniotakis. Trading wind generation from short-term probabilistic forecasts of wind power. *IEEE Transactions on Power Systems*, 22(3):1148–1156, 2007.

H. Raiffa and R. Schlaifer. *Applied statistical decision theory*. Division of Research – Harvard Business school, 1964.

K. Skytte. The regulating power market on the Nordic power exchange Nord Pool: an econometric analysis. *Energy Economics*, 21(4):295–308, 1999.

C. Weber. Adequate intraday market design to enable the integration of wind energy into the European power systems. *Energy Policy*, 38(7):3155–3163, 2010.

PAPER E

Risk Averse Bidding of Wind Power - Formulation and Properties

Authors:
T. Jónsson, S. M. Ryan, M. Zugno, P. Pinson

Published in:
IMM Technical Report 2012-03

Risk Averse Bidding of Wind Power - Formulation and Properties

Tryggvi Jónsson[1,2] Sarah M. Ryan[3] Marco Zugno[2] Pierre Pinson[2]

Nomenclature

Main symbols:

ρ_k	Wind power producer revenues at trading period k
W_k	Wind power production at trading period k
π_k	Market price at trading period k
C_k	Negative wind power producer revenues due to imbalance at trading period k
ψ_k	Unit regulation costs for positive and negative imbalances at trading period k
$W^{(max)}$	Installed wind power capacity
r_k	Quantile of wind power distribution at trading period k
P_k	Probability of imbalance direction at trading period k
a_v	Parameter determining the width of the bound to the optimal bid in the decision space
a_p	Parameter determining the width of the bound to the optimal bid in the probability space

Superscripts:

(S)	Referring to the day-ahead market
$(\uparrow/\downarrow)$	Referring to the real-time market
$(\uparrow)$	Referring to up-regulation in the real-time market
$(\downarrow)$	Referring to down-regulation in the real-time market
$*$	Optimal
$\sim$	Contracted at the day-ahead market
$\widehat{\ }$	Forecast

[1]ENFOR A/S, Lyngsø Allé 3, DK-2970 Hørsholm, Denmark
[2]DTU Informatics, Technical University of Denmark, Richard Petersens Plads, building 321, DK-2800 Kgs. Lyngby, Denmark
[3]Dept. of Industrial and Manufacturing Systems Engineering, Iowa State University, 3004 Black Engineering Building, 50011, Ames, IA, USA

1 Introduction

The recent year's tremendous growth in installed wind power generation capacity worldwide has fuelled growing interest in how electricity generated by these plants is best offered to the market. A pioneer work on the topic is presented in Bremnes (2004) which shows analytically that the optimal bid for a wind energy producer in the day-ahead market is a particular quantile of a predictive generation density. Building further on these findings, the authors of this report present in Zugno et al. (2012) a case study where trading of wind power, entirely based on forecasts, during a 10 month period is simulated.

The biggest limitation of the strategy presented in Zugno et al. (2012) is that it only yields an optimal bid as long as the quantity traded is small enough not to affect the market outcome in any way. As soon as the strategy is adopted for a price making quantity, the deviations from the point forecast can act to increase the probability of deviations in that direction being penalised. Thus the effects of the strategy risk becoming exactly the opposite of what is intended. This situation can be the result of either a single price making producer adopting the strategy or prompted a collective adaptation of the strategy by a number of wind power producers (given that their production at any given time is highly correlated). Even though both of these scenarios have the same effect, the appropriate countermeasures are most likely different. Whereas a single price making producer has to explicitly consider the full extent of the feedback his actions create on the market, a small producer can still take advantage of the fact that the market is indifferent to his individual actions. His main concerns are therefore to add the knowledge that other small producers are also strategic in their bidding, e.g. by taking a more game theoretical approach to his bidding.

The strategy presented in Zugno et al. (2012) also pays no explicit regard to the risk involved. The hours of severe losses are merely avoided by restricting the deviation from the point forecast either in terms of percentage of the point forecast or in terms of probability. These constraints on the bid are imposed by the TSO although how much deviation would be accepted is not clear. The reasoning for regarding this choice as sufficient consideration for risk is twofold. Firstly, most likely will any popular restriction of the variance of the revenue would lead to larger deviations from the point forecast than allowed by the TSO. Secondly, the revenue risk is only relevant on a quarterly or annual basis and due to the many independent decisions made within one year (8760 on a non-leap year to be exact) that maximising expectations is sufficient.

Generally speaking however the need for some risk awareness is undisputed since applying the optimal quantile strategy directly without restrictions yields

several hours of excessive losses during the test period in Zugno et al. (2012). Then due to the fact that the producers are only subject to downside risk these losses are not countered by huge gains. Moreover, even though the practical constraints seem to be sufficient in the case study there exist (in theory at least) scenarios where a producer might suffer large losses despite the aforementioned restrictions. This is because putting a limit on the deviation from the point forecast only addresses the part of the risk that arises from the uncertain production and not the part that is owed to the volatility of the regulation prices / penalties. In other words the possibility of a large loss arising from a small deviation times a large penalty is not addressed by the restrictions in Zugno et al. (2012). Thus excessive losses could be suffered e.g. in a more volatile market / period than the one considered in Zugno et al. (2012). This aside, the market feedback from a price maker's decisions might prompt an increased risk of excessive losses despite retaining the bid within a certain limit from the point forecast and market circumstances being similar to that in the previously mentioned case study. So in summary, the incorporation of a more comprehensive risk measure in the bidding strategy would strengthen the theoretical grounds for the strategy already developed and contribute to a more seamless adoption to other markets and extensions.

The aim of this report is to derive and analyse the methods for wind power trading which account for risk and are applicable for a price maker in the market. At first the general formulation of the risk averse bidding problem is derived analytically and the effect of the price taker assumption discussed. Similar to Morales et al. (2010) and Dent et al. (2011), the risk criteria considered is the Conditional Value-at-Risk (CVaR). Afterwards, an operational formulation of the problem in a stochastic programming framework is obtained and the generation of the scenarios necessary for solving it informally discussed. Finally the characteristics of such a strategy are demonstrated through a small case study and the resulting bids compared to the bids found by the strategy in Zugno et al. (2012). Readers of this report are assumed to have basic knowledge about the general functionalities of Nord Pool's markets and about strategic bidding of wind power. A more comprehensive introduction to these aspects is given in Zugno et al. (2012).

2 Being a Price Maker

Before going any further, spending a few words on what being a price maker or a price taker involves and why the concepts are relevant in the context of this report is in order. In a perfect competitive market, all participants are price takers since the do not affect the market outcome in any way by the actions. A price maker in a particular market on the other hand can influence the price

on the market it is involved in by its trades. Since the potential influence on the market is owed (in this case) to a prominent share in the electricity supply the actual market power of a producer may vary both between the markets he's active on and might also be not constant in time. More precisely a wind power producer[1] with a production capacity that is large enough to affect the spot price in a single price area (say DK-1) may loose some of his impact during hours when there is no congestion on the transmission lines to the surrounding areas.

Furthermore, a producer's impact may change from being on the supply side in one market to being on the demand side in another. On the spot market though, it is clear that it is the volume bid to the market that affects the price as it is indeed that volume that enters the supply function and shifts it to the right. The same wind power producer and his actions on the spot market is a source for demand on the regulation market. That is their imbalances are what prompts the demand for regulation power. However at the same time this very same wind power affects the supply of regulating power indirectly as it has the ability to push less cost efficient yet flexible power generators to the right of the equilibrium price. So the impact on opposite sides of the supply / demand might act as counterbalancing to some extent. This is the case as long as the wind power producer can't be a direct supplier of regulating power. Finally it is important to realise that the market power of a particular collection of wind turbines is not the same on the spot market and the regulation market even in situations where the spot price is unique for the area in question. This is because the different parties are involved in the different markets (e.g. not everybody need to regulate).

So in conclusion, abandoning the price taker assumption prompts that the following relationships need to be accounted for:

- The impact of the bid quantity ($\widetilde{W}_k$) on the spot price ($\pi_k^{(S)}$) and the regulation price ($\pi_k^{(\uparrow/\downarrow)}$) / penalty ($\psi_k^{(\uparrow/\downarrow)}$)
- The impact of the price maker's imbalance $\left(W_k - \widetilde{W}_k\right)$ on the regulation price / penalty through the demand for regulating power
- The impact of the price maker's imbalance on the regulation price / penalty through impact on the supply of regulating power

This aside, the regulation prices / penalties are known to be dependent on the spot prices. Now assuming that all the mentioned variables actually impact the prices the spot price should be written as a function of the bid wind power, $\pi_k^{(S)}(\widetilde{W}_k)$, and the regulation prices / penalties as a function of the bid wind, the

[1] or an aggregation of a number of producers with highly correlated production / behaviour

produced wind power and the spot price $\pi_k^{(\uparrow/\downarrow)}(\widetilde{W}, W_k, \pi_k^{(S)}) / \pi_k^{(\uparrow/\downarrow)}(\widetilde{W}, W_k, \pi_k^{(S)})$. Obviously, it has to be investigated whether accounting for all these relationships is necessary but for the time being we will assume that to be the case.

3 Problem Formulation

In this report we continue along the lines of Zugno et al. (2012) and consider the bidding decision to be taken for each hour individually. This is in contrast to the formulations of Morales et al. (2010) and Dent et al. (2011) which consider all 24 bidding decisions for the upcoming day simultaneously. A further discussion on the differences between those two approaches in theory and practise is given in the final section of this report. In this section analytical expressions for the expected revenue and the CVaR are derived to the extent possible. The formulation presented here is mainly adopted from Rockafellar and Uryasev (2000, 2002), Schultz and Tiedemann (2006), Chen et al. (2009).

As shown in Zugno et al. (2012) the revenue ρ_k for hour k can be written in the following ways:

$$\begin{aligned}
\rho_k &= \pi_k^{(S)} \widetilde{W}_k \\
&\quad + I\{W_k > \widetilde{W}_k\}(W_k - \widetilde{W}_k)\pi_k^{(\downarrow)} + I\{W_k < \widetilde{W}_k\}(W_k - \widetilde{W}_k)\pi_k^{(\uparrow)} \\
&= \pi_k^{(S)} W_k + (\widetilde{W}_k - W_k)\pi_k^{(S)} \\
&\quad + I\{W_k > \widetilde{W}_k\}(W_k - \widetilde{W}_k)\pi_k^{(\downarrow)} + I\{W_k < \widetilde{W}_k\}(W_k - \widetilde{W}_k)\pi_k^{(\uparrow)} \qquad (1) \\
&= \pi_k^{(S)} W_k \\
&\quad - I\{W_k > \widetilde{W}_k\}(W_k - \widetilde{W}_k)\underbrace{(\pi_k^{(S)} - \pi_k^{(\downarrow)})}_{\psi_k^{(\downarrow)}} + I\{W_k < \widetilde{W}_k\}(W_k - \widetilde{W}_k)\underbrace{(\pi_k^{(\uparrow)} - \pi_k^{(S)})}_{\psi_k^{(\uparrow)}}.
\end{aligned}$$

Same place it is shown that a risk neutral producer is interested in the bid, $\widetilde{W}_k$ that maximises its expected revenues, i.e.

$$\widetilde{W}_k^{(*)} = \arg\max_{\widetilde{W}_k} \mathbb{E}[\rho_k | \widetilde{W}_k] \qquad (2)$$

which is shown to be equivalent to solving

$$\widetilde{W}_t^{(*)} = \arg\max_{\widetilde{W}_t} \mathbb{E}\left[C_t^{(\uparrow/\downarrow)}\right] \qquad (3)$$

where

$$C_t^{(\uparrow/\downarrow)} = I\{W_k < \widetilde{W}_k\}(W_k - \widetilde{W}_k)\psi^{(\uparrow)} - I\{W_k > \widetilde{W}_k\}(W_k - \widetilde{W}_k)\psi_k^{(\downarrow)} \qquad (4)$$

if the market is unaffected by the producer's actions, i.e it is price taker.

Taking the expectation of Eq. (1) yields either

$$\begin{aligned}
\mathbb{E}[\rho_k|\widetilde{W}_k] &= \mathbb{E}[W_k\pi^{(S)}|\widetilde{W}_k] \\
&\quad - \mathbb{E}[I\{W_k > \widetilde{W}_k\}(W_k - \widetilde{W}_k)(\pi_k^{(S)} - \pi_k^{(\downarrow)})|\widetilde{W}_k] \\
&\quad + \mathbb{E}[I\{W_k < \widetilde{W}_k\}(W_k - \widetilde{W}_k)(\pi_k^{(\uparrow)} - \pi_k^{(S)})|\widetilde{W}_k] \\
&= \int_0^{W^{(max)}} W_k d\mathbb{P}_W \int_{\pi^{(S)}=-\infty}^{\infty} \pi_k^{(S)}(\widetilde{W}) d\mathbb{P}_{\pi^{(S)}} \\
&\quad - \int_{\pi^{(S)}=-\infty}^{\infty} \int_{W_k=\widetilde{W}}^{W^{(max)}} \int_{\psi^{(\downarrow)}=0}^{\infty} [W_k - \widetilde{W}_k]\psi^{(\downarrow)}(\widetilde{W}_k, W_k, \pi_k^{(S)}) d\mathbb{P}_{\psi^{(\downarrow)}} d\mathbb{P}_W d\mathbb{P}_{\pi^{(S)}} \\
&\quad + \int_{\pi^{(S)}=-\infty}^{\infty} \int_{W_k=0}^{\widetilde{W}} \int_{\psi^{(\uparrow)}=0}^{\infty} [W_k - \widetilde{W}_k]\psi^{(\uparrow)}(\widetilde{W}, W_k, \pi_k^{(S)}) d\mathbb{P}_{\psi^{(\uparrow)}} d\mathbb{P}_W d\mathbb{P}_{\pi^{(S)}}
\end{aligned} \tag{5}$$

or

$$\begin{aligned}
\mathbb{E}[\rho_k|\widetilde{W}_k] &= \mathbb{E}[\widetilde{W}_k\pi_k^{(S)}|\widetilde{W}_k] \\
&\quad + \mathbb{E}[I\{W_k > \widetilde{W}_k\}(W_k - \widetilde{W}_k)\pi^{(\downarrow)}|\widetilde{W}_k] \\
&\quad + \mathbb{E}[I\{W_k < \widetilde{W}_k\}(W_k - \widetilde{W}_k)\pi^{(\uparrow)}|\widetilde{W}_k] \\
&= \widetilde{W}_k \int_{\pi^{(S)}=-\infty}^{\infty} \pi_k^{(S)}(\widetilde{W}) d\mathbb{P}_{\pi^{(S)}} \\
&\quad + \int_{\pi^{(S)}=-\infty}^{\infty} \int_{W_k=\widetilde{W}}^{W^{(max)}} \int_{\pi^{(\downarrow)}=-\infty}^{\pi^{(S)}} [W_k - \widetilde{W}_k]\pi_k^{(\downarrow)}(\widetilde{W}_k, W_k, \pi_k^{(S)}) d\mathbb{P}_{\pi^{(\downarrow)}} d\mathbb{P}_W d\mathbb{P}_{\pi^{(S)}} \\
&\quad + \int_{\pi^{(S)}=-\infty}^{\infty} \int_{W_k=0}^{\widetilde{W}} \int_{\pi^{(\uparrow)}=\pi^{(S)}}^{\infty} [W_k - \widetilde{W}_k]\pi_k^{(\uparrow)}(\widetilde{W}, W_k, \pi_k^{(S)}) d\mathbb{P}_{\pi^{(\uparrow)}} d\mathbb{P}_W d\mathbb{P}_{\pi^{(S)}}
\end{aligned} \tag{6}$$

where in both equations, $d\mathbb{P}_x = f(x)dx$ where in turn $f(x)$ is the probability density function (PDF) of x. In order to ease the notation in the following, $\pi_k^{(S)}(\widetilde{W})$ will be written as $\pi_k^{(S)}$. Likewise we will note $\pi_k^{(\uparrow/\downarrow)}(\widetilde{W}, W_k, \pi_k^{(S)})$ and $\psi_k^{(\uparrow/\downarrow)}(\widetilde{W}, W_k, \pi_k^{(S)})$ as $\pi_k^{(\uparrow/\downarrow)}$ and $\psi_k^{(\uparrow/\downarrow)}$ respectively.

In Eq. 5 the expectations in the first term can be separated without loss of generality. This is because the wind power actually produced has no impact on the prices. Instead, any correlation between W_k and $\pi_k^{(S)}$ can be explained by the correlation between $\widetilde{W}_k$ and $\pi_k^{(S)}$. The remaining terms are however inseparable in the general setting. Only if the producer is a price taker, the triple integrals can be separated into a wind power part and a price part as shown in Zugno et al. (2012). Between the formulations in Eqs. (5) and (6) the former has the appeal in the price taker case that the term for the spot market can be omitted in the optimisation making it a maximisation of the (non-positive) imbalance costs instead of the revenue. When the price taker assumption is abandoned however, the contribution from the spot market has to be considered as well. This in turn makes the choice between the two formulations less obvious.

A producer who is not completely risk neutral and characterises his risk in terms of CVaR seeks a solution to

$$\widetilde{W}_t^{(*)} = \arg\max_{\widetilde{W}_t} \left\{ \mathbb{E}\left[C_t^{(\uparrow/\downarrow)}\right] + \lambda \mathrm{CVaR}_\alpha \left[C_t^{(\uparrow/\downarrow)}\right] \right\} \tag{7}$$

or similarly in terms of the revenue as:

$$\widetilde{W}_t^{(*)} = \arg\max_{\widetilde{W}_t} \left\{ \mathbb{E}\left[\rho_t\right] + \lambda \mathrm{CVaR}_\alpha \left[\rho_t\right] \right\} \tag{8}$$

where in both cases $\mathrm{CVaR}_\alpha[\cdot]$ is the expected cost/revenue given that it deceeds the α-quantile (α is in the lower tail) of the cost/revenue and λ, $0 \leq \lambda \leq 1$, is a parameter indicating the risk attitude of the producer.

Generally the CVaR-term on for a confidence level α (with α in the left tail) is defined as

$$\mathrm{CVaR}_\alpha(X) = \eta_\alpha - \frac{1}{\alpha}\mathbb{E}\left[\max\left\{(\eta_\alpha - X), 0\right\}\right] \tag{9}$$

where η_α is the α-Value-at-Risk (VaR_α) or

$$\eta_\alpha = F_X^{-1}(\alpha) \tag{10}$$

where $F_X(\cdot)$ is the cumulative density function (CDF) of X.

If the prices and thereby the penalties are fixed we find that the CDF of the imbalance costs can be found as

$$\begin{aligned} F_C(x) &= \mathbb{P}\left[C^{(\uparrow/\downarrow)} \leq x\right] \\ &= \mathbb{P}\left[\psi^{(\uparrow)}\left(W - \widetilde{W}\right) I\left\{W < \widetilde{W}\right\} - \psi^{(\downarrow)}\left(W - \widetilde{W}\right) I\left\{W > \widetilde{W}\right\} \leq x\right] \\ &= \mathbb{P}\left[W < \widetilde{W} \cap \psi^{(\uparrow)}\left(W - \widetilde{W}\right) \leq x\right] + \mathbb{P}\left[W > \widetilde{W} \cap -\psi^{(\downarrow)}\left(W - \widetilde{W}\right) \leq x\right] \\ &= \mathbb{P}\left[W \leq \widetilde{W} + \frac{x}{\psi^{(\uparrow)}}\right] + \mathbb{P}\left[W \geq \widetilde{W} - \frac{x}{\psi^{(\downarrow)}}\right] \\ &= F_W\left(\widetilde{W} + \frac{x}{\psi^{(\uparrow)}}\right) + 1 - F_W\left(\widetilde{W} - \frac{x}{\psi^{(\downarrow)}}\right) \end{aligned} \tag{11}$$

which yields a PDF

$$f_C(x) = \frac{\partial}{\partial x} F_C(x) = \frac{1}{\psi^{(\uparrow)}} f_w\left(\frac{x}{\psi^{(\uparrow)}} + \widetilde{W}\right) + \frac{1}{\psi^{(\downarrow)}} f_w\left(-\frac{x}{\psi^{(\downarrow)}} + \widetilde{W}\right) \tag{12}$$

and thus

$$\begin{aligned} \mathbb{E}\left[\max\left\{\left(\eta_\alpha - C^{(\uparrow/\downarrow)}\right), 0\right\}\right] = &\frac{1}{\psi^{(\uparrow)}} \int_{-\infty}^{\eta_\alpha} (\eta_\alpha - c) f_w\left(\frac{c}{\psi^{(\uparrow)}} + \widetilde{W}\right) dc \\ &+ \frac{1}{\psi^{(\downarrow)}} \int_{-\infty}^{\eta_\alpha} (\eta_\alpha - c) f_w\left(-\frac{c}{\psi^{(\downarrow)}} + \widetilde{W}\right) dc. \end{aligned} \tag{13}$$

Now let

$$
\begin{aligned}
c &= \psi^{(\uparrow)} \min\left\{W-\widetilde{W},0\right\} - \psi^{(\downarrow)} \max\left\{W-\widetilde{W},0\right\} \\
dc &= \left[\psi^{(\uparrow)} I\{\widetilde{W}>W\} - \psi^{(\downarrow)} I\{\widetilde{W}<W\}\right] dw
\end{aligned}
$$

and obtain

$$
\begin{aligned}
&\mathbb{E}\left[\max\left\{\left(\eta_\alpha - C^{(\uparrow/\downarrow)}\right),0\right\}\right] \\
&= \frac{\psi^{(\uparrow)} I\{\widetilde{W}>W\} - \psi^{(\downarrow)} I\{\widetilde{W}<W\}}{\psi^{(\uparrow)}} \\
&\quad \cdot \left[\int_{-\infty}^{\infty} \max\left\{\left(\eta_\alpha - \psi^{(\uparrow)} \min\left\{W-\widetilde{W},0\right\} + \psi^{(\downarrow)} \max\left\{W-\widetilde{W},0\right\}\right),0\right\}\right. \\
&\qquad \left. \cdot f_w\left(\frac{\psi^{(\uparrow)} \min\left\{W-\widetilde{W},0\right\} - \psi^{(\downarrow)} \max\left\{W-\widetilde{W},0\right\}}{\psi^{(\uparrow)}} + \widetilde{W}\right) dw\right] \\
&\quad + \frac{\psi^{(\uparrow)} I\{\widetilde{W}>W\} - \psi^{(\downarrow)} I\{\widetilde{W}<W\}}{\psi^{(\downarrow)}} \\
&\quad \cdot \left[\int_{-\infty}^{\infty} \max\left\{\left(\eta_\alpha - \psi^{(\uparrow)} \min\left\{W-\widetilde{W},0\right\} + \psi^{(\downarrow)} \max\left\{W-\widetilde{W},0\right\}\right),0\right\}\right. \\
&\qquad \left. \cdot f_w\left(-\frac{\psi^{(\uparrow)} \min\left\{W-\widetilde{W},0\right\} - \psi^{(\downarrow)} \max\left\{W-\widetilde{W},0\right\}}{\psi^{(\downarrow)}} + \widetilde{W}\right) dw\right] \qquad (14) \\
&= \frac{1}{\psi^{(\uparrow)}}\left[\psi^{(\uparrow)} \int_0^{\frac{\eta_\alpha+\psi^{(\uparrow)}\widetilde{W}}{\psi^{(\uparrow)}}} \left(\eta_\alpha - \psi^{(\uparrow)}\left(W-\widetilde{W}\right)\right) f_w\left(\frac{\psi^{(\uparrow)}\left(W-\widetilde{W}\right)}{\psi^{(\uparrow)}} + \widetilde{W}\right) dw\right. \\
&\quad \left. + \psi^{(\downarrow)} \int_{\frac{\psi^{(\downarrow)}\widetilde{W}-\eta_\alpha}{\psi^{(\downarrow)}}}^{W^{(max)}} \left(\eta_\alpha + \psi^{(\downarrow)}\left(W-\widetilde{W}\right)\right) f_w\left(-\frac{\psi^{(\downarrow)}\left(W-\widetilde{W}\right)}{\psi^{(\uparrow)}} + \widetilde{W}\right) dw\right] \\
&\quad + \frac{1}{\psi^{(\downarrow)}}\left[\psi^{(\uparrow)} \int_0^{\frac{\eta_\alpha+\psi^{(\uparrow)}\widetilde{W}}{\psi^{(\uparrow)}}} \left(\eta_\alpha - \psi^{(\uparrow)}\left(W-\widetilde{W}\right)\right) f_w\left(\frac{\psi^{(\uparrow)}\left(W-\widetilde{W}\right)}{\psi^{(\downarrow)}} + \widetilde{W}\right) dw\right. \\
&\quad \left. + \psi^{(\downarrow)} \int_{\frac{\psi^{(\downarrow)}\widetilde{W}-\eta_\alpha}{\psi^{(\downarrow)}}}^{W^{(max)}} \left(\eta_\alpha + \psi^{(\downarrow)}\left(W-\widetilde{W}\right)\right) f_w\left(-\frac{\psi^{(\downarrow)}\left(W-\widetilde{W}\right)}{\psi^{(\downarrow)}} + \widetilde{W}\right) dw\right]
\end{aligned}
$$

$$
\begin{aligned}
&= \int_0^{\frac{\eta_\alpha+\psi^{(\uparrow)}\widetilde{W}}{\psi^{(\uparrow)}}} \left[\left(\eta_\alpha - \psi^{(\uparrow)}\left(W-\widetilde{W}\right)\right)\cdot \right. \\
&\qquad \left. \left(f_w(W) + \frac{\psi^{(\uparrow)}}{\psi^{(\downarrow)}} f_w\left(\widetilde{W} - \frac{\psi^{(\uparrow)}}{\psi^{(\downarrow)}}\left(W-\widetilde{W}\right)\right)\right)\right] dw \\
&\quad + \int_{\frac{\psi^{(\downarrow)}\widetilde{W}-\eta_\alpha}{\psi^{(\downarrow)}}}^{W^{(max)}} \left[\left(\eta_\alpha + \psi^{(\downarrow)}\left(W-\widetilde{W}\right)\right)\cdot \right. \\
&\qquad \left. \left(\frac{\psi^{(\downarrow)}}{\psi^{(\uparrow)}} f_w\left(\widetilde{W} - \frac{\psi^{(\downarrow)}}{\psi^{(\uparrow)}}\left(W-\widetilde{W}\right)\right) + f_w(W)\right)\right] dw.
\end{aligned}
\tag{14, cont}
$$

Similarly for ρ we get

$$
\begin{aligned}
F_\rho(x) &= \mathbb{P}[\rho \le x] \\
&= \mathbb{P}\left[W < \widetilde{W} \;\&\; \pi^{(S)}\widetilde{W} + \pi^{(\uparrow)}\left(W-\widetilde{W}\right) \le x\right] \\
&\quad + \mathbb{P}\left[W > \widetilde{W} \;\&\; \pi^{(S)}\widetilde{W} + \pi^{(\downarrow)}\left(W-\widetilde{W}\right) \le x\right] \\
&= \mathbb{P}\left[W \le \frac{x}{\pi^{(\uparrow)}} + \widetilde{W}\left(1-\frac{\pi^{(S)}}{\pi^{(\uparrow)}}\right)\right] + \mathbb{P}\left[\widetilde{W} \le W \le \frac{x}{\pi^{(\downarrow)}} + \widetilde{W}\left(1-\frac{\pi^{(S)}}{\pi^{(\downarrow)}}\right)\right] \\
&= F_W\left(\frac{x}{\pi^{(\uparrow)}} + \widetilde{W}\left(1-\frac{\pi^{(S)}}{\pi^{(\uparrow)}}\right)\right) + F_W\left(\frac{x}{\pi^{(\downarrow)}} + \widetilde{W}\left(1-\frac{\pi^{(S)}}{\pi^{(\downarrow)}}\right)\right) - F_W\left(\widetilde{W}\right)
\end{aligned}
\tag{15}
$$

thus yielding

$$
\begin{aligned}
f_\rho(x) &= \frac{\partial}{\partial x} F_\rho(x) \\
&= \frac{1}{\pi^{(\uparrow)}} f_W\left(\frac{x}{\pi^{(\uparrow)}} + \widetilde{W}\left(1-\frac{\pi^{(S)}}{\pi^{(\uparrow)}}\right)\right) + \frac{1}{\pi^{(\downarrow)}} f_W\left(\frac{x}{\pi^{(\downarrow)}} + \widetilde{W}\left(1-\frac{\pi^{(S)}}{\pi^{(\downarrow)}}\right)\right)
\end{aligned}
\tag{16}
$$

which in turn renders

$$
\begin{aligned}
\mathbb{E}[\max\{(\eta_\alpha-\rho),0\}] &= \frac{1}{\pi^{(\uparrow)}}\int_{-\infty}^{\eta_\alpha} (\eta_\alpha - r) f_w\left(\frac{r}{\pi^{(\uparrow)}} + \widetilde{W}\left(1-\frac{\pi^{(S)}}{\pi^{(\uparrow)}}\right)\right) dr \\
&\quad + \frac{1}{\pi^{(\downarrow)}}\int_{-\infty}^{\eta_\alpha} (\eta_\alpha - r) f_w\left(\frac{r}{\pi^{(\downarrow)}} + \widetilde{W}\left(1-\frac{\pi^{(S)}}{\pi^{(\downarrow)}}\right)\right) dr.
\end{aligned}
\tag{17}
$$

Following the same procedure as before and let

$$
\begin{aligned}
r &= \pi^{(S)}\widetilde{W} + \pi^{(\uparrow)}\min\left\{W-\widetilde{W},0\right\} + \pi^{(\downarrow)}\max\left\{W-\widetilde{W},0\right\} \\
dr &= \left[\psi^{(\uparrow)} I\left\{\widetilde{W} > W\right\} - \psi^{(\downarrow)} I\left\{\widetilde{W} < W\right\}\right] dw
\end{aligned}
$$

and thereby obtain

$$
\begin{aligned}
&\mathbb{E}\left[\max\left\{\left(\eta_\alpha-\rho\right),0\right\}\right]\\
&=\frac{\psi^{(\uparrow)}I\left\{\widetilde{W}>W\right\}-\psi^{(\downarrow)}I\left\{\widetilde{W}<W\right\}}{\pi^{(\uparrow)}}\\
&\cdot\left[\int_{-\infty}^{\infty}\max\left\{\left(\eta_\alpha-\pi^{(S)}\widetilde{W}-\pi^{(\uparrow)}\min\left\{W-\widetilde{W},0\right\}-\pi^{(\downarrow)}\max\left\{W-\widetilde{W},0\right\}\right),0\right\}\right.\\
&\quad\cdot f_w\left(\frac{\pi^{(S)}\widetilde{W}+\pi^{(\uparrow)}\min\left\{W-\widetilde{W},0\right\}+\pi^{(\downarrow)}\max\left\{W-\widetilde{W},0\right\}}{\pi^{(\uparrow)}}\right.\\
&\qquad\left.\left.+\widetilde{W}\left(1-\frac{\pi^{(S)}}{\pi^{(\uparrow)}}\right)\right)dw\right]\\
&+\frac{\psi^{(\uparrow)}I\left\{\widetilde{W}>W\right\}-\psi^{(\downarrow)}I\left\{\widetilde{W}<W\right\}}{\pi^{(\downarrow)}}\\
&\cdot\left[\int_{-\infty}^{\infty}\max\left\{\left(\eta_\alpha-\pi^{(S)}\widetilde{W}-\pi^{(\uparrow)}\min\left\{W-\widetilde{W},0\right\}-\pi^{(\downarrow)}\max\left\{W-\widetilde{W},0\right\}\right),0\right\}\cdot\right.\\
&\quad\cdot f_w\left(\frac{\pi^{(S)}\widetilde{W}+\pi^{(\uparrow)}\min\left\{W-\widetilde{W},0\right\}+\pi^{(\downarrow)}\max\left\{W-\widetilde{W},0\right\}}{\pi^{(\downarrow)}}\right.\\
&\qquad\left.\left.+\widetilde{W}\left(1-\frac{\pi^{(S)}}{\pi^{(\downarrow)}}\right)\right)dw\right]\\
&=\int_0^{\frac{\eta_\alpha+\widetilde{W}\left(\pi^{(\uparrow)}-\pi^{(S)}\right)}{\pi^{(\uparrow)}}}\left[\left(\eta_\alpha-\pi^{(S)}\widetilde{W}-\pi^{(\uparrow)}\left(W-\widetilde{W}\right)\right)\cdot\right.\\
&\qquad\left.\left(\frac{\psi^{(\uparrow)}}{\pi^{(\uparrow)}}f_w\left(W\right)+\frac{\psi^{(\uparrow)}}{\pi^{(\downarrow)}}f_w\left(\widetilde{W}+\frac{\pi^{(\uparrow)}}{\pi^{(\downarrow)}}\left(W-\widetilde{W}\right)\right)\right)\right]dw\\
&+\int_{\frac{\eta_\alpha-\widetilde{W}\left(\pi^{(S)}-\pi^{(\downarrow)}\right)}{\pi^{(\downarrow)}}}^{W^{(max)}}\left[\left(\eta_\alpha-\pi^{(S)}\widetilde{W}-\pi^{(\downarrow)}\left(W-\widetilde{W}\right)\right)\cdot\right.\\
&\qquad\left.\left(\frac{\psi^{(\downarrow)}}{\pi^{(\uparrow)}}f_w\left(\widetilde{W}+\frac{\pi^{(\downarrow)}}{\pi^{(\uparrow)}}\left(W-\widetilde{W}\right)\right)+\frac{\psi^{(\downarrow)}}{\pi^{(\downarrow)}}f_w\left(W\right)\right)\right]dw.
\end{aligned}
\tag{18}
$$

Considering the prices to be fixed, as is done in Eqs. (14) and (18), allows for a closed form solution of the problem to be obtained (Dent et al. (2011)). The prices are however stochastic and as shown below the price expectation integrals can not be separated from the wind expectation integral. Thus the certainty equivalence principle does not apply

anymore. With stochastic prices, Eq. (14) & (18) become

$$\begin{aligned}
&\mathbb{E}\left[\max\left\{\left(\eta_\alpha(\boldsymbol{\psi}) - C^{(\uparrow/\downarrow)}\right), 0\right\}\right] \\
&= \int_0^\infty \int_0^\infty \int_0^{\frac{\eta_\alpha(\boldsymbol{\psi})+\psi^{(\uparrow)}\widetilde{W}}{\psi^{(\uparrow)}}} \left(\eta_\alpha(\boldsymbol{\psi}) - \psi^{(\uparrow)}\left(W - \widetilde{W}\right)\right) \\
&\quad \cdot \left(f_w(W) + \frac{\psi^{(\uparrow)}}{\psi^{(\downarrow)}} f_w\left(\widetilde{W} - \frac{\psi^{(\uparrow)}}{\psi^{(\downarrow)}}\left(W - \widetilde{W}\right)\right)\right) f_{\boldsymbol{\psi}}(\boldsymbol{\psi}) dw d\boldsymbol{\psi} \\
&\quad + \int_0^\infty \int_0^\infty \int_{\frac{\psi^{(\downarrow)}\widetilde{W} - \eta_\alpha(\boldsymbol{\psi})}{\psi^{(\downarrow)}}}^{W^{(max)}} \left(\eta_\alpha(\boldsymbol{\psi}) + \psi^{(\downarrow)}\left(W - \widetilde{W}\right)\right) \\
&\quad \cdot \left(\frac{\psi^{(\downarrow)}}{\psi^{(\uparrow)}} f_w\left(\widetilde{W} - \frac{\psi^{(\downarrow)}}{\psi^{(\uparrow)}}\left(W - \widetilde{W}\right)\right) + f_w(W)\right) f_{\boldsymbol{\psi}}(\boldsymbol{\psi}) dw d\boldsymbol{\psi}.
\end{aligned} \tag{19}$$

and

$$\begin{aligned}
&\mathbb{E}\left[\max\left\{\left(\eta_\alpha(\boldsymbol{\pi}) - \rho\right), 0\right\}\right] \\
&= \int_{-\infty}^\infty \int_{\pi^{(S)}}^\infty \int_{-\infty}^{\pi^{(S)}} \int_0^{\frac{\eta_\alpha(\boldsymbol{\pi})+\widetilde{W}\left(\pi^{(\uparrow)}-\pi^{(S)}\right)}{\pi^{(\uparrow)}}} \left(\eta_\alpha(\boldsymbol{\pi}) - \pi^{(S)}\widetilde{W} - \pi^{(\uparrow)}\left(W - \widetilde{W}\right)\right) \\
&\quad \cdot \left(\frac{\psi^{(\uparrow)}}{\pi^{(\uparrow)}} f_w(W) + \frac{\psi^{(\uparrow)}}{\pi^{(\downarrow)}} f_w\left(\widetilde{W} + \frac{\pi^{(\uparrow)}}{\pi^{(\downarrow)}}\left(W - \widetilde{W}\right)\right)\right) f_{\boldsymbol{\pi}}(\boldsymbol{\pi}) dw d\boldsymbol{\pi} \\
&\quad + \int_{-\infty}^\infty \int_{\pi^{(S)}}^\infty \int_{-\infty}^{\pi^{(S)}} \int_{\frac{\eta_\alpha(\boldsymbol{\pi}) - \widetilde{W}\left(\pi^{(S)}-\pi^{(\downarrow)}\right)}{\pi^{(\downarrow)}}}^{W^{(max)}} \left(\eta_\alpha(\boldsymbol{\pi}) - \pi^{(S)}\widetilde{W} - \pi^{(\downarrow)}\left(W - \widetilde{W}\right)\right) \\
&\quad \cdot \left(\frac{\psi^{(\downarrow)}}{\pi^{(\uparrow)}} f_w\left(\widetilde{W} + \frac{\pi^{(\downarrow)}}{\pi^{(\uparrow)}}\left(W - \widetilde{W}\right)\right) + \frac{\psi^{(\downarrow)}}{\pi^{(\downarrow)}} f_w(W)\right) f_{\boldsymbol{\pi}}(\boldsymbol{\pi}) dw d\boldsymbol{\pi}
\end{aligned} \tag{20}$$

respectively where

$$\boldsymbol{\psi} = \begin{bmatrix} \psi^{(\downarrow)} & \psi^{(\uparrow)} \end{bmatrix}$$
$$\boldsymbol{\pi} = \begin{bmatrix} \pi^{(\downarrow)} & \pi^{(\uparrow)} & \pi^{(S)} \end{bmatrix}$$

are multivariate stochastic variables with the appropriate covariance structure.

What is still missing in the expressions are the formulations of $\eta_\alpha(\cdot)$ in terms of the wind and the price / penalty variables. Assuming that both the penalty and the imbalance had a parametric distribution and were independent of each other an analytical expression for the variance of the cost can be found (in terms of $\psi^{(\uparrow/\downarrow)}$) as

$$\begin{aligned}
\mathbb{V}\left[\psi(W - \widetilde{W})\right] = \mathbb{V}[\psi]\left(\mathbb{E}\left[(W - \widetilde{W})\right]\right)^2 + \mathbb{V}\left[(W - \widetilde{W})\right](\mathbb{E}[\psi])^2 \\
+ \mathbb{V}[\psi]\mathbb{V}\left[(W - \widetilde{W})\right]
\end{aligned} \tag{21}$$

from which η_α could be derived. The distribution of W is however known to be best characterised by non-parametric techniques and the same probably goes for the imbalance penalties / prices (although probably nothing should be ruled out in this regard).

More importantly though $\psi^{(\uparrow/\downarrow)}$ and $(W - \widetilde{W})$ are not necessarily independent. Even though η_α could be found with the help of Eq. (21), an analytical solution to the optimisation problem would be hard, if not impossible, to obtain. Thus a discrete formulation of the problem using scenarios of the cost is probably a more likely road to success.

4 Operational Risk-Averse Bidding

4.1 Bidding as a Price Taker

Now assume that a set of N cost/revenue scenarios, ζ_s, $s \in \mathcal{S}$, is available and that they are ordered such that $\zeta_1 < \zeta_2 < \ldots < \zeta_N$. Then by defining the index k_α such that

$$\sum_{k=1}^{k_\alpha} p_k \leq \alpha < \sum_{k=1}^{k_\alpha+1} p_k,$$

where p_s is the probability of scenario s, the mean-risk bidding optimisation problem can be written as

$$\begin{aligned}\widetilde{W}_t^{(*)} &= \arg\max_{\widetilde{W}_t} \left\{ (1-\lambda)\mathbb{E}\left[\zeta(\widetilde{W})\right] + \lambda \mathrm{CVaR}_\alpha\left[\zeta(\widetilde{W})\right] \right\} \\ &= \arg\max_{\widetilde{W}_t} \left\{ (1-\lambda) \sum_{s\in\mathcal{S}} p_s \zeta_s(\widetilde{W}) \right. \\ &\left. + \lambda \left(\eta_\alpha(\widetilde{W}) - \frac{1}{\alpha}\left[\sum_{k=1}^{k_\alpha} p_k \zeta_k(\widetilde{W}) + \left(\sum_{k=k_\alpha+1}^{N} p_k - (1-\alpha) \right) \zeta_{k_\alpha}(\widetilde{W}) \right] \right) \right\}\end{aligned} \tag{22}$$

where, depending on whether the objective is formulated in terms of cost or revenue, $\zeta_s(\widetilde{W})$ is either defined as

$$\zeta_s(\widetilde{W}) = I\left\{W_s > \widetilde{W}\right\}(W_s - \widetilde{W})\psi_s^{(\downarrow)} + I\left\{W_s < \widetilde{W}\right\}(W_s - \widetilde{W})\psi_s^{(\uparrow)} \tag{23}$$

or

$$\zeta_s(\widetilde{W}) = \pi_s^{(S)}\widetilde{W}_s + I\left\{W_s > \widetilde{W}\right\}(W_s - \widetilde{W})\pi_s^{(\downarrow)} + I\left\{W_s < \widetilde{W}\right\}(W_s - \widetilde{W})\pi_s^{(\uparrow)} \tag{24}$$

respectively. As before $\eta_\alpha(\widetilde{W})$ is the α-VaR or

$$\eta_\alpha(\widetilde{W}) = \mathrm{VaR}_\alpha(\widetilde{W}) = F^{-1}_{\zeta(\widetilde{W})}(\alpha)$$

Finally the producer's risk attitude is characterised by the parameter λ, $0 \leq \lambda \leq 1$, which takes the value 0 for the completely risk-neutral producer and the value 1 for total risk-aversion.

Now rewrite Eq. (22) as

$$\widetilde{W}_t^{(*)} = \arg\max_{\widetilde{W}} \left\{ (1-\lambda) \sum_{s\in\mathcal{S}} p_s \zeta_s(\widetilde{W}) + \lambda \left(\eta_\alpha(\widetilde{W}) - \frac{1}{\alpha} \sum_{s\in\mathcal{S}} p_s \xi_s(\widetilde{W}) \right) \right\} \tag{25}$$

$$s.t. \quad \xi_s(\widetilde{W}) \geq \eta_\alpha(\widetilde{W}) - \zeta_s(\widetilde{W}) \tag{26}$$

$$\xi_s(\widetilde{W}) \geq 0 \tag{27}$$

and introduce two auxiliary variables

$$\Delta W_s^{(\uparrow)}(\widetilde{W}) \leq W_s - \widetilde{W} \tag{28}$$

$$\Delta W_s^{(\downarrow)}(\widetilde{W}) \leq \widetilde{W} - W_s \tag{29}$$

$$\Delta W_s^{(\uparrow)}(\widetilde{W}), \Delta W_s^{(\downarrow)}(\widetilde{W}) \leq 0. \tag{30}$$

Consequently Eq. (23) & (24) can be written as

$$\zeta_s(\widetilde{W}) = \Delta W_s^{(\downarrow)}(\widetilde{W}) \psi_s^{(\downarrow)} + \Delta W_s^{(\uparrow)}(\widetilde{W}) \psi_s^{(\uparrow)} \tag{31}$$

and

$$\begin{aligned} \zeta_s(\widetilde{W}) &= \pi_s^{(S)} \widetilde{W} + \Delta W_s^{(\downarrow)}(\widetilde{W}) \pi_s^{(\downarrow)} + \Delta W_s^{(\uparrow)}(\widetilde{W}) \pi_s^{(\uparrow)} \\ &= \pi_s^{(S)} W_s + \Delta W_s^{(\downarrow)}(\widetilde{W}) \psi_s^{(\downarrow)} + \Delta W_s^{(\uparrow)}(\widetilde{W}) \psi_s^{(\uparrow)} \end{aligned} \tag{32}$$

respectively. The augmented optimisation problem (25) subject to (26) - (30) can be solved, for given values of α and λ, as an LP problem with a maximum

$$\left(\widetilde{W}^{(*)}, \eta_\alpha^{(*)}(\widetilde{W}^{(*)}), \Delta W^{(\uparrow,*)}(\widetilde{W}^{(*)}), \Delta W^{(\downarrow,*)}(\widetilde{W}^{(*)}) \right)$$

for which it holds that

$$\eta_\alpha^{(*)}(\widetilde{W}^{(*)}) = \mathrm{VaR}_\alpha \left[\zeta(\widetilde{W}^{(*)}) \right] \tag{33}$$

$$\eta_\alpha^{(*)}(\widetilde{W}^{(*)}) - \frac{1}{\alpha} \sum_{s\in\mathcal{S}} p_s \xi_s(\widetilde{W}) = \mathrm{CVaR}_\alpha \left[\zeta(\widetilde{W}^{(*)}) \right] \tag{34}$$

thus making $\widetilde{W}^{(*)}$ also the optimal solution of (22).

4.2 Bidding as a Price Maker

Abandoning the price taker assumption can be done in two steps. First by assuming that the producer is only a price taker on the day-ahead market (where there are more producers and volume involved) but is a price maker or has some sort of market power on the regulation market. Subsequently the the producer can be assumed to possess market power on both markets. Whether the possibility of being a price maker only on the regulation market is realistic will not be addressed in detail for the time being.

However given that there is less volume "traded" on the regulation market and that there are fewer potential actors on that market, this scenario seems intuitively plausible.

The main difference between solving the bidding problem for a price maker and a price taker is that the scenarios (or the scenario probabilities) now depend on the decision. Essentially we are still interested in solving the problem given in Eq. (25) only with the decision dependent scenarios. If we discretise the decision space such that we have a set, $\mathcal{W}$, of finite number of decisions intervals and for each $w \in \mathcal{W}$ we have a corresponding set, $\mathcal{S}^w$ of cost/revenue scenarios that have a constant probabilities on the entire span of w. Then the problem in (25) can be revised to

$$\widetilde{W}_t^{(*)} = \arg\max_{w \in \mathcal{W}} C^w(w;\alpha,\lambda) \tag{35}$$

where

$$C^w(w;\alpha,\lambda) = \max\left\{ (1-\lambda) \sum_{s\in\mathcal{S}^w} p_s \zeta_s(\widetilde{W}) + \lambda \left(\eta_\alpha(\widetilde{W}) - \frac{1}{\alpha} \sum_{s\in\mathcal{S}^w} p_s \xi_s(\widetilde{W}) \right) \right\} \tag{36}$$

still subject to (26)-(30) and with $\zeta(\widetilde{W})$ defined by (31) or (32).

Given a set $\mathcal{W}$ containing N_w decisions and for each $w \in \mathcal{W}$ a corresponding set of N_s cost/revenue scenarios, the two-stage problem in (35) & (36) can be solved as is. This will however of course require generation of $N_w \times N_s$ scenarios in total which rather quickly becomes a substantial amount.

An alternative to generating N_w different scenario sets, is only to generate a single set of cost/revenue scenarios and let the scenario probabilities, $p_{s,w}$, vary between different w's. Generally this is possible if zero scenario probabilities are allowed. However as the variations in the bid won't in any case alter the range of possible outcomes, this can be done for this particular case without having to assign zero scenario probabilities. So again let $\mathcal{W}$ be a set of bidding decisions, $\mathcal{S}$ be a set of cost/revenue scenarios and $\boldsymbol{P}_s$ be an $N_s \times N_w$ matrix of scenario probabilities, with element (s,w) stating the probability of scenario s under decision w. Furthermore let $\widetilde{w}_i$ be a bidding decision on the interval $w_i \in \mathcal{W}$. Finally define a (column) vector of binary variables $\boldsymbol{z}$ of length N_w and with elements z_{w_i}. Then then we can write the bidding problem as a mixed integer problem:

$$\widetilde{W}_t^{(*)} = \arg\max_{\widetilde{W}} \left\{ (1-\lambda) \sum_{s\in\mathcal{S}} p_s \zeta_s(\widetilde{W}) + \lambda \left(\eta_\alpha - \frac{1}{\alpha} \sum_{s\in\mathcal{S}} p_s \xi_s(\widetilde{W}) \right) \right\} \tag{37}$$

$$s.t. \quad \xi_s(\widetilde{W}) \geq \eta_\alpha(\widetilde{W}) - \zeta_s(\widetilde{W}) \tag{38}$$

$$\xi_s(\widetilde{W}) \geq 0 \tag{39}$$

$$\Delta W_s^{(\uparrow)}(\widetilde{W}) \leq W_s - \widetilde{W} \tag{40}$$

$$\Delta W_s^{(\downarrow)}(\widetilde{W}) \leq \widetilde{W} - W_s \tag{41}$$

$$\Delta W_s^{(\uparrow)}(\widetilde{W}), \Delta W_s^{(\downarrow)}(\widetilde{W}) \leq 0 \tag{42}$$

$$z_{w_i}\underline{w}_i \leq \widetilde{w}_i \leq z_{w_i}\overline{w}_i \tag{43}$$

$$\sum_{w_i \in \mathcal{W}} z_{w_i} = 1 \tag{44}$$

$$\widetilde{W} = \sum_{i=1}^{N_w} w_i \tag{45}$$

$$p_s = \sum_{i=1}^{N_w} \boldsymbol{P}_s(s,i) z_{w_i} = \boldsymbol{P}_s(s,:)\boldsymbol{z} \tag{46}$$

where $\underline{w}_i$ and $\overline{w}_i$ are the lower and the upper bound of w_i respectively and $\zeta(\widetilde{W})$ still defined by (31) or (32). So given the necessary scenarios, this mixed integer formulation of the problem can then be used to optimise the bids of a producer that only has market power on the regulation market as well as for a producer that also has market power on the day-ahead market. Whereas in the former case, one still has the choice between optimising in terms of his imbalance costs or in therm of his revenues, the revenue formulation is probably the only sensible formulation for a producer with full market power. This is because the first one is still not in any control over his spot market revenues and thus can look away from them in the optimisation. In contrast, the second one can diminish the value of his lower imbalance cost by reducing his spot market revenues in the process.

4.3 Objective - Revenue vs. Imbalance Costs

The choice between the two possible formulations of the objective function is not obvious. In Zugno et al. (2012) the cost formulation is chosen since it can be shown that maximising the expected deviation from perfect information revenue (or the expected imbalance costs) the same as maximising the expected revenue for a price taker. Once any nonlinear measure of risk becomes an explicit part of the objective however this is no longer true - Regardless of whether you only consider production risk or you consider the production and the price risk together. This in turn yields different optimums depending on the formulation chosen. Summarised in one sentence the difference for a mixed strategy $(0 < \lambda < 1)$ is that whereas the CVaR for the cost formulation pulls the bid towards the expected production, the CVaR for the revenue pulls the bid towards the bid yielding the lowest probability of negative revenue.

In order to further illustrate the difference between the two consider the following toy example. Assume that we have for a given hour 10 equally probable scenarios of wind power production so

$$\begin{bmatrix} w_{s_1} & w_{s_2} & \dots & w_{s_{10}} \end{bmatrix} = \begin{bmatrix} 0 & 1 & \dots & 9 \end{bmatrix} MWh/h$$
$$p_i = 0.1 \quad \forall i = 1,2,\dots,10.$$

Furthermore assume that up-and down-regulation are equally probable for that same hour and that the market prices (conditioned upon their realisation where appropriate) are fixed at

$$\pi^{(S)} = 20, \quad \pi^{(\uparrow)} = 30, \pi^{(\downarrow)} = 10 \Rightarrow \psi^{(\uparrow)} = \psi^{(\downarrow)} = 10.$$

Finally let $\alpha = 0.1$ and assume that wind power is always produced, i.e. that what's not sold day-ahead is sold at the down regulation price. Given all this, the bid maximising both the expected revenues and the (non-positive) expected imbalance cost is the expected production or $4.5 MWh/h$. The CVaR however is maximised at $0 MWh/h$ for the revenue formulation but at $4.5 MWh/h$ for the cost formulation.

What makes the maximum CVaR be at zero for the revenue formulation is that since the prices are fixed such that the down regulation price is positive, a non-negative revenue is guaranteed by bidding zero into the market. Then making the prices stochastic and the probability of negative down regulation price positive pushes the bid again away from zero - still contributing to a lower bid than a pure optimisation of the expected revenue would though. The push towards the expected production in the other case however is a result of the fact that unless very different probabilities of each imbalance sign the worst case scenarios are to be found at both ends of the revenue distribution. Hence the push towards the expected value.

Which of the two formulations is the more appropriate one is to some extent a matter of preference and there are arguments in favour of either one. For one the producer's financial health is in the end affected by his revenues and therefore one can argue that revenue risks should be considered when power is bid to the market. This was also the initial objective of the strategy in Zugno et al. (2012) which was only revised since the cost formulation was equivalent. For a risk-averse producer, an additional appeal of the revenue formulation is that it offers the bid that truly minimises the probability of loosing money. Hence the revenue formulation can be said to be more conservative than the cost formulation. However it is important for the system operation standpoint that the volume bid to the market reflects the actual future production. This prompted the constraint that the bid should be within a certain limit from the point forecast in Zugno et al. (2012) and for the revenue formulation of the CVaR bidding strategy, this constraint is still likely to be necessary in the same form as before. In contrast optimising the CVaR in the cost formulation essentially has the same effect as that constraint. Thus with a carefully chosen value of λ will in some ways account for this constraint implicitly and what is more do it in a more intelligent manner. In addition, the coherence of CVaR implies that

$$\mathrm{CVaR}_\alpha[\rho] \leq \mathrm{CVaR}_\alpha[\rho^{(S)}] + \mathrm{CVaR}_\alpha[\rho^{(\uparrow/\downarrow)}]$$

where

$$\rho^{(S)} = \pi_s^{(S)} W_s$$
$$\rho^{(\uparrow/\downarrow)} = \Delta W_s^{(\downarrow)}(\widetilde{W})\psi_s^{(\downarrow)} + \Delta W_s^{(\uparrow)}(\widetilde{W})\psi_s^{(\uparrow)}$$

and $\rho^{(S)}$ consists of two stochastic variables, neither of which the is in control of. So one can argue that he/she who actually is responsible for trading wind power should focus on maintaining as little deviation as possible from the perfect scenario and let someone else take care of the revenue risk as such - possibly along with the producer's total revenue risk if it has a diverse production portfolio. So in addition to general taste, the appropriate formulation might also depend on how the general structure of the company owning the turbines is. For a producer only owning wind turbines the revenue formulation might be more appropriate while the cost formulation might be better

suited for a large company with a diverged production portfolio. For both objectives it is important to realise though that long-term goals for risk can be derived directly from the hourly risk criteria. Due to the lack of apparent better choice it is decided to try out both formulation in attempt to shed more light on the consequences of adopting either formulation of the strategy.

5 Scenario Generation

In order to solve the problem in the formulation just described, scenarios for production and market outcomes are necessary. In this section generation of such scenarios are loosely discussed. First the method used to obtain the scenarios used in the case study later presented are discussed. Thereafter, some thoughts on how these scenarios could be constructed properly are presented.

5.1 Simple Scenarios

In order to find the optimal bid in terms of revenue, each scenario $s \in \mathcal{S}$ consists of simulated realisations of 4 different variables. These are the wind power production, W_s, the spot price, $\pi_s^{(S)}$, and the up-and down regulation penalties, $\psi_s^{(\uparrow)}$ & $\psi_s^{(\downarrow)}$. For the cost formulation, the same variables are needed apart from the spot price. For now (and in the price taker test case presented in the next section) we'll assume that there isn't any type of dependence between the wind power production and the prices so that wind power scenarios and market scenarios can be created independently of each other. Doing so allows us to create a wind scenario only by drawing random realisations of the estimated CDF for that particular time. For the market, its sequential arrangement prompts a hierarchy in the prices which somehow has to be taken into account when market scenarios are generated. Therefore it is decided to model the density of the penalties conditional to the actual spot price and adopt the following scheme for generating the scenarios (including the wind power):

For generating each $s \in \mathcal{S}$:

1. Generate a vector $\boldsymbol{r}$ with IID elements $r_i \sim U(0,1) \forall i,\ i = 1,\ldots,4$
2. Set $\pi_s^{(S)} = F^{-1}_{\pi^{(S)}}(r_1)$
3. Set $I_s^{(\psi)} = I(\psi^{(\uparrow)} > 0) - I(\psi^{(\downarrow)} < 0) = F_I^{-1}(r_2)$
4. Set $W_s = F_W^{-1}(r_3)$
5. If $I_s^{(\psi)} = -1$
   (a) Estimate $F_{\psi^{(\downarrow)}}(x; \pi^{(S)}, I_s^{(\psi)})$
   (b) Set $\psi_s^{(\downarrow)} = F^{-1}_{\psi^{(\downarrow)}}(r_4; \pi^{(S)}, I_\psi)$

(c) Set $\psi_s^{(\uparrow)} = 0$

else if $I_s^{(\psi)} = 1$

(a) Estimate $F_{\psi^{(\uparrow)}}(x; \pi_s^{(S)}, I_s^{(\psi)})$

(b) Set $\psi_s^{(\uparrow)} = F^{-1}_{\psi^{(\uparrow)}}(r_4; \pi_s^{(S)}, I_s^{(\psi)})$

(c) Set $\psi_s^{(\downarrow)} = 0$

else $\psi_s^{(\uparrow)} = \psi_s^{(\downarrow)} = 0$

For the cost formulation, the spot prices are not a part of the scenarios and thus unconditional densities for the penalties are required. However since

$$F_\psi(x) = \int_{-\infty}^{\infty} F_\psi(x; \pi^{(S)}) d\pi^{(S)}$$

by generating a large number of scenarios as described above and discarding the spot prices is a completely valid alternative to constructing new densities.

Regarding forecasts, those are required for the following variables:

1. The day-ahead spot price, $\pi^{(S)}$
2. The wind power production, W
3. The imbalance sign, $I_s^{(\psi)} = I(\psi^{(\uparrow)} > 0) - I(\psi^{(\downarrow)} < 0)$
4. The regulation penalties, conditioned on it being different from zero, i.e. $\psi^{(\uparrow)} | I^{(\psi)} = 1$ and $\psi^{(\downarrow)} | I^{(\psi)} = -1$

5.2 Further Development

The scenario generation scheme listed before is complete in the sense that all realisations all necessary variables are created based obtainable predictive densities. Moreover, should the assumption that there is no relationship between our wind power production and the market outcome holds, the method for scenario generation outlined above complete. Whereas it's difficult to see any reason for this assumption not to hold for the spot market, since it is settled before the production is realised, the situation is more complicated for the regulation market. First of all, unless the producer's turbines are relatively isolated geographically, the production of the turbines and the remaining turbines in the system is going to be positively correlated. Then if this correlation is present, the question becomes whether or not the actual production in the system affects the market outcome or not. Now the imbalance sign (defined by price) is determined by the system imbalance (and whether or not the prompt a penalty) which in turn intuitively seems influenced by that of the wind turbines - At least during hours of medium to high production.

As previously mentioned, the relationship between the wind power production and regulation penalty is two sided. For one, increased offering of wind power in the spot

market prompts a greater supply of relatively cheap regulating power since flexible units otherwise cleared on the spot market will now be offering regulative power. The increased share of wind power however also typically prompts a greater demand for balancing power which then counteracts with the increased supply. In addition, the generation units capable of supplying balancing power all operate with some substantial marginal cost. Therefore even if you only look at the supply side there is a limit on how low the regulation price can be. Thus at some point the increased share of wind in the cleared volume starts to increase the penalty again. Empirical evidence supporting these statements can be viewed in Jónsson et al. (2012a).

So for the purpose of better scenario generation, both for a price taker and a price maker, it would be interesting to first model a joint distribution between one's own production errors and those of the system and subsequently joint that distribution with the regulation market densities e.g. through copulas by the method outlined in Pinson et al. (2009). Although easier said than done, this task should be well within what's achievable.

On a more overall note, there are several other factors that impact the regulation prices which impact the regulation market outcome. An example of two of the more important ones of these factors are the demand side imbalance and to which degree exporting/importing the imbalances to neighbouring areas exists, if at all. These variables are of course not a part of the required scenario explicitly. Basing the regulation market scenarios on that for these extra variables however could help towards gaining a more accurate description of the probability density of the imbalance penalties.

Once models for the aforementioned joint densities have been developed, the scenario reduction technique from Nicole Growe-Kuska and Romisch (2003) could be adopted to create scenarios for the price maker solution. In short, the forward selection method of Nicole Growe-Kuska and Romisch (2003) calculates the euclidean distances between every scenario in a given set of scenarios, selects a reduced number of scenarios that conserve the moments of the original set and reassigns scenario probabilities. So given a number of different scenarios sets for different wind power bid to the market, each of these scenarios sets could be reduced to the same pre-determined scenarios that match the unconditional revenue distribution.

6 A (Really) Small Case Study

Finally we present a small case study to illustrate the characteristics of the bidding behaviour of a producer adopting the strategy here described. Before the actual bidding results are presented, a brief discussion of the forecasts constructed for the purpose is given.

6.1 Forecasts

For all variables, the procedure for obtaining the forecasts for all the continuous variables is similar. First a point forecast is made and then prediction intervals are estimated using methods that explicitly forecast each quantile for a range of pre-determined set of quantiles. All models are tuned on data for the period from November 1st 2008 - January 31st 2010.

The point forecasts are obtained in the following manner:

- The wind power forecasts stem from WPPT, a statistically based and commercially based prediction software Nielsen et al. (2002) (see www.enfor.dk for further information)
- The spot price predictions are found using the model presented in Jónsson et al. (2012c).
- The imbalance penalty forecasts are found by a Holt-Winters model similar to the one described in Jónsson et al. (2012a).

For all variables, the time-adaptive quantile regression method described in Møller et al. (2008) and Jónsson et al. (2012b) are used to predict density quantiles of nominal proportion between 0.05 and 0.95 in steps of 0.05. For the wind power no further modelling is done and the 0 and installed capacity set as the 0 and 100% quantiles. For the prices and penalties, the Conditional Autoregressive Value-at-Risk (CAViaR) Gorr and Hsu (1985), Engle and Manganelli (2004), Taylor (2008) model are used to predict the $0.01, 0.025, 0.975, 0.99$ quantiles as well. Then the highest and the lowest observations during the data period are set as the 0 and 100% quantiles.

Finally, the imbalance sign probabilities are obtained by the Holt-Winters model described in Jónsson et al. (2012a).

6.2 Bidding Behaviour

In order to illustrate the workings of the bidding strategy and the different formulations of the objective, the strategy is tested for a single hour. The hour chosen is the 10th hour of July 13th 2009 for which we have the forecasts shown in Figure 1. These forecasts are then used to generate 10000 scenarios for the all variables involved using the previously described scenario generation procedure and subsequently reduced to 100 by the method of Nicole Growe-Kuska and Romisch (2003). After that the optimal bid is calculated using GAMS for $\alpha = 0.05$ and $\alpha = 0.1$ and the value of λ is varied between 0 and 1 in steps of 0.1 and compared to the bids obtained by the strategy formulated in Zugno et al. (2012).

In Figure 2, the resulting bids shown for different values of λ. As expected, the bids derived from the revenue formulation of the objective decreases with increased risk aversion. The fact that they don't go all the way down to 0 is a result of some of the

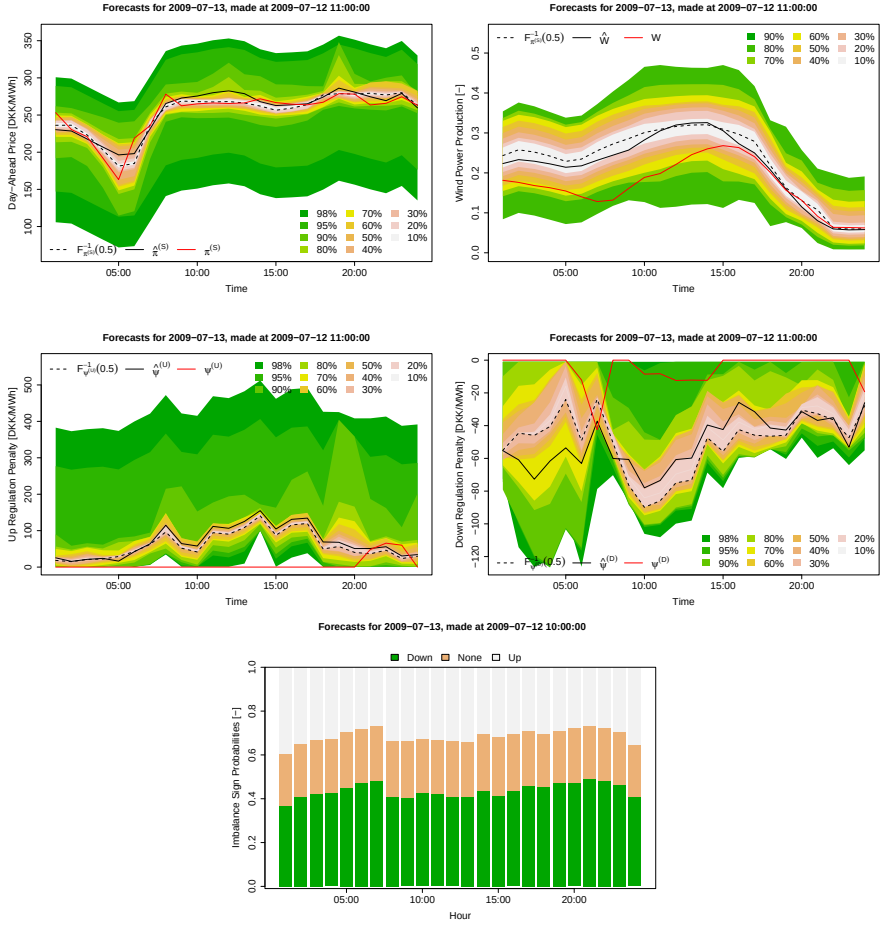

Figure 1: Forecasts for July 13th 2009 made at noon the day before

scenarios containing negative down regulation price and that down regulation has a slightly higher probability than up regulation. However since the probability of the two penalising imbalance signs isn't severely different, the bid from the cost formulation doesn't change all that much with λ. The bid is nonetheless being pulled towards the point forecast but large tail of the up-regulation penalty density keeps it above the point forecast though for every value of λ. As shown in Figure 3, the CVaR behaves according to expectations from the bids. In Figure 4 the estimated density of the revenues from the 10000 scenarios is plotted for different values of lambda. As can be seen, the density doesn't change all that much on the scale of the plot. The expected value is decreasing though and the distribution goes from being two peaked to a single peak. However if some quantiles in the very leftmost tail of the distribution are viewed though some change becomes apparent as shown in Figure 5.

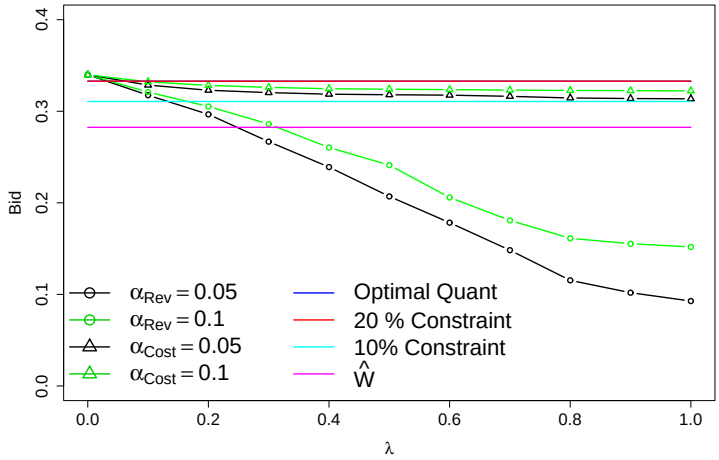

Figure 2: The optimal bids for the mean-CVaR bidding strategy for different values of λ along with bids from the newsvendor strategy. The unconditional optimal bid does not show since it is equal to the 20% constraint one.

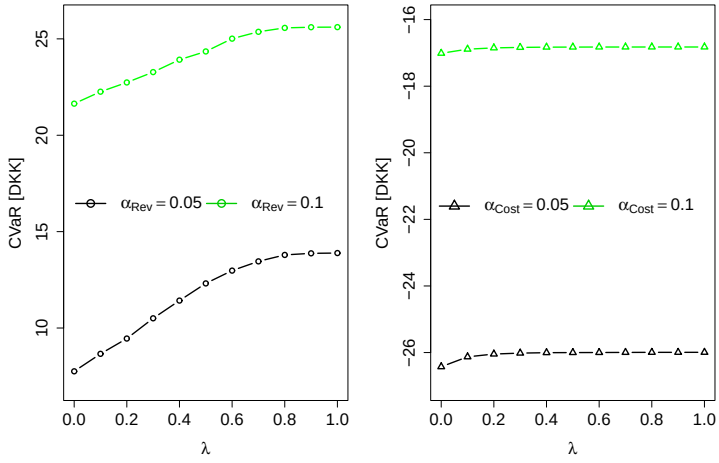

Figure 3: The CVaR for different values of λ and for the two formulations of the objective.

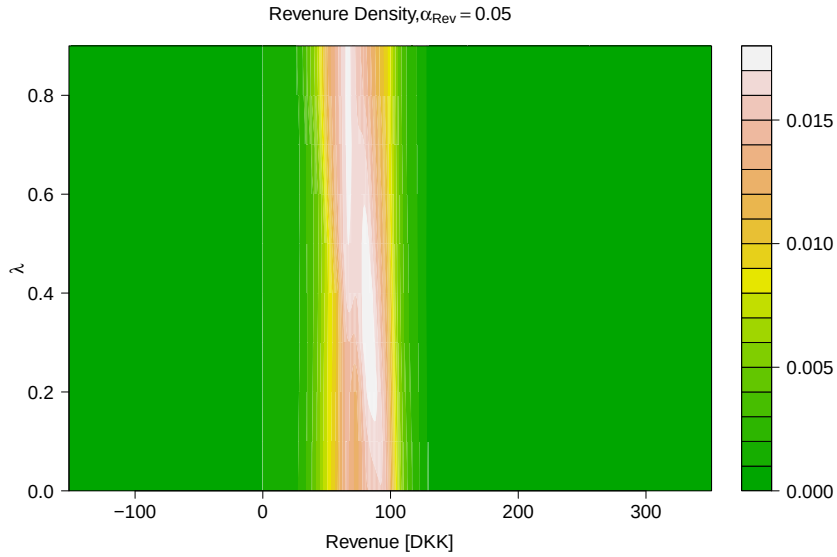

Figure 4: The density of the revenues for $\alpha = 0.05$ for different values of λ

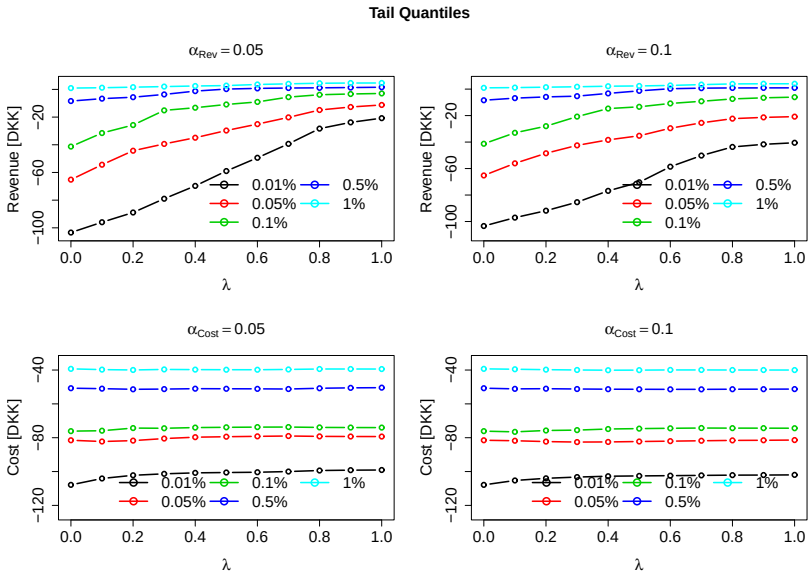

Figure 5: Movement in the leftmost tail of the cost / revenue distribution for different values of λ

7 Concluding Remarks

A framework for risk averse bidding of wind power to day-ahead electricity market has been derived. Should a risk-averse strategy for bidding be adopted, the CVaR seems like an appropriate choice due to it is concerned with the worst possible outcomes. This property is appealing for daily trading of wind power where the main focus of risk management should be on avoiding the few potential occurrences of excessive losses from the real-time market.

The framework here presented addresses the bidding and the risk on an hourly basis. Extending the framework to consider multiple periods simultaneously, e.g. 24 hours as done in Morales et al. (2010), is easy though. It simply involves swapping the hourly value for the sum of multiple ones within the terms of the objective functions. The scenario generation for such model would become considerably more complex since it would have to accommodate the temporal correlation of all the variables.

Regardless of whether the trading is considered on a daily or an hourly basis it is important to realise that long-term risk management goals are beyond reach with these types of strategies. This is also important to consider when the choice between the two formulations of the objective value presented is made. In light of all this, the relevancy and effect of short-term risk management in context with such efforts on longer time scales would be interesting to carry out.

References

John B. Bremnes. Probabilistic wind power forecasts using local quantile regression. *Wind Energy*, 7(1):47–54, 2004.

Youhua (Frank) Chen, Minghui Xu, and Zhe George Zhang. A Risk-Averse Newsvendor Model Under the CVaR Criterion. *Operations Research*, 57(4):1040–1044, 2009.

Chris J. Dent, Janusz W. Bialek, and Benjamin F. Hobbs. Opportunity cost bidding by wind generators in forward markets: Analytical results. *IEEE Transactions on Power Systems*, 26(3):1600–1608, 2011.

Robert F. Engle and Simone Manganelli. CAViaR: Conditional Autoregressive Value-at-Risk by Regression Quantiles. *Journal of Business adn Economic Statistics*, 22(4):367–381, 2004.

W.L. Gorr and C. Hsu. An Adaptive Filtering Procedure for Estimating Regression Quantiles. *Management Science*, 31(8):1019–1029, 1985.

Tryggvi Jónsson, Pierre Pinson, Henrik Aa. Nielsen, and Henrik Madsen. Exponential smoothing approaches for prediction in real-time electrcity markets. *Energy Economics*, (submitted), 2012a.

Tryggvi Jónsson, Pierre Pinson, Henrik Aa. Nielsen, and Henrik Madsen. Predictive densities for day-ahead electricity prices using time-adaptive quantile regression. *European Journal of Operational Research*, (submitted), 2012b.

Tryggvi Jónsson, Pierre Pinson, Henrik Aalborg Nielsen, Henrik Madsen, and Torben Skov Nielsen. Forecasting electricity spot prices accounting for wind power predictions. *IEEE Transactions on Sustainable Energy*, In PRESS, 2012c.

Jan Kloppenborg Møller, Henrik Aalborg Nielsen, and Henrik Madsen. Time-adaptive quantile regression. *Computational Statistics and Data Analysis*, 52(3):1292–1303, 2008.

Juan M. Morales, Antonio J. Conejo, and Juan Pérez-Ruiz. Short-term trading for a wind power producer. *IEEE Transactions on Power Systems*, 25(1):554–564, 2010.

Holger Heitsch Nicole Growe-Kuska and Werner Romisch. Scenario reduction and scenario tree construction for power management problems. In *IEEE PowerTech Conference*, Bologna, Italy, June 23-26 2003.

Torben Skov Nielsen, Henrik Aalborg Nielsen, and Henrik Madsen. Prediction of wind power using time-varying coefficient functions. In *15th IFAC World Congress*, Barcelona, Spain, 2002.

Pierre Pinson, George Papaefthymiou, B. Klockl, Henrik Aalborg Nielsen, and Henrik Madsen. From probabilistic forecasts to statistical scenarios of short-term wind power production. *Wind Energy*, 12(1):51–62, 2009.

R. Tyrrell Rockafellar and Stanislav Uryasev. Optimization of Conditional Value-at-Risk. *The Journal of Risk*, 2(3):21–41, 2000.

R. Tyrrell Rockafellar and Stanislav Uryasev. Conditional Value-at-Risk for General Loss Distributions. *Journal of Banking and Finance*, 26(7):1443–1471, 2002.

Rudiger Schultz and Stephan Tiedemann. Conditional Value-at-Risk in Stochastic Programs with Mixed-Integer Recourse. *Mathematical Programming Series B*, 105(2-3): 365–386, 2006.

James W. Taylor. Using Exponentially Weighted Quantile Regression to Estimate Value at Risk and Expected Shortfall. *Journal of Financial Econometrics*, 6(3):382–406, 2008.

Marco Zugno, Tryggvi Jónsson, and Pierre Pinson. Trading wind energy based on probabilistic forecasts of wind generation and market quantities. *Wind Energy*, In PRESS, 2012.

PAPER F

Forecasting Electricity Spot Prices Accounting for Wind Power Predictions

Authors:
T. Jónsson, P. Pinson, H. Aa. Nielsen, H. Madsen, T.S. Nielsen

Accepted for publication in:
IEEE Transactions on Sustainable Energy (2012)

Forecasting Electricity Spot Prices Accounting for Wind Power Predictions

Tryggvi Jónsson[1,2] Pierre Pinson[2] Henrik Aa. Nielsen[1] Henrik Madsen[2] Torben Skov Nielsen[1]

Abstract

A two-step methodology for forecasting of electricity spot prices is introduced, with focus on the impact of predicted system load and wind power generation. The non-linear and non-stationary influence of these explanatory variables is accommodated in a first step based on a non-parametric and time-varying regression model. In a second step, time-series models i.e. ARMA and Holt-Winters, are applied to account for residual autocorrelation and seasonal dynamics. Empirical results are presented for out-of-sample forecasts of day-ahead prices in the Western Danish price area of Nord Pool's Elspot, during a two year period covering 2010-2011. These results clearly demonstrate the practical benefits of accounting for the complex influence of these explanatory variables.

1 Introduction

The participants in deregulated electricity markets rely, among other things, on forecasts of future prices for bidding and optimizing the dispatch of their generation units. Methods for deriving such forecasts can be divided into two fundamentally different categories: economical equilibrium models that mimic the actual pricing model, and statistical ones. The former models are able to provide excellent forecasts when given sufficiently accurate information (see e.g. Vehviläinen and Pyykkönen (2005), Fleten and Wallace (1998) and references therein). This information is however seldom available to individual market participants. In addition, the presence of non-dispatchable yet cheap generation units in the system implies that this information might be impossible to obtain since their production is indeed stochastic. Statistical approaches then appear to be a relevant alternative.

The increased focus on curbing carbon emissions worldwide has led to vast investments in renewable energy sources and in particular wind power. Many of these emerging energy sources, wind power included, share a characteristic in being non-dispatchable due to the varying availability of the fuel, which also cannot be stored. Consequently these sources are ill-suited for long term contracts, leaving only markets with relatively short

[1]ENFOR A/S, Lyngsø Allé 3, DK-2970 Hørsholm, Denmark
[2]DTU Informatics, Technical University of Denmark, Richard Petersens Plads, building 321, DK-2800 Kgs. Lyngby, Denmark

time between gate-closure and delivery as a realistic option for selling the production. Inevitably the prices at these markets are affected by this additional supply Jónsson et al. (2010), Giabardo et al. (2010), Morales et al. (2011), Skytte (1999), Morthorst (2003).

The impact of renewable energy is superimposed on already existing price features such as non-stationarity, periodicity, mean reverting spikes, positive skewness and high kurtosis along with intra- and inter-day serial correlation Conejo et al. (2005), Panagiotelis and Smith (2008), Kosater and Mosler (2006). These features arise from the distinct characteristics of electricity as a commodity. Firstly, lack of direct storability along with the specialized and technically limited transmission system required, makes arbitrage over time and space difficult Sewalt and de Jong (2003), Boogert and Dupont (2005). Secondly, demand for electricity is highly inelastic while exhibiting strong seasonalities in the short term. Meanwhile the supply function is discontinuous, convex and steeply increasing at the high production end Taylor and McSharry (2007), Panagiotelis and Smith (2008), Karakatsani and Bunn (2008). The aim of the present paper is to propose a forecasting methodology which allows for accommodating the effect of the emerging renewable sources as well as the characteristics described in Conejo et al. (2005), Panagiotelis and Smith (2008), Kosater and Mosler (2006), Karakatsani and Bunn (2008).

In Jónsson et al. (2010), predicted power production is shown to significantly impact the distribution moments of day-ahead electricity prices through a Danish case study. Motivated by these findings, the present paper introduces a two-step methodology for issuing point forecasts for electricity spot prices, accounting for the impact of predicted load and wind power production. First, a time-varying function is estimated, jointly mapping the predicted hourly load and wind power production to a corresponding spot price. The function is built based on a conditional parametric regression model for which the parameters are estimated adaptively. In addition, past observations are discounted exponentially as new ones become available. The resulting flexibility in the model serves the purpose of accommodating both the non-linear relationship between the explanatory variables and the prices, as well as the non-stationarity of all the processes involved. Although here a conditional parametric model is chosen for the inclusion of the wind power and load as explanatory variables, other model types might be just as suitable. For instance including the forecast wind power production along with the load in the adaptive wavelet neural-network model of Wu and Shahidehpour (2010). Regardless of the model chosen, the main message of this paper remains intact: that wind power production, where present, impacts the prices to such extent that it should be accounted for in a forecasting model for electricity spot prices.

In the second stage, the remaining residuals are modeled using well known models from the time series analysis literature. These models are an additive double seasonal Holt-Winters model and a recursively estimated seasonal AR model. All models are estimated under robust criteria in order to protect the parameter estimates from the effects of excessive price spikes. Models and parameters are optimized in terms of weighted least squares residuals.

The sole focus of this paper is deriving a model that describes the expected spot prices on a day-ahead basis. Although the authors recognize proper modeling of forecast uncertainty and price spikes as paramount in forecasting electricity spot prices, the empir-

ical features of the prices are such that appropriate uncertainty or spike modeling will easily comprise a full paper of its own. The model presented in this paper can however be combined with a price spike model (e.g. those presented in Lu et al. (2005), Amjady and Keynia (2010)). Same goes for a model for predictive densities such as the ones described in Panagiotelis and Smith (2008) and Higgs (2009).

The context of the empirical results presented in this paper is the Western Danish price area (DK-1) of the Nord Pool's Elspot market. Operational data for the period from November 1st 2008 until December 31st 2011 are considered and used to evaluate the model's day-ahead forecasting skill. Furthermore, the value of the time-adaptivity and robustness is illustrated by comparing the performance of the proposed approach against its time-invariant and non-robust counterparts. Despite focus being on this market only, the fact that results on the influence of wind power forecasts on electricity prices similar to those of Jónsson et al. (2010) have been obtained for other areas, e.g. Germany and Spain Morales et al. (2011), indicates that similar forecasting methodology could be applied successfully in the context of other markets.

The remainder of the paper is structured as follows. The market and data on which the empirical work is based are described in Section 2. Section 3 presents the models and Section 4 the obtained empirical results. Finally concluding remarks are given in Section 5.

2 Empirical Background

Elspot is a day-ahead market for physical delivery of electric power, operated by Nord Pool Spot ASNord Pool Spot AS (2012) in the entire Scandinavia (Denmark, Finland, Norway and Sweden) and in Estonia.

On Elspot, contracts for next day physical delivery are traded for hourly periods. Prices are set as the intersection between the aggregated supply and demand curves for each hour of the day, right after gate-closure at noon. The intersection of the curves representing all bids in the entire market region defines the system price. The system price, in addition to serve as reference for financial contracts, is the price at which physical contracts are settled if transmission capacity is sufficient throughout the entire region.

Due to limited transmission capacity however, both between and within the member countries, the market region is divided into several price areas. If the scheduled flow between price areas exceeds the corresponding transmission capacity, area prices that differ from the system price are calculated. On such occasions, the area prices are identical among areas that have sufficient capacity on their interconnections. Areas on each side of a congested connection however have different prices. The area prices are the ones at which contracts for physical delivery are settled.

The context of the empirical results presented in the following is the Western Danish price area (DK-1) of Elspot. The area comprises Jutland and Funen along with the islands west of the Størebælt channel and has relatively strong connections to both Nor-

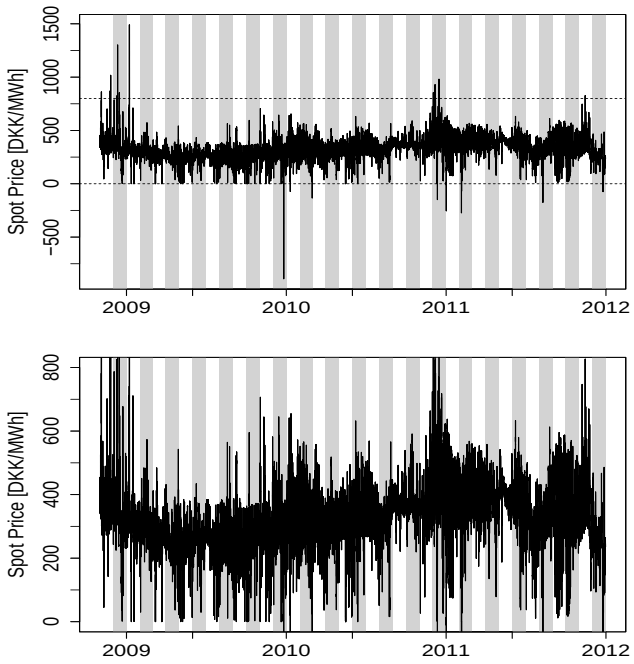

Figure 1: Time series plots of the spot prices throughout the considered period.

way and Sweden to the north and Germany to the south. As of August 20, 2010 the DK-1 area also has a 600 MW link to the Eastern Danish price area (DK-2). Furthermore, the area has a large share of its annual electricity consumption (about 25%) generated by wind turbines.

The data set used consists of hourly observed area prices along with forecasts of both wind power production and consumption in the area. Both forecasts are issued before gate-closure and have a temporal resolution of 1 hour. The observed prices are taken from the website of the Danish transmission system operator (TSO), Energinet.dk (Energinet.dk (2012)). The load forecasts are the ones made publicly available by Nord Pool through their website (Nord Pool Spot AS (2012)). The wind power production forecasts however stem from a statistically based wind power prediction software Nielsen et al. (2002). Time series plots of the prices for the considered period are shown in Fig. 1. Whereas the top plot shows the full series, the bottom one shows the sereis on a scale truncated a 0 and 800 DKK / MWh.

3 Model for Spot Prices

3.1 The Rationale Behind the Proposed Modeling Approach

As more than half of the annual electricity production in the Nordic region is hydro power based Nord Pool Spot AS (2010), the prices at the Elspot market are inevitably dominated by the water stock in the hydro power reservoirs in Norway, Sweden and Finland. This stock however varies relatively slowly compared to the resolution and lead-times of the desired forecasts. Indeed the fact that data for these are published with a resolution of one week should be enough to convince one that such data has no explanatory value in day-ahead price forecasts with a resolution of a single hour. Instead, the impact of the water stock appears as a slow drift in the price series with this resolution. Because of this, it is decided only to implicitly include the impact of hydro stock, along with other slowly varying fundamentals such as fuel prices, by adaptive estimation of the model parameters.

In Jónsson et al. (2010) the ratio between predicted wind power production and forecast consumption is shown to affect the area spot prices in DK-1 substantially. On a similar note, forecast wind power production is shown to appear in the supply function as a stochastic threshold in Giabardo et al. (2010). The reason for wind power to have such a strong influence on prices is owed to how it fundamentally differs from most other energy sources that significantly contribute to the supply. Whereas conventional power plants can be scheduled to steadily produce a certain amount of energy over a longer period, wind turbines literally produce as the wind blows. In addition, the absence of fuel costs allows wind turbines to produce at a marginal cost close to 0. This low marginal cost causes wind power to enter the supply function to the very left and thereby horizontally shifts the supply function.

The stochastic fuel availability moreover implies that those responsible for bidding wind power into the market have to rely on production forecasts for their decisions. As a consequence, the supply function comprises the production forecasts available at gate-closure and not the realized volume. For this reason, forecasts of future production are the appropriate form of wind power for any inference on its relation to the prices. This aside, forecasting in practice has to be based on predictions of both wind power production and load. Thus following Jonsson (1994) the model is entirely and based on forecast values for the explanatory variables.

In contrast to Jónsson et al. (2010) the two explanatory variables enter the former model step individually and not as a ratio. This is because that formulation was found to yield better forecasts of the prices.

In Nogales et al. (2002) lagged values of measured load are found to have significant explanatory power in a model for the spot prices. Past demand has however no direct effect on the current spot prices. It is therefore likely that the effect seen in Nogales et al. (2002) is owed to that in the absence of actual load forecasts the lagged demands serve as implicit prediction of the load. The high number of lags, especially seasonal ones,

found significant in Nogales et al. (2002) support this conclusion. Thus with access to an actual load forecast, no attempt to include past demand in the model was made.

3.2 Spot Price as a Function of Forecast Wind Power Production and Load

An excellent general description of the methodology and estimation procedure used to describe the spot prices as a function of wind power and load forecasts is given in Cleveland and Devlin (1988) (without recursivity) and in Nielsen et al. (2000), Pinson et al. (2007)(including recursivity and robustness respectively). However, in order to make this paper self-contained, an outline of the method is given here, tailored to the application at hand.

Let a model for the spot price at time t, $\pi_t^{(S)}$, be denoted as

$$\pi_t^{(S)} = \boldsymbol{\theta}_t(\boldsymbol{u}_t) + \varepsilon_t \tag{1}$$

where $\boldsymbol{\theta}_t(\cdot)$ is a function of a set of explanatory variables, $\boldsymbol{u}_t$, and ε_t is a noise term, centered and a with a finite variance. Thus, the model (1) is a non-linear and non-parametric regression model.

The function $\boldsymbol{\theta}(\cdot)$, is approximated using polynomials by fitting a linear model at a number of distinct *fitting points*. More specifically let $\boldsymbol{u} = \begin{bmatrix} u_1 & u_2 \end{bmatrix}^T$ denote a particular fitting point and let $\boldsymbol{p}_d(\boldsymbol{u})$ denote a column vector containing the terms in the corresponding polynomial of order d. Here $d = 2$ has been chosen after trials with $d \in \{1,2,3\}$ yielding $\boldsymbol{p}_2(\boldsymbol{u}) = \begin{bmatrix} 1 & u_1 & u_2 & u_1^2 & u_1 u_2 & u_2^2 \end{bmatrix}^T$.

Now define

$$\boldsymbol{\phi}_{u,t}^T = \begin{bmatrix} \phi_{u_1,t} & \cdots & \phi_{u_2^2,t} \end{bmatrix} \tag{2}$$

a column vector of coefficients such that the model

$$\pi_t^{(S)} = \boldsymbol{p}_2^T(\boldsymbol{u}_t)\boldsymbol{\phi}_{u,t} + e_t \tag{3}$$

describes the prices in the close vicinity of the fitting point $\boldsymbol{u}$ where e_t is a noise term, centered and with a finite variance.

The parameters in (3) are estimated using recursive and robust weighted least squares. That is

$$\widehat{\boldsymbol{\phi}}_{u,t} = \arg\min_{\boldsymbol{\phi}_{u,t}} \sum_{s=1}^{t} \lambda^{t-s} w_u(\boldsymbol{u}_s) \left(g(e_s,\tau)\right)^2 \tag{4}$$

where $e_t = \pi_t^{(S)} - \boldsymbol{p}_2^T(\boldsymbol{u}_t)\boldsymbol{\phi}_{u,t}$ and $0 < \lambda < 1$ is a forgetting factor that exponentially discounts observations over time. Furthermore, $w_u(\boldsymbol{u}_t)$ is a weight, assigned to observation $\boldsymbol{u}_t$ as a function of its distance to the fitting point $\boldsymbol{u}$. Finally, $g(\cdot,\cdot)$ is the *Huber*

influence function Huber (1981), defined as

$$g(e_t, \tau) = \text{sgn}(e_t) \cdot \min\{|e_t|, \tau\}, \tag{5}$$

where τ is the cut-off value or the maximum influence a single observation is allowed to have on the estimate.

The weights are assigned as

$$w_u(\boldsymbol{u}_t) = W\left(\frac{||\boldsymbol{u}_t - \boldsymbol{u}||}{h(\boldsymbol{u})}\right) \tag{6}$$

where $W(\cdot)$ is a function taking non-negative arguments, $||\cdot||$ denotes the Euclidean norm and $h(\boldsymbol{u})$ is the bandwidth applied in the fitting point $\boldsymbol{u}$. Following Cleveland and Devlin (1988) and Nielsen et al. (2000) a tri-cube kernel is used to determine the weights. That is

$$W(x) = \begin{cases} (1-x^3)^3 & \text{if } x \in [0;1) \\ 0 & \text{otherwise} \end{cases} \tag{7}$$

which entails weights between 0 and 1.

It can be shown (see e.g. Pinson et al. (2007) or Madsen (2008), Ch. 11) that the adaptive parameter estimates in Eq. (4) can be found recursively as

$$\widehat{\boldsymbol{\phi}}_{u,t} = \widehat{\boldsymbol{\phi}}_{u,t-1} + w_u(\boldsymbol{u}_t)\boldsymbol{R}_{u,t}^{-1}\boldsymbol{p}_2(\boldsymbol{u}_t)g\left(e_{t|t-1}, \tau\right) \tag{8}$$

where

$$e_{t|t-1} = \pi_t^{(S)} - \boldsymbol{p}_2^T(\boldsymbol{u}_t)\widehat{\boldsymbol{\phi}}_{u,t-1} \tag{9}$$

and

$$\boldsymbol{R}_{u,t} = \lambda \boldsymbol{R}_{u,t-1} + w_u(\boldsymbol{u}_t)\frac{\partial g(e_t,\tau)}{\partial e_t}\boldsymbol{p}_2(\boldsymbol{u}_t)\boldsymbol{p}_2^T(\boldsymbol{u}_t). \tag{10}$$

Abruptly changing parameter estimates are avoided by following Nielsen et al. (2000) and defining the effective forgetting factor, λ_t^* as

$$\lambda_t^* = 1 - (1-\lambda)w_u(\boldsymbol{u}_t)\frac{\partial g(e_t,\tau)}{\partial e_t} \tag{11}$$

and subsequently update (10) so it becomes

$$\boldsymbol{R}_{u,t} = \lambda_t^* \boldsymbol{R}_{u,t-1} + w_u(\boldsymbol{u}_t)\frac{\partial g(e_t,\tau)}{\partial e_t}\boldsymbol{p}_2(\boldsymbol{u}_t)\boldsymbol{p}_2^T(\boldsymbol{u}_t). \tag{12}$$

Finally, $\boldsymbol{\theta}_t(\boldsymbol{u})$ is estimated by

$$\widehat{\boldsymbol{\theta}}_t(\boldsymbol{u}) = \boldsymbol{p}_2^T(\boldsymbol{u})\widehat{\boldsymbol{\phi}}_{u,t} \tag{13}$$

and estimates for other values of $\boldsymbol{u}_t$ than the fitting points are found by linear interpolation.

In contrast to fitting 24 hour-specific models, a single conditional parametric model is estimated for all hours of the day simultaneously. The rationale behind this choice is twofold. First the apparent diurnal seasonality in the prices is mainly caused by that of the demand. Thus the seasonality is implicitly accounted for by the inclusion of the load forecast as an explanatory variable. Secondly, the consumption pattern is in most cases quite similar among consecutive hours. Thus, fitting hour-specific model in many cases leads to the exclusion of observations of similar circumstances from neighboring hours. The absence of obvious regime shifts in the consumption pattern makes alternative segmentation also problematic. Besides, all data split results in longer time passing between observations prompting a lower forgetting factor and thereby less stable parameters over time. So the dynamics of the spot price most local in time along with seasonalities not owed to the demand and wind are left to be accommodated in the second model step. A consequence of adopting this fitting procedure is that the results from the former step are only to be viewed for model building purposes and not evaluated on their own. This is because the missing diurnal variation in the function will inflate the performance measures.

For estimation, the independent variables, i.e. forecast wind power and load, are scaled such that $u_i \in [-1,1]\ \forall i$ using the range of each variable in the training set to perform the scaling. Fitting points are then chosen as 24 equidistant ones in each dimension. It was decided not to optimize neither the position of the fitting points nor their number since results from a few different sets of fitting points indicated that little would be gained from their inclusion in the optimization. Such optimization is however possible, e.g. by methods presented in Wahba (1990) and Hastie et al. (2001).

The model parameters are estimated using a nearest neighbor bandwidth which implies that the actual bandwidth varies with the local density of the data. That is, the bandwidth for each fitting point is chosen such that a certain fraction γ of the observations fulfill $||\boldsymbol{u}_s - \boldsymbol{u}|| \leq h(\boldsymbol{u})$. The actual bandwidth for each fitting point is found empirically from the training set. Put differently, the bandwidth for each particular fitting point is set as the γ-quantile of the Euclidean distances between that fitting point and the observations in the training set.

The actual values of γ, λ and τ are selected by a least squares optimization of the forecasts issued at noon the day before delivery. More precisely let $\widehat{\pi}^{(S)}_{t+k|t}$ denote the forecast spot price for time $t+k$ issued at time t. Every day at noon, forecasts are issued for the period from midnight to midnight the following day and then no forecasts are made until noon the next day, when forecasts for the same lead times are generated. This implies that forecasts for individual hours of the day always have the same lead time. This scenario resembles the practical one and these forecasts are termed *day-ahead forecasts* in the following and noted as $\widehat{\pi}^{(S)}_{DA(t)}$. This notation implies that for an observation $\pi^{(S)}_t$ the corresponding day-ahead forecast is $\widehat{\pi}^{(S)}_{DA(t)} = \widehat{\pi}^{(S)}_{t|t-13}$ if t corresponds to the first hour of the day. If the observation is from the second hour of the day, $\widehat{\pi}^{(S)}_{DA(t)} = \widehat{\pi}^{(S)}_{t|t-14}$,

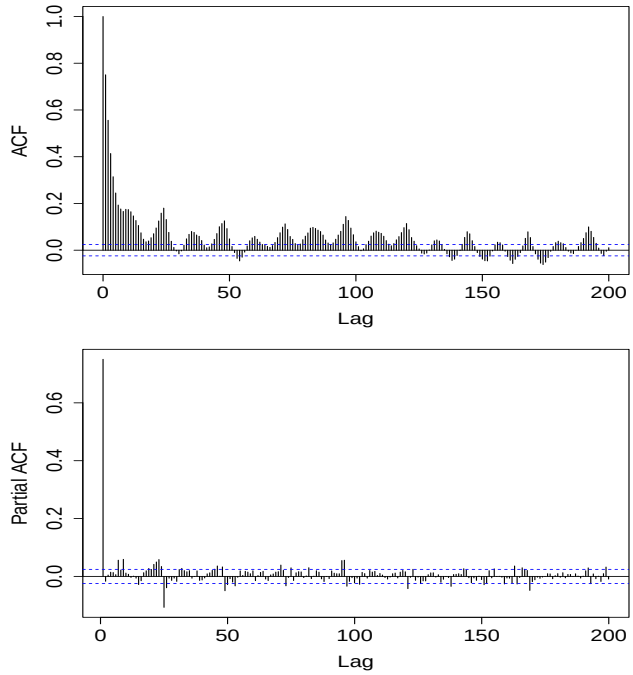

Figure 2: ACF (left) and PACF (right) for the residuals arising from the first model step.

and so forth. The optimal values of the tuning parameters are then found as

$$\begin{bmatrix} \gamma^* \\ \lambda^* \\ \tau^* \end{bmatrix} = \underset{\gamma,\lambda,\tau}{\arg\min}\, \mathrm{RMSE}_{DA}(\gamma,\lambda,\tau). \tag{14}$$

where

$$\mathrm{RMSE}_{DA}(\gamma,\lambda,\tau) = \sqrt{\frac{1}{N}\sum_{t=1}^{N}\left(\pi_t^{(S)} - \widehat{\pi}_{DA(t)}^{(S)}\right)^2}. \tag{15}$$

3.3 Residual models

The purpose of the model's second step is to account for autocorrelation and seasonal patterns that are not explained by the load and the wind power. Out of the models tried for the second step of the model, two models turned out to be superior to the others and yet quite compatible. These models are seasonal AR model with robust and adaptively

estimated parameters, and a seasonal additive Holt-Winter model, also estimated under a robust criteria.

The autocorrelation function (ACF) and the partial autocorrelation function (PACF) for the residuals from the first model step are shown in Figure 2. Despite that the residual series is not completely stationary, its ACF and PACF are used to identify potentially appropriate orders of AR and MA terms to include in second step model. Afterwards a survey of different model orders is conducted in order to determine the most appropriate structure. From this survey, a model on the form

$$\varepsilon_{t+k} = \boldsymbol{z}_t^T(k)\boldsymbol{\beta}_t(k) + \nu_{t+k} \tag{16}$$

is found to be appropriate for $k \leq 24$. The vectors $\boldsymbol{z}_t(k)$ and $\boldsymbol{\beta}_t(k)$ are defined as

$$\boldsymbol{z}_t(k) = \begin{bmatrix} 1 & \varepsilon_{t-1} & \varepsilon_{t-2} & \cdots \\ \varepsilon_{t+k-24} & \varepsilon_{t+k-48} & \varepsilon_{t+k-168} \end{bmatrix}^T \tag{17}$$

$$\boldsymbol{\beta}_t(k) = \begin{bmatrix} \beta_{0,t,k} & \beta_{1,t,k} & \cdots & \beta_{6,t,k} \end{bmatrix}^T, \tag{18}$$

where in turn $\beta_{j,t,k}$ are parameters to be estimated recursively. Moreover, ε_t is defined by Eq. (1) and ν_t is a new noise term also centered and with finite variance. Put differently, separate model parameters are estimated for each lead time, relevant for a day-ahead forecast, that correspond to the lagged values of the forecast error from the first model step (ε). Obviously for $k = 23$, $\varepsilon_{t-1} = \varepsilon_{t+k-24}$ and correspondingly for $k = 24$, $\varepsilon_t = \varepsilon_{t+k-24}$. In these special cases, the dimension of the design matrix is reduced so that each observation is only represented once. Other model structures, such as including a moving average term were considered but the one here describes was found to be the most appropriate one.

The parameter estimates are obtained similarly to what already has been described for the first step of the model or as

$$\widehat{\boldsymbol{\beta}}_t = \arg\min_{\boldsymbol{\beta}_t} \sum_{s=1}^{t} \lambda^{t-s} \left(g(\nu_t, \tau)\right)^2. \tag{19}$$

where $\nu_t = \varepsilon_t - \boldsymbol{z}_t^T\boldsymbol{\beta}_{t-1}$, $g(\cdot,\cdot)$ is defined by Eq. (5) and $0 < \lambda < 1$ is a forgetting factor as before. Hereafter, the AR model with these parameter estimates will be referred to as RLS-AR. The difference between the two procedures is merely that the kernel weights, $w_u(\cdot)$, are omitted from all the equations so that Eq. (8) and (12) become

$$\widehat{\boldsymbol{\beta}}_t = \widehat{\boldsymbol{\beta}}_{t-1} + \boldsymbol{R}_t^{-1}\boldsymbol{z}_t g(\nu_t, \tau) \tag{20}$$

$$\boldsymbol{R}_t = \lambda_t^* \boldsymbol{R}_{t-1} + \frac{\partial g(\nu_t, \tau)}{\partial \nu_t}\boldsymbol{z}_t\boldsymbol{z}_t^T. \tag{21}$$

respectively, where

$$\lambda_t^* = 1 - (1-\lambda)\frac{\partial g(\nu_t, \tau)}{\partial \nu_t}. \tag{22}$$

The Holt-Winters model was initially introduced in Winters (1960) for one seasonal cycle while extension to multiple cycles is described in Taylor (2003). The model that

eventually yielded the best prediction skill for ε_t only has a single daily seasonal cycle. However since the benchmark model for $\pi_t^{(S)}$ was found to benefit substantially from including a weekly seasonality as well, a formulation for a double seasonal model is given here. The transition from a double seasonal model to a single seasonal one merely involves omitting the second seasonality from all equations.

The purely additive form of the Holt-Winters model is used (see e.g. Hyndman et al. (2002) for a comparison between additive and multiplicative Holt-Winters models). The model contains a mean term, μ_t, and two separate seasonal indices, D_t and W_t. The period of D_t is 24 while that of W_t is 168, corresponding the within-day and within-week seasonalities respectively. A standard non-robust Holt-Winters model can be denoted as

$$\mu_t = \alpha_\mu \left(\varepsilon_t - (D_{t-24} + W_{t-168})\right) + \left(1 - \alpha_\mu\right) \mu_{t-1} \tag{23}$$

$$D_t = \alpha_D \left(\varepsilon_t - (\mu_t + W_{t-168})\right) + (1 - \alpha_D) D_{t-24} \tag{24}$$

$$W_t = \alpha_W \left(\varepsilon_t - (\mu_t + D_{t-24})\right) + (1 - \alpha_W) W_{t-168} \tag{25}$$

where the α's are smoothing parameters to be estimated. Once the different terms of the model are updated, the k-step ahead forecast is found as

$$\widehat{\varepsilon}_{t+k|t} = \mu_t + D_{t+k-24} + W_{t+k-168}. \tag{26}$$

The inclusion of a trend term in the model was considered but the resulting improvement in forecasting skill was found to be insignificant.

Writing Eq. (23) - (25) on their error correction form and adopting the formulae for robustness from Gelper et al. (2010) yields

$$\mu_t = \mu_{t-1} + \alpha_\mu g(v_t, \tau) \tag{27}$$

$$D_t = D_{t-24} + \alpha_D g(v_t, \tau) \tag{28}$$

$$W_t = W_{t-168} + \alpha_W g(v_t, \tau) \tag{29}$$

where, as before, $v_t = \varepsilon_t - \widehat{\varepsilon}_{t|t-1}$ and $g(\cdot,\cdot)$ is the Huber influence function given by Eq. (5).

For both models, a single set of tuning parameters was estimated for all lead times. As for the first step, the parameters are optimized with respect to the day-ahead RMSE as formulated in Eq. (14) and (15). Certainly these parameters could be optimized for each hour of the day. A search for initial values indicated however, that improvement in forecasting skill achieved by doing so would only be marginal. This choice does not in any way alter the validity of the model and the results obtained but only indicates that some of the parameters might by slightly sub-optimal.

4 Empirical Results

The parameters in the two model steps are estimated sequentially based on the first 14 months of the data set or from November 2008 and through December 2009. The remaining two years of data are then used as an independent test period. For estimation,

Table 1: Estimated parameters and forecasting skill for the first model step and the reference models

Explanatory Variables(s)	Estimation Setup	γ	λ	τ	In-sample RMS(S)E [DKK]	In-sample RMS(S)E [−]	In-sample MA(S)E [DKK]	In-sample MA(S)E [−]	Out-of-sample RMS(S)E [DKK]	Out-of-sample RMS(S)E [−]	Out-of-sample MA(S)E [DKK]	Out-of-sample MA(S)E [−]
Wind Power & Load Forecasts	Recursive & Robust	0.8529	0.9877	55.67	51.10	0.663	28.33	0.705	50.89	0.676	35.05	0.732
	Recursive only	0.9018	0.9901	—	52.33	0.679	29.84	0.742	51.85	0.686	35.52	0.742
	Time-invariant	0.0821	—	—	52.05	0.676	32.07	0.798	101.54	1.349	86.17	1.799
Load Forecasts	Recursive & Robust	0.7887	0.9831	53.38	56.24	0.730	30.66	0.763	58.79	0.781	39.09	0.816

prices above 800 DKK / MWh and below 0 DKK / MWh are excluded to avoid unstable parameters. Performance estimates presented in the following are based on all observations though.

In order to illustrate the contribution from different features of the model, different reference models are estimated and their RMSE and Mean Absolute Error (MAE) compared to that of the proposed model. The RMSE and the MAE are both presented in two versions:

1. On the price's real scale (in DKK), and
2. as a skill relative to the daily persistence (RMSSE and MASE).

That is, the measures are scaled by the corresponding measures for a daily persistence forecast as suggested by Hyndman and Koehler (2006). More formally, the RMSE is scaled by

$$\sqrt{\frac{1}{N_{per}-24}\sum_{t=25}^{N_{per}}\left(\pi_t^{(S)}-\pi_{t-24}^{(S)}\right)^2} \tag{30}$$

and the MAE is scaled by

$$\frac{1}{N_{per}-24}\sum_{t=25}^{N_{per}}\left|\pi_t^{(S)}-\pi_{t-24}^{(S)}\right| \tag{31}$$

where N_{per} is the number of observations in the sample for which the measure is calculated. This scaling yields a relative error measure that is unbiased towards forecasting ability of high and low prices and does not call for any data trimming due to the prices being zero or close to that. A more detailed discussion on the RMSSE, MASE and forecast accuracy measures in general can be found in Hyndman and Koehler (2006).

For the first model step the in-sample and out-of-sample performance is compared to that of:

1. its time-invariant and non-robust counterpart,
2. its non-robust counterpart,
3. a model estimated in the same manner but only taking load as an explanatory variable.

Finally, the forecasting skill of the combined models is compared to the that of

1. two seasonal persistence models, one with a daily period, and another with a weekly period,
2. the previously described Holt-Winters and RLS-AR models applied directly to the spot price series.
3. a series of 24 ARIMAX models, one for each hour of the day with the forecast wind and load as external regressors.

In line with such type of models in the existing literature (e.g. Conejo et al. (2005), Nogales et al. (2002)) the ARIMA models are fit in terms of $log(\pi_t^{(S)} + 1000)$. The model order for each hour is decided on by minimizing the Bayesian Information Criteria (BIC)Hastie et al. (2001) for the training period. The external variables are considered both on their original scale and log-transformed as suggested by Nogales et al. (2002). After calculating the predictions, they are transformed to the original scale by the exponential of the prediction plus half the estimated variance. The set of external variables that yielded the best forecasting skill was the one with the log-transformed wind power and load forecasts for which results are reported in the following.

The fitting points for the former model step are chosen as 24 equidistant ones in each dimensions thus yielding a grid of 24^2 equidistant fitting points in total. For each point, the coefficient vector, $\boldsymbol{\phi}$, is initialized by setting all its elements to 0.1. The corresponding matrix inverse variance-covariance matrix, $\boldsymbol{R}_0$, is chosen as a diagonal one with non-zero elements as 10^{-6}. Thereafter the first 1008 observations are taken for initialization and are excluded from the performance measure. Hence the tuning parameters are optimized in context of the previously mentioned training period apart from its first 42 days. During the initialization period, the robust criteria is relaxed in order to obtain frequent updates of $\boldsymbol{R}_t$. This is necessary because of the poor initial guesses for the coefficients.

The parameters are optimized as described in the previous section, using the quasi-Newton Broyden-Fletcher-Goldfarb-Shanno (BFGS) method. The estimated parameters are shown in Table 1 along with the corresponding in- and out-of-sample RMSE.

The results indicate that the inclusion of wind power forecasts and the recursive parameter estimation are worth the effort since the top two models significantly outperform the bottom two. Especially the recursive parameter estimation seems to paramount since the performance of the time invariant model degrades excessively during the test period. In terms of performance, the benefits of the robust estimation are less obvious. However, given the spiky behavior of the spot prices, it is generally sound to robustify the estimation process in order to protect the model from abrupt changes caused by a single spike. In light of the varying volatility of the prices, making τ recursive, as described in Pinson et al. (2007) and Sejling et al. (1994), could be more appropriate. No such efforts were made for this paper though.

A forgetting factor of $\lambda = 0.9877$ translates to that $1/(1-0.9877) = 81.3$ latest observations are effective in the parameter estimation which corresponds to around 3.5 days. Owed to the locally weighted and robust estimation however, the effective forgetting factor, $\lambda^{(*)}$ is somewhat higher and varies between fitting points. In Nielsen et al. (2000) a procedure to estimate the actual memory of the model is proposed. Following this procedure and averaging over time as well as the 576 fitting points yields a mean number of effective observations, $\overline{\eta} = 281.8$ hours and a corresponding average effective forgetting factor of $\overline{\lambda}^{(*)} = 0.9965$.

The function which the model approximates is shown for one instance in Figure 3. This function is then updated each day at noon by adjusting the model's coefficients to observations from the current day. Subsequently, forecasts are calculated from next day's

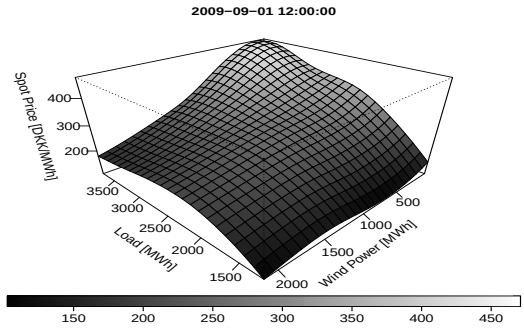

Figure 3: Surface plot of the spot prices as a function of the forecast wind power production and load at noon on September 1st 2009

input forecasts, i.e. the wind power and the load forecast. This is done by bilinear interpolation between the four fitting points surrounding the input forecasts. In other words, the price forecast for a set of input forecasts for a given hour, $\boldsymbol{u}_{t+k}$, is found as the corresponding point on the linear plane joining the four nearest fitting points. Alternatively generalization to values other than fitting points could be done non-linearly, e.g. by one of the multidimensional spline techniques presented in Hastie et al. (2001). In light of the high number of fitting points used here, linear interpolation was however deemed adequate.

The initial values for the coefficients, $\boldsymbol{\beta}_0$, in the second step AR model are found from a standard AR model, i.e. not recursively estimated, using observations for the first 42 days of the data set. The inverse of the corresponding variance-covariance matrix is taken as $\boldsymbol{R}_0$. For the Holt-Winters model, an initial value for the μ-term (μ_0) is found as the mean price during the first 42 days of the training period. The seasonal terms are initialized as the difference between μ_0 and the average price for the individual hours during the same 42 days. In the same way as for the first step, the first 42 days of observations are disregarded in the optimization of the tuning parameters. The benchmark models are initialized in the same manner, only using the spot price series instead of the residuals from the former step.

Again, least squares estimates of the parameters are sought yielding the ones summarized in the second column of Table 2. The corresponding in- and out of-sample residual RMSEs and MAEs (in DKK and scaled) are given in the remaining columns along with that of the benchmark models.

Apart from the obvious fact that the proposed models drastically outperform the more naive benchmarks, the table reveals that the decaying unscaled performance between the training- and test periods may, to a certain degree, be explained by the somewhat greater volatility of the prices during the test period. This applies to both the full model and the intermediate step and further supports what already has been said about recursive robustification.

Table 2: RMSE for the day-ahead forecasts

Model		Parameters	In-sample				Out-of-sample			
			$RMS(S)E$		$MA(S)E$		$RMS(S)E$		$MA(S)E$	
			[DKK]	[−]	[DKK]	[−]	[DKK]	[−]	[DKK]	[−]
Bench-marks	Period Mean	—	75.61	0.981	45.50	1.132	95.45	1.268	69.75	1.456
	Daily persistence	—	77.02	1.000	40.22	1.000	75.30	1.000	47.90	1.000
	Weekly persistence	—	74.37	0.965	41.69	1.037	79.83	1.060	52.42	1.094
	ARIMAX	—	69.20	0.898	35.93	0.894	64.21	0.853	43.26	0.903
	RLS-AR	$[\lambda, \tau] = [0.9889, 92.78]$	50.03	0.725	31.27	0.808	55.87	0.742	37.73	0.788
	Holt-Winters	$[\alpha_\mu, \alpha_D, \alpha_W, \tau] = [0.0116, 0.0903, 0.1009, 112.39]$	52.88	0.756	31.73	0.820	57.81	0.768	40.34	0.842
Two step	RLS-AR	$[\lambda, \tau] = [0.9915, 240.63]$	47.55	0.680	27.95	0.722	48.15	0.640	32.77	0.684
	Holt-Winters	$[\alpha_\mu, \alpha_D, \tau] = [0.0042, 0.1245, 32.98]$	46.81	0.669	27.23	0.704	49.07	0.652	33.66	0.703

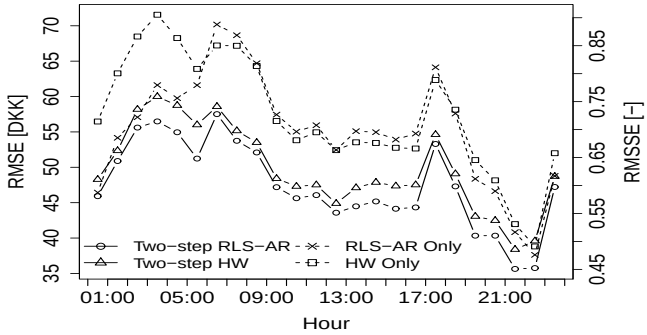

Figure 4: RMSE for individual lead times during the test period in DKK (left axis) and as percentages of the average price for the period (right axis).

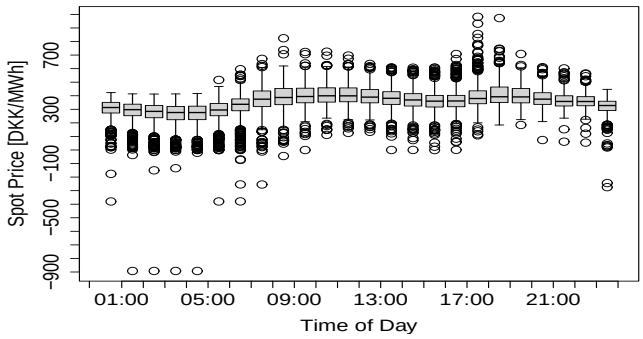

Figure 5: An hour-by-hour box plot of the spot prices during the test period. Whiskers are placed at 1.5 times the interquartile range.

The forecasting skill of the Holt-Winters and the RLS-AR models applied to the residuals of the non-parametric model is also clearly superior to that of the models applied to the spot prices directly. As shown in Figure 4, which plots the hourly residual RMSE for the bottom four models in Table 2, the superiority is a result of the two step models consistently outperforming the other models almost throughout the entire day. It is only in the first hour of the day that the benchmark RLS-AR model performs similarly to the two-step ones. This is because the forecasts for these hours are the ones with the shortest lead times and thus based on very recent observations.

The performance varies somewhat between hours but seems to coincide with the severity of the price spikes that occurred during the test period. This can be seen on the box plot in Figure 5 where the spot price distribution within each hour of the day is illustrated. The hours with the highest RMSE are among the ones when the most extreme prices occur.

Table 3: Out-of-sample performance of the proposed model during weekdays, weekends and holidays separately

Model	Day Type	RMS(S)E		MA(S)E	
		[DKK]	[-]	[DKK]	[-]
RLS-AR	Weekdays	44.94	0.637	31.03	0.696
	Weekends	51.74	0.635	34.90	0.654
	Holidays	73.79	0.683	50.52	0.715
Holt-Winters	Weekdays	44.39	0.6287	30.67	0.6874
	Weekends	52.95	0.650	35.86	0.672
	Holidays	74.54	0.690	52.05	0.737

The model's forecasting skill during normal weekdays, weekends and public holidays is listed in Table 3. In terms of the unscaled measures, the performance seems to vary quite substantially between different types of days. However, the performance measures relative to that of the persistence forecast reveal that much of this variation is due to the alternating price volatility during the different day types. One has to bear in mind though that the unbalanced sample sizes between the different categories make this kind of comparison unreliable. That is, the small number of holidays makes performance assessment during these days vulnerable for any extraordinary circumstances.

As previously mentioned, the explanatory power of the input forecasts used in the model's first step is owed to their reflection of the volumes bid to the market. The forecasting skill of the model can therefore be expected to be affected by how closely the input forecasts are related to the volume cleared on the market. Increased quality of the input forecast will therefore not necessarily improve the price forecasts unless resemblance with the bidding behavior is increased as well.

Overall, there seems to be little skill difference between the residual Holt-Winters and the residual RLS-AR models. In light of the fact that both mainly rely on the same information from the past this is understandable. Since both models are relatively easy to implement, choosing one out of the two thus comes down to personal preferences of the one implementing the model. The Holt-Winters model has the advantage though that price spikes are less likely to be reflected in forecasts for the following days since it does not explicitly use previous values for prediction. For the same reason, the Holt-Winters model is more robust operationally since missing observations will only affect the model update but will not prevent predictions from being issued.

5 Conclusions and Future Work

A two step methodology for day-ahead forecasting of electricity spot prices has been presented. Whereas the first step accounts for the prices' dependence on forecast load

and wind power production, the second step accommodates autocorrelation and seasonalities. The time-adaptive version of the model was shown to comfortably outperform its time-invariant counterpart. Hence, adaptive parameter estimation must be concluded to be relevant for the modeling of this phenomena. In terms of forecasting skill the interest of employing the robust approach is less obvious. However, the robust estimation protects the model's parameters from abrupt changes, caused by few excessive spikes. Thereby the model is enabled to follow the progress of the average prices more closely without manual inference. The time-varying price volatility suggest though that robustification should be made recursive.

Out-of-sample empirical results, obtained by mimicking practical circumstances, indicate that the model is well suited for practical use - both in terms of methodology and forecasting skill. In order to obtain complete forecasts of the electricity spot prices, the model here presented should be accompanied by a model for prediction intervals. Given the results of Jónsson et al. (2010), such intervals would most likely be conditional upon fundamental factors, e.g. forecast wind power production and load. Whether modeling of higher order moments also requires time-adaptivity will be an interesting question to answer. Given the characteristics of the prices however, time-adaptivity is likely to be as essential in such models as it is here.

Even though the share of wind power in the generation portfolio is relatively large in DK-1, accounting for predicted wind power production is likely to be beneficial in other markets as well. For instance the findings of Morales et al. (2011) hint that the methodology presented here could be successfully applied to the Spanish case. Here the fundamental difference between wind power and conventional power plants plays an essential role. In addition, the EU's target of having 20% of its energy consumption produced by renewable sources by 2020 and similar initiatives in the USA imply that price forecasting methods accounting for wind power production and renewable energy sources in general may have a more widespread applicability in the near future. In this context the inclusion of e.g. solar and wave power in the model parallel to their emergence would be interesting. Although both theoretically possible and not hard to implement, the inclusion of 1 or 2 more variables in the model calls for a more cautiously chosen variables or merger of them in order to ensure frequent enough updates of the parameters in all fitting points.

Acknowledgment

The authors would like to express their gratitude to the editors and the anonymous reviewers for providing useful comments that improved the paper substantially. Tryggvi Jónsson is partially sponsored by the Danish Agency for Science, Technology and Innovation which is hereby acknowledged. Pierre Pinson was partly supported by the European Commission through the EU FP6 project Anemos.plus (contract No 038692) and by the Danish Council for Strategic Research, Technology and Production through the Ensymora project (10-093904 / DSF).

References

Nima Amjady and Farshid Keynia. Electricity market price spike analysis by a hybrid data model and feature selection technique. *Electric Power Systems Research*, 80(3): 318–327, 2010.

Alexander Boogert and Dominique Dupont. On the effectiveness of the anti-gaming policy between the day-ahead and real-time electricity markets in the Netherlands. *Energy Economics*, 27(5):752–770, 2005.

William S. Cleveland and Susan J. Devlin. Locally weighted regression: An approach to regression analysis by local fitting. *Journal of the American Statistical Association*, 83 (403):596–610, 1988.

Antonio J. Conejo, Javier Contreras, Rosa Espínola, and Miguel A. Plazas. Forecasting electricity prices for a day-ahead pool-based electric energy market. *International Journal of Forecasting*, 21(3):435–462, 2005.

Energinet.dk. Website, January 2012. URL http://www.energinet.dk.

Stein-Erik Fleten and Stein W. Wallace. Power scheduling with forward contracts. In *Proceedings of the Nordic MPS*, Molde, Norway, 1998.

Sarah Gelper, Roland Fried, and Cristophe Croux. Robust forecasting with exponential and Holt-Winters smoothing. *Journal of Forecasting*, 29(3):285–300, 2010.

Paolo Giabardo, Marco Zugno, Pierre Pinson, and Henrik Madsen. Feedback, competition and stochasticity in a day ahead electricity market. *Energy Economics*, 32(2): 292–301, 2010.

Trevor Hastie, Robert Tibshirani, and Jerome Friedman. *The Elements of Statistical Learning - Data Mining, Inference and Prediction*. Springer, New York, USA, 2001.

Helen Higgs. Modelling price and volatility inter-relationships in the Australian wholesale spot electricity markets. *Energy Economics*, 31(5):748–756, 2009.

Peter J. Huber. *Robust Statistics*. John Wiley & Sons, Inc., Hoboken, NJ, USA, 1981.

Rob J. Hyndman and Anne B. Koehler. Another look at measures of forecast accuracy. *International Journal of Forecasting*, 22(4):679–688, 2006.

Rob J. Hyndman, Anne B. Koehler, Ralph D. Snyder, and Simone Grose. A state space framework for automatic forecasting using exponential smoothing methods. *International Journal of Forecasting*, 18(3):439–454, 2002.

Bo Jonsson. Prediction with a linear regression model and errors in a regressor. *International Journal of Forecasting*, 10(4):549–555, 1994.

Tryggvi Jónsson, Pierre Pinson, and Henrik Madsen. On the market impact of wind energy forecasts. *Energy Economics*, 32(2):313–320, 2010.

Nektaria V. Karakatsani and Derek W. Bunn. Forecasting electricity prices: The impact of fundamentals and time-varying coefficients. *International Journal of Forecasting*, 24 (4):764–785, 2008.

Peter Kosater and Karl Mosler. Can Markov regime-switching models improve power-price forecasts? Evidence from German daily power prices. *Applied Energy*, 83(9): 943–958, 2006.

Xin Lu, Zhao Yang Dong, and Xue Li. Electricity market price spike forecast with data mining techniques. *Electric Power Systems Research*, 73(1):19–29, 2005.

Henrik Madsen. *Time Series Analysis*. Chapman & Hall / CRC, London, UK, 2008.

Juan M. Morales, Antonio J. Conejo, and Juan Pérez-Ruiz. Simulating the impact of wind production on locational marginal prices. *IEEE Transactions on Power Systems*, 26(2):820–828, 2011.

Poul Erik Morthorst. Wind power and the conditions at a liberalized power market. *Wind Energy*, 6(3):297–308, 2003.

Henrik Aa. Nielsen, Torben S. Nielsen, Alfred K. Joensen, Henrik Madsen, and Jan Holst. Tracking time-varying coefficient functions. *International Journal of Adaptive Control and Signal Processing*, 14(8):813–828, 2000.

Torben Skov Nielsen, Henrik Aalborg Nielsen, and Henrik Madsen. Prediction of wind power using time-varying coefficient functions. In *15th IFAC World Congress*, Barcelona, Spain, 2002.

Francisco J. Nogales, Javier Contreras, Antonio J. Conejo, and Rosario Espínola. Forecasting next-day electricity prices by time series models. *IEEE Transactions on Power Systems*, 17(2):342–348, 2002.

Nord Pool Spot AS. Production split, November 2010. URL http://www.nordpoolspot.com/reports/Production_split/.

Nord Pool Spot AS. Website, January 2012. URL http://www.nordpoolspot.com.

Anastasios Panagiotelis and Michael Smith. Bayesian density forecasting of intraday electricity prices using multivariate skew-t distributions. *International Journal of Forecasting*, 24(4):710–727, 2008.

Pierre Pinson, Henrik Aalborg Nielsen, and Henrik Madsen. Robust estimation of time-varying coefficient functions - application to the modeling of wind power production. Technical report, Department of Informatics and Mathematical Modelling, Technical University of Denmark, 2007.

Ken Sejling, Henrik Madsen, Jan Holst, Ulla Holst, and Jan-Eric Englund. Methods for recursive robust estimation of ar parameters. *Computational Statistics & Data Analysis*, 17(5):509–536, 1994.

Michael Sewalt and Cyriel de Jong. Negative prices in electricity markets. *Commodities Now. Available at http://www.erasmusenergy.com/articles/91/1/Negative-prices-in-electricity-markets/Page1.html*, 2003.

Klaus Skytte. The regulating power market on the nordic power exchange nord pool: An econometric analysis. *Energy Economics*, 21(4):295–308, 1999.

James W. Taylor. Short-term electricity demand forecasting using double seasonal exponential smoothing. *Journal of Operational Research Society*, 54(8):799–805, 2003.

James W. Taylor and Patrick E. McSharry. Short-term load forecasting methods: An evaluation based on european data. *IEEE Transactions on Power Systems*, 22(4):2213–2219, 2007.

Iivo Vehviläinen and Tuomas Pyykkönen. Stochastic factor model for electricity spot price - the case of the nordic market. *Energy Economics*, 27(2):351–367, 2005.

Grace Wahba. *Spline Models for Observational Data*. SIAM, Philadelphia, PA, USA, 1990.

Peter R. Winters. Forecasting sales by exponentially weighted moving averages. *Management Science*, 6(3):324–342, 1960.

Lei Wu and Mohammad Shahidehpour. A hybrid model for day-ahead price forecasting. *IEEE Transactions on Power Systems*, 25(3):1519–1530, 2010.

PAPER G

Predictive Densities for Day-Ahead Electricity Prices using Time-Adaptive Quantile Regression

Authors:
T. Jónsson, P. Pinson, H. Aa. Nielsen, H. Madsen

Submitted to:
European Journal of Operational Research (2012)

Predictive Densities for Day-Ahead Electricity Prices Using Time-Adaptive Quantile Regression

Tryggvi Jónsson[1,2] Pierre Pinson[2] Henrik Madsen[2] Henrik Aa. Nielsen[1]

Abstract

Solving many of the problems actors in modern electricity markets are faced on a daily basis requires scenarios of the day-ahead price. These scenarios are generated using predictive densities for the same prices. A semi-parametric methodology for generating such densities is presented, comprising a time-adaptive quantile regression model for the 5-95% quantiles and a description of the distribution tails by exponential distribution. The forecasting skill of the proposed model is compared to that of 4 benchmark approaches and the well known GARCH model during a 3 year period. Whereas the benchmarks are outperformed in terms of general forecasting skill the superiority of the semi-parametric model over the GARCH model lies in the former's ability to generate reliable quantile estimates.

1 Introduction

Probabilistic forecasts of the day-ahead wholesale price in the form of predictive densities are required to solve many of the challenges faced by participants in today's electricity markets. For instance, optimal bidding strategies for wind power producers like the ones described in Morales et al. (2010) and Jónsson et al. (2012) require such forecasts for scenario generation. Similarly, scenarios of the day-ahead prices are used for pricing of hydro power in Fleten and Kristoffersen (2008) and Fleten and Kristoffersen (2007) and for optimal bidding of other types of generation units in Heredia et al. (2010). This aside, foreseeable developments in the electricity sector such as continuing growth of renewable energy technologies and the emergence of flexible demand, are likely to further boost the demand for such forecasts.

The aim of this paper is to present a methodology for density forecasting of day-ahead electricity prices that permits generation of operational scenarios. First and foremost such a model should produce reliable density forecasts of the untransformed prices. For the purpose of scenario generation it is important that the forecasts properly describe the full density of the prices (instead of certain quantiles only as is sometimes the case

[1]ENFOR A/S, Lyngsø Allé 3, DK-2970 Hørsholm, Denmark
[2]DTU Informatics, Technical University of Denmark, Richard Petersens Plads, building 321, DK-2800 Kgs. Lyngby, Denmark

for applications in risk management concerned with a single variable). Once a proper description of the density is obtained, scenarios respecting price's correlation structure are easily obtainable using the scenario generation framework presented in Pinson et al. (2009).

The unique features of electricity as a commodity prompt some distinct characteristics of its price. In order to maintain a stably operating transmission network, supply and demand must be matched constantly and instantaneously. In addition, since electricity can not be stored directly in an efficient manner, production must take place synchronous with consumption. Together this makes arbitrage over time and space close to impossible (Boogert and Dupont, 2005, Sewalt and de Jong, 2003). Electricity consumption however is highly inelastic in the short-term and exhibits multiple strong seasonal patterns (Taylor and McSharry, 2007). The supply function on the other hand is discontinuous, convex and steeply increasing in the high production end (Panagiotelis and Smith, 2008, Karakatsani and Bunn, 2008). All together this results in electricity prices which in most markets exhibit most or all of the following features: strong multiple periodicities, intra-and inter-day correlation, non-stationarity, positive skewness, high kurtosis, mean reverting spikes and general excessive volatility (Jónsson et al., 2010, Conejo et al., 2005, Panagiotelis and Smith, 2008).

Density forecasting of day-ahead electricity prices has received increased attention in the recent years. The most popular approach in the existing literature on the matter is to describe the density by some variant of the Generalised AutoRegressive Conditional Heteroskedasticity model (GARCH), uni- or multivariate (García-Martos et al., 2011, Diongue et al., 2009, Higgs, 2009, and references therein), often with the aid of a jump-diffusion model (Haugom et al., 2011, Chan et al., 2008). Disappointingly though rigorous measures of the forecasting skill of the density model are in most cases not reported. Alternative approaches are quite rare in the literature but exist though. Panagiotelis and Smith (2008) presents a novel approach for Bayesian density forecasting by a vector autoregressive model with skew-t noise and puts forward measures of the overall fit of the forecast density. All inference is however done on a logarithmic transformed data and no scheme for conversion to the original scale is discussed. Such a scheme is nevertheless paramount for a proper conversion of any forecast for a non-linear and non-stationary process like electricity prices. It is therefore hard to pinpoint how their model would perform on the real scale and compared to other types of models. Finally, Deng and Jiang (2004) and Serinaldi (2011) present interesting methods for modelling the first 4 moments of the conditional price densities with alternative probability density functions.

In the broadest sense, there are two different approaches to model density: adopting parametric assumptions and non/semi-parametric modelling. The parametric approaches have the appeal that the full density of the modelled process is characterised by very few parameters. This in turn makes a single model sufficient for obtaining a description of the whole density. This very same feature is however also the main drawback of parametric approaches since it constrains the density shape. The non-or semi-parametric approaches on the other hand do not suffer from this shape inflexibility since assumptions about the distributional shape are either none or conditioned to a certain domain. These approaches however involve either severely increased model

complexity, a handsome growth in the number of models to be estimated or even both.

Using data from the Western Danish price area for Nord Pool's Elspot, models for conditional price densities from both categories will be derived, analysed and compared in the following. As a parametric approach, and as a form of baseline approach, modelling the standard deviation of a Gaussian distribution is attempted through a series of formulations of the well known ARCH / GARCH models (Engle, 1982, Bollerslev, 1986) and similar regression models. Alternatively, a non-parametric Quantile Regression (QR) (Koenker and Basset, 1978, Koenker, 2005, Møller et al., 2008) model is derived for quantiles ranging from 0.05 to 0.95. In order to overcome the shortcomings of QR regarding modelling of distribution tails, that model is coupled with a model for the tails which assumes these to be exponentially distributed. All models have time-varying regression parameters and describe the density of deviations from the expected price, here found by the model described in Jónsson et al. (2012). Generally any well tuned model for the expected prices could be applied though. The expected price also serves as an explanatory variable for the models, either on its own or along with the forecast load.

In addition to comparing the models with each other, their performance is compared to that of four benchmark approaches. These are the i) empirical density of the price, often referred to as climatology forecasts in meteorology, ii) the empirical Gaussian density of the prices, iii) a Gaussian density whose mean and standard deviation are estimated by exponential smoothing and iv) a kernel density estimation model . The continuous ranked probability score ($\overline{CRPS}$) (Matheson and Winkler, 1976, Gneiting and Raftery, 2007) and the related continuous ranked probability skill score ($CRPSS$) are used for comparison of the two model's forecasting skill. In terms of these measures, both models are shown to outperform the benchmarks. It is also demonstrated by reliability diagrams that even though the CRPSS of these two models types is quite compatible, it is only the QR-Exponential model that produces reliable density forecasts.

The remainder of this paper is structured as follows: Section 2 describes the functions of Nord Pool and the data, then developing into an empirical analysis in order to highlight the main data features to be modelled subsequently. The models and related parameter estimation are described in Section 3 while further analysis and genuine comparison of their forecasting skill are the focus of Section 4. Finally, concluding remarks are given in Section 5.

2 The Data

2.1 Nord Pool's Elspot

Nord Pool's Elspot is a day-ahead market for physical delivery of electricity which covers 5 different countries. By default, the day-ahead price should be the same in the entire market region unless prevented by transmission bottlenecks. Gate-closure is every day at noon for exchange during the upcoming day. The prices are set with hourly

resolution as the intersection between the aggregated supply and demand curves. At first, curves for the whole region are constructed and their intersection constitutes the system price - The price at which trades are settled if transmission capacity is sufficient. If however, the resulting production and consumption schedules prompt congestion in the transmission network, two or more area prices are calculated. The area prices are found in the same manner as the system price. The supply and demand curves however only comprise the bids within the area where transmission capacity is sufficient along with full utilisation of congested lines. Further information can be found at Nord Pool Spot AS (2011).

The empirical work of this paper is based data from the Western Danish price area (DK-1). The data covers a period of almost exactly three years of from December 21st 2008 and through December 2011. The data set comprises hourly forecast and observed day-ahead prices for the area, forecast system load and the area's forecast wind power production. The point forecasts for the prices are found by the model described in Jónsson et al. (2012) while the load forecasts were obtained from Nord Pool's website, www.nordpoolspot.com. Finally, the wind power forecasts originate from a statistically based wind power prediction software (see Nielsen et al. (2002)).

2.2 Data Analysis

In order to demonstrate the previously described characteristics of the prices and to establish the necessary properties of a model for their density, a brief empirical data analysis is presented. Let $\pi_t^{(S)}$ denote the day-ahead electricity price for hour t. The top plot in Figure 1 shows a time series plot of $\pi_t^{(S)}$ for the whole data period. From the plot, some of the features mentioned in the previous section are apparent. The prices' mean and volatility varies constantly throughout the series and price spikes are quite frequent. From the bottom two plots in Figure 1, which show time series plots of $\pi_t^{(S)}$ for March 2009 and January 2010, the daily and weekly seasonal cycles of the prices are apparent as well as some of the other features previously mentioned.

Figure 2 shows the residual series

$$\varepsilon_t = \pi_t^{(S)} - \widehat{\pi}_t^{(S)} \tag{1}$$

where $\widehat{\pi}_t^{(S)}$ is the forecast price generated by the model in Jónsson et al. (2012), issued before at 11:00 on the day before delivery. The horizontal lines on plot represent the $\alpha/2$ and the $1-\alpha/2$ empirical quantiles of the residuals.

The variation of the mean and volatility is far less severe for ε_t series than for $\pi_t^{(S)}$. Furthermore, the magnitude of the spikes in the residual series is severely reduced compared to the unfiltered prices. The reduction of these features makes ε_t better suited for parametric modelling than $\pi_t^{(S)}$ and will yield more stable parameters over time for any type of model.

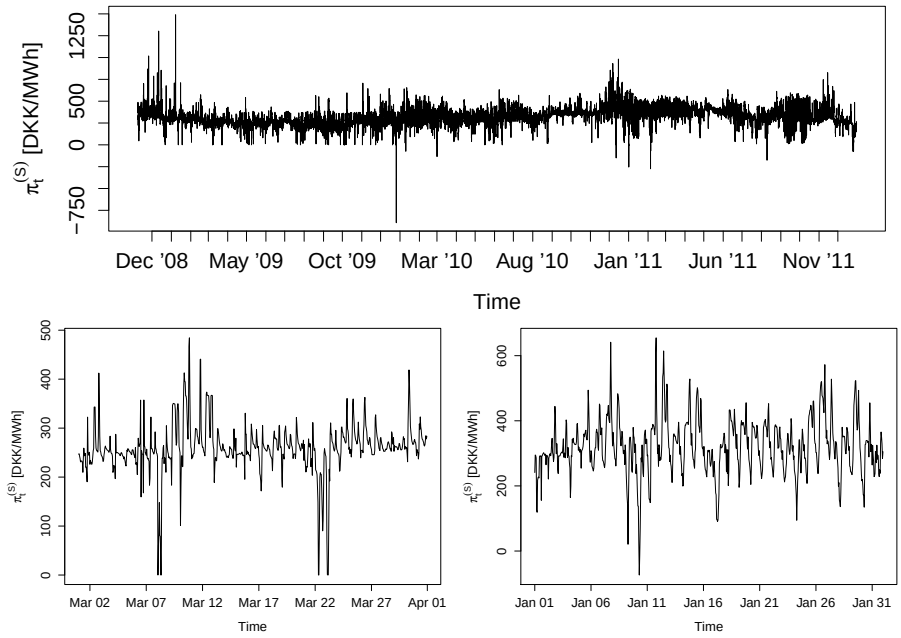

Figure 1: Time series plots of $\pi_t^{(S)}$ for the whole period (top), March 2009 (bottom left) and January 2010 (bottom right)

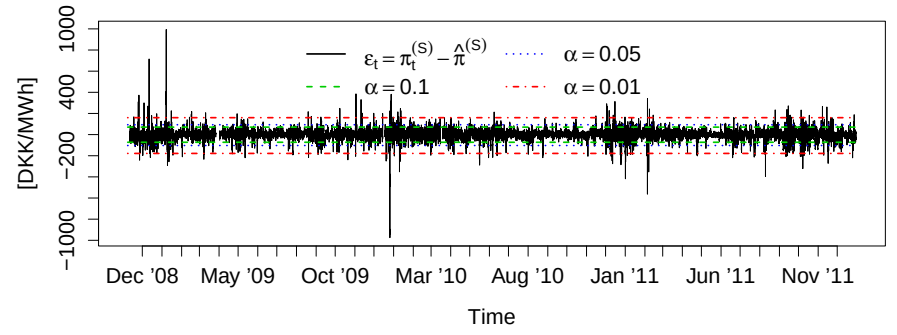

Figure 2: Time series plots of ε_t.

Another appeal of modelling the density of ε_t is that it does not exhibit nearly as much diurnal variation as that of $\pi_t^{(S)}$. Also dependence of the mean on exogenous variables vanishes. This can be seen from the plots in Figures 3 and 4.

Figure 3 shows the mean (μ), standard deviation (σ), skewness(γ) and Pearson's kurtosis (κ) of ε_t and $\pi_t^{(S)}$ conditional to different explanatory variables. Three variables are

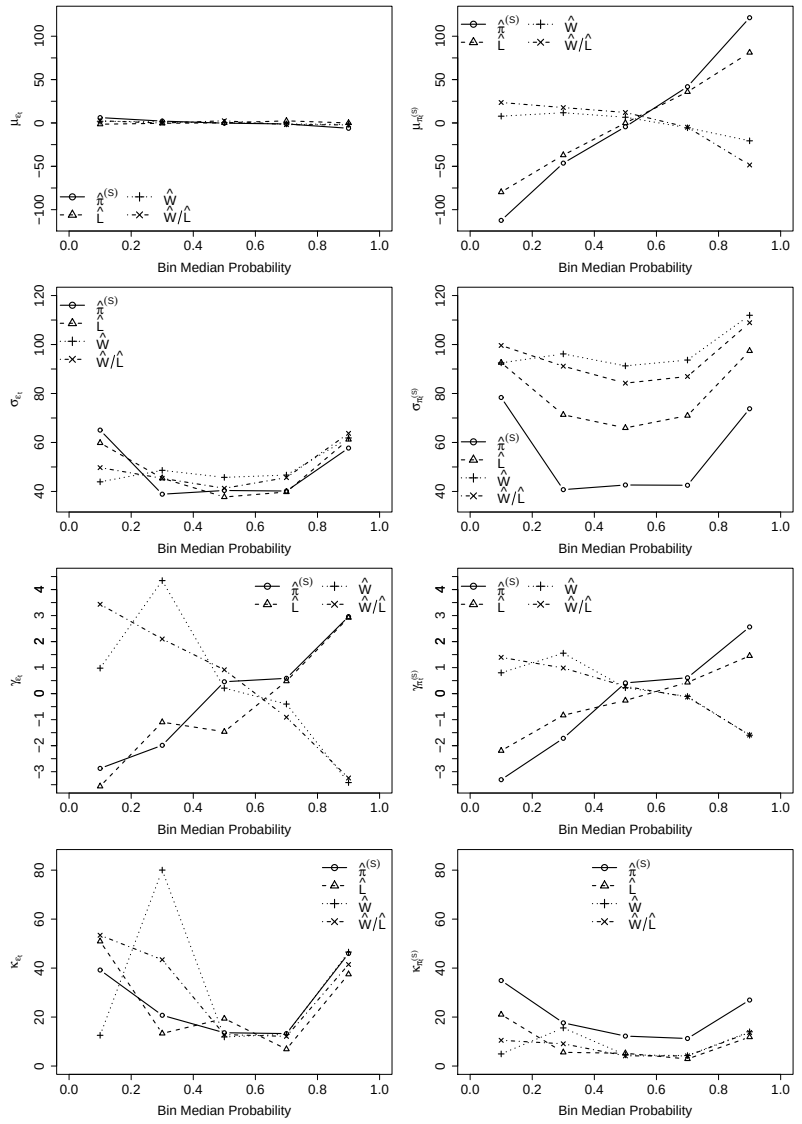

Figure 3: Conditional centred moments of ε_t (left column) and $\pi_t^{(S)}$ (right column).

considered here and a fourth one derived from the others. These are the price forecast $\widehat{\pi}_t^{(S)}$, the forecast system load $\widehat{L}_t$, the forecast wind power production $\widehat{W}_t$ and the forecast wind power penetration $\frac{\widehat{W}_t}{\widehat{L}_t}$. In order to ease the comparison between ε_t and $\pi_t^{(S)}$,

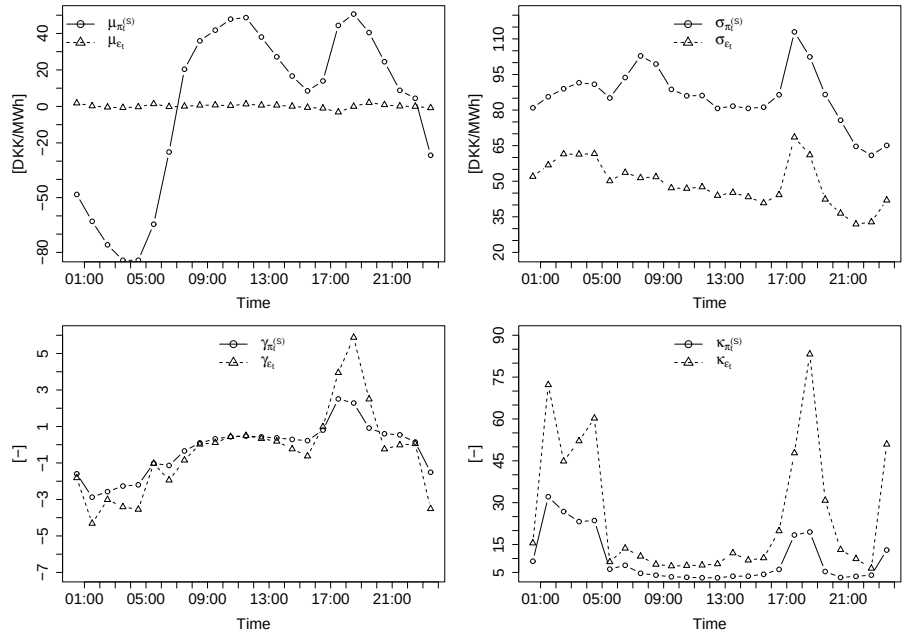

Figure 4: Hourly centred moments of ε_t and $\pi_t^{(S)}$.

the empirical mean of $\pi_t^{(S)}$ has been subtracted from the corresponding conditional means.

The plots in Figure 3 reveal that the impact of the explanatory variables on the mean becomes neglectable for ε_t while it is quite strong for $\pi_t^{(S)}$. Apart from the lower standard deviation and somewhat elevated kurtosis, the relationship patterns between seem to be consistent between ε_t and $\pi_t^{(S)}$ for the higher order moments. An explanation for the higher kurtosis of ε_t is to be found in the most excessive price spikes which, due to the lowered σ, raise κ. The strongest relation seems to be with the expected price and since the other variables have already been taken into account in the derivation of $\widehat{\pi}_t^{(S)}$, it seems reasonable to start out with a density model depending on the expected price and subsequently add the other variables and examine whether predictive skill is improved or not. In addition to the analysis based on moments only presented here, the dependencies were also verified visually for full densities supporting the aforementioned conclusions. Calibration assessment presented later on will permit to verify the suitability of distribution assumptions.

Figure 4 shows hourly values of the μ, σ, γ and κ for the two series. Comparison of the two lines in each plot reveals that by subtracting $\widehat{\pi}_t^{(S)}$, much of the diurnal variation in the density is mitigated and what daily seasonality remains coincides well with the relationship between $\widehat{\pi}_t^{(S)}$ and the density of ε_t. Hence a model relying on $\widehat{\pi}_t^{(S)}$ to ex-

plain the density of $\pi_t^{(S)}$ through ε_t will not require an explicit daily seasonality term as a model directly modelling the density of $\pi_t^{(S)}$ would.

3 Models for Density Forecasts

3.1 Benchmarks

Four relatively simple benchmark models are constructed, which the more elaborate models will be measured against. These models are:

I The empirical unconditional quantiles of the prices.

II A time-invariant Gaussian density, i.e. a density defined by the empirical unconditional standard deviation of the prices.

III A simple exponential smoothing of the standard deviation.

IV A kernel density model estimated using, all past data, the last week worth of data, the last 500 and the last 1000 observations available.

For model I, the predictions are obviously constant. The sample quantile $Q_{\pi^{(S)}}(\tau)$ with nominal proportion τ is found as

$$Q_{\pi^{(S)}}(\tau) = \inf\{\pi_t^{(S)} : \tau \leq F_{\pi^{(S)}}(x)\} \tag{2}$$

where $F_{\pi^{(S)}}(x)$ is the empirical Cumulative Density Function (CDF) of $\pi_t^{(S)}$. In other words, $Q_{\pi^{(S)}}(\tau)$ is the value for which it holds that

$$\frac{1}{N}\sum_{i=1}^{N} \mathbf{1}\{\pi_i^{(S)} \leq Q(\tau)\} = \tau \tag{3}$$

where N is the number of observations in the data set.

The prediction intervals obtained by model II are also constant. They are taken from a normal distribution with a standard deviation, $\sigma_{\pi^{(S)}}$:

$$\sigma_{\pi^{(S)}} = \sqrt{\frac{1}{N-1}\sum_{i=1}^{N}(\overline{\pi}^{(S)} - \pi_i^{(S)})^2} \tag{4}$$

where $\overline{\pi}^{(S)} = \frac{1}{N}\sum_{i=1}^{N}\pi_i^{(S)}$.

Model III is a two-stage exponential smoothing of the mean ($\mu_{\pi^{(S)},t}$) and the standard deviation ($\sigma_{\pi^{(S)},t}$) of $\pi_t^{(S)}$ which can be written as

$$\begin{aligned} \mu_{\pi^{(S)},t} &= \alpha\pi_t^{(S)} + (1-\alpha)\widehat{\mu}_{\pi^{(S)},t-1} \\ \sigma^2_{\pi^{(S)},t} &= \alpha\left(\pi_t^{(S)} - \mu_{\pi^{(S)},t}\right)^2 + (1-\alpha)\sigma^2_{\pi^{(S)},t-1} \end{aligned} \tag{5}$$

where α is found as

$$\alpha^* = \arg\min_{\alpha} \sum_{t=1}^{N} \left(\left(\pi_t^{(S)} - \widehat{\mu}_{\pi^{(S)},t} \right)^2 - \widehat{\sigma}_{\varepsilon,t}^2 \right)^2 \tag{6}$$

where in turn $\widehat{\sigma}_{\varepsilon,t}^2$ is the estimate of $\widehat{\sigma}_{\pi^{(S)},t}^2$ from just before noon on the previous day.

Finally model IV is a kernel density estimation of the Probability Density Function (PDF) of ε_t:

$$\widehat{f}_t(\varepsilon;h) = \frac{1}{nh} \sum_{i=t-N_{est}+1}^{t} K\left(\frac{\varepsilon - \varepsilon_i}{h} \right) \tag{7}$$

where $K(\cdot)$ is a Gaussian kernel

$$K(x;\sigma) = \frac{1}{\sqrt{2\pi}\sigma} e^{-\frac{x^2}{2\sigma^2}}, \tag{8}$$

N_{est} is the number of observations used for the estimation at each time and h is the bandwidth, chosen according to the method described in Sheather and Jones (1991). Four lengths of estimation periods are tried, all previous data available, data for the last week ($N_{est} = 168$), and the last 500 and 1000 available observations. Afterwards, the CDF is obtained by numerical integration of the estimated PDF. Using the $N_{est} = 168$ observations for estimation at each time yielded the best performance out of the four and thus it is the corresponding performance that is reported in the following. Just like for model III, the density estimated just before noon on the day before realisation is used to produce the forecast for time t.

3.2 Gaussian Models

The underlying assumption for the parametric models tried here is that the residuals are conditionally Gaussian. Thereby the relationship between the spot prices and the point forecast from Jónsson et al. (2012) can be written as

$$\pi_t^{(S)} = \widehat{\pi}_{t|t-k}^{(S)} + z_t \sigma_{\varepsilon,t} \tag{9}$$

where z_t is a sequence of Independent and Identically Distributed (IID) standard normal variables and $\sigma_{\varepsilon,t}$ is the standard deviation of ε_t from Eq. (1). An autoregressive model is used in the second step of the model for the expected price. Thus assuming a non-zero $\mathbb{E}[\varepsilon_t]$ and consequently adopting an AR-GARCH model for ε_t is superfluous which in turn renders

$$\sigma_{\varepsilon,t}^2 = \mathbb{E}[\varepsilon_t^2]. \tag{10}$$

Hence all the models for Gaussian density forecasts derived in this section involve modelling of ε_t^2 which is plotted in the top panel of Figure 5. Relative to the scale of the plot, ε_t^2 seems to have a level close to zero but with quite frequent spikes. Autocorrelation

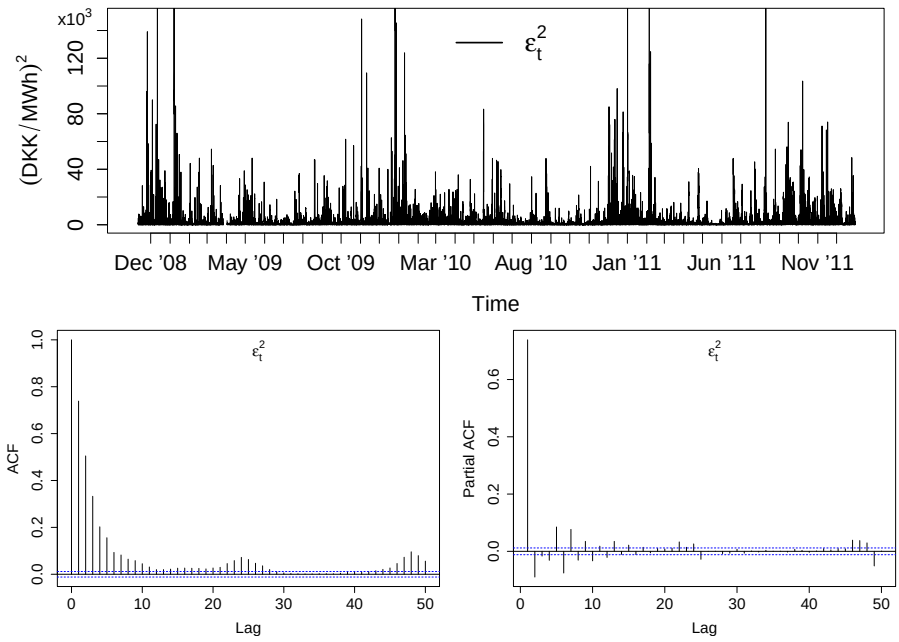

Figure 5: Time series plot of ε_t^2 (top) and the series ACF and PACF (bottom).

and partial autocorrelation functions (ACF and PACF respectively) for ε_t^2 is shown in the bottom panel of Figure 5. The ACF and the PACF suggest a low order ARCH or GARCH model is sufficient.

It can be shown (see e.g. Bollerslev (1986)) that a GARCH model of order (q, p), describing $\sigma_{\varepsilon,t}$ can be written as

$$\begin{aligned} \widehat{\sigma}_{\varepsilon,t} &= \sqrt{h_t} \\ h_t &= \alpha_0 + \sum_{i=1}^{q} \alpha_i \varepsilon_{t-i}^2 + \sum_{j=1}^{p} \beta_j \nu_{t-j} \end{aligned} \tag{11}$$

where

$$\nu_t = \varepsilon_t^2 - h_t, \quad \nu_t \sim \mathcal{N}(0, \sigma_\nu). \tag{12}$$

For $p = 0$ the model in Eq. 11 becomes an ARCH(q) model and M exogenous variables can be introduced in the model by adding an extra term so such that

$$h_t = \alpha_0 + \sum_{i=1}^{q} \alpha_i \varepsilon_{t-i}^2 + \sum_{j=1}^{p} \beta_j \nu_{t-j} + \sum_{u=1}^{M} \gamma_u x_{u,t} \tag{13}$$

where $\boldsymbol{x}_t = [x_{1,t}, \ldots, x_{M,t}]^T$ is a vector of length M including the regressors for time t.

Based the preceding data analysis and the ACF and PACF for ε_t^2 in Figure 5, 10 different model formulations are chosen for analysis. Experiments with the models revealed that only the forecast spot price and load had some merit in terms of forecasting skill. Thus the formulations are given here explicitly in terms of these variables:

$$\begin{aligned}
&\text{I} && h_t = \alpha_{0,t} + \alpha_{1,t}\varepsilon_{t-1}^2 + \beta_{1,t}v_{t-1}\\
&\text{II} && h_t = \alpha_{0,t} + \alpha_{1,t}\varepsilon_{t-1}^2\\
&\text{III} && h_t = \alpha_{0,t} + \alpha_{1,t}\varepsilon_{t-1}^2 + \beta_{1,t}v_{t-1} + \gamma_{1,t}\widehat{\pi}_t^{(S)}\\
&\text{IV} && h_t = \alpha_{0,t} + \alpha_{1,t}\varepsilon_{t-1}^2 + \gamma_{1,t}\widehat{\pi}_t^{(S)}\\
&\text{V} && h_t = \alpha_{0,t} + \alpha_{1,t}\varepsilon_{t-1}^2 + \beta_{1,t}v_{t-1} + \gamma_{1,t}\widehat{\pi}_t^{(S)} + \gamma_{2,t}\widehat{L}_t\\
&\text{VI} && h_t = \alpha_{0,t} + \alpha_{1,t}\varepsilon_{t-1}^2 + \gamma_{1,t}\widehat{\pi}_t^{(S)} + \gamma_{2,t}\widehat{L}_t\\
&\text{VII} && h_t = \alpha_{1,t}\varepsilon_{t-1}^2 + \beta_{1,t}v_{t-1} + \gamma_{1,t}\widehat{\pi}_t^{(S)}\\
&\text{VIII} && h_t = \alpha_{1,t}\varepsilon_{t-1}^2 + \gamma_{1,t}\widehat{\pi}_t^{(S)}\\
&\text{IX} && h_t = \alpha_{0,t} + \gamma_{1,t}\widehat{\pi}_t^{(S)}\\
&\text{X} && h_t = \gamma_{1,t}\widehat{\pi}_t^{(S)}
\end{aligned}$$

The parameters, α, β, γ and θ are estimated recursively (as described in (Madsen, 2008, ch. 11) and Jónsson et al. (2012)) with the forgetting factor λ chosen as

$$\lambda^* = \arg\min_{\lambda} \sum_{t=1}^{N} v_t^2. \tag{14}$$

The regression parameters, α, β and γ are estimated separately for each lead-time. In this particular case translates into estimating hourly specific parameters. A prediction formula can be written generally for models I - X as

$$\widehat{h}_{t|t-k} = \alpha_{0,t-k}(k) + \alpha_{1,t-k}(k)\varepsilon_{t-k}^2 + \sum_{i=1}^{p}\beta_{i,t-k}(k)v_{t-k} + \sum_{j=1}^{M}\gamma_{j,t}(k)x_{j,t} \tag{15}$$

The alternative approach of estimating a single set of parameters for single step predictions and issue predictions iteratively was found to perform worse than this prediction scheme.

3.3 Time Adaptive Quantile Regression

The QR model derived is based on the time adaptive QR-framework described in Møller et al. (2008). The QR model is used to describe the distribution of ε_t between the 5% and the 95% quantiles. Afterwards, this model is coupled with a separate model for the tails.

There exists a vast literature on Quantile Regression in general. In Koenker (2005), a detailed description of everything from fundamental properties to latest developments in the field is provided.

The most basic form for a QR model (Koenker and Basset, 1978) for the variable ε_t and a pre-specified quantile, τ is written as

$$Q_{\varepsilon_t,t}(\tau) = F^{-1}_{\varepsilon_t,t}(\tau) = \boldsymbol{x}_t^T \boldsymbol{\beta}(\tau) + e_t \tag{16}$$

where $F^{-1}_{\varepsilon_t,t}(\tau)$ is the inverse CDF of ε_t, $\boldsymbol{x}_t$ is a (column)vector of explanatory variables and e_t is a noise term, centred at zero and with a finite variance. Finally, $\boldsymbol{\beta}(\tau)$ is a (column)vector of model parameters, estimated by solving a linear program:

$$\widehat{\boldsymbol{\beta}}(\tau) = \underset{\boldsymbol{\beta}(\tau)}{\arg\min} \sum_{i=1}^{N} \Big(\varepsilon_t - \boldsymbol{x}_t^T \boldsymbol{\beta}(\tau)\Big) \Big(\tau - \mathbf{1}(\varepsilon_t < \boldsymbol{x}_t^T \boldsymbol{\beta}(\tau))\Big) \tag{17}$$

In the model here derived, the non-linear relationship between ε_t and the explanatory variables is accounted for by representing $\boldsymbol{x}_t$ by B-splines. Furthermore, the estimation data set is updated as new observations become available and at the same time, the oldest observations are discarded. Then a new estimate of the regression parameters is obtained by solving (17). Estimating the parameters on relatively recent values only has the drawback that deviations from the average behaviour are quickly discarded. In order to ensure a broader coverage of the explanatory variables' previous values in the estimation set, its updating is done on a number of partitions or bins. Each bin contains observations falling within a pre-specified range and every time a new observation becomes available, it replaces the oldest observation in the corresponding bin. Meanwhile, other bins containing data for different values of the variable remain intact. Afterwards the data bins are combined into a single estimation set which then contains a broader range of observations than it otherwise would. The updating procedure is described more thoroughly in Møller et al. (2008).

In light of the analysis presented earlier on, we start out with a QR-model of the form

$$Q_{\varepsilon_t,t}(\tau) = s(\widehat{\pi}_t^{(S)})\boldsymbol{\beta}_t(\tau) + e_t = \sum_{i=1}^{K} b_i(\widehat{\pi}_t^{(S)})\beta_{i,t}(\tau) + e_t \tag{18}$$

where b_i are natural cubic B-spline basis functions with no intercept term. Furthermore, K is the number of knots used for the spline fitting and e_t is an error term, centred and with finite variance. The remaining candidates for explanatory variables, L_t, W_t and $\frac{W_t}{L_t}$ are subsequently added to the model one by one. Both a spline representation is considered as well as their inclusion as a linear term. The model that yields the highest forecasting skill has the form

$$Q_{\varepsilon_t,t}(\tau) = \sum_{i=1}^{K} b_i(\widehat{\pi}_t^{(S)})\beta_{i,t}(\tau) + \widehat{L}_t\gamma_t(\tau) + e_t. \tag{19}$$

That is, in addition to the spline representation of the forecast spot price, the forecast load is also included in the model as a linear term. The variables for the wind power proved not the enhance the model's forecasting skill nor did representing $\widehat{L}_t$ by splines.

Since the optimal memory of the model is likely to vary between different values of τ, a best model setup is found for each individual value of τ. This calls for a skill score that can rate a single quantile forecast and not the entire CDF. Following the suggestions of (Gneiting and Ranjan, 2011, and references therein) such score is defined from (17) as

$$\overline{\text{SSc}} = -\frac{1}{N}\sum_{t=1}^{N}\left(\mathbf{1}(\varepsilon_t \leq \widehat{Q}_{\varepsilon_t,t}(\tau)) - \tau\right)\left(\varepsilon_t - \widehat{Q}_{\varepsilon_t,t}(\tau)\right) \tag{20}$$

and is used to evaluate a model's forecasting skill for a given nominal quantile τ and subsequently to decide on the meta parameters of the model in (19).

The number and placement of bins and knots is chosen as the setup yielding the highest value of $\overline{\text{SSc}}$, for the estimation period, out of 6 setups. For setups I - III, bin edges are placed at $F_{\widehat{\pi}^{(S)}}(\tau)$, $\tau \in \{0, 0.25, 0.75, 1\}$ where denotes the empirical CDF of $\widehat{\pi}^{(S)}$ for the same period. The bin edges for setups IV - VI however are chosen as $\tau \in \{0,1\}$. The knots are placed at $\tau \in \{0, 0.25, 0.5, 0.75, 1\}$ for setups I and IV, at $\tau \in \{0, 0.125, 0.25, 0.5, 0.75, 0.875, 1\}$ for setups II and V and at $\tau \in \{0, 0.25, 0.75, 1\}$ for setups III and VI.

For deciding on the appropriate bin size, N_B, for each of the aforementioned setups, the following scheme is adopted for each value of τ:

1. For setups I - III: Estimate $\overline{\text{SSc}}(N_B)$ for $N_B \in \{200, 400, \ldots, 1200\}$.
   For setups IV - VI: Estimate $\overline{\text{SSc}}(N_B)$ for $N_B \in \{200, 400, \ldots, 3200\}$.
2. Find the bin size N_B^{*1}, $N_B^{*1} = \arg\max_{N_B} \overline{\text{SSc}}(N_B)$.
3. Estimate $\text{SSc}(N_B)$ for $N_B \in \{N_B^{*1} - 150, N_B^{*1} - 100, \ldots, N_B^{*1} + 150\}$
4. Again find $N_B^{*2} = \arg\max_{N_B} \overline{\text{SSc}}(N_B)$ out of the new set of N_B's.
5. Estimate $\text{SSc}(N_B)$ for $N_B \in \{N_B^{*2} - 40, N_B^{*2} - 30, \ldots, N_B^{*2} + 40\}$
6. Decide on $N_B^{*3} = \arg\max_{N_B} \overline{\text{SSc}}(N_B)$ out of the third set of N_B's as the bin size for that particular value of τ.

3.4 Estimating the Distribution Tail for QR Predictions

One of the drawbacks of quantile regression is that it only provides a description of particular quantiles. Thus one has to assume some shape of the CDF for values of τ for which a model has not been estimated. This becomes especially problematic when a description of the distribution tails is desired since they are unlikely to be well approximated by inter- or extrapolation.

For any risk management however a proper description of the tails is paramount. Likewise such description is also important to have for scenario generation. Without it, the scenarios will not reflect properly the full range of possible outcomes.

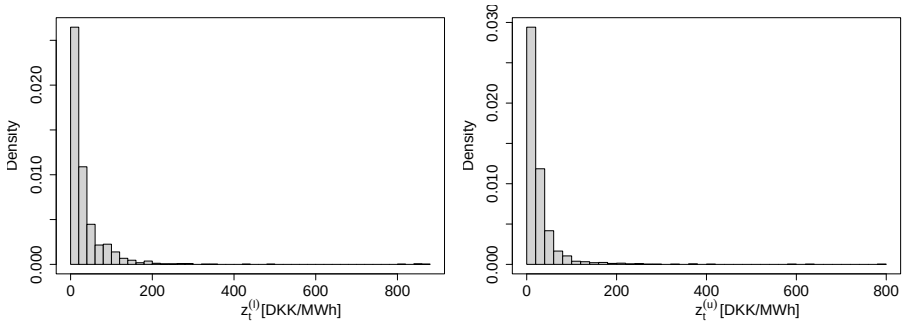

Figure 6: Histograms of the $z_t^{(l)}$ (left) and the $z_t^{(u)}$ (right)

Therefore, a quantile regression model for an unbounded process like the one just described must be accompanied by a model for the tails. In order to obtain such a model we now define two new variables, $z_t^{(l)}$ and $z_t^{(u)}$, as

$$z_t^{(l)} = \max\{\widehat{Q}_{\varepsilon_t,t}(0.05) - \varepsilon_t, 0\}, \quad z_t^{(u)} = \max\{\varepsilon_t - \widehat{Q}_{\varepsilon_t,t}(0.95), 0\}. \tag{21}$$

Indeed the choice of defining the coverage of the tail models as the data exceeding or deceeding the 95% and 5% quantiles respectively is somewhat arbitrary. Here we will not go into detail in this discussion but these values seem to be a reasonable choice since the quantile regression seems to perform well up to these values. On the other hand, by estimating quantiles further out in the tails would dilute the estimation data for the tail models severely. Also for this reason, we restrict ourselves to models with parametric assumptions as obtaining a description of the full density will always end up in a parametric assumption for the extremes.

In Figure 6, histograms of these two variables are plotted using data for the whole period and the best performing QR model found. Not surprisingly, the densities of $z_t^{(l)}$ and $z_t^{(u)}$ seem to be exponentially decaying for increasing values. Thus assuming exponential distribution for $z_t^{(l)}$ and $z_t^{(u)}$ seems reasonable.

For an exponentially distributed variable x the PDF $f(x;\lambda)$ and the CDF $F(x;\lambda)$ are defined as

$$f(x;\lambda) = \begin{cases} \lambda e^{-\lambda x} & \text{for } x \geq 0 \\ 0 & \text{for } x < 0 \end{cases}, \quad F(x;\lambda) = \begin{cases} 1 - e^{-\lambda x} & \text{for } x \geq 0 \\ 0 & \text{for } x < 0 \end{cases} \tag{22}$$

where λ is the rate-parameter defined as one over the mean of x.

The estimate of λ at time t, $\widehat{\lambda}_t$, is obtained by maximum likelihood estimation using all data available until time t. It easily shown that such estimate of the rate-parameter is found as

$$\widehat{\lambda}_t = \frac{1}{\overline{x}_t} = \frac{1}{\frac{1}{N_t}\sum_{i=1}^{N_t} x_i} \tag{23}$$

where N_t is the number of observations available at time t.

4 Numerical Results

4.1 Evaluation of Forecasting Skill

For comparison of forecast quality the average Continuous Ranked Probability Score ($\overline{\text{CRPS}}$) (Matheson and Winkler, 1976) and the related Continuous Ranked Probability Skill Score (CRPSS) are used. For a single observation, x_o and a corresponding predicted CDF, $\widehat{F}(x)$, the CRPS is defined as

$$\text{CRPS} = \int_{-\infty}^{\infty} \left(\widehat{F}(x) - F_o(x)\right)^2 dx \tag{24}$$

where

$$F_o(x) = H(x - x_o) = \begin{cases} 0 & \text{if } x - x_o < 0 \\ 1 & \text{if } x - x_o \geq 0 \end{cases}. \tag{25}$$

is the well-known Heaviside function. Subsequently $\overline{\text{CRPS}}$ is found as

$$\overline{\text{CRPS}} = \frac{1}{N} \sum_{i=1}^{N} \text{CRPS}_i. \tag{26}$$

The CRPSS for a certain model is defined as

$$\text{CRPSS} = 1 - \frac{\overline{\text{CRPS}}_{model}}{\overline{\text{CRPS}}_{ref}} \tag{27}$$

where $\overline{\text{CRPS}}_{model}$ is the average CRPS for the model and $\overline{\text{CRPS}}_{ref}$ is that for a chosen reference model. The reference model is commonly chosen as the empirical quantiles, i.e. benchmark model II, which is also the case here.

In order to allow for a fair comparison of the performance of all the derived models, two sets of $\overline{\text{CRPS}}$ values are reported. One is estimated using a set of quantiles, τ_1, ranging from 0 to 1 in steps of 0.05. For the other one, τ_2, the set of quantiles used includes additional quantiles in the tails of the distribution. That is the sets τ_1 and τ_2 are defined as

$$\begin{aligned} \tau_1 &\in \{0, 0.05, 0.10, \ldots, 0.95, 1\} \\ \tau_2 &\in \{\tau_1, 0.005, 0.01, 0.025, 0.975, 0.99, 0.995\}. \end{aligned} \tag{28}$$

In both cases the empirical minimum and maximum for the whole data set are used for the 0 and 1 quantiles respectively.

Table 1: The $\overline{\text{CRPS}}$ for the best performing models.

Model		Parameters	Training Period $\tau \in \boldsymbol{\tau}_1$	Training Period $\tau \in \boldsymbol{\tau}_2$	Test Period $\tau \in \boldsymbol{\tau}_1$	Test Period $\tau \in \boldsymbol{\tau}_2$
Benchmark	I	—	50.76	48.62	56.64	54.52
	II	—	51.97	49.82	56.50	54.37
	III	$\alpha = 0.0119$	48.96	47.03	47.53	45.41
	IV	$N_{est} = 168$	46.17	44.32	42.26	40.04
Gaussian	III	$\lambda = 0.9954$	23.50	21.39	25.35	23.24
	V	$\lambda = 0.9956$	23.43	21.33	25.28	23.16
	VI	$\lambda = 0.9039$	23.18	21.08	25.07	22.97
QR-E	I	See Table 2	22.71	21.26	25.18	23.06

4.2 Estimation Results

For all models, parameter estimation is done using the data or from December 21st 2008 until December 31st 2009. The remaining 2 years are used as an independent test set. These data sets will be referred to as the training set and the test set from here on.

Table 1 lists the $\overline{\text{CRPS}}$ of the best performing models from previous section along with the corresponding parameter estimates for the benchmark and the parametric models. The model parameters for the QR-E model are however given in Table 2. Among the benchmarks, the kernel density estimation model outperforms the other ones. This was the case for all values of N_{est} tried although $N_{est} = 168$ was the one for which the difference was largest. The exponential smoothing model was also found to outperform the time-invariant benchmarks although it performs poorer than the kernel model.

The best performing parametric models are the GARCH-X model with $\widehat{\pi}_t^{(S)}$ as explanatory variable (III) and the GARCH-X and ARCH-X models with both $\widehat{\pi}_t^{(S)}$ and $\widehat{L}_t$ as exogenous variables (V and VI respectively). Although the ARCH-X model outperforms the other two, the difference in $\overline{\text{CRPS}}$ is small. Furthermore, the forgetting factor λ is suspiciously low for the ARCH-X model as it can not rely on the moving average term to accommodate the short term dynamics of σ_{ε_t}. Thus the forgetting factor of the two GARCH models is of a much desirable magnitude in terms of parameter stability.

The τ-specific bin sizes, N_B for the QR-E model are listed in Table 2 along with the placement of the spline knots and the bin edges. According to expectations, the largest amount of data is used to estimate the quantiles close to the tails. Then on both sides of the median there are quantiles for which the model as a relatively short memory indicating more rapidly varying dynamics. Closer to the median the memory increases again since the point forecasts have accommodated most dynamic changes there. All in all, the merits of the model's flexibility, compared to the parametric models, transpire through the longer memory of the QR-E model, thus allowing for a more stable regression parameters.

The rate parameters for $z_t^{(l)}$ and $z_t^{(u)}$ are, like for the other models updated daily using all available data at the estimation time. The corresponding $\overline{\text{CRPS}}$ values are listed in Table 3, along with that of climatology forecasts for the tails. The table shows that a slightly better description of the lower tail is obtained through by the exponential model than by the climatology forecasts. Disappointingly however the opposite is the case for the upper tail. One has to bear in mind though that only the Exponential model is applicable in practise since the other one utilises future information at every prediction time which is especially misleading for models describing extreme occurrences.

4.3 Model Comparison

Barplots of the CRPSSs for the test period are presented in Figure 7, using $\tau \in \boldsymbol{\tau}_1$ and $\tau \in \boldsymbol{\tau}_2$ as earlier defined. Overall the more elaborate models seem to outperform the benchmarks by a significant margin. The difference between the Gaussian and the QR-E models may appear negligible.

For any type of risk management or scenario generation, the reliability of the density forecasts is essential. Most risk management models, such as Value-at-Risk (VaR) or Conditional Value-at-Risk (CVaR), aim at minimising losses at or beyond a certain quantile of the loss probability distribution. Thus an unreliable density estimate will severely affect all risk assessment. Similarly for scenario generation which often is used for generating inputs to models such as VaR and CVaR, an unreliable density forecasts will yield scenarios that do not cover the full spectrum of possible outcomes. Moreover since uncertainty generally tends to be underestimated in density forecasts (Chatfield, 2000, ch. 7.7), unreliable density forecast will generally prompt risk to be underestimated.

Table 2: The best bin sizes (N_B) found for each value of τ.

τ	N_B	τ	N_B	τ	N_B	τ	N_B	τ	N_B
0.05	1710	0.25	210	0.45	810	0.65	790	0.85	550
0.10	1790	0.30	230	0.50	760	0.70	820	0.90	1090
0.15	2000	0.35	210	0.55	800	0.75	840	0.95	1280
0.20	200	0.40	300	0.60	740	0.80	550		
Knots:		$\widehat{\pi}_t^{(S)} \in \{-158.85, 240.25, 275.61, 311.64, 675.07\}$							
Bin Edges:		$\widehat{\pi}_t^{(S)} \in \{-\infty, 240.25, 311.64, \infty\}$							

Table 3: The $\overline{\text{CRPS}}$ for the tail models, estimated for $\tau \in \boldsymbol{\tau}_1$.

Period:	Q_{clim}		Exp$(\widehat{\lambda})$	
	Lower Tail	Upper Tail	Lower Tail	Upper Tail
Training	22.93	27.65	22.93	27.59
Test	22.51	12.15	22.09	12.90

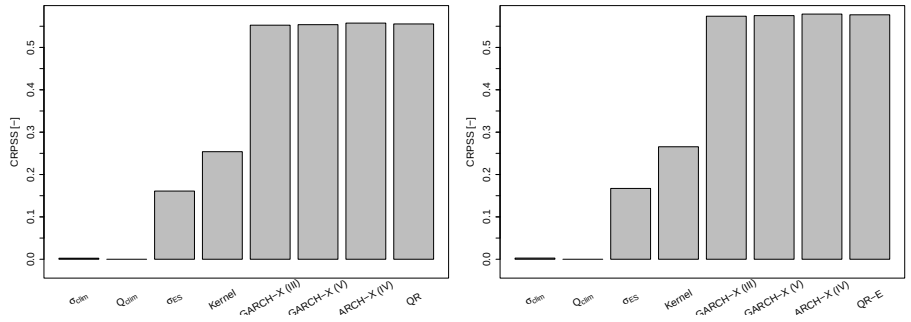

Figure 7: Barplot of the CRPSS for the models listed in Table 1 for the test period estimated on $\tau \in \boldsymbol{\tau}_1$ (left) and on $\tau \in \boldsymbol{\tau}_2$ (right).

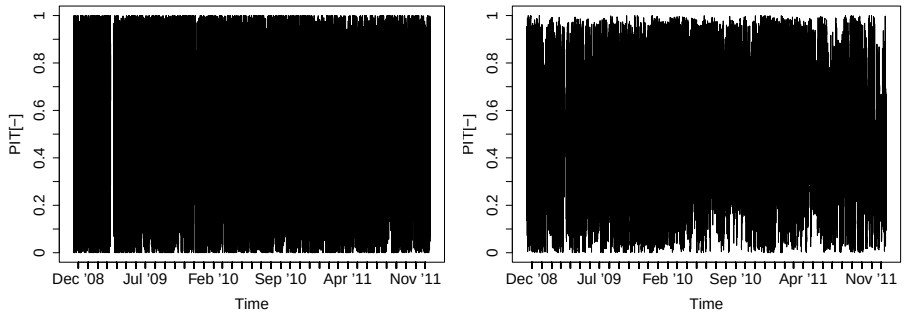

Figure 8: The PIT of ε_t the ARCH-X model (left) and the QR-E model (right).

For this reason the reliability of the models derived in previous section is examined.

A thorough discussion of the concept of reliability is given in Bröcker and Smith (2007) and Pinson et al. (2010) so only a brief introduction will be given here. Ideally a series of N forecasts for the τth quantile of the density of ε_t, $\widehat{Q}_{\varepsilon_t,t}(\tau)$, should satisfy

$$\widetilde{\tau} = \frac{1}{N}\sum_{t=1}^{N} \mathbf{1}(\varepsilon_t \leq \widehat{Q}_{\varepsilon_t,t}(\tau)) = \tau. \tag{29}$$

How reliable forecasts from a particular model are is commonly reported either as a comparison of $\widetilde{\tau}$ and τ or as the bias of $\widetilde{\tau}$, i.e. $\tau - \widetilde{\tau}$. For a finite data set, some deviation a non-zero bias of $\widetilde{\tau}$ is natural within a certain band around τ and both Bröcker and Smith (2007) and Pinson et al. (2010) present estimation procedures for this band. These intervals are commonly referred to as consistency intervals and correspondingly they are illustrated as consistency bars on reliability diagrams.

Pinson et al. (2010) suggest that the Auto-Correlation of the Probability Integral Transformation (PIT) (Gneiting et al., 2007) should be accounted for in the estimation of consistency intervals for reliability diagrams. Using the predictive densities obtained by

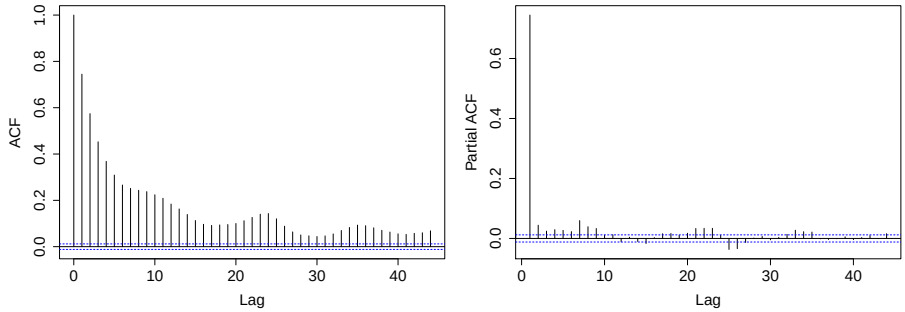

Figure 9: The rank ACF and PACF for the PIT of the forecasts from the QR-E model.

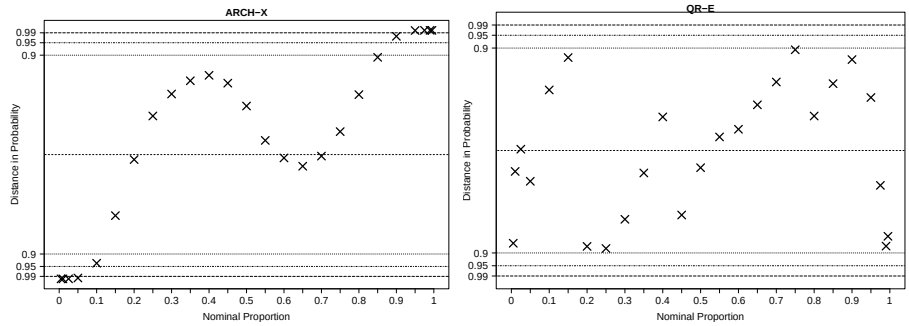

Figure 10: Reliability diagrams on probability paper for the GARCH-X models (top-left and right), the ARCH-X model (bottom-left) and the QR-E model (bottom-right).

the models described here, PIT of ε_t is found as

$$PIT(\varepsilon_t) = \widehat{F}_t(\varepsilon_t) \tag{30}$$

and should be uniformly distributed between 0 and 1. The PITs for the four models are plotted in Figure 8. The plots reveal that even though the PITs seems to be close to uniform on a time-invariant plot, like a histogram, for the whole period this is not the case in the short-term as the PIT seems a drifting mean for all models.

Figure 9 shows the rank ACFs for the QR-E model. The figure reveals considerable autocorrelation in the PIT which need to be accounted for when reliability of the forecasts is evaluated. The ACFs for the other models look similar.

Therefore the methodology presented in Pinson et al. (2010) for constructing consistency intervals for the reliability diagrams is adopted. Reliability diagrams, plotted on probability paper (see Bröcker and Smith (2007)) are shown for the four models in Figure 10. For the QR-E model, the reliability hypothesis can not be rejected at the 10%

level for all quantiles. For the ARCH-X model however, the hypothesis is rejected for 9 out of the 25 quantiles at the 5% significance level. Furthermore, going to the 1% level only reduces this number to 8. For the two GARCH models the results are even worse. Thus one must conclude that even though the two models score similarly in terms of CRPSS, the Gaussian models fail to produce reliable probabilistic forecasts. The reliability diagrams are a clear testimony of the shortcomings of the Gaussian assumption. The assumed shape of the density causes centre quantiles to be generally overestimated while the tail quantiles are underestimated. This indicates that ε_t has in fact a sharper density with higher kurtosis than a standard Normal distribution - Even conditionally.

4.4 Properties of the QR-E Model

Table 4 lists the CRPSS for the QR-E forecasts and the $\overline{\text{CRPS}}$ for both that model and the climatology one within each estimation bin for $\widehat{\pi}_t^{(S)}$ the training and the test set. That is, the quantile forecasts have been segmented by the 1st and the 3rd sample quartiles and the CRPSS estimated for each bin.

First and foremost the table shows that the QR-E model consistently outperform the climatological model regardless of the expected price. Apart from that, the table reveals that the the superiority of the QR-E model is greater in situations where the prices are expected to be high or low. The fact that the difference in $\overline{\text{CRPS}}$ between the intermediate bin and the bins outside the inter-quartile range is at least 70% larger for the benchmark model than for the QR-E model is a testimony of this. These results are not surprising since a static reference model is generally expected to give the best result under ordinary circumstances at the cost of less frequent events. Thus, greater improvements should be expected for $\widehat{\pi}_t^{(S)}$ above and below average by using a more elaborate model.

The varying performance of the QR-E model in the outer bins is partly due to their varying update frequency between the two periods. During the training period the average spot price is lower than during the test period. The segmentation on the other hand is done according to the empirical quantiles of the whole data set. Thus the bin

Table 4: The $\overline{\text{CRPS}}$ for the predictions from the QR-E model and the climatology quantiles, segmented according to $\widehat{\pi}_t^{(S)}$

Range	$\overline{\text{CRPS}}$				CRPSS	
	QR-E		Q_{clim}		QR-E vs. Q_{clim}	
	Training	Test	Training	Test	Training	Test
$-295.43 \leq \widehat{\pi}_t^{(S)} \leq 266.87$	21.48	36.63	51.03	67.20	0.5790	0.4549
$266.87 \leq \widehat{\pi}_t^{(S)} \leq 381.27$	18.07	19.97	27.74	35.08	0.3487	0.4307
$381.27 \leq \widehat{\pi}_t^{(S)} \leq 867.74$	47.89	24.23	76.61	90.93	0.3749	0.7335

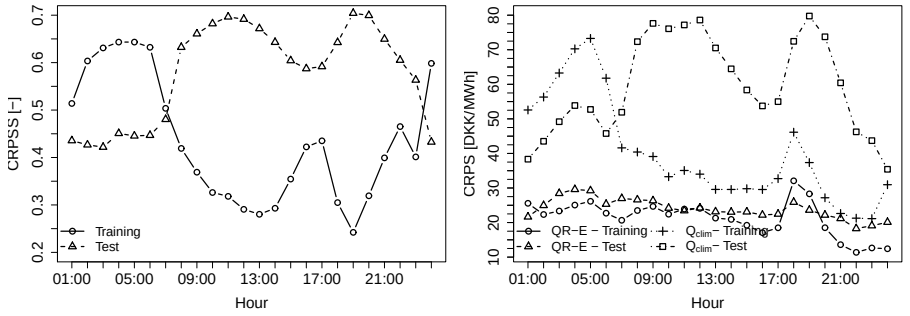

Figure 11: Hourly CRPSS for the QR-E model (left) and the hourly CRPS values for the QR-E model and the climatology one (right).

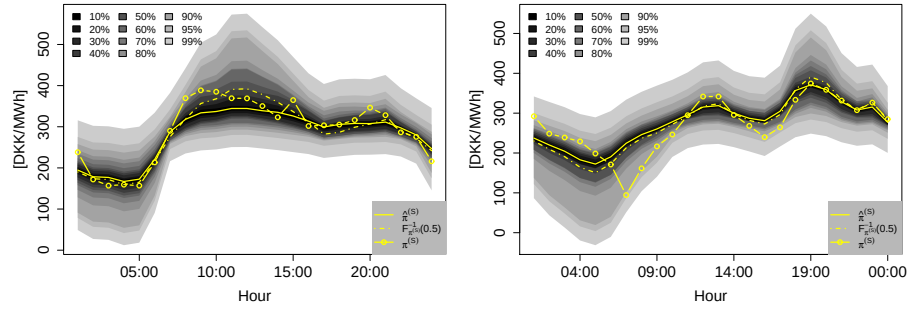

Figure 12: Forecasts generated by the QR-E model on 15/9 2009 at 10:00 for 16/9 2009 (left) and forecasts issued on 23/1 2010 at 10:00 for 24/1 2010 (right).

containing the high expected prices is updated less frequently than the low price bin during the training period. On the contrary, the low price bin represents expected prices further from the mean during the test period than during the training period. This prompts the question of whether time-varying bin edges would be appropriate. No effort for obtaining such model was made though.

Figure 11 illustrates the CRPSS and the $\overline{\text{CRPS}}$ for each hour of the day which in this case is also for each lead-time. Again the instability of the CRPSS seems to be mainly driven by the varying skill of the climatology quantiles. In the context of Jónsson et al. (2012), it is interesting to see the peak (poorest performance) of the climatology model in the early evening hours. These were observed in forecast quality of the model presented in Jónsson et al. (2012) and since the CRPS closely related to the Mean Absolute Error (MAE) for point forecasts, the appearance of these is natural for the climatology model. Interestingly however, this peak is by far less severe in the curves representing the QR-E model. It was shown in Jónsson et al. (2012) that this poor performance during these hours was due to more volatile prices. Thus it is pleasant to see that the combination of

the model from Jónsson et al. (2012) and the QR-E model is able capture this increased volatility to some extent.

Two examples of the density forecasts from the QR-E model are shown in Figure 12. The plots in the figure illustrate well how the density of $\pi_t^{(S)}$ varies with the expected price.

5 Concluding Remarks

A model able to generate reliable density forecasts for the day-ahead electricity prices at Nord Pool's Elspot has been presented. Time-adaptive quantile regression is used to describe the density between the 5% and the 95% quantiles. The distribution tails are then approximated by an exponential distribution. The proposed methodology is shown to consistently outperform 4 different benchmark approaches for every hour of the day and regardless of the level of the prices. Compared to the parametric Gaussian models also presented in this paper, the QR-E model has the advantage that is produces quantile forecasts that are reliable.

The density model is built as an independent extension of the point forecasts presented in Jónsson et al. (2012) which simplifies the modelling process considerably. The expected price could however be obtained by any other well-tuned model serving the same purpose. Unlike the majority of procedures in the existing literature, the modelling is done on untransformed data allowing for directly deriving density forecasts on the actual scale of the prices. Furthermore, as the results presented in this paper are derived by mimicking practical data availability, the model can be applied as presented for online density forecasting of the prices.

The type of forecasts here presented are valuable for various applications. For one, the model's predictions can be used directly for determining the optimal structure of block bids (see Nord Pool Spot AS, 2011, for definition) in markets where such bids are accepted. Secondly, the model can be used for generating the scenarios necessary to solve the decision problems described in Morales et al. (2010), Jónsson et al. (2012), Fleten and Kristoffersen (2008, 2007), Heredia et al. (2010). In the scenario generation process, the auto-correlation of the PIT needs to be accounted for, e.g. by applying the scenario generation framework from Pinson et al. (2009). The sequential clearing of many liberalised electricity markets, e.g. the Scandinavian and the Spanish ones, makes density forecasts of the day-ahead prices vital for any generation of market scenarios - Even though the day-ahead prices are not explicitly required in the scenarios. This is because other market variables are either strongly influenced or even directly dependent upon the day-ahead prices. Thus accounting for the whole range of potential outcomes on the day-ahead market is vital for obtaining a set of scenarios spanning the whole density of possible realisations on other markets.

Despite that a complete model has been found there are several possibilities for improving it. First of all, from Figure 8 a relatively slow drift in the realised PIT can be

detected. For a time-varying process like the spot prices are, such effects will never be fully prevented. Although it would be interesting to see whether an auto-regressive or a moving average term could mitigate this behaviour of the PIT. This could either be done in the Quantile auto-regression framework discussed in Koenker (2005, section 8.3 pp. 260-265) or as an exponential smoothing model like the one described in Taylor (2008, and references therein). Secondly, alternative definition of the bin edges, e.g. in terms of sample quantiles over a given period could be interesting to pursuit.

Thirdly, even though the parametric models presented here yielded unreliable forecasts, there are several extensions to the models that might successfully mitigate that problem. For instance some of a mixture model might help in this regard. The mixture model could be either a discrete one, e.g. a Hidden Markov model, or a continuous latent model could be applied. Another interesting possibility would be a double stochastic (G)ARCH-X model (Madsen, 2008). This would serve the purpose of accommodating the shifts between periods of excessive volatility and periods of relative tranquillity better than the exponential smoothing does. Also other parametric distributions could be considered. For such models, one should bear in mind that some form for adaptivity in the parameters is paramount for a non-stationary process like the spot prices are.

Finally, given a larger data set, revisiting the exponential tail models would be worthwhile. For one, even though the centre part of the density of ε_t does not exhibit any apparent diurnal variation, it seems plausible that the tail quantiles would do so due to the higher demand during the day. For the data set at hand however, hourly estimation however dilutes the data set so severely that estimation of a seasonal model for the tail would be meaningless. A larger data set would also allow for investigation of whether a limited memory is appropriate for estimation of the tail.

References

Tim Bollerslev. Generalized autoregressive conditional heteroskedasticity. *Journal of Econometrics*, 31(3):307–327, 1986.

Alexander Boogert and Dominique Dupont. On the effectiveness of the anti-gaming policy between the day-ahead and real-time electricity markets in the Netherlands. *Energy Economics*, 27(5):752–770, 2005.

Jochen Bröcker and Leonard A. Smith. Increasing the reliability of reliability diagrams. *Weather and Forecasting*, 22(3):651–661, 2007.

Kam Fong Chan, Philip Gray, and Bart van Campen. A new approach to characterizing and forecasting electricity price volatility. *International Journal of Forecasting*, 24(4): 728–743, 2008.

Christopher Chatfield. *Time Series Forecasting*. Chapman & Hall / CRC, London, UK, 2000.

Antonio J. Conejo, Javier Contreras, Rosa Espínola, and Miguel A. Plazas. Forecasting electricity prices for a day-ahead pool-based electric energy market. *International Journal of Forecasting*, 21(3):435–462, 2005.

Shi-Jie Deng and Wenjiang Jiang. *Modelling prices in competitive electricty markets*, chapter 7 - Quantile-Based Probabilistic Models for Electricity Prices, pages 161–176. John Wiley & Sons, 2004.

Abdou Ka Diongue, Dominique Guegan, and Bertrand Vignal. Forecasting electricity spot market prices with a k-factor GIGARCH process. *Applied Energy*, 86(4):505–510, 2009.

Robert F. Engle. Autoregressive conditional heteroscedasticity with estimates of the variance of United Kingdom inflation. *Econometrica*, 50(4):987–1007, 1982.

Stein-Erik Fleten and Trine Krogh Kristoffersen. Stochastic programming for optimizing bidding strategies of a Nordic hydropower producer. *European Journal of Operational Research*, 181(2):916–928, 2007.

Stein-Erik Fleten and Trine Krogh Kristoffersen. Short-term hydropower production planning by stochastic programming. *Computers & Operations Research*, 35(8):2656–2671, 2008.

Carolina García-Martos, Julio Rodríguez, and María Jesús Sánchez. Forecasting electricity prices and their volatility using unobserved components. *Energy Economics*, 33(6): 1227–1239, 2011.

Tilman Gneiting, Fadoua Balabdaoui, and Adrian E. Raftery. Probabilistic forecasts, calibration and sharpness. *Journal of the Royal Statistical Society Series B - Statistical Methodology*, 69(2):243–268, 2007.

Tilmann Gneiting and Adrian E. Raftery. Strictly proper scoring rules, prediction and estimation. *Journal of the American Statistical Association*, 102(477):369–378, 2007.

Tilmann Gneiting and Roopesh Ranjan. Comparing density forecasts using threshold and quantile weighted prober scoring rules. *Journal of Business and Economic Statistics*, 29(3):411–422, 2011.

Erik Haugom, Sjur Westgaard, Per Bjarte Solibakke, and Gudbrand Lien. Realized volatility and the influence of market measures on predictability: Analysis of Nord Pool forward electricity data. *Energy Economics*, 33(4):1206–1215, 2011.

F.-Javier Heredia, Marcos J. Rider, and Cristina Corchero. Optimal bidding strategies for thermal and generic programming units in the day-ahead electricity market. *IEEE Transactions on Power Systems*, 25(3):1504–1518, 2010.

Helen Higgs. Modelling price and volatility inter-relationships in the Australian wholesale spot electricity markets. *Energy Economics*, 31(5):748–756, 2009.

Tryggvi Jónsson, Pierre Pinson, and Henrik Madsen. On the market impact of wind energy forecasts. *Energy Economics*, 32(2):313–320, 2010.

Tryggvi Jónsson, Pierre Pinson, Henrik Aalborg Nielsen, Henrik Madsen, and Torben Skov Nielsen. Forecasting electricity spot prices accounting for wind power predictions. *IEEE Transactions on Sustainable Energy*, In PRESS, 2012.

Tryggvi Jónsson, Sarah M. Ryan, Marco Zugno, and Pierre Pinson. Risk averse bidding of wind power: Formulation and properties. Technical report, DTU Informatics, 2012. 2012-03.

Nektaria V. Karakatsani and Derek W. Bunn. Forecasting electricity prices: The impact of fundamentals and time-varying coefficients. *International Journal of Forecasting*, 24 (4):764–785, 2008.

Roger Koenker. *Quantile Regression*. Cambridge University Press, New York, NY, USA, 2005.

Roger Koenker and Gilbert Basset. Regression quantiles. *Econometrica*, 46(1):33–50, 1978.

Henrik Madsen. *Time Series Analysis*. Chapman & Hall / CRC, London, UK, 2008.

James E. Matheson and Robert L. Winkler. Scoring rules for continuous probability distributions. *Management Science*, 22(10):1087–1095, 1976.

Jan Kloppenborg Møller, Henrik Aalborg Nielsen, and Henrik Madsen. Time-adaptive quantile regression. *Computational Statistics and Data Analysis*, 52(3):1292–1303, 2008.

Juan M. Morales, Antonio J. Conejo, and Juan Pérez-Ruiz. Short-term trading for a wind power producer. *IEEE Transactions on Power Systems*, 25(1):554–564, 2010.

Torben Skov Nielsen, Henrik Aalborg Nielsen, and Henrik Madsen. Prediction of wind power using time-varying coefficient functions. In *15th IFAC World Congress*, Barcelona, Spain, 2002.

Nord Pool Spot AS. The power market, August 2011. URL http://www.nordpoolspot.com/How-does-it-work/.

Anastasios Panagiotelis and Michael Smith. Bayesian density forecasting of intraday electricity prices using multivariate skew-t distributions. *International Journal of Forecasting*, 24(4):710–727, 2008.

Pierre Pinson, George Papaefthymiou, B. Klockl, Henrik Aalborg Nielsen, and Henrik Madsen. From probabilistic forecasts to statistical scenarios of short-term wind power production. *Wind Energy*, 12(1):51–62, 2009.

Pierre Pinson, Patrick McSharry, and Henrik Madsen. Reliability diagrams for nonparametric density forecasts of continuous variables: accounting for serial correlation. *Quarterly Journal of the Royal Meteorological Society*, 136(646):77–90, 2010.

Francesco Serinaldi. Distributional modeling and short-term forecasting of electricity prices by generalized additive models for location, scale and shape. *Energy Economics*, 33(4):1216–1226, 2011.

Michael Sewalt and Cyriel de Jong. Negative prices in electricity markets. *Commodities Now. Available at http://www.erasmusenergy.com/articles/91/1/Negative-prices-in-electricity-markets/Page1.html*, 2003.

Simon J. Sheather and M. C. Jones. A reliable data-based bandwidth selection method for kernel density estimation. *Journal of the royal statistical society. Series B*, 53(3):683–690, 1991.

James W. Taylor. Using exponentially weighted quantile regression to estimate value at risk and expected shortfall. *Journal of Financial Econometrics*, 6:382–406, 2008.

James W. Taylor and Patrick E. McSharry. Short-term load forecasting methods: An evaluation based on european data. *IEEE Transactions on Power Systems*, 22(4):2213–2219, 2007.

PAPER H

Exponential Smoothing Approaches for Prediction in Electricity Regulation Markets

Authors:
T. Jónsson, P. Pinson, H. Aa. Nielsen, H. Madsen

Submitted to:
Energy Economics (2012)

Exponential Smoothing Approaches for Prediction in Real-Time Electricity Markets

Tryggvi Jónsson[1,2] Pierre Pinson[2] Henrik Aa. Nielsen[1] Henrik Madsen[2]

Abstract

Alternative bidding strategies for wind power are commonly evaluated based on constant expectations for the real-time prices in the literature. This is the case despite the potential gains of accounting for the varying price dynamics are obvious and necessary under practical circumstances. In this paper, methods for accommodating the short-term dynamics of the prices are derived and analysed. The models presented are all based on the well known Holt-Winters model with a daily seasonal cycle, either in its conventional form or conditioned upon exogenous variables chosen among forecasts of: (i) the day-ahead price, (ii) the system load and (iii) the system wind power penetration. The proposed models' superiority over the aforementioned commonly applied climatology model is subsequently demonstrated by a case study, mimicking practical forecasting for a 3 year period during 2008-2011.

1 Introduction

In parallel to recent years' rapid growth in electricity generation by renewable energy sources, producers are increasingly urged to sell their generation though the market. This has triggered the interest of both researchers and practitioners in proposing optimal bidding strategies for renewable energy producers as balance responsible parties (BRPs) in deregulated electricity markets. Especially wind power has been in focus due to its leading role among recently emerged renewable energy sources. The wind power producer's point of view will also be considered here for the sake of an example. Although other market participants may be interested in the forecasting of regulation market quantities for similar reasons. Wind power production is a stochastic process with limited predictability on a day-ahead basis. Accordingly bidding strategies for wind power producers are derived as a stochastic optimisation problem. The optimisation's objective commonly is to minimise a function of the expected cost and risk induced by their (involuntary) participation in the real-time imbalance market (also referred to as regulation market) (Bremnes, 2004, Matevosyan and Söder, 2006, Pinson

[1]ENFOR A/S, Lyngsø Allé 3, DK-2970 Hørsholm, Denmark
[2]DTU Informatics, Technical University of Denmark, Richard Petersens Plads, building 321, DK-2800 Kgs. Lyngby, Denmark

et al., 2007, Zugno et al., 2012, Morales et al., 2010, Gibescu et al., 2008, Galloway et al., 2006, Rahimiyan et al., 2011).

The unit regulation costs (per MWh of imbalance) in the real-time market are dynamic and asymmetric (Skytte, 1999). As shown by Gneiting (2010) for the general case and by Bremnes (2004) for wind power specifically, this makes common bidding procedures solely based on the expected generation for every lead time sub-optimal. Instead, the bid maximising expected revenues is found to be a particular quantile of predictive production densities. The nominal proportion of this quantile is a direct function of expected unit regulation costs in the real-time market, also referred to as imbalance penalties. Despite their obvious impact on the performance of trading strategies, these quantities are often assumed deterministic and known (Matevosyan and Söder, 2006), or modelled based on long-term averages (Pinson et al., 2007, Gibescu et al., 2008, Galloway et al., 2006) thus disregarding the short-term dynamics of the real-time market. Under similar assumptions Boogert and Dupont (2005) conclude that gaming in general can not be profitable. Recently though, Zugno et al. (2012), Morales et al. (2010) and Rahimiyan et al. (2011) have taken into account short-term variations in the penalties with considerable benefits. The drawback of the approach Morales et al. (2010) and Rahimiyan et al. (2011) take for modelling the real-time market is that it is not able to accommodate negative prices which are the reality of many electricity markets. Furthermore, information which in not available before the market gate-closure is utilised. In contrast, the results of Zugno et al. (2012) are obtained using the forecasting methodology described in the present paper, hence yielding optimal bids based entirely on predictions from readily available information prior to gate closure.

The objective of this paper is to rigorously model and predict imbalance penalties at lead-times of interest when trading wind power on a day-ahead market, in an exponential smoothing framework. The very characteristics of electricity markets prompt the task of modelling the real-time electricity prices to differ substantially from conventional time-series modelling. Excessive volatility and skewness aside, anti-gaming policies have in many cases caused these prices to have unique dynamic features. For one, the widely adopted dual pricing scheme for regulating power (which implies different pricing for producers in surplus and deficit) induces a regime-switching behaviour of the prices. In other words, the dynamics of the two prices are heavily affected by the net balance of the system. Additionally, some markets have real-time prices that are bounded by the day-ahead price (e.g. the Danish and the Spanish ones) or capped in another manner (e.g. the PJM and the New England markets in the USA) to discourage gaming even further. This feature magnifies the state dependency of the prices since they either share characteristics with the day-ahead prices or have their own unique dynamics. Furthermore, this policy arguably inflates the volatility in the real-time market through reduced supply.

Conditioning models for the real-time prices on the net balance of the whole system is paramount for capturing relevant price dynamics. This in turn makes popular time series models like the seasonal ARMA model used in Morales et al. (2010) inadequate, since this type of model does not account for this regime-switching behaviour. Olsson and Söder (2008) introduced a Markov-switching seasonal ARIMA model with time-inhomogeneous transition probabilities for addressing this issue, though with the

following pitfalls. Firstly, the transition probabilities are time-invariant, hence ignoring the short-term variations in state probabilities, while such variations are shown to be substantial in this paper. Secondly the lack of auto-correlation between day-ahead lags causes the time-inhomogeneous transition probabilities to converge to the homogeneous ones rather quickly, and for lead-times shorter than those required for bidding into a day-ahead market. Put differently, the transition probability matrices for lead-times required for day-ahead trading of wind power contain only the empirical steady state distribution during the period the estimation is based on.

The idea behind the prediction approach introduced here is to take advantage of the formulation of imbalance costs as the product of two variables: (i) a categorical one representing the sign of the net system balance, and (ii) a penalty part describing the magnitude of imbalance penalties when active. Combining predictions for these two variables by applying the law of total expectation then yields the expected imbalance costs. Both variables are modelled using Holt-Winters models (Winters, 1960) with a daily seasonal cycle, either in its conventional form or conditioned by exogenous variables. The proposed approach is to be evaluated against the climatological benchmark, for each individual variable and for the final expected imbalance penalties.

The remainder of the paper is structured as following: Section 2 gives an overview of the empirical context of the paper and describes the data used for the analysis. Afterwards, the necessary definitions and data analysis is presented in Section 3. The models and parameter estimation procedures are given in Section 4 followed by numerical results in Section 5. Finally, concluding remarks are given in Section 6.

2 Electricity Exchanges and the Specifics of Nord Pool

2.1 Generalities

Day-ahead electricity markets are the result of a general movement around the world towards deregulation in the electricity industry over the past two decades. The aim of the deregulation policies has been to replace regulated regional or national monopolies with competitive market environments. Although the actual implementation varies between countries and regions, the basic functionalities remain similar among those who have adopted these policies. A market is organised, typically by an independent market operator, where producers and retailers trade electricity with gate-closure on the day before the physical exchange or even later. In addition, so-called over-the-counter (OTC) contracts are common. These are agreements for electricity exchange with delivery periods ranging from days or weeks up to years. Finally, a real-time market (often termed imbalance market) is operated where deviations from previously entered contracts are settled in real-time.

Due to the expensive and highly specialised system required for transmitting electricity,

the transmission systems have typically either remained under public control or with a thoroughly regulated private monopoly. Depending on location these monopolies are referred to as a Transmission System Operator (TSO) or an Independent System Operator (ISO) which then also acts as a market operator. Similar structure is widely adopted for the distribution network.

The TSOs are responsible for the operation of the transmission network and thereby for maintaining the balance between supply and demand, which is crucial for the operation of the system. The real-time market is therefore in many cases operated by the TSO even though other markets are operated by a third party. Trading on these market is often discouraged by a market structure unfavourable for speculation or gaming. In addition, producers are obliged to bid their full available capacity into the day-ahead market in some areas.

2.2 Nord Pool and the Danish Electricity Market

The Danish electricity market is a part of the Nord Pool market which is the world's first multinational electricity market. It was founded by Statnett SF and Svenska Kraftnät (the Norwegian and the Swedish TSOs respectively) in 1996. Since it has been gradually expanded to encompass Denmark, Finland and Estonia as well. In 2002 physical exchange activities were demerged into a separate company, Nord Pool Spot which operates the markets. Nord Pool Spot ASA is jointly owned by Statnett SF, Svenska Kraftnät (30% each), the Danish and the Finnish TSOs, Energinet.dk and Fingrid Oy respectively (20% each). Nord Pool's market share is one of the highest in the world with 72% of the total Nordic consumption traded on its markets in 2009 (Nord Pool Spot AS, 2010). In 2010 and 2011 the market share rose to 74% and 75% respectively (Nord Pool Spot AS, 2011b, 2012).

The market region is divided into 10 price areas, bordered by bottlenecks in the transmission grid and with internal transmission capacity practically infinite. Denmark comprises two of these areas, one on either side of the Storebælt channel.

Nord Pool runs two different markets for physical exchange of electricity, Elspot and Elbas. Elspot is a day-ahead market with gate-closure at noon on the day before delivery. Here producers and retailers bid for the sale and purchase of electricity in hourly intervals. Once the bids are collected, a system price is determined as the intersection between the aggregated supply and demand curves. The system price is the price at which physical exchange is settled during hours where transmission across the grid bottlenecks does not reach their capacity. Besides, the system price serves as a reference price for almost all financial derivatives linked to Nord Pool. In case the desired transmission across price area borders reaches its capacity, multiple area prices are defined. An area price is determined by the same procedure as the system price however only considering the bids from the particular area and the full utilisation of the connections to the surrounding areas as price independent bids. Elbas is opened for trading once the Elspot prices have been published and has gate-closure 1 hour prior to delivery. Elbas is a bid-ask market where bids for either purchase or sale of electricity are placed.

The bids are prioritised according to price and submission time and are settled at the bid price. The acceptance of a bid across price areas is subject to capacity availability. Almost the entire exchange takes place on Elspot, which is responsible for more than 99% of the total exchanged volume each year. A more detailed description of the market environment and price settlement is provided in Nord Pool Spot AS (2011a).

In addition, the national TSOs each run a real-time market in their countries for balancing the transmission grid. Markets for supplier imbalances and retailer imbalances are run separately and with different pricing schemes. For the retailers a single-price is defined at which those short of their contracted volume buy the surplus of those having overestimated their consumption at the time. In contrast, two prices are defined on the suppliers' market. The producers short of their contracts buy their deficits at the up-regulation price while those overproducing sell their surplus at the down-regulation price. The regulation prices are bounded by the Elspot prices so that the up-regulation price can never deceed it and the down-regulation price can never exceed it. Furthermore, imbalances that negate the total system imbalance are not penalised. This implies that at any given time, either the up-regulation or the down-regulation price is equal to the spot price.

2.3 Available Data for the Study

The data which the empirical results of this paper are based on comprise hourly data for the period from November 2008 and through December 2011. The data set contains hourly spot-and regulation prices for the Western Danish price area of Elspot (DK-1) along with forecast system load, wind power production and spot prices for the same area. All forecasts are issued before noon on the day before delivery and like the price data have a temporal resolution of one hour. The observed prices and the load forecasts have been made publicly available by Nord Pool through their website, www.nordpoolspot.com. The spot price forecast is obtained by the method described in Jónsson et al. (2012) and the wind power forecasts stem from a commercially available wind power prediction software (Nielsen et al., 2002). Due to difference currency conversion procedures between Nord Pool and Energinet.dk, prices are rounded off to the first decimal.

3 Problem Formulation and Data Analysis

The purpose of the data analysis that follows is to establish the necessary properties of models for the imbalance cost and to identify potentially influential exogenous variables. Only results that seemed to deserve further inspection are presented.

3.1 Background and Variable Definition

Let $\pi_t^{(S)}$ be the day-ahead area price at hour t and let $\pi_t^{(\downarrow)}$ and $\pi_t^{(\uparrow)}$ be the down-and up regulation prices for the same hour respectively. In addition, let $\psi_t^{(\downarrow)}$ and $\psi_t^{(\uparrow)}$ denote the down-and up regulation penalty during hour t respectively, defined as

$$\psi_t^{(\downarrow)} = \pi_t^{(S)} - \pi_t^{(\downarrow)} \tag{1}$$
$$\psi_t^{(\uparrow)} = \pi_t^{(\uparrow)} - \pi_t^{(S)}. \tag{2}$$

Zugno et al. (2012), Pinson et al. (2007) and Bremnes (2004) all show the bid that maximises the expected hourly revenue of a price taking wind power producer, $\widetilde{W}_t^*$, to be found as

$$\widetilde{W}_t^* = F_{W_t}^{-1}\left(\frac{\widehat{\psi}_{t|t-k}^{(\downarrow)}}{\widehat{\psi}_{t|t-k}^{(\downarrow)} + \widehat{\psi}_{t|t-k}^{(\uparrow)}}\right) \tag{3}$$

where $F_{W_t}^{-1}(\cdot)$ is the inverse cumulative density function (CDF) of the wind power production during hour t. Furthermore,

$$\widehat{\psi}_{t|t-k}^{(\downarrow)} = \mathbb{E}\left[\psi_t^{(\downarrow)}|\chi_{t-k}\right] \tag{4}$$
$$\widehat{\psi}_{t|t-k}^{(\uparrow)} = \mathbb{E}\left[\psi_t^{(\uparrow)}|\chi_{t-k}\right] \tag{5}$$

are the expected imbalance penalties, conditional on the information available before gate-closure of the spot market, χ_{t-k}. In order to ease the notation, $\widehat{\psi}_{t|t-k}^{(\downarrow)}$ and $\widehat{\psi}_{t|t-k}^{(\uparrow)}$ will be noted as $\widehat{\psi}_t^{(\downarrow)}$ and $\widehat{\psi}_t^{(\downarrow)}$ from here on. For the same purpose $\mathbb{E}[\cdot|\chi_t]$ is denoted $\mathbb{E}[\cdot]$ in the following.

The regulatory framework of Nord Pool implies that the following conditions are fulfilled at all times:

$$\pi_t^{(\uparrow)} \geq \pi_t^{(S)} \Rightarrow \psi_t^{(\uparrow)} \geq 0 \quad \forall t \tag{6}$$
$$\pi_t^{(\downarrow)} \leq \pi_t^{(S)} \Rightarrow \psi_t^{(\downarrow)} \geq 0 \quad \forall t \tag{7}$$
$$\pi_t^{(\uparrow)} = \pi_t^{(S)} \Rightarrow \psi_t^{(\uparrow)} = 0 \quad \text{if } \pi_t^{(\downarrow)} < \pi_t^{(S)} \quad \forall t \tag{8}$$
$$\pi_t^{(\downarrow)} = \pi_t^{(S)} \Rightarrow \psi_t^{(\downarrow)} = 0 \quad \text{if } \pi_t^{(\uparrow)} > \pi_t^{(S)} \quad \forall t. \tag{9}$$

The first two conditions are a result of the fact that the real-time prices are bounded by the spot price while the later two conditions are owed to that only producers that contribute to the overall imbalance are penalised. From a producer's point of view, these conditions allow for the relationship between the spot market and the real-time market to be categorised in three discrete states. These are down-regulation hours (production

surpluses penalised), no regulation hours (no imbalances penalised) and up-regulation hours (production deficits penalised) and are defined mathematically as

$$I_t^{(\psi)} = \operatorname{sgn}\{\psi_t^{(\uparrow)} - \psi_t^{(\downarrow)}\} = \begin{cases} 1 & \text{during up-regulation hours} \\ 0 & \text{during hours of no regulation penalty} \\ -1 & \text{during down-regulation hours} \end{cases}. \tag{10}$$

Note that for the system operator, these states are not necessarily the same since it operates in higher temporal resolution with the actual physical balance of the system, which can change signs within an hour and is seldom precisely zero. The no regulation hours thus comprise both hours of no physical regulation and hours where balancing power has been inexpensive enough not to prompt a penalty for those subject to the regulation. However, since the producer's main objective is to maximise his revenue, regardless of the exact physical balance of the system, it is primarily the price differences that are relevant for the producer. Consequently, the following modelling efforts are all done in terms of the price difference and not the physical imbalance.

By applying the law of total expectation, Eqs. (4) and (5) can be written as

$$\mathbb{E}\left[\psi_t^{(\uparrow)}\right] = \mathbb{P}(\psi_t^{(\uparrow)} > 0) \cdot \mathbb{E}\left[\psi_t^{(\uparrow)} | \psi_t^{(\uparrow)} > 0\right] + \mathbb{P}(\psi_t^{(\uparrow)} = 0) \cdot 0 \tag{11}$$

$$\mathbb{E}\left[\psi_t^{(\downarrow)}\right] = \mathbb{P}(\psi_t^{(\downarrow)} > 0) \cdot \mathbb{E}\left[\psi_t^{(\downarrow)} | \psi_t^{(\downarrow)} > 0\right] + \mathbb{P}(\psi_t^{(\downarrow)} = 0) \cdot 0. \tag{12}$$

This allows for partitioning the problem into estimation of the probabilities of regulation in each direction, hereafter termed the imbalance sign, and forecasting of the penalties conditioned on them being different from zero.

The appeal of dividing the problem up like this is twofold. Firstly, the chance of obtaining an acceptable description of the penalties, when actually realised, is higher. Especially this is the case when the use of external explanatory variables is considered since certain circumstances could for instance otherwise result in either a zero penalty or extremely high penalty thus mitigating the observed effect of that variable. Secondly, this approach allows for a more intuitive approach for scenario generation. On the other hand, for applications where only the expected penalty is required, estimating a model on the full series (including the zeros) could perform similarly if no helpful explanatory variables are found.

From a modelling perspective, working with the penalties, opposed to the actual prices has some advantages as well. For one, the penalties have a constant lower boundary at zero, which to some extent can mitigate high positive residuals. More importantly though, the penalty forecasts are applicable at all horizons, both day-ahead and intraday. Combined with the current available information about the spot prices, they form a prediction for the regulation prices. Finally, a model for the penalties is more versatile in terms of applications. When for instance the strategy in Zugno et al. (2012) is extended, first to accommodate the price risk of a price taking producer and subsequently to a price maker, the problem is most easily solved by stochastic programming which in turn calls for stochastic scenarios to be generated (Jónsson et al., 2012). Due to the

hierarchical structure of the market, scenarios that respect the regulatory framework of the market are best found via predictions of the regulation penalties and not the prices (Jónsson, 2012).

Finally for estimation and analysis purposes, three additional variables are defined. Following standard estimation procedures for a multinomial regression model, $I_t^{(\psi)}$ can be decomposed into a (row)vector of binary variables as

$$\begin{aligned} \boldsymbol{I}_t^{(\uparrow/\downarrow)} &= \left[\begin{array}{ccc} I_{t,1}^{(\uparrow/\downarrow)}, & I_{t,2}^{(\uparrow/\downarrow)}, & I_{t,3}^{(\uparrow/\downarrow)} \end{array} \right] \\ &= \left[\begin{array}{ccc} \mathbf{1}\{\pi_t^{(\downarrow)} < \pi_t^{(S)}\}, & \mathbf{1}\{\pi_t^{(S)} = \pi_t^{(\downarrow)} = \pi_t^{(\uparrow)}\} & \mathbf{1}\{\pi_t^{(\uparrow)} > \pi_t^{(S)}\} \end{array} \right] \end{aligned} \tag{13}$$

for which it holds that

$$\sum_{i=1}^{3} I_{i,t}^{(\uparrow/\downarrow)} = 1.$$

For the penalties, let

$$\begin{aligned} \widehat{\psi}_{t|>0}^{(\downarrow)} &= \mathbb{E}\left[\psi_t^{(\downarrow)} | \psi_t^{(\downarrow)} > 0\right] \\ \widehat{\psi}_{t|>0}^{(\uparrow)} &= \mathbb{E}\left[\psi_t^{(\uparrow)} | \psi_t^{(\uparrow)} > 0\right] \end{aligned} \tag{14}$$

and let $\psi_{t|>0}^{(\downarrow)}$ and $\psi_{t|>0}^{(\uparrow)}$ be the corresponding observations which are undefined during up-and down-regulation hours respectively and otherwise equal to $\psi_t^{(\downarrow)}$ and $\psi_t^{(\uparrow)}$ respectively.

3.2 Non-stationarity

The penalty series, $\psi_{t|>0}^{(\uparrow/\downarrow)}$ include a few spikes of such magnitude that their inclusion in an estimation set for a statistical model would lead to parameter estimates solely focusing on capturing these extremes. Thus these extremes are removed from the data set after being chosen by the procedure described in Jónsson (2012). The unmodified time series are plotted in the top row of Figure 1 where the removed observations have been marked with a cross. In total there are removed 85 and 29 observations from the up-and down regulation penalty series respectively. Cleaned versions of the series are shown in the bottom row of the same figure. They reveal considerable time-variations in the first and second order moments of the penalties. The mean constantly fluctuates and volatile periods with quite frequent price spikes are followed by periods of relative tranquillity.

Table 1, summarises the empirical probabilities, $\overline{\boldsymbol{I}}^{(\uparrow/\downarrow)}$, for the states of $\boldsymbol{I}_t^{(\uparrow/\downarrow)}$. The table reveals the dominance of down regulation in long-term expectation while the other two states' probabilities are quite similar.

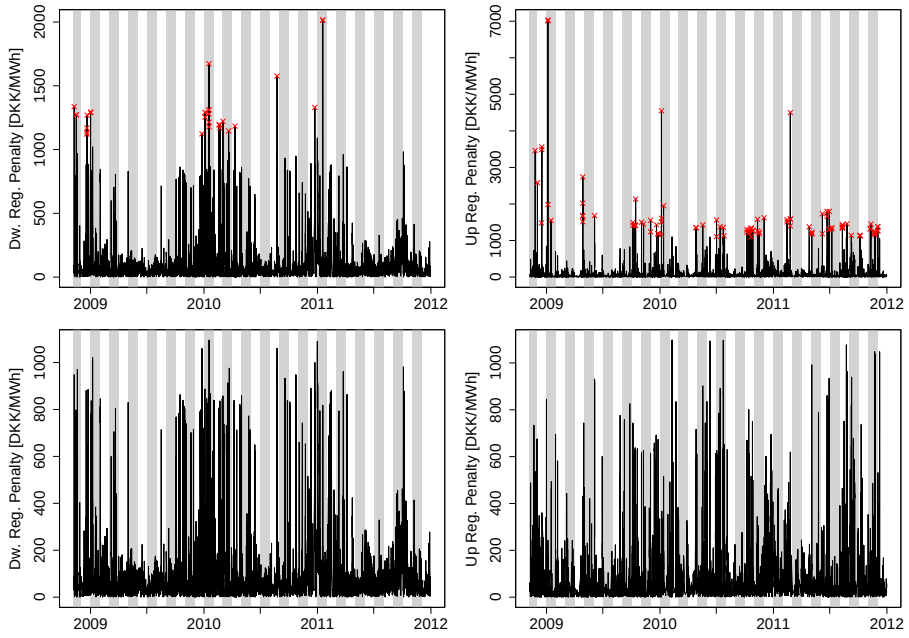

Figure 1: Time series plot of the down-and up-regulation penalties (left and right respectively) with the excluded observations marked.

Let $\widehat{\boldsymbol{I}}_t^{(\uparrow/\downarrow)}$ denote the exponentially smoothed average if $\boldsymbol{I}_t^{(\uparrow/\downarrow)}$, updated at every time t by

$$\widehat{\boldsymbol{I}}_t^{(\uparrow/\downarrow)} = \lambda \boldsymbol{I}_t^{(\uparrow/\downarrow)} + (1-\lambda)\widehat{\boldsymbol{I}}_{t-1}^{(\uparrow/\downarrow)} \tag{15}$$

where $0 < \lambda < 1$ is a smoothing parameter. Should the probabilities of each regulation scenario be constant over the period from T_0 until T_N, $\widehat{\boldsymbol{I}}_t^{(\uparrow/\downarrow)}$, should oscillate around $\overline{\boldsymbol{I}}^{(\uparrow/\downarrow)}$ with deviations inversely related to λ. However as the plots in Figure 2 illustrate, this is not the case for the imbalance sign probabilities. The bottom two plots show the tracking of a series simulated from a trinomial distribution with probabilities of each instance equal to the empirical probabilities from Table 1. The top two plots on the other hand, show the tracking of the actual occurrences of regulation in each direction. Forgetting factors $\lambda = 0.99$ and $\lambda = 0.999$ were applied for the two plots on the left and on the right respectively.

Table 1: The nominal probabilities of $\boldsymbol{I}^{(\uparrow/\downarrow)}$ for the data period.

$\downarrow$	$\sim$	$\uparrow$
39.00%	29.30%	31.70%

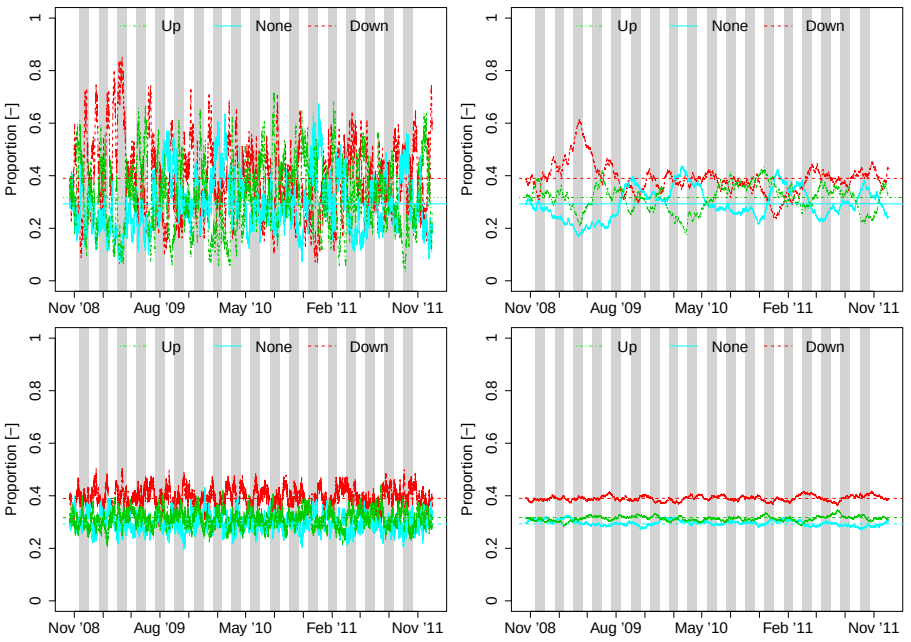

Figure 2: Exponentially smoothed state probabilities of the observed $\boldsymbol{I}^{(\uparrow/\downarrow)}$ (top row) and the simulated $\boldsymbol{I}^{(\uparrow/\downarrow)}$ (bottom row) with $\lambda = 0.99$ (left column) and $\lambda = 0.999$ (right column). The horizontal lines represent the nominal probabilities for the whole period.

For both λ's the observed series deviates considerably more from the empirical probabilities and seems to drift distinctively away from them over shorter periods. The plots therefore provide a clear indication that greater knowledge about next day's imbalance sign can be obtained by considering the probabilities more local in time.

3.3 Seasonality

Mainly driven by the daily and weekly cycles of the consumption, electricity prices are generally known to have the same seasonal cycles. Thus it seems natural to examine the seasonalities of $\boldsymbol{I}_t^{(\uparrow/\downarrow)}$ and $\psi_{t|>0}^{(\uparrow/\downarrow)}$.

Figure 3 shows the hourly averages of $\boldsymbol{I}_t^{(\uparrow/\downarrow)}$ and $\psi_{t|>0}^{(\uparrow/\downarrow)}$ for each hour of the day and the week relative to the corresponding empirical means. For the imbalance sign there is an apparent diurnal variation for the up- and no-regulation hours. For the down-regulation hours, the diurnal variation is less distinctive yet there seems to be some evidence of such behaviour. Furthermore, the frequency of up-regulation hours seems

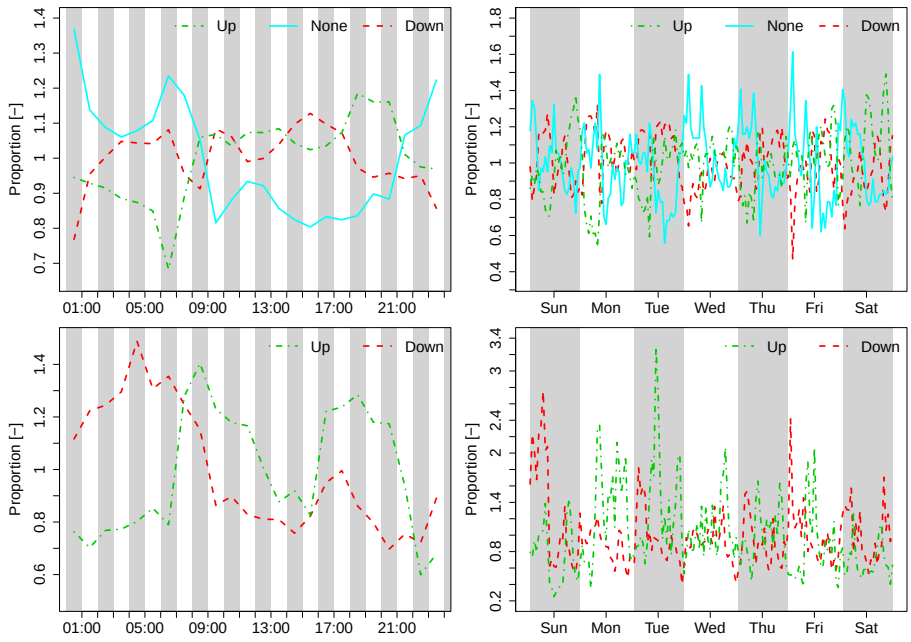

Figure 3: The intra-day and intra-week variations (left and right columns respectively) of the imbalance sign (top row) and the imbalance penalties (bottom row) relative to the corresponding empirical average.

to exhibit stronger diurnal variation during the weekends than during working days whereas the opposite is observed for the no regulation hours. The diurnal variation of the frequency of down-regulation hours seems to be quite consistent throughout the week.

The penalties have an obvious diurnal seasonality where the up-regulation penalties are generally above average during the day and below average during the night while the down-regulation penalties exhibit the opposite pattern. Given the high share of hours where $\psi_{t|>0}^{(\uparrow/\downarrow)}$ is not defined, segmenting the penalties according to the hour of the week dilutes the data quite severely. The excessive fluctuations seen in the bottom-right plot of Figure 3 should therefore be interpreted with caution. The magnitude aside the daily seasonal cycle seems to be consistent throughout the entire week.

3.4 Exogenous Variables

Figure 4 illustrates the impacts of external variables detected for the imbalance sign and penalties. The plots in the figure are constructed by segmenting the data into 10 equally populated bins according to the value of the variable on the x-axis and the sign

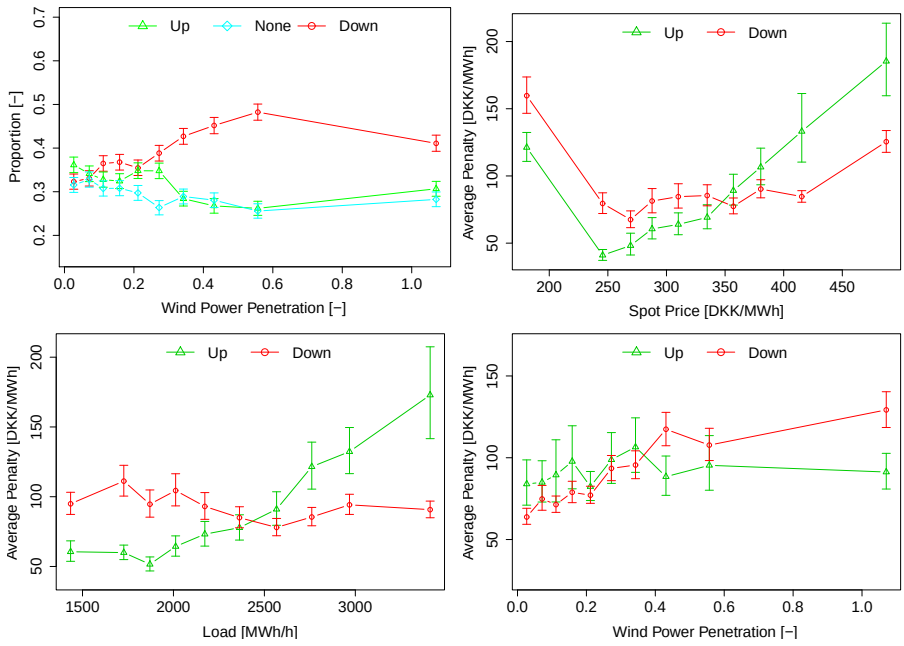

Figure 4: The empirical frequency of each imbalance sign as a function of the forecast wind power penetration (top-left) and the average imbalance penalties as a function of the forecast spot price (top-right), the forecast load (bottom-left) and the predicted wind power penetration (bottom-right).

frequency or average penalty for each bin plotted against the bin median. Along with the mean of each bin, 95% confidence intervals are drawn, found by bootstrapping (see (Efron and Tibshirani, 1986)). The top-left plot in Figure 4 shows the empirical frequencies of each imbalance sign as a function of the forecast wind power penetration. The wind power penetration is defined as the ratio between the forecast wind power production and the forecast load. The purpose of its usage, instead of the actual production forecasts, is to account wind power's varying ability to affect the market outcome depending on demand (Jónsson et al., 2010). The remaining three plots in Figure 4 show the average imbalance penalties as a function of the forecast spot price (top-right), load (bottom-left) and wind power penetration (bottom-right).

The top-left plot indicates a considerable relation between the forecast wind power penetration and the imbalance sign once this production is realised. The top-right plot shows that both penalties are significantly affected by the forecast spot price. Even though some of the middle points are not significantly different from their neighbours, there are significant differences between points further apart. Similar conclusions can be drawn for the impact of the forecast load on the up regulation penalty and for the impact of forecast wind power penetration on the down regulation penalty. The forecast load

however does not seem to impact the down regulation penalty more than marginally. Likewise the up regulation penalties seem to be merely affected by the forecast wind power penetration.

The previously demonstrated time-variation and seasonal cycles of $\boldsymbol{I}_t^{(\uparrow/\downarrow)}$ and $\psi_{t|>0}^{(\uparrow/\downarrow)}$ is not taken into account here. It hence prevents any final conclusions to be drawn from the plots. The question of whether or not the imbalance sign and penalties are affected by these variables will be answered by examining whether a model including this information has a forecasting skill superior to a model that does not.

4 Holt-Winters Model for the Imbalance Sign and Penalty

The Holt-Winters model (HW model) is a pragmatic approach to model seasonal time series. The standard formulation of the HW model, suitable for series with a single seasonal pattern, was introduced by Winters (1960). In Taylor (2003) the HW model is extended to accommodate multiple seasonal patterns. The model can be formulated either as an additive or a multiplicative one and Hyndman et al. (2008) and Hyndman et al. (2002) provide an excellent overview of different possible formulations. In light of the vast existing literature on the generalities of HW models, the discussion is limited here to the relevant formulations used at various modelling stages.

4.1 Standard Holt-Winters

For a stochastic process, $\boldsymbol{Y}_t = [y_0, y_1, \ldots]$ for $t = [0, 1, \ldots]$, an additive double seasonal HW model without a trend term can be written as:

$$\mu_t = \alpha_\mu (y_t - (S_{t-s_1}^{(1)} + S_{t-s_2}^{(2)})) + (1-\alpha)\mu_{t-1} \tag{16}$$

$$S_t^{(1)} = \alpha_{S^{(1)}} (y_t - (\mu_t + S_{t-s_2}^{(2)})) + (1-\alpha_{S^{(1)}}) S_{t-s_1}^{(1)} \tag{17}$$

$$S_t^{(2)} = \alpha_{S^{(2)}} (y_t - (\mu_t + S_{t-s_1}^{(1)})) + (1-\alpha_{S^{(2)}}) S_{t-s_2}^{(2)} \tag{18}$$

where s_1 and s_2 are the periods of seasonal components $S^{(1)}$ and $S^{(2)}$ respectively while α_μ, $\alpha_{S^{(1)}}$ and $\alpha_{S^{(2)}}$ are smoothing parameters. After the updating step in Eqs. (16) - (18), the k-step ahead prediction, $\widehat{y}_{t+k|t}$, can be found as

$$\widehat{y}_{t+k|t} = \mu_t + S_{t-s_1+k}^{(1)} + S_{t-s_2+k}^{(2)}. \tag{19}$$

Similarly, a multiplicative HW model for $\boldsymbol{Y}_t$ with two seasonal cycles can be defined as:

$$\mu_t = \alpha_\mu (y_t / (S^{(1)}_{t-s_1} S^{(2)}_{t-s_2})) + (1-\alpha)\mu_{t-1} \tag{20}$$

$$S^{(1)}_t = \alpha_{S^{(1)}} (y_t / (\mu_t S^{(2)}_{t-s_2})) + (1-\alpha_{S^{(1)}}) S^{(1)}_{t-s_1} \tag{21}$$

$$S^{(2)}_t = \alpha_{S^{(2)}} (y_t / (\mu_t S^{(1)}_{t-s_1})) + (1-\alpha_{S^{(2)}}) S^{(2)}_{t-s_2} \tag{22}$$

for which the definitions of s_1 and s_2 are as before while

$$\widehat{y}_{t|t-k} = \mu_t S^{(1)}_{t-s_1+k} S^{(2)}_{t-s_2+k} \tag{23}$$

By defining the one step prediction error as

$$\varepsilon_{t|t-1} = y_t - \widehat{y}_{t|t-1} \tag{24}$$

and following Gelper et al. (2010), the models can be made robust by defining

$$y^{(*)}_t = \widehat{y}_{t|t-1} + g(\varepsilon_{t|t-1}, \tau) \tag{25}$$

where $g(\cdot, \tau)$ is the Huber influence function

$$g(u,\tau) = \begin{cases} u & \text{if } |u| <= \tau \\ \text{sgn}(u) \cdot \tau & \text{if } |u| > \tau \end{cases} \tag{26}$$

and substitute $y^{(*)}_t$ for y_t in Eqs. (16) - (18) or Eqs. (20) - (22).

In compliance with the common formulation of the HW model in the literature Eqs. (16) - (18) can be written on their more compact error correction form as

$$\mu_t = \mu_{t-1} + \alpha_\mu g(\varepsilon_{t|t-1}, \tau) \tag{27}$$

$$S^{(1)}_t = S^{(1)}_{t-s_1} + \alpha_{S^{(1)}} g(\varepsilon_{t|t-1}, \tau) \tag{28}$$

$$S^{(2)}_t = S^{(2)}_{t-s_2} + \alpha_{S^{(2)}} g(\varepsilon_{t|t-1}, \tau). \tag{29}$$

It is readily seen that letting $\tau = \infty$ yields a non-robust HW model.

Should a single seasonal pattern be sufficient, Eqs. (18), (22) and (29) are simply omitted from the models. Correspondingly, the second seasonal term vanishes from the prediction equations (23) and (19).

4.2 Conditional Holt-Winters Model

In order to account for the effects of external variables, e.g. forecast spot price, wind power penetration and load, the previously described HW models can be conditioned on exogenous variables. Let $\boldsymbol{X}_t = [x_0, x_1, \ldots]$ for $t = [0, 1, \ldots]$ be a variable on which $\boldsymbol{Y}_t$ arbitrarily depends on. Inspired by Cleveland and Devlin (1988), let $\boldsymbol{x}_i$, $i \in [1, \ldots, M]$

be a particular fitting point in a set of M distinct fitting points in $\boldsymbol{X}_t$. At each $\boldsymbol{x}_i$ a HW model like the ones given either by Eqs. (20)-(22) or by (27)-(29) can describe the dynamics of $\boldsymbol{Y}_t$ in the close vicinity of $\boldsymbol{x}_i$. A model fully describing $\boldsymbol{Y}_t$ can then be found as a series of M different HW models each on the same form as given previously. Now however, the smoothing in each model at time t is not only done in time but also by weighting the observations according to the Euclidean distance between x_t and $\boldsymbol{x}_i$. The weights are assigned as

$$v_{\boldsymbol{x}_i}(x_t) = V\left(\frac{||x_t - \boldsymbol{x}_i||}{h(\boldsymbol{x}_i)}\right) \tag{30}$$

where $V(\cdot)$ is a function taking non-negative arguments, $||\cdot||$ denotes the Euclidean norm and $h(\boldsymbol{x}_i)$ is the bandwidth applied in the fitting point $\boldsymbol{x}_i$. Following Cleveland and Devlin (1988) and Nielsen et al. (2000) a tri-cube kernel used to determine the weights. That is

$$V(u) = \begin{cases} (1-u^3)^3 & \text{if } u \in [0;1) \\ 0 & \text{otherwise} \end{cases} \tag{31}$$

which entails weights between 0 and 1. A nearest-neighbour bandwidth is employed here. This implies that the actual bandwidth varies with the local density of the data since $h(\boldsymbol{x}_i)$ is set as the range of the $(\gamma \cdot 100)\%$ closest observation to each $\boldsymbol{x}_i$ where $0 \leq \gamma \leq 1$ is the relative bandwidth, common for all fitting points.

Now define $\boldsymbol{\alpha} = [\ \alpha_\mu \quad \alpha_{S^{(1)}} \quad \alpha_{S^{(2)}}\ ]$ and subsequently find the effective smoothing parameters at time t and for fitting point $\boldsymbol{x}_i$ as

$$\boldsymbol{\alpha}^{(eff)}(t,i) = \boldsymbol{\alpha} v_{\boldsymbol{x}_i}(x_t). \tag{32}$$

The robust conditional HW model thus consists of M models, for which the additive version of the updating formulae for the ith model can be written as

$$\mu_{t,i} = \mu_{t-1,i} + \alpha_\mu^{(eff)}(t,i) g(\varepsilon_{t|t-1}, \tau) \tag{33}$$

$$S_{t,i}^{(1)} = S_{t-s_1,i}^{(1)} + \alpha_{S^{(1)}}^{(eff)}(t,i) g(\varepsilon_{t|t-1}, \tau) \tag{34}$$

$$S_{t,i}^{(2)} = S_{t-s_2,i}^{(2)} + \alpha_{S^{(2)}}^{(eff)}(t,i) g(\varepsilon_{t|t-1}, \tau). \tag{35}$$

Similarly the updating scheme for the ith multiplicative HW model becomes

$$\mu_{t,i} = \alpha_\mu^{(eff)}(t,i)(y_t^{(*)} / (S_{t-s_1}^{(1)} S_{t-s_2}^{(2)})) + (1 - \alpha_\mu^{(eff)}(t,i))\mu_{t-1,i} \tag{36}$$

$$S_{t,i}^{(1)} = \alpha_{S^{(1)}}^{(eff)}(t,i)(y_t^{(*)} / (\mu_t S_{t-s_2}^{(2)})) + (1 - \alpha_{S^{(1)}}^{(eff)}(t,i)) S_{t-s_1}^{(1)} \tag{37}$$

$$S_{t,i}^{(2)} = \alpha_{S^{(2)}}^{(eff)}(t,i)(y_t^{(*)} / (\mu_t S_{t-s_1}^{(1)})) + (1 - \alpha_{S^{(2)}}^{(eff)}(t,i)) S_{t-s_2}^{(2)} \tag{38}$$

For a value of x_t with $\boldsymbol{x}_i \leq x_t \leq \boldsymbol{x}_{i+1}$, $y_{t+k|t}$ is found by linear interpolating between $\widehat{y}_{t+k|t,i}$ and $\widehat{y}_{t+k|t,i+1}$.

Although in principle the number of variables used to condition upon could be infinity, one should take caution in doing so due to the risk of sparse updates in the points located close to the edges of the multidimensional space.

4.3 Parameter Estimation

Let $\boldsymbol{\beta}$ be the model parameters:

$$\boldsymbol{\beta} = \begin{cases} [\ \boldsymbol{\alpha} \quad \tau\ ] & \text{for the standard HW model} \\ [\ \boldsymbol{\alpha} \quad \gamma \quad \tau\ ] & \text{for the conditional HW model} \end{cases} \tag{39}$$

Due to the binary nature of the $\boldsymbol{I}_t^{(\uparrow/\downarrow)}$, only the additive formulation of the HW model is feasible for modelling the imbalance sign. Given N observations of $\boldsymbol{I}^{(\uparrow/\downarrow)}$, an estimate $\boldsymbol{\beta}$ can be derived by Maximum Likelihood (ML) estimation or

$$\widehat{\boldsymbol{\beta}} = \arg\max_{\boldsymbol{\beta}} \ell(\boldsymbol{\beta}) \tag{40}$$

where $\ell(\boldsymbol{\beta})$ is the log-likelihood function for a trinomial variable:

$$\begin{aligned} \ell(\boldsymbol{\beta}) = \sum_{t=1}^{N} \Big\{ & I_{t,1}^{(\uparrow/\downarrow)} \log p_{t,1}(\boldsymbol{\beta}) + I_{t,3}^{(\uparrow/\downarrow)} \log p_{t,3}(\boldsymbol{\beta}) \\ & + (1 - (I_{t,1}^{(\uparrow/\downarrow)} + I_{t,3}^{(\uparrow/\downarrow)})) \log(1 - p_{t,1}(\boldsymbol{\beta}) - p_{t,3}(\boldsymbol{\beta})) \Big\} \end{aligned}$$

where in turn $p_{t,i}(\boldsymbol{\beta}) = \mathbb{P}\left(I_{t,i}^{(\uparrow/\downarrow)} = 1 \middle| \boldsymbol{\beta}\right)$. Since a finite value for τ is not meaningful in the context of binary variables, it is fixed at $\tau = \infty$ for $\boldsymbol{I}_t^{(\uparrow/\downarrow)}$

After the updating and the forecasting steps, the inverse logit-transformation is applied for deriving the posterior probabilities for the imbalance sign:

$$\begin{aligned} \widehat{\mathbb{P}}_{t+k|t}\left(I_{t+k}^{(\psi)} = -1\right) = \widehat{\mathbb{P}}_{t+k|t}\left(I_{t+k,1}^{(\uparrow/\downarrow)} = 1\right) &= \frac{\exp\left(\widehat{I}_{t+k|t,1}^{(\uparrow/\downarrow)}\right)}{1 + \exp\left(\sum_{i\in\{1,3\}} \widehat{I}_{t+k|t,i}^{(\uparrow/\downarrow)}\right)} \\ \widehat{\mathbb{P}}_{t+k|t}\left(I_{t+k}^{(\psi)} = 1\right) = \widehat{\mathbb{P}}_{t+k|t}\left(I_{t+k,3}^{(\uparrow/\downarrow)} = 1\right) &= \frac{\exp\left(\widehat{I}_{t+k|t,3}^{(\uparrow/\downarrow)}\right)}{1 + \exp\left(\sum_{i\in\{1,3\}} \widehat{I}_{t+k|t,i}^{(\uparrow/\downarrow)}\right)} \\ \widehat{\mathbb{P}}_{t+k|t}\left(I_{t+k}^{(\psi)} = 0\right) = \widehat{\mathbb{P}}_{t+k|t}\left(I_{t+k,2}^{(\uparrow/\downarrow)} = 1\right) &= \frac{1}{1 + \exp\left(\sum_{i\in\{1,3\}} \widehat{I}_{t,i}^{(\psi)}\right)} \\ &= 1 - \left(\widehat{\mathbb{P}}\left(I_{t+k}^{(\psi)} = -1\right) + \widehat{\mathbb{P}}\left(I_{t+k}^{(\psi)} = 1\right)\right). \end{aligned}$$

For the penalties, both the multiplicative and the additive formulations of the HW models are tried. The estimation procedure is the same for both models though. An estimate of $\boldsymbol{\beta}$ is found by minimising the sum of squared residuals after limiting the forecast to zero or

$$\widehat{\boldsymbol{\beta}} = \arg\max_{\boldsymbol{\beta}} \sum_{i=1}^{N} \left(\psi_{i|>0}^{(\uparrow/\downarrow)} - \max\{0, \widehat{\psi}_{i|>0}^{(\uparrow/\downarrow)}\}\right)^2. \tag{41}$$

In the estimation process, the practical situation for day-ahead bidding of wind power is mimicked. More specifically, the models are fit in the context of forecasts made at 11:00 on the day before realisation. Hence, the lead-time k is identical among forecasts made for each hour of the day but distinct between different hours of the day. So estimates for the hour between 00:00 and 01:00 are found using $k = 13$ while $k = 37$ for the hour between 23:00 and 00:00.

5 Empirical Results

Various versions of the model described in previous section are fit to the data in order to conclude on the appropriate structure. The first 14 months of the data set are taken for parameter estimation and the subsequent 2 years are used as an independent test period. So the data from before January 1st 2010 is taken for estimation while data from 2010 and 2011 is used as a test set. In terms of seasonal cycles, the following model structures are tried:

I Exponential smoothing, i.e. no seasonalities included.

II Single seasonal HW-model with a daily period, i.e. $S^{(1)} = 24$.

III Single seasonal HW-model with a weekly period, i.e. $S^{(1)} = 168$.

IV Double seasonal HW-model with daily and weekly periods, i.e. $S^{(1)} = 24$ and $S^{(2)} = 168$.

Unconditional models are fitted for all three series as well as conditional ones. For the imbalance penalties, conditioning on the forecast spot price, wind power penetration and load, one at a time, is tried as well as every possible combination of two out of these three variables. For the imbalance sign however, the model is only conditioned on the forecast wind power penetration. For all conditional models, fitting points are chosen as the deciles of the explanatory variables in the training set. Since there are in total 56 different versions of the penalty models tried, results are only presented for a few of the best performing ones.

For all models, only one set of parameters is estimated across all lead times and all fitting points for the conditional models. Although this along with the somewhat arbitrarily chosen fitting points might lead to sub-optimal results for individual lead times and fitting points, the obtained results are decisive enough to serve the objective of this paper. Should the model be implemented in practise however, the extra effort of estimating more locally optimal parameters in all likelihood would be worthwhile.

5.1 Imbalance Sign Probabilities

For a more intuitive comparing of the models and to allow comparison between periods, the Discrete Ranked Probability Skill Score (RPSS_D) (Weigel et al., 2007) is calcu-

lated and compared for the models. The RPSS_D is found as

$$\begin{aligned}\text{RPSS}_D &= 1 - \frac{\frac{1}{N}\sum_{t=1}^{T_N}\text{RPS}_{\widehat{\boldsymbol{I}}_t^{(\uparrow/\downarrow)},t}}{\frac{1}{N}\sum_{t=1}^{T_N}\text{RPS}_{\overline{\boldsymbol{I}}^{(\uparrow/\downarrow)},t}} \\ &= 1 - \frac{\sum_{t=1}^{T_N}\sum_{k=1}^{3}\left(\sum_{i=1}^{k}\widehat{I}_{t,i}^{(\uparrow/\downarrow)} - \sum_{i=1}^{k}I_{t,i}^{(\uparrow/\downarrow)}\right)^2}{\sum_{t=1}^{T_N}\sum_{k=1}^{3}\left(\sum_{i=1}^{k}\overline{I}_{i}^{(\uparrow/\downarrow)} - \sum_{i=1}^{k}I_{t,i}^{(\uparrow/\downarrow)}\right)^2 + D}\end{aligned} \tag{42}$$

where $\text{RPS}_{\widehat{\boldsymbol{I}}_t^{(\uparrow/\downarrow)},t}$ and $\text{RPS}_{\overline{\boldsymbol{I}}^{(\uparrow/\downarrow)},t}$ are the Ranked Probability Scores (Epstein, 1969, Murphy, 1969, 1971) of the estimated posterior probabilities and the climatology forecasts respectively. Furthermore, D is a bias correction term found as

$$D = \frac{1}{N}\sum_{k=1}^{3}\sum_{i=1}^{k}\left[\overline{I}_i^{(\uparrow/\downarrow)}\left(1 - \overline{I}_i^{(\uparrow/\downarrow)} - 2\sum_{j=i+1}^{k}\overline{I}_j^{(\uparrow/\downarrow)}\right)\right]. \tag{43}$$

The estimated parameters along with the corresponding RPSS_D are summarised in Table 2. First and foremost, the table reveals that all models have forecasting skill significantly superior to the constant probability model as all *RPSS*s are considerably higher than 0. The difference in forecast skill between the conditional models and the unconditional ones seems to be insignificant. Put in context with the optimal bandwidth found this seems reasonable. Viewing the performance during both periods, it seems as the models with the daily seasonal term seem to be slightly superior to the others. The performance of all the models including a seasonal terms seems to be quite similar though. A visualisation of a single set of forecasts is given in Figure 5.

In Figure 6, reliability diagrams for the unconditional and the conditional version of model II are depicted, along with 95% consistency bars (Following the terminology of Bröcker and Smith (2007)). The diagrams are based on segmenting the predicted probabilities into 5 equally populated bins which averages represent the predicted probabilities. The consistency bars are constructed by bootstrapping 10000 samples with

Table 2: Estimated parameters and RPSS_D for the different model setups investigated

Model		Model parameters				RPSS_D	
		γ	α_μ	$\alpha_{S(1)}$	$\alpha_{S(2)}$	Training set	Test set
Unconditional	I	—	0.0018	—	—	0.5063	0.4796
	II	—	0.0114	0.1161	—	0.5154	0.4815
	III	—	0.0188	—	0.0838	0.5105	0.4778
	IV	—	0.0126	0.1174	0.0626	0.5152	0.4806
Conditional	I	0.9365	0.0022	—	—	0.5052	0.4811
	II	0.9629	0.0090	0.1541	—	0.5141	0.4816
	III	0.8837	0.0203	—	0.0924	0.5072	0.4778
	IV	0.9886	0.0104	0.1460	0.0608	0.5140	0.4808

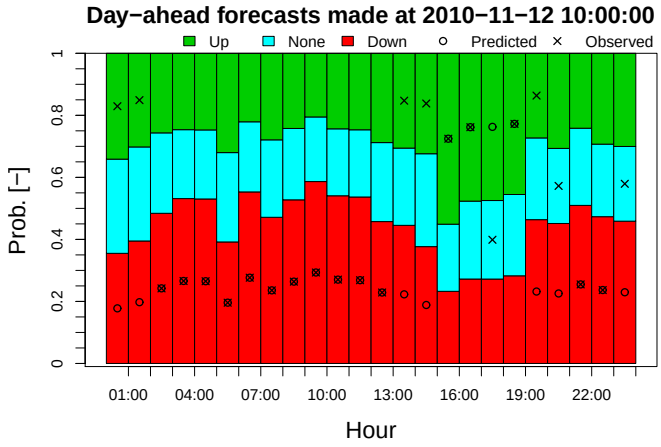

Figure 5: Stacked bar plot showing the posterior imbalance sign probabilities estimated at 10:00 on November 12th 2010 for November 13th. The most likely imbalance sign and the observed one are marked.

replacement for each point (Efron and Tibshirani, 1986, Atger, 2004, Bröcker and Smith, 2007) accounting for the autocorrelation of the probability transformation integral (PIT) as described in Pinson et al. (2010).

For both models and both periods, the predictions can not be deemed unreliable at the 5% significance level. The unconditional and the conditional models therefore seem to perform quite similarly. Hence it must be concluded that the forecast wind power penetration has no significant impact on the imbalance sign – At least not when defined in terms of price differences and under such a family of models.

The reason for the lack of improved forecasting skill most likely lies in the time-variation of the imbalance sign probabilities – both periodical variations and drift. Since they are not taken into account in Figure 4, the increased probability of down-regulation could be the result of generally higher wind power penetration during the night and that periods of high down-regulation frequency coincide with periods of high wind power production.

As a final remark, it should be noted that the segmentation of the predicted probabilities implies that their position in the horizontal dimension is subject to uncertainty just as their vertical position. Especially this uncertainty could be large in the bins including the highest and the lowest probabilities since the distribution of elements in these bins is likely to be skewed, positively and negatively respectively. This property could however only inflate the reliability uncertainty and thus can not impact the conclusions of this paper. Although an interesting problem, the construction of these two-dimensional consistency bars is beyond the scope of this paper.

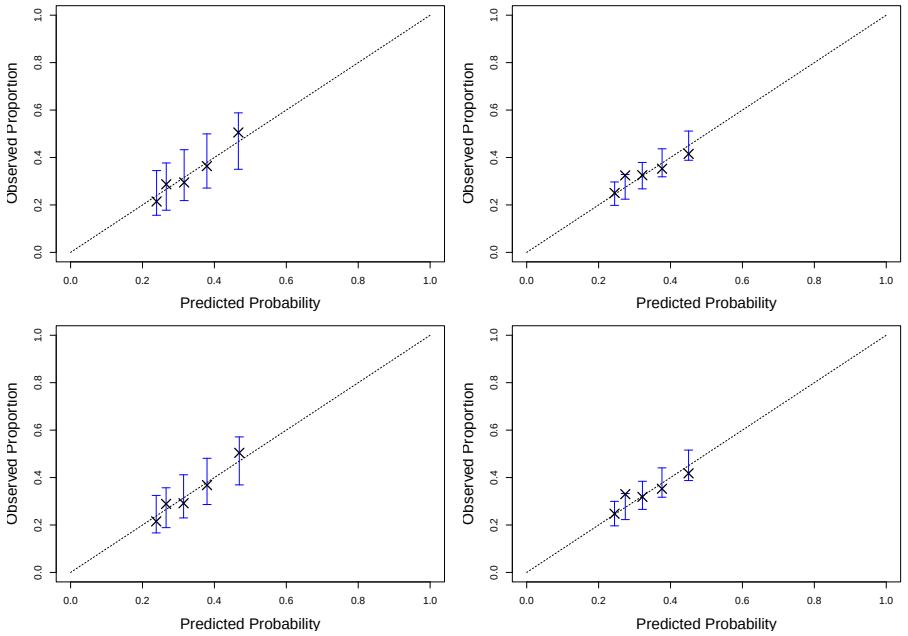

Figure 6: Reliability diagrams for the unconditional (top row) and the conditional (bottom row) models with diurnal cycle for the training and the test periods (left and right columns respectively).

5.2 Imbalance Penalties

The imbalance penalty forecasts are evaluated in terms of the Root Mean Square Error (RMSE)

$$\mathrm{RMSE} = \sqrt{\frac{\sum_{t=1}^{N}\left(\psi_t^{(\uparrow/\downarrow)} - \widehat{\psi}_t^{(\uparrow/\downarrow)}\right)^2}{N}} \tag{44}$$

and in terms of the R^2 measure defined as

$$\mathrm{R}^2 = 1 - \frac{\sum_{t=1}^{N}\left(\psi_t^{(\uparrow/\downarrow)} - \widehat{\psi}_t^{(\uparrow/\downarrow)}\right)^2}{\sum_{t=1}^{N}\left(\psi_t^{(\uparrow/\downarrow)} - \overline{\psi^{(\uparrow/\downarrow)}}_t\right)^2} \tag{45}$$

where $\overline{\psi^{(\uparrow/\downarrow)}}_t$ is the empirical mean of the penalties during the corresponding period. Thus, similar to the RPSS_D, the R^2 measures the relative improvement in forecasting skill compared to the climatological models. For the sake of comparison, Table 3 summarises the standard deviations of the series themselves.

Tables 4 and 5 list the estimated model parameters and the corresponding performance measures for the up-and down-regulation penalty models. The best performing models are conditional ones, all of which involve conditioning upon the forecast spot price. Moreover, the models include either solely a mean term or a mean and a daily seasonal term. None of the models however perform particularly well and their residual RMSE is only slightly less than the series standard deviation. In light of the optimal smoothing parameters, which yield long model memory, this is not surprising.

The long memory, combined with the high value of τ and the residual RMSE values indicate that the model is only capable of tracking the relatively long-term average penalty and its variations. Spiking behaviour remains undescribed though. This suggest that such behaviour is mainly owed to factors that become known after the clearing of the spot market. It would therefore be interesting to estimate the expected penalties based on scenarios. These would in turn be based on scenarios for some of the factors mainly impacting the regulation penalty, e.g. wind power and load forecasting errors and remaining capacity on the interconnections to neighbouring areas.

Table 3: Standard Deviation of the down-and up-regulation penalties

Period	Down	Up
Training	109.81	97.56
Test	135.85	118.73

Table 4: The estimated model parameters along with performance measures for the best performing up-regulation penalty models

Seasonality	X_t	γ	τ	α_μ	$\alpha_{S(1)}$	In-Sample RMSE	In-Sample R^2	Out-of-Sample RMSE	Out-of-Sample R^2
	$\pi^{(S)}$ & L	0.2647	793	0.0082	—	92.68	0.0974	116.93	0.0301
Additive	L	0.5372	625	0.0028	0.0447	91.93	0.1120	116.87	0.0311
	$\pi^{(S)}$ & L	0.5223	701	0.0030	0.0533	92.87	0.0938	114.47	0.0705
Multiplicative	$\pi^{(S)}$ & L	0.4252	695	0.0050	0.0202	93.57	0.0801	117.13	0.0268

Table 5: The estimated model parameters along with performance measures for the best performing down-regulation penalty models

Seasonality	X_t	γ	τ	α_μ	$\alpha_{S(1)}$	In-Sample RMSE	In-Sample R^2	Out-of-Sample RMSE	Out-of-Sample R^2
	—-	—	1197	0.0040	—	108.46	0.0243	133.07	0.0405
Additive	—	—	599	0.0022	0.0465	107.22	0.0466	132.35	0.0508
	$\pi^{(S)}$	0.9634	74	0.0005	0.1419	110.18	-0.0067	133.15	0.0393
	$\pi^{(S)}$ & W	0.4491	584	0.0007	0.1523	106.52	0.0590	129.24	0.0948
	$\pi^{(S)}$ & L	0.6975	611	0.0006	0.0936	107.30	0.0452	131.04	0.0695
Multiplicative	—	—	600	0.0023	0.0451	106.51	0.0592	132.10	0.0544
	$\pi^{(S)}$ & W	0.3768	574	0.0418	0.0587	106.38	0.0614	129.59	0.0900

5.3 Unconditional Expected Imbalance Penalties

Finally the models' ability to provide the optimal quantile value for the wind power trading application described in Section 3.1 is examined. Now recall that the bid that optimises the hourly expected revenue of a price taking wind power producer is the $\widehat{q}$-quantile of the CDF for the wind power production where

$$\widehat{q}_t = \frac{\widehat{\psi}_t^{(\downarrow)}}{\widehat{\psi}_t^{(\downarrow)} + \widehat{\psi}_t^{(\uparrow)}} \tag{46}$$

also recalling that $\widehat{\psi}_t^{(\downarrow)}$ and $\widehat{\psi}_t^{(\uparrow)}$ are the unconditional expectations for the penalties, given by Eqs. (11) and (12) respectively.

The market design implies that the realisation of q is a binary number for the hours where imbalances in either direction are penalised. For hours when imbalances are not penalised, q is not defined as it implies division by 0. However during these hours, any bid between 0 and full production can be seen as the correct one. So q is defined as

$$q_t = \frac{\psi_t^{(\downarrow)}}{\psi_t^{(\downarrow)} + \psi_t^{(\uparrow)}} = \begin{cases} 1 & \text{if } \psi_t^{(\downarrow)} > 0 \\ 0 & \text{if } \psi_t^{(\uparrow)} > 0 \\ \text{Undefined} & \text{if } \psi_t^{(\downarrow)} = \psi_t^{(\uparrow)} = 0 \end{cases} \tag{47}$$

In order to evaluate the quality of $\widehat{q}_T$ the RPSS_D (Eq. (42)) is calculated for the hours when q_t is defined during the test period. The climatology model for q is used as a reference. This implies that the optimal quantile estimate $\overline{q}$ is constant throughout the period and found by substituting the period averages for $\widehat{\psi}_t^{(\uparrow/\downarrow)}$ in Eq. (46). The estimate of $\widehat{q}$ is found using (i) the unconditional model with a daily seasonal cycle for $\widehat{\boldsymbol{I}}_t^{(\uparrow/\downarrow)}$, (ii) the model conditioned upon the forecast spot price and wind power penetration for $\widehat{\psi}_{t|>0}^{(\downarrow)}$ and (iii) the model conditional to the forecast spot price and load for $\widehat{\psi}_{t|>0}^{(\uparrow)}$. This yields $\text{RPSS}_D = 0.2954$ and thus the proposed model outperforms the empirical probability by a significant margin.

6 Conclusions and Discussion

The foregoing study shows that analysis of real-time electricity markets can be significantly improved by the inclusion of a model describing the short-term variations of the market dynamics. This is the case both for studies of strategic bidding of renewable energy in the markets and for the more general discussions about the presence and profitability of gaming on electricity markets. Despite the fact that the presented empirical results are somewhat area specific, a number of relevant similarities between the specifics of the Nord Pool and of other electricity markets suggests that similar results could be obtained for other markets as well.

The results presented in this paper are derived in a framework tailored for day-ahead bidding of wind power into the market, with its specific lead times. Even though conditioning the model upon the forecast wind power penetration did not result in an improved model, the conditional Holt-Winters framework is likely to be more relevant for other variables and for shorter lead times. For instance, one interesting aspect to investigate in the context of predictions with shorter lead times would be to include updated wind power and load forecasts when they become available.

Although the forecasting skill of the proposed model might seem low to some readers, one has to bare in mind that the process it described is mainly driven by errors from well tuned forecasting models and unforeseeable events like plant malfunctions. In light of this, the observed forecasting quality is quite satisfactory. From the market operator's point of view however, the results of this paper might be worrying since hinting that profitable gaming on the electricity market is possible. Thus, it is clear that anti gaming policies have to be revised if the desire is to maintain a gaming free market. Given the current carbon emission curbing targets in various parts of the world however, the potential benefits of gaming for producers of, and systems highly penetrated with, electricity by renewable sources have to be considered while structuring such reforms.

The models presented in this paper are adapted to the purpose of facilitating the bidding strategy presented in Zugno et al. (2012). Thus expectations of the imbalance penalties are sought conditional only to the information available before the gate-closure of the market are considered. Constructing similar models for scenario generation purposes however does not necessarily call for such availability restrictions. In that case, models can be constructed based on realisations of the variables affecting the penalties, e.g. spot price, regulation need and interconnection capacity to neighbouring areas. In that case accounting for the interdependence between simulated variables becomes paramount, e.g. by the method presented in Pinson et al. (2009).

References

Frédéric Atger. Estimation of the reliability of ensemble-based probabilistic forecasts. *Quarterly Journal of the Royal Meteorological Society*, 130(597):627–646, 2004.

Alexander Boogert and Dominique Dupont. On the effectiveness of the anti-gaming policy between the day-ahead and real-time electricity markets in the Netherlands. *Energy Economics*, 27(5):752–770, 2005.

John B. Bremnes. Probabilistic wind power forecasts using local quantile regression. *Wind Energy*, 7(1):47–54, 2004.

Jochen Bröcker and Leonard A. Smith. Increasing the reliability of reliability diagrams. *Weather and Forecasting*, 22(3):651–661, 2007.

William S. Cleveland and Susan J. Devlin. Locally weighted regression: An approach to regression analysis by local fitting. *Journal of the American Statistical Association*, 83 (403):596–610, 1988.

Brad Efron and Robert Tibshirani. Bootstrap methods for standard errors, confidence intervals, and other measures of statistical accuracy. *Statistical Science*, 1(1):54–77, 1986.

E Epstein. A scoring system for probability forecasts of ranked categories. *Journal of Applied Meteorology*, 8(6):985–987, 1969.

S. Galloway, G. Bell, G. Burt, J. McDonald, and T. Siewerski. Managing the risk of trading wind energy in a competitive market. *Generation, Transmission and Distribution, IEEE Proceedings*, 153(1):106–114, 2006.

Sarah Gelper, Roland Fried, and Cristophe Croux. Robust forecasting with exponential and Holt-Winters smoothing. *Journal of Forecasting*, 29(3):285–300, 2010.

M. Gibescu, W. L. Kling, and E. W. Van Zwet. Bidding and regulating strategies in a dual imbalance pricing system: case study for a Dutch wind producer. *International Journal of Energy Technology and Policy*, 6(3):240–253, 2008.

Tilmann Gneiting. Quantiles as optimal point forecasts. *International Journal of Forecasting*, 27(2):197–207, 2010.

Rob J. Hyndman, Anne B. Koehler, Ralph D. Snyder, and Simone Grose. A state space framework for automatic forecasting using exponential smoothing methods. *International Journal of Forecasting*, 18(3):439–454, 2002.

Rob J. Hyndman, Anne B. Koehler, J. Keith Ord, and Ralph D. Snyder. *Forecasting with Exponential Smoothing - The State Space Approach*. Springer, New York, USA, 2008.

Tryggvi Jónsson. *Forecasting and decision making in electricity markets with focus on wind energy*. PhD thesis, DTU Informatics, Technical University of Denmark, Kgs. Lyngby, Denmark, 2012.

Tryggvi Jónsson, Pierre Pinson, and Henrik Madsen. On the market impact of wind energy forecasts. *Energy Economics*, 32(2):313–320, 2010.

Tryggvi Jónsson, Pierre Pinson, Henrik Aalborg Nielsen, Henrik Madsen, and Torben Skov Nielsen. Forecasting electricity spot prices accounting for wind power predictions. *IEEE Transactions on Sustainable Energy*, In PRESS, 2012.

Tryggvi Jónsson, Sarah M. Ryan, Marco Zugno, and Pierre Pinson. Risk averse bidding of wind power: Formulation and properties. Technical report, DTU Informatics, 2012. 2012-03.

J. Matevosyan and L. Söder. Minimization of imbalance cost trading wind power on the short-term power market. *IEEE Transactions on Power Systems*, 21(3):1396–1404, 2006.

Juan M. Morales, Antonio J. Conejo, and Juan Pérez-Ruiz. Short-term trading for a wind power producer. *IEEE Transactions on Power Systems*, 25(1):554–564, 2010.

Allan H. Murphy. On the ranked probability skill score. *Journal of Applied Meteorology*, 8(6):988–989, 1969.

Allan H. Murphy. A note on the ranked probability skill score. *Journal of Applied Meteorology*, 10(1):155–156, 1971.

Henrik Aa. Nielsen, Torben S. Nielsen, Alfred K. Joensen, Henrik Madsen, and Jan Holst. Tracking time-varying coefficient functions. *International Journal of Adaptive Control and Signal Processing*, 14(8):813–828, 2000.

Torben Skov Nielsen, Henrik Aalborg Nielsen, and Henrik Madsen. Prediction of wind power using time-varying coefficient functions. In *15th IFAC World Congress*, Barcelona, Spain, 2002.

Nord Pool Spot AS. Exchange Information - Highest market share ever for Nord Pool Spot, January 2010. URL http://www.nordpoolspot.com/Message-center-container/Exchange-list/Exchange-information/No-022010-NPS---Highest-market-share-ever-for-Nord-Pool-Spot-/?year=2010&month=1.

Nord Pool Spot AS. The power market, August 2011a. URL http://www.nordpoolspot.com/How-does-it-work/.

Nord Pool Spot AS. Exchange Information - Highest volume ever for Nord Pool Spot, January 2011b. URL http://www.nordpoolspot.com/Message-center-container/Exchange-list/Exchange-information/No-052011--Highest-volume-ever-for-Nord-Pool-Spot/?year=2011&month=1.

Nord Pool Spot AS. Exchange Information - Figures show record volume for Nord Pool Spot, January 2012. URL http://nordpoolspot.com/Message-center-container/Exchange-list/2012/1/No-022012---Figures-show-record-volume-for-Nord-Pool-Spot/?year=2012&month=1.

Magnus Olsson and Lennart Söder. Modeling real-time balancing power market prices using combined SARIMA and Markov processes. *IEEE Transactions on Power Systems*, 23(2):443–450, 2008.

Pierre Pinson, Christophe Chevallier, and George N. Kariniotakis. Trading wind generation from short-term probabilistic forecasts of wind power. *IEEE Transactions on Power Systems*, 22(3):1148–1156, 2007.

Pierre Pinson, George Papaefthymiou, B. Klockl, Henrik Aalborg Nielsen, and Henrik Madsen. From probabilistic forecasts to statistical scenarios of short-term wind power production. *Wind Energy*, 12(1):51–62, 2009.

Pierre Pinson, Patrick McSharry, and Henrik Madsen. Reliability diagrams for nonparametric density forecasts of continuous variables: accounting for serial correlation. *Quarterly Journal of the Royal Meteorological Society*, 136(646):77–90, 2010.

Morteza Rahimiyan, Juan M. Morales, and Antonio J. Conejo. Evaluating alternative offering strategies for wind producers in a pool. *Applied Energy*, 88(12):4918–4926, 2011.

K. Skytte. The regulating power market on the Nordic power exchange Nord Pool: an econometric analysis. *Energy Economics*, 21(4):295–308, 1999.

James W. Taylor. Short-term electricity demand forecasting using double seasonal exponential smoothing. *Journal of Operational Research Society*, 54(8):799–805, 2003.

Andreas P. Weigel, Mark A. Liniger, and Christof Appenzeller. The discrete brier and ranked probability skill scores. *Monthly Weather Review*, 135(1):118–124, 2007.

Peter R. Winters. Forecasting sales by exponentially weighted moving averages. *Management Science*, 6(3):324–342, 1960.

Marco Zugno, Pierre Pinson, and Tryggvi Jónsson. Trading wind energy based on probabilistic forecasts of wind generation and market quantities. *Wind Energy*, In PRESS, 2012.